UNIVERSIDAD DE GRANADA

PROGRAMA DE DOCTORADO DE BIOMEDICINA

INSTITUTO DE PARASITOLOGÍA Y BIOMEDICINA "LÓPEZ-NEYRA", CSIC

Analysis of LRRK2 localization towards understanding the pathogenic mechanisms underlying Parkinson's Disease

Marian Blanca Ramírez

Tesis doctoral

2017

Editor: Universidad de Granada. Tesis Doctorales
Autora: Marian Blanca Ramírez
ISBN: 978-84-9163-556-7
URI: http://hdl.handle.net/10481/48377

El doctorando / The *doctoral candidate* **Marian Blanca Ramírez** y los directores de la tesis / and the thesis supervisor/s **Sabine Nicole Navarro Hilfiker**

Garantizamos, al firmar esta tesis doctoral, que el trabajo ha sido realizado por el doctorando bajo la dirección de los directores de la tesis y hasta donde nuestro conocimiento alcanza, en la realización del trabajo, se han respetado los derechos de otros autores a ser citados, cuando se han utilizado sus resultados o publicaciones.

/

Guarantee, by signing this doctoral thesis, that the work has been done by the doctoral candidate under the direction of the thesis supervisor/s and, as far as our knowledge reaches, in the performance of the work, the rights of other authors to be cited (when their results or publications have been used) have been respected.

Lugar y fecha / Granada, 30 de Mayo de 2017

Director/es de la Tesis / *Thesis supervisor/s;*

Doctorando / *Doctoral candidate*:

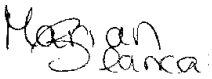

Acknowledgments

A special thanks to my supervisor Sabine Hilfiker for thinking of me when she gave me the grant for my PhD, for all her tips about science and life, and despite all the craziness from the past months, for always thinking I could do better.

I would like to thank everyone from my lab, because although this might sound as a cliché, I truly believe that without them I would not have been able to go along this pathway. Thanks to Patri, because even though it did not seem that way in the beginning, she has become one of my best friends. For having helped me out when I first got in the lab, for being there for me, even in the distance, and specially when things did not work out for me in any aspect of my life. Thanks to Jesus, because if our friendship survived this, I doubt there is much more out there that could break it up! Thank you for sharing a million of hours in the lab with me, for our great talks, and for reminding me the world can be a better place. Thanks to Belencilla, who came last, but never least! For our lunches together, for the best thesis present ever, and for always always taking care of me. Thanks to Pilar, for showing me people can be a better version of themselves. Thanks to Antonio, for hanging out with me when I needed it, and for always counting on me when I was not there. Thanks to Ele, because her stories are an inspiration for me. Thanks to María, for sharing great music with me, apart from the hard-drive! Thanks to Mar, for sharing her enthusiasm when we all needed it, as well as very good party times. I would like to thank the two extra lab members, Mariascen, because her enthusiasm rubs off everyone who is around her, thanks for being such a great person, and thanks for being my friend; and Laura, thanks for all your microscopy tips and for getting me the best present that I could have to conclude this time with.

Thanks to all my friends, to Natalia, for our endless whatssapp conversations and for always encouraging me to keep on loving science, to Maca, for listening to me no matter what, to Dario, for being one of my best friends. To my English friends, for answering the tons of geeky questions about uses of English, and for being there for me in the distance.

I am also grateful to Maddy Parsons and Elisa Greggio for giving me the opportunity to work in their lab and live in Padova and in my beloved city of London. Thanks to everyone in their lab, for helping me set out my experiments and with my English and Italian.

Thanks to my sister, my favourite person in the world, because of her and despite her my life keeps on changing. Thanks to my dad, for being my dad, and to the rest of my family, for loving me and coping with me in stressful times.

Thanks to my mum for having existed.

Index

I. Summary/Resumen....6

II. Abbreviations....8

III. Introduction....11

1. Parkinson's Disease....13

2. LRRK2....14

a. Enzymatic activities....15

i. Kinase domain....15

ii. GTPase domain....19

b. LRRK2 interactors....23

3. Microtubules....25

a. Microtubules....25

i. Tubulin isotypes....27

ii. Post translational modifications....27

b. Links between MT stability and neurodegeneration....31

c. MTs and vesicular trafficking events 32

4. LRRK2 function....34

a. endomembrane trafficking....34

b. signalling pathways....36

c. cytoskeletal dynamics....37

IV. Objectives....40

V. Materials and Methods....41

VI. Results....51

1. LRRK2 and Parkinson´s disease: from lack of structure to gain of function....51

2. LRRK2: from kinase to GTPase to microtubules and back....52

3. GTP binding regulates cellular localization of Parkinson's disease-associated LRRK2..53

4. LRRK2: a death effector filament protein?....54

5. Alterations in motility as a cellular readout for pathogenic LRRK2 in Parkinson's Disease.....58

VII. Discussion.....60

VIII. Conclusions/Conclusiones.....68

IX. References.....71

X. List of Papers.....94

I. Summary

Mutations in leucine rich repeat kinase 2 (LRRK2) represent the most common cause of familial Parkinson's Disease (PD), and variants in this gene modify risk for sporadic PD. Thus, the study of LRRK2 is key towards elucidating the mechanism(s) underlying both familial and sporadic disease entities. Towards this goal, previous studies have reported an interaction between LRRK2 and microtubules (MTs). However, the determinants within LRRK2 responsible for such interactions, and the possible downstream alterations in MT-mediated transport events remain unknown.

Here, we first we demonstrate that most pathogenic LRRK2 mutants as well as pharmacological LRRK2 kinase inhibition causes an enhanced association of LRRK2 with a subset of stable MTs, displaying a filamentous phenotype. This is in contrast to wildtype LRRK2, which displays a largely cytosolic localization. Second, we find that this association can be modulated upon altering the levels of detyrosinated tubulin, whereas the MT acetylation status does not seem to play a direct role. Such association may cause subsequent MT destabilization. Third, we elucidate the molecular determinants of this interaction to be regulated by LRRK2 GTP binding. We find that two synthetic mutants (R1398L; R1398L/T1343V) as well as a protective risk variant for PD (R1398H) decrease GTP binding which causes a rescue of this phenotype. Treatment with two novel GTP binding inhibitors also reverts such altered localization of pathogenic or kinase-inhibited LRRK2. Finally, such altered subcellular localization is induced by GTP analogs, providing formal proof-of-concept that altered LRRK2 GTP binding causes such altered subcellular localization.

Altogether, our findings indicate a preferential association of pathogenic mutant and pharmacologically kinase-inhibited LRRK2 with stable MTs, which may directly or indirectly impact upon various MT-mediated vesicular trafficking events.

Resumen

Mutaciones en leucine rich repeat kinase 2 (LRRK2) representan la causa más común de la Enfermedad de Parkinson (EP) familiar, y variaciones en este gen modifican el riesgo de EP esporádico. Por ello, el estudio de LRRK2 es clave para intentar dilucidar el mecanismo responsable de ambas formas de la enfermedad: familiar y esporádica. Con este fin, estudios previos han descrito la interacción entre LRRK2 y microtúbulos (MTs). Sin embargo, los determinantes implicados en esta interación, así como los efectos "downstream" que se deriven de ella, aún son desconocidos.

En esta tesis, primero demostramos que la mayoría de los mutantes patogénicos, así como su versión farmacológicamente inhibida de la actividad kinasa, intensifican la asociación de LRRK2 con un grupo de MTs estables, mostrando un fenotipo filamentoso. Esto se contrapone con wildtype LRRK2, que muestra una localización predominantemente citosólica. Segundo, encontramos que esta asociación puede ser modulada mediante la alteración de los niveles de tubulina destirosinada, mientras que el estado de acetilación de los MTs no parece jugar un papel de manera directa. Esta asociación puede desembocar en la desestabilización de los MTs. Tercero, dilucidamos que los determinantes moleculares de esta interacción requieren la unión de GTP. Encontramos que dos mutantes sintéticos (R1398L; R1398L/T1343V), así como una variante de riesgo protectora para EP (R1398H) dismininuyen la unión a GTP, lo cual revierte este fenotipo. El tratamiento con dos nuevos inhibidores de GTP también revierte la localización alterada mostrada por LRRK2 patogénico y kinasa inactivo. Finalmente, esta localización alterada es inducida por analógos de GTP, lo cual representa una prueba formal de que la alteración de la unión de GTP a LRRK2 es la causa de esta alteración en su localización subcelular.

Teniendo todo esto en cuenta, nuestros resultados indican una asociación preferencial de LRRK2 patogénico así como de su versión farmacológicamente inhibida de la actividad kinasa con MTs estables, lo cual puede directa o indirectamente tener un efecto en varios de los eventos implicados en el tráfico de vesículas a través de MTs.

II. Abbreviations

4E-BP: eIF4E (eukaryotic initiation factor 4E)-binding protein

α-TAT-1: α-tubulin acetyltransferase-1

Ac: acetylation

AD: Alzheimer's disease

ArfGAP1: ADP-ribosylation factor GTPase-activating protein 1

ArhGEF7: rho guanine nucleotide exchange factor 7

CAP-Gly: cytoskeleton-associated protein glycine-rich

CCPs: cytosolic carboxypeptidase family

Cdk1: cyclin-dependent kinase 1

CK1α: casein kinase I α

CLIP170: cytoplasmic linker protein 70

DVL1-3: dishevelled proteins 1-3

COR: C-terminus of ROC

ER: endoplasmic reticulum

FADD: fas associated death domain protein

GAD: G proteins activated by nucleotide-dependent dimerization

GAP: GTPase activating protein

GEF: guanine nucleotide exchange factor

GDP: guanosine diphosphate

GDI: guanine nucleotide dissociation inhibitor

GSK-3β: glycogen synthase kinase-3β

GTP: guanosine triphosphate

HDAC6: histone deacetylase family member 6

KIF5: kinesin like protein 5

KIF6B: kinesin like protein 6

KIF-2: kinesin family-2

KIF-1A: kinesin like protein 2

LBs: Lewy bodies

LRP6: low-density lipoprotein receptor-related protein 6

LRR: leucine rich repeats

LRRK2: leucine rich repeat kinase 2

MAP: microtubule-associated protein

MAP1B: microtubule-associated protein 1B

MAPK: mitogen-activated protein kinase

MCAK: mitotic centromere-associated kinesin

MEC: mechanosensory

MEK: mitogen-activated protein kinase kinase/extracellular signal–regulated kinase

MTs: microtubules

NFTs: neurofibrillary tangles

PAK6: p21 (RAC1) activated kinase 6

Pam: palmitoylation

PD: Parkinson's disease

PKA: protein kinase A

PP1/PP2A: protein phosphatase 1/2A

PTMs: post-translational tubulin modifications

Rac1: ras-related c3 botulinum toxin substrate 1

RGS2: regulator of G protein signalling 2

RILP: rab7-interacting lysosomal protein

ROC: ras of complex

SIRT-2: sirtuin type-2

SNpc: substantia nigra pars compacta

Syk: spleen tyrosine kinase

TGN: trans-Golgi network

TTL: tyrosine tubulin ligase

TTLL: tubulin tyrosine ligase-like

TRADD: TNFR1-associated death domain protein

Vps34: protein phosphatidylinositol-3-OH kinase

Wnt: wingless signalling pathway

III. Introduction

1. Parkinson's disease (PD)

Parkinson's disease (PD) was described for the first time by James Parkinson in his essay on the shaking palsy in 1817 [1]. PD is a progressive and incurable disease and it is currently the most prevalent neurodegenerative disorder in the Western world after Alzheimer's disease, with approximately 6 million people worldwide suffering from it. PD is an age-related disease which affects between 1-2% of the population above the age of 65 and up to ~4% in those above 85 years [2]. Since the incidence increases as the population ages, neurodegenerative diseases will become an ever-growing social and economic burden on society.

The main pathological hallmarks of PD are progressive degeneration and death of pigmented dopaminergic neurons of the substantia nigra *pars compacta* (SNpc), which project to the striatum (primarily to the putamen), impairing the nigrostriatal dopaminergic pathway [3] (Figure 1A, 1B). Since this pathway is mainly involved in the execution of movement [4], the loss of dopaminergic neurons of the SNpc that causes striatal dopamine deficiency provokes the characteristic motor symptoms of PD. The other cardinal pathological sign is the presence of Lewy bodies (LBs) (Figure 1C), which are proteinaceous cytoplasmic inclusions mainly composed of aggregated α-synuclein and ubiquitin [5].The cellular consequences of LBs remain unclear, and there is evidence supporting both a potential neuroprotective role, with misfolded proteins getting accumulated in order to block cellular damage, or a neurodegenerative role, with accumulated proteins inducing toxicity [6].

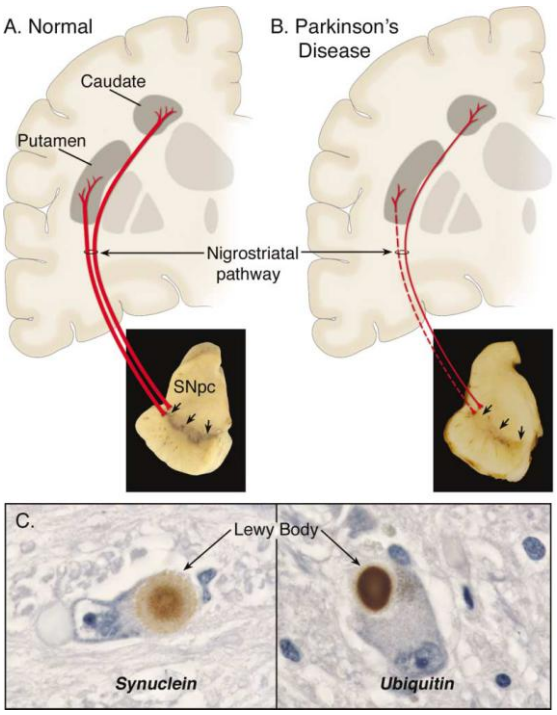

Figure 1: Schematic comparison of the nigrostriatal pathway in a normal and in a PD brain. PD has been described to induce a loss of dopaminergic neurons from the *substantia nigra pars compacta*, which project to the striatum (the putamen and the caudate nucleus), thereby impairing the nigrostriatal pathway. A cardinal hallmark for PD is the presence of abnormal aggregation of proteins such as α-synuclein or ubiquitin, which form proteinaceous structures known as Lewy Bodies**.** Adapated from [6].

The main motor symptoms of PD include rigidity, tremor, postural instability, hypokinesia (reduced amplitude of movement) and bradykinesia (slowness of movement) [7]. The clinical motor symptoms of PD appear after a threshold loss of around 60-70% of SNpc dopaminergic neurons and 80% depletion of striatal dopamine [6]. As the disease progresses, other neurotransmitter pathways in the brain are also affected, giving rise to non-motor symptoms including cognitive decline, psychiatric problems and a range of autonomic disturbances [8]. There are also various early manifestations of the disease, such as anosmia [9].

In addition, not all dopaminergic neurons are affected in the disease, and neurons other

than dopaminergic neurons are prone to cellular demise as well [10]. Currently, there is no cure for the disease, and treatments are only based on alleviating symptoms. In fact, the classical treatment involving exogenous dopamine replacement via the administration of Levodopa (an intermediate in dopamine synthesis), has been shown with time to produce dyskinesia (involuntary movements) and motor fluctuations, supporting the need for better therapies [11].

PD is largely sporadic, with the exact pathological mechanism(s) remaining unclear. Indeed, the use of identified toxins such as MPP+ or rotenone has been linked to PD, highlighting a role for mitochondria and oxidative stress [5]. However, around 8-10% of PD cases are due to mutations in identified loci called *PARK* genes that have been shown to be linked to familial PD [12] (Table 1). *PARK1* encodes for α-synuclein [13], which tends to aggregate and constitutes one of the main components of LBs. Both point mutations as well as triplication of the α-synuclein gene are associated with autosomal-dominant, early-onset PD [13-16]. Another early-onset gene is *PARK2*, encoding for Parkin, which is an E3-ubiquitin ligase recruited to defunct mitochondria [17]. Point mutations in this gene are known to segregate with the disease in a recessive fashion, which is generally characterized by the absence of LBs, although these have also been found in some particular cases [18, 19]. *PARK6* encodes for PINK1 [20], which is also associated to mitochondria. Mutations in this gene represent the second most frequent cause of autosomal-recessive early-onset PD after mutations in *PARK2*. Overall, the known function(s) of those genes imply various mechanisms related to abnormal protein homeostasis, altered vesicular trafficking and mitochondrial dysfunction.

Finally, genome-wide association studies have revealed other genes variations in which increases or decreases disease risk (included in Table 1) [21]. Altogether, the finding that not only environmental factors, but also various monogenic forms contribute to PD pathogenesis helps to shed light into elucidating the molecular basis underlying this disease.

Reference	Locus	Chromos.	Gene	Inheritance	Transmission
Polymeropoulos, 1996; Farrer, 1999 [22, 23]	PARK1/4	4q21-q23	SNCA (α-synuclein)	AD and sporadic, high penetr.	Early/ late onset PD
Matsumine, 1997 [24]	PARK2	6q25-q27	PRKN (parkin)	AR and sporadic	Early onset PD
Valente, 2001 [25]	PARK6	1p36-p35	PINK-1	AR	Early onset PD
Van Duijn CM , 2001 [26]	PARK7	1p36	DJ-1	AR	Early onset PD
Funayama, 2002 [27]	PARK8	12p11-q13	LRRK2	AD and sporadic, incomplete penetr.	Late onset PD
Satake, 2009 [28]	PARK16	1q32	RAB7L1	Risk factor	Late onset PD
Vilariño-Güell,2011[29]	PARK17	16q11	VPS35	Risk factor/ AD	Late onset PD

Table 1: Loci involved in PD: PARK genes. List of the PARK genes specifying chromosome position (chromos.), name of the gene, kind of inheritance and type of disease transmission. Adapted from Fernandez et al. (unpublished).

2. LRRK2

The *PARK8* locus encodes for *Leucine-Rich Repeat Kinase 2* (*LRRK2*) [30, 31]. LRRK2 is a 2527 amino acid protein and comprises several interaction domains such as ANK repeats, Leucine-Rich Repeats (LRR) and a WD40 domain. In addition, the protein contains a catalytic core composed of a Ras Of Complex (ROC) domain with GTPase activity, followed by a C-terminal of ROC domain (COR), with this combination being characteristic of ROCO proteins, and a kinase domain [32]. Mutations in LRRK2 represent the most common genetic cause of late-onset PD with an autosomal-dominant inheritance [30, 31], affecting up to 5% of individuals with a family history of the disease (which can go up to 40% depending on ethnic background), and 3% of sporadic cases, although there is incomplete penetrance [32] (Table 1). To date, nine mutations have been shown to clearly segregate with the disease: N1437H, R1441C/G/H/S in the ROC domain, Y1699C in the COR domain and I2012T, G2019S and

I2020T in the kinase domain [30, 31, 33-35]. Importantly, all of these mutations are located in the central region of the protein where the two catalytic domains are (GTPase and kinase domains), implying that a change in enzymatic activity may lead to the pathogenic form of the protein.

Furthermore, two variants have been described to increase risk for sporadic PD, one located in the COR domain, R1628P [36], and the other in the WD40, G2385R [37]. Interestingly, a recent study has also identified for the first time a point mutation, R1398H, that seems to be protective for PD [38], and individuals carrying risk factors (R1628P and/or G2385R) together with this protective variant showed a reduced risk for the disease [38-40] (Figure 2).

Altogether, current knowledge pin-points LRRK2 as a key player for both sporadic and familiar forms of the disease, which makes its study essential for understanding the pathological mechanism(s) that cause PD.

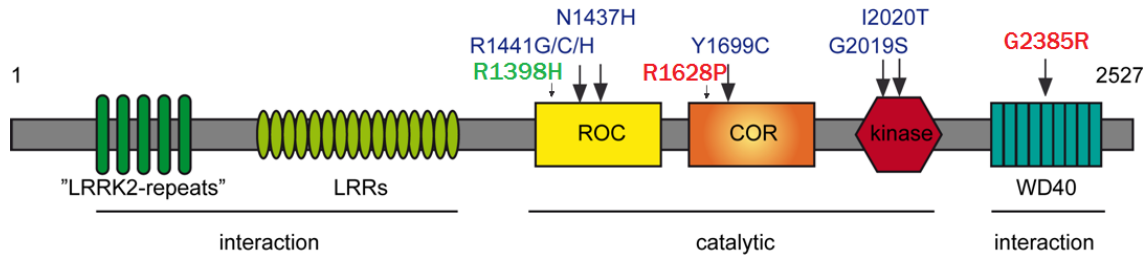

Figure 2: LRRK2 structure and mutations. Schematic representation of the LRRK2 protein, with interaction domains: LRRK2-repeats, LRRs and WD40; and a catalytic domain: ROC-COR and kinase domain. Mutations which segregate with PD are annotated in blue, a protective variant is indicated in green, and two risk mutations are highlighted in red. Taken from [5].

a. Enzymatic activities of LRRK2

i. Kinase domain

The LRRK2 kinase domain constitutes, together with the GTPase domain, the catalytic core of the protein. It is flanked by the ROC-COR domain at the N-terminus and the WD40 repeats at the C-terminus. Equally to all ROCO proteins, LRRK2 belongs to the serine/threonine kinase group [41]. The activation mechanism among serine/threonine kinases is quite conserved, and it usually involves the autophosphorylation of one or more residues in the activation loop, which then induces a conformational change associated with altered ATP binding and/or substrate interaction [42, 43].

Several studies have reported altered kinase activity associated with PD mutations. For most mutations, contradictory results have been obtained, with some studies showing an enhancement due to the I2020T or R1441 mutations [44-46], or reporting no change [47, 48], and the risk variant G2385R displaying lower kinase activity [46, 49]. However, the most frequent mutation in LRRK2, G2019S, linked to both familial and sporadic PD, has consistently been reported to increase the *in vitro* kinase activity 3-4 fold, leading to a hyperactive form of the protein [30, 31, 50]. Thus, it is tempting to speculate that altered kinase activity may cause pathogenicity. Indeed, numerous studies have linked enhanced kinase activity with neurotoxic effects, which were reverted by either genetic or pharmacological kinase activity inhibition [51-53]. Moreover, a recent study looking at substrate phosphorylation in intact cells has reported for the first time increased phosphorylation of a subset of Rab proteins, which was caused by all pathogenic mutants, thus further supporting the relevance of kinase activity in the disease, and the therapeutic potential of kinase inhibitors [54]. Structurally distinct and highly specific kinase inhibitors have been developed. Early studies described CZC-54252 [55] and TAE684 [56, 57], which were shown to effectively inhibit LRRK2 kinase activity, although they are unable to cross the blood brain barrier. More recently, new and highly specific LRRK2 kinase inhibitors with higher permeability through the blood brain barrier have been found including IN1 [58], GSK2578215A [59], GNE-7915 and GNE-0877[57] as well as MLi2 [60], which is currently the most specific LRRK2 kinase inhibitor synthesised so far.

Since LRRK2 was discovered in 2004, many efforts have focused on identifying specific substrates for its kinase activity. However, despite years of research and several candidates proposed, such as moesin, 4E-BP [eIF4E (eukaryotic initiation factor 4E)-binding protein], β-tubulin or tau protein [47, 61-63], it was not until 2016 when a set of specific bona fide substrates were found. Alessi's group has pointed towards the Rab family of small GTPases, showing for the first time that a subset of Rabs, including Rab8, Rab10 and Rab12 are directly phosphorylated by LRRK2 kinase activity *in vitro* and *in vivo* [54], even though the cellular consequences of such phosphorylation events remain unknown.

The LRRK2-mediated phosphorylation of Rab proteins seems to modulate their association with their regulatory proteins, such as Guanine Nucleotide Dissociation Inhibitor (GDI) or GTPase activating proteins (GAPs). The reported lack of association of phosphorylated Rabs with these proteins may cause the accumulation of phosphorylated, inactive Rab proteins in their membrane compartments, and/or their mislocalization. In either case, all pathogenic LRRK2 mutants were found to increase phosphorylation of Rabs in intact cells, even though only one them, the G2019S mutant, displays increased *in vitro* kinase activity, thus raising the question as to how the other mutants might enhance Rab phosphorylation [54].

Apart from substrate phosphorylation, and like many other protein kinases, LRRK2 can phosphorylate itself at numerous identified autophosphorylation sites. However, only some of these sites have been confirmed *in vivo,* including S1292, T1410 and T1491 [64-70]. Various additional phosphorylation sites have been identified in LRRK2, with most of them clustering in the N-terminus (S910, S935, S955, S973) [48, 71, 72] and one in the ROC domain (S1444) [73] (Figure 4). Firstly, these were described as autophosphorylation sites, since the use of specific kinase inhibitors impeded phosphorylation at these sites. However, *in vitro* kinase assays have demonstrated that they are not directly phosphorylated by LRRK2 [74, 75], but rather other kinases/phosphatases have been reported to regulate these so-called cellular phosphorylation sites. For example, protein kinase A (PKA) has been shown to phosphorylate S1444 [73], IκB

kinase seems to phosphorylate Ser 935 in macrophages [76], casein kinase I α (CK1α) has been shown to phosphorylate S910/935 in adult mouse striatum [77], and protein phosphatase 1/2A (PP1/PP2A) inhibitors have been reported to restore phosphorylation at S910/S935 [78] (Figure 3) .

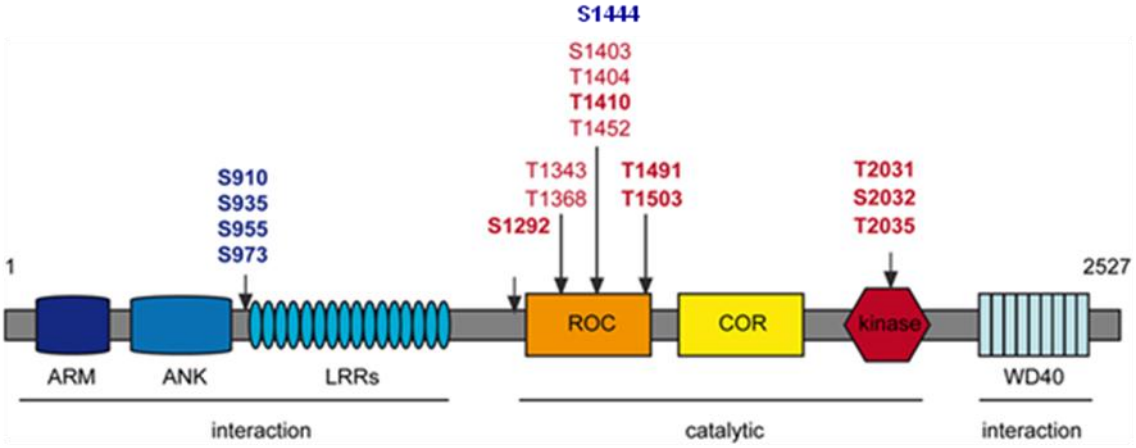

Figure 3: LRRK2 phosphorylation sites. Schematic representation of LRRK2 phosphorylation sites. Cellular sites are annotated in blue, and autophosphorylation sites are indicated in red, with the ones determined *in vivo* highlighted in bold.

Phosphorylation at S910 and S935 has been proven to mediate the interaction of LRRK2 with 14-3-3 proteins. Hence, it has been suggested that 14-3-3 binding to LRRK2 could protect it from being dephosphorylated at these two phosphorylation sites, as well as correlate with differential LRRK2 localization. Thus, LRRK2 was proposed to show a cytosolic distribution when phosphorylated at S910/935 and bound to 14-3-3, but accumulate into discrete cytoplasmic pools when S910/S935 are in a dephosphorylated state and thus 14-3-3 binding is impaired, and the same distribution has been observed when making S/A mutations at those sites. Similarly, pathogenic mutants which present decreased phosphorylation at the cellular sites have been shown to relocalize into cytoplasmic pools [48, 51, 74, 75, 79, 80].

Interestingly, 14-3-3 proteins have been reported to exert a neuroprotective role for PD, with a rescue of neurite shortening induced by the G2019S mutant upon 14-3-3 protein

overexpression, and a further enhancement of the neurite phenotype when inhibiting 14-3-3 binding to LRRK2 by using peptides such as difopein, which binds to 14-3-3 proteins with very high affinity [81].

Along these lines, S910/935 dephosphorylation upon pharmacological kinase inhibition has also been proposed to induce LRRK2 redistribution into cytoplasmic pools. However, some studies highlighted an apparent difference between this relocalization pattern and the one shown when artificially mutating the N-terminal phosphorylation sites, with the first looking more stylized [74] and colocalizing with tubulin [75, 82], subsequently termed as "filamentous structures", and the latter resembling dot-like structures. Interestingly, recent studies have also reported the presence of filamentous structures when analyzing most pathogenic mutants, altogether suggesting that an alteration in LRRK2 subcelullar localization might be involved in PD pathogenesis. Therefore, elucidating the exact mechanism(s) by which LRRK2 undergoes such abnormal relocalization is crucial [66, 79, 82, 83].

ii. GTPase Domain

The GTPase domain of LRRK2 is characterized by having a ROC domain followed by a COR domain, which makes LRRK2 a member of the ROCO protein family, a novel multi-domain family of small GTPases. According to the ROCO protein type of structure, the LRRK2 GTPase domain is composed of five regions: a P-loop or GDP/GTP binding domain, followed by switch I and switch II motifs that undergo conformational changes upon GTP binding, and G4 and G5 motifs [84] (Figure 4).

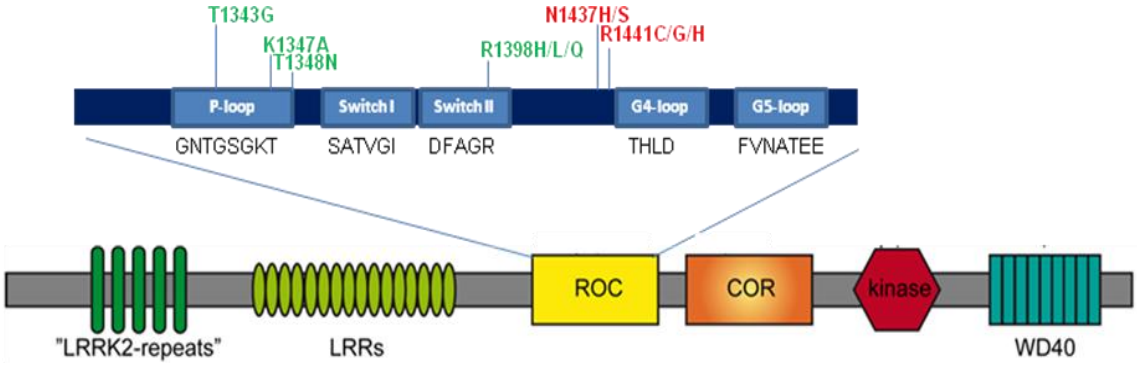

Figure 4: LRRK2 GTPase domain. Schematic representation of the ROC domain: P-loop, Switch I, Switch II, G4-loop and G5-loop domain. Synthetic mutations altering the GTPase activity are annotated in green, and pathogenic mutations clustering in the ROC domain are indicated in red. Adapted from [85].

G proteins, also known as guanine nucleotide-binding proteins, are commonly known as "molecular switches", since they share a mechanism in which the protein cycles between an on-state, when it is GTP bound and exhibits higher affinity for effectors, and an off-state, when GTP gets hydrolysed, leaving the protein bound to GDP and stopping the signal [86]. The exact mechanism by which the LRRK2 GTPase works is unclear, and two possible models have been suggested.

One scenario proposes that LRRK2 works as a GAD (G proteins activated by nucleotide-dependent dimerization). GADs have been characterized as having very low nucleotide affinity and fast nucleotide dissociation rate, consistent with LRRK2 GTPase and other ROCO protein data [87-89]. Moreover, the hydrolysis rate of the monomeric LRRK2 ROC domain is more than 700-fold slower than that of dimeric full-length LRRK2, with approximately 1.5 fold more nucleotide affinity of monomeric ROC, as compared to dimeric LRRK2 ROC–COR–kinase fragments, further supporting the GAD model [89, 90]. In addition, impaired GTP binding mutations such as K1347A and T1348N have been shown to exist as monomers [91, 92], perhaps indicating that LRRK2 is only active when forming dimers. *In*

vitro assays have suggested that LRRK2 predominately exists as a homodimer [93-95] although a recent study has proposed the opposite, so this should be taken with caution [96].

GAD proteins are known to undergo dimerization through the COR domain, and several studies have indicated that the LRRK2 COR domain plays an essential role in the dimerization process [85, 87, 97], although other domains such as the ROC domain or the WD40 have also been reported to regulate dimerization [98, 99]. Interestingly, some of the pathogenic mutations clustering at the GTPase domain (R1441 and Y1699) seem to be located at the interface between the ROC and the COR domain, potentially limiting/altering the interaction between the two domains and thus impairing GTPase activity, according to the GAD model.

Alternatively, LRRK2 could work as a typical small GTPase, undergoing the GTP/GDP switch by the requirement of accessory proteins namely GEFs (guanine nucleotide exchange factors) and GAPs (GTPase activating proteins). Consistent with this model, a putative GEF (Rho Guanine Nucleotide Exchange Factor 7(ArhGEF7)) [100] and two GAPs (regulator of G protein signaling 2 (RGS2) and ADP-ribosylation factor GTPase-activating protein 1 (ArfGAP1)) [101-103] for LRRK2 have been identified. ArhGEF7 has been shown to act as a GEF for LRRK2 in HEK293 cells. It successfully enhanced GTP binding of the R1441C mutant about 2 fold. ArhGEF7 was also found to be phosphorylated by LRRK2, and to enhance LRRK2 autophosphorylation [100]. Further, a recent study has shown trans-Golgi clustering which occurs via enhanced interaction between LRRK2 and ArhGEF7, and in turn modulates Rab7L1 localization to the trans-Golgi network (TGN). This interaction is inhibited by CK1α mediated phosphorylation of the N-terminus of LRRK2 [77]. Altogether, these data indicate complex and mutual regulation between LRRK2 and ArhGEF7.

Little is known about RGS2, apart from its potential role in regulating neuronal toxicity by inhibiting LRRK2 kinase activity, although independently of its GTPase activity, which might propose a new mode of action for GAPs [103]. The other described GAP for LRRK2, ArfGAP1, has been reported to enhance both wild type and mutant LRRK2 GTP hydrolysis, displaying a higher association for GTP-locked mutants such as R1441C, and a diminished

interaction with non-GTP bound mutants, such as R1398L or T1343N. Consistent with a role as a GAP for LRRK2, ArfGAP1 could rescue LRRK2 mutant toxicity both *in vitro* and *in vivo*, increasing cortical neuronal viability in mice, and reverting dopaminergic neuron loss in flies, respectively [104]. In contrast, another study showed that silencing of ArfGAP1 expression could rescue G2019S LRRK2-induced neurite shortening in primary rat cortical neurons, and the same occurred when silencing LRRK2 in an overexpressing ArfGAP1 system. The two independent studies both showed that ArfGAP1 can be directly phosphorylated by LRRK2, which activates ArfGAP1, and this has been shown to either enhance [102] or inhibit LRRK2 kinase activity [104]. Therefore, more work will be needed to entangle the exact mechanism for the ArfGAP1-mediated LRRK2 regulation and its cellular consequences.

Multiple studies have been performed to analyze the effects of LRRK2 pathogenic mutants on GTPase activity, as well as the impact of artificial mutations on those activities. Pathogenic mutations in the ROC-COR domain (R1441C/G/H and Y1699C) have been consistently shown to alter GTP binding/GTP hydrolysis [71, 89, 101, 102, 105-108]. Another ROC-COR mutant, N1437H, was described to increase GTP binding, but no change in guanosine triphosphosphate (GTP) hydrolysis was found [33]. Some of these alterations in GTP binding/GTP hydrolysis correlated with enhanced kinase activity, although overall results have been rather inconsistent [51, 88, 106, 107, 109]. Since pathogenic mutations in the ROC-COR domain have been repetitively shown to impair the proper functioning of the GTPase activity, GTP binding inhibition has been proposed as a therapeutic approach which could revert the ROC-COR mutation-induced effects. Importantly, a recent study has developed the first two identified GTP binding inhibitors for LRRK2 (compounds 68 and 70) which were shown to decrease GTP binding at nanomolar concentrations *in vitro* on both wild-type and PD-linked mutants, with a concomitant reduction of kinase activity. These two compounds attenuated neuronal degeneration in SH-SY5Y cells and mouse primary neurons, and one of the two which was tested *in vivo* (compound 68) successfully reduced both GTP binding and kinase activity [110]. Remarkably, another study has identified a new compound that, similarly to compound

68, was shown to inhibit GTP binding and rescue R1441C-induced mitochondrial and lysosomal transport impairments in neurites of SH-SY5Y cells.

Taken together, these data suggest that abnormal LRRK2 GTP binding may be involved in regulating transport of organelles in neurites, which may comprise an early event underlying neurodegeneration, such that LRRK2 GTP binding inhibitors may represent a novel strategy for PD treatment [111]. However, the mechanism(s) by which pathogenic LRRK2 mutants cause such organelle transport deficits in a manner dependent on altered GTP binding remains unknown. In addition, further work is needed to clarify the mode of action of the LRRK2 GTPase domain and to further understand how and whether the two enzymatic domains regulate each other, which may provide important insight into the pathogenic effects of the various distinct LRRK2 mutations.

b. LRRK2 interactors

LRRK2 has been described to interact with a large number of proteins. In fact, a recent study has suggested that LRRK2 could behave as a "hub", with more than 250 interactors identified to date, amongst which 62 have been confirmed under more controlled conditions [112]. Hence, LRRK2 may be linked to many different functions within the cell (see also next section).

Here, we focus on its interaction with cytoskeletal proteins, which has been largely confirmed in the literature. In 2006, Gloeckner and co-workers showed for the first time colocalization of overexpressed wildtype LRRK2 with β-tubulin [45]. Another study further found that LRRK2 could directly phosphorylate β-tubulin in mouse brain samples, being enhanced by the G2019S mutant [63]. Moreover, Gandhi et al. revealed an interaction with both α and β-tubulin heterodimers, which was shown to only require the ROC domain, thus hypothesising that tubulin could act as an effector for the LRRK2 GTPase activity. However, pulldown experiments with preloaded GTP/GDP indicated that the interaction was independent on the guanine nucleotide state of LRRK2 [113]. Interestingly, Caesar et al showed enhanced

GTPase activity when incubating LRRK2 with tubulin [114], and another work reported differences in β-tubulin interactions with PD mutants at R1441 site and phosphomimetic mutants at the ROC domain [115]. Further, inhibiting kinase activity by a specific kinase inhibitor enhanced LRRK2 interaction with tubulin as assessed by Förster Resonance Energy Transfer (FRET) [114].

Dauer's lab showed enhanced colocalization with α-tubulin of all pathogenic mutants in the ROC-COR domain, as well as with the I2020T mutation, and Godena and coworkers corroborated R1441C and Y1699C mutants colocalizing more with microtubules (MTs) in a recent study [83]. Taken together, LRRK2 interaction with MTs has been largely validated and PD mutants impairing GTP hydrolysis/GTP binding and/or modulating the LRRK2 kinase activity by kinase inhibitors seems to alter this association. However, the exact mechanism by which LRRK2 interacts with tubulin, and how pathogenic mutants could modulate that interaction remains to be elucidated.

In addition to tubulin, MT-associated proteins (MAPs) have been shown to interact with LRRK2 as well. One of the most consistently reported interactions is the one occurring with tau. Kawamaki et al. showed tau to be directly phosphorylated by LRRK2, with G2019S and I2020T mutants showing enhanced phosphorylation. Interestingly, this only occurred when tau was bound to tubulin, and resulted in microtubule destabilization [116]. In addition, they found LRRK2 to enhance tau phosphorylation by interacting with glycogen synthase kinase-3β (GSK-3β), thus giving LRRK2 a dual role in regulating tau phosphorylation [117]. Interestingly, tau neuropathology, including hyperphosphorylation and mislocalization of tau into big aggregates, has also been reported in some human *postmortem* PD brains carrying pathogenic LRRK2 mutations [30, 118-120] as well as in transgenic mice expressing pathogenic LRRK2 [121, 122]. In addition, a recent study showed enhanced hyperphosphorylated and insoluble tau in a tau mouse model when overexpressing LRRK2, which further supports a LRRK2-mediated regulation of tau [62]. Another MAP, Microtubule-Associated Protein 1B (MAP1B), has also been reported to interact with LRRK2 and to rescue LRRK2-mediated toxicity when

coexpressed with pathogenic LRRK2 mutants, possibly by inhibiting LRRK2 kinase activity [123]. Lastly, there is growing evidence for LRRK2 interacting with other components of the cytoskeletal system. For instance, neurite outgrowth alterations have been reported due to LRRK2 modulation of Ras-related C3 botulinum toxin substrate 1(Rac1) (a main player in actin cytoskeleton remodelling) [123], ArfGEF7 [124], ArfGAP1 [102] RGS2 [103], and more recently, through the LRRK2-mediated P21 (RAC1) Activated Kinase 6 (PAK6) regulation [125]. An additional mechanism via phosphorylating Rab8 can also be envisioned, since the former has also been shown to play a role in neurite outgrowth through regulating actin/MT reorganization [126]. Collectively, the widely reported interactions with various cytoskeletal proteins suggest a potential role for LRRK2 in modulating cytoskeletal processes, especially those related to MTs.

3. Microtubules

Microtubules (MTs) are polymers composed of a basic structure of two tubulin subunits (one α and one β) which constitutively interact to form a heterodimer. These heterodimers assemble in a polarized manner to form protofilaments, which can bind to each other by side-to-side contacts, leading to MT formation [127].

MT assembly is a process that requires the incorporation of new tubulin heterodimers having GTP bound at the β-tubulin binding site, namely "the E-site". Within the dimer, at the interface between the two subunits, there is another GTP binding site, "the N-site", which does not get hydrolysed, hence maintaining the integrity of the tubulin dimer. Conversely, GTP at the E-site of the heterodimer will switch to GDP when a new dimer will get incorporated into the + end of the MT. This process occurs in a polarized manner, thus the α-tubulin of the new heterodimer will face the β-tubulin of the one already integrated, creating a pattern of GDP dimers towards the MT - end, and GTP towards the + end, with the latter forming the GTP cap.

Importantly, there is a certain point in which MTs instead of growing start rapidly shrinking, in a process that has been termed as "catastrophe". It may also occur that the

shrinking phase stops, thus MTs would be "in pause", which can be followed by a subsequent growing phase, so then they would be "rescued" [128]. The continuous cycle between these stochastic events constitutes the "dynamic instability" typically associated with MTs [129]. According to the time passed between assembly and disassembly, MTs can be classified as stable or dynamic, with an observed *in vitro* half-life of 1-2 h or 2-5 min, respectively [130, 131] (Figure 5).

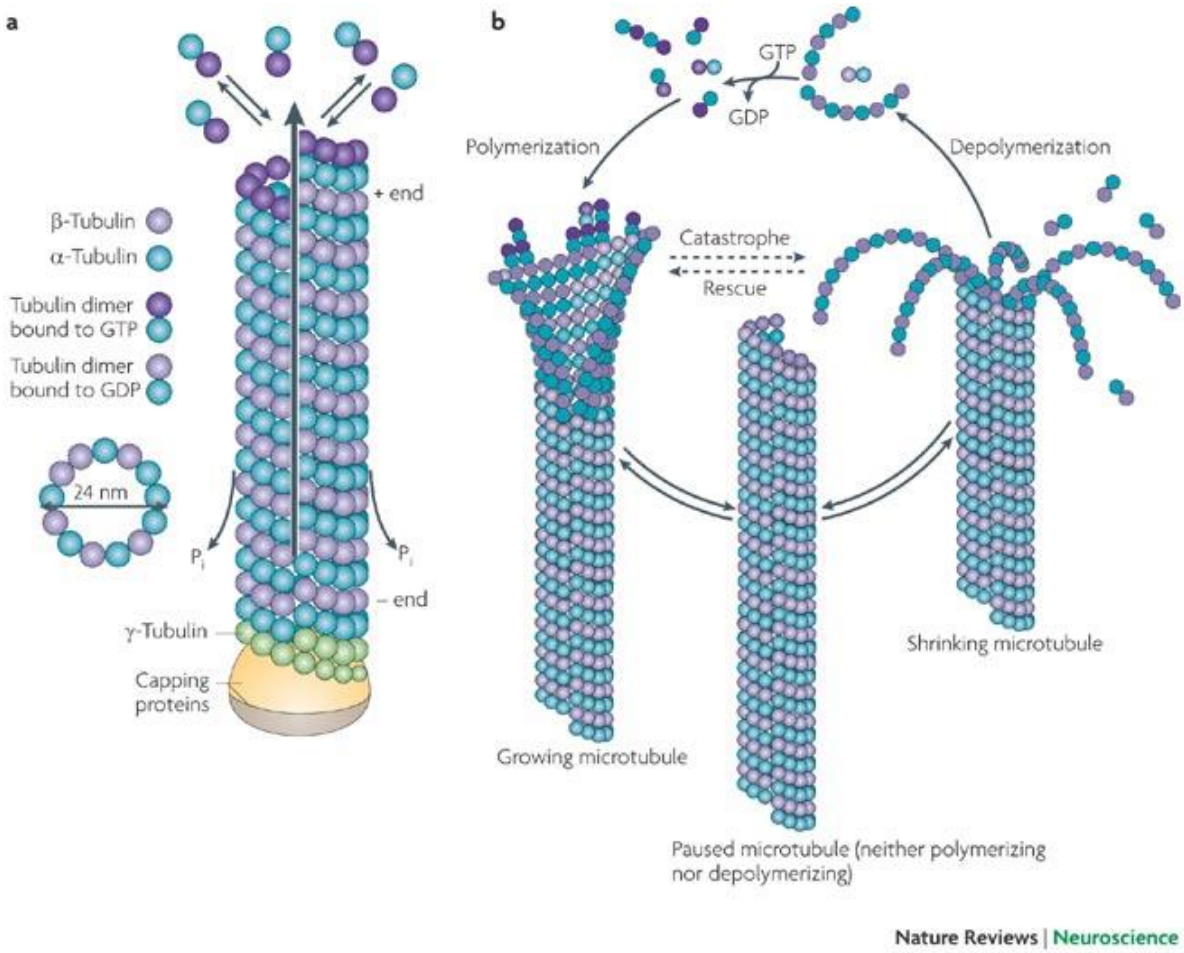

Figure 5: MT assembly. Schematic representation of the MT assembly process. αβ-tubulin dimers get assembled in a polarized manner forming a protofilament, with a γ-tubulin cap at the - end. GTP mediates the incorporation of new αβ-tubulin dimers to the + end, thus establishing a gradient of GDP-bound tubulin dimers towards the - end and GTP-bound tubulin dimers towards the + end. MTs cycle between the growing and the shrinking processes, sometimes stopping at a paused intermediate phase. This whole process is known as MT instability. Adapted from [132].

The core structure of MTs is very well conserved, being composed of globular bodies of α/β heterodimers that are involved in MT assembly. In contrast, the C-terminal tails of tubulin which project out of the shaft are not responsible for the proper formation of the MT lattice and can be extremely variable. Indeed, the tubulin heterogeneity known as "the tubulin code" [131] is mainly rendered by modifications at the C-terminal tubulin tails, which arise principally from two sources: i) tubulin isotypes, and ii) post-translational tubulin modifications (PTMs).

a. tubulin isotypes

Mammalian tubulin genes are composed of 9α and 9β tubulin isotypes, the latter being more divergent in their C-tails [133]. Tubulin isotypes are combined so as to generate distinct MTs that can in turn determine specific binding of MT-associated proteins, and/or be subjected to PTMs (see below), which may then lead to diverse MT functions. Indeed, mutations in mechanosensory (MEC) α-tubulin and β-tubulin have been shown to cause unbundling of MTs and enhanced affinity of the motor protein dynein with mistrafficking effects in cargo(es), and defects in neurite outgrowth and mislocalization of synaptic vesicles, respectively [134]. In addition, a neuron-specific β-tubulin isotype, TUBB3, has been shown to decrease MT stability *in vitro*. This may be important for maintaining a "sufficiently dynamic" MT network in neurons, as a greater percentage of MTs are stable in those cells as compared to other cells, thereby allowing for the occurrence of dynamic processes such as growth cone guidance or neural progenitor mitosis [135].

b. post-translational modifications (PTMs)

MTs are known to be modified by multiple PTMs. As mentioned before, the C-tails of the heterodimers are located on the outer surface of MT filaments, thus being more accessible for the enzymes that catalyze PTMs such as α-detyrosination [136, 137] and related Δ2-tubulin [138] and Δ3-tubulin modifications [139], α/β-(poly)glutamylation [140, 141], α/β-

(poly)glycylation [142] and α-palmitoylation [143]. However, there are some identified PTMs that also occur inside the MT lumen, such as α-tubulin acetylation [144], α/β-tubulin polyamination [145], β-phosphorylation [146-149] and as recently described, β-tubulin acetylation [150]. Tubulin can also be ubiquitinated [151], arginylated [152], glycosylated [153], methylated [154], S-nitrosylated [155] and sumoylated [156], although little is known about these PTMs to date (Figure 6).

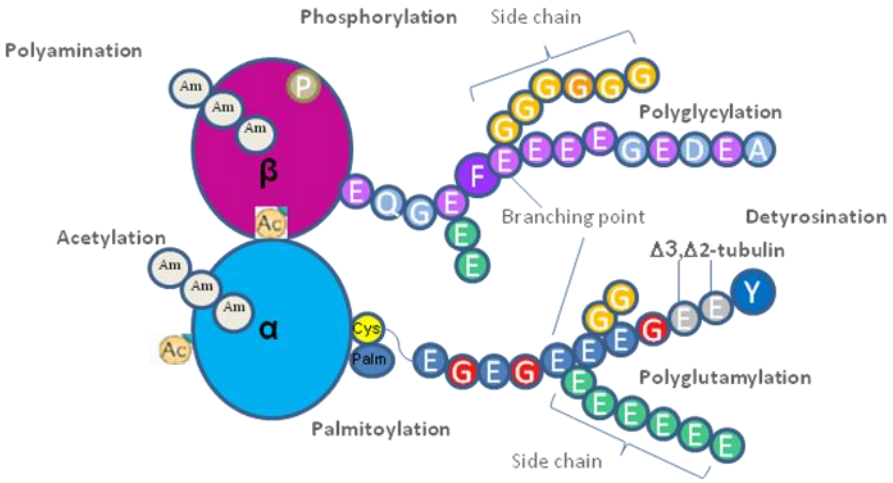

Figure 6: Tubulin PTMs

Schematic representation of tubulin PTMs. C-terminal tails can undergo polyglycylation and/or polyglutamlyation, in both α and β-tubulin, whilst palmitoylation (Pam) and detyrosination (Δ2, Δ3 -tubulin) have only been reported to occur at the α-tubulin monomer. On the luminal side, acetylation (Ac) can tag α-tubulin as well as β-tubulin. Phosphorylation (P) and polyamination (Am) have also been shown to modify the luminal face of the α/β-tubulin monomers. Adapted from [157, 158].

Several of the enzymes that catalyze these processes have been identified. Probably the best characterized mechanism so far is α-tubulin acetylation, which consists of the incorporation of an acetyl group at the K-40 residue of α-tubulin, which is quite conserved among all isotypes with the exception of the human TUBA8, which has been shown not to undergo acetylation [159]. Tubulin acetylation is catalyzed in a very specific manner by α-tubulin acetyltranferase-1 (α-TAT-1) and mechanosensory abnormality protein 17 (Mec-17) [160]. Conversely, two other

enzymes have been identified to mediate the reverse process (deacetylation), namely histone deacetylase family member 6 (HDAC6) [161] and sirtuin type-2 (SIRT-2), although the latter one plays a minor role [162]. Extra targets such as histones have been found for both of them, which should be taken into account when performing knockout experiments.

Since α-tubulin acetylation has been shown to preferentially accumulate on stable MTs, an acetylation-mediated stabilizing mechanism has been proposed. However, no current causal evidence in that respect has been found, and a potential explanation suggests that based on the "longevity" of stable MTs and the very low-rate activity of α-TAT-1, this could in turn make this type of MT more prone to be acetylated [163]. Furthermore, and in contrast to the initially suggested stabilizing mechanism, a recent study has reported the opposite effect, with α-TAT-1 overexpression increasing susceptibility of MTs to be disrupted by nocodazole, with the reverse observed upon knockout experiments of α-TAT-1. Strikingly, this was equally shown when overexpressing the catalytically inactive form of the enzyme, thus suggesting that MT destabilization may be induced irrespective of the acetylation activity of α-TAT-1 [164]. Acetylated MTs have been reported to display preferential binding by certain motor proteins such as kinesin like protein 5 (KIF5); thus, acetylation may play a role in modulating cargo trafficking [165]. Finally, additional work on this PTM by Chu and colleagues has revealed for the first time that β-tubulin can also be acetylated at its K-252 residue, which was shown to be catalyzed by the acetyltransferase San [150]. Taken together, whilst there seems to be an apparent link with acetylation preferentially decorating stable MTs, the precise mechanism(s), and the effects of acetylation on MT stability remain to be clarified.

The identity of the enzyme that catalyzes the removal of the last tyrosine residue of the α-tubulin C-tail is lacking, whereas its counterpart enzyme has been already identified, namely tyrosine tubulin ligase (TTL) [166-168]. Interestingly, whereas detyrosination seems to occur when tubulin is already incorporated into MTs, and thus specifically targeting "longer-lived" MTs, TTL-mediated retyrosination only takes place within tubulin dimers [167, 168], hence linking tyrosinated tubulin to unpolymerized and/or "short-lived" MTs. Importantly, the existing

association of detyrosinated tubulin to long-lasting MTs has led to the assumption that detyrosinated tubulin *per se* may directly enhance MT stability [169-171]. However, an inhibitory binding for identified MAPs, namely depolymerizing enzymes such as Kinesin Family-2 (KIF-2) or mitotic Centromere-Associated Kinesin (MCAK) [172, 173] exhibited by detyrosinated over tyrosinated tubulin, or the enhanced affinity for certain severing proteins such as spastin, shown by detyrosinated MTs [174] leads to the possibility that detyrosination may regulate MT stability by differentially recruiting enzymes, which could modulate the MT polymerization process. Similarly, plus end-tracking proteins with Cytoskeleton-Associated Protein Glycine-rich (CAP-Gly), such as Cytoplasmic Linker Protein 70 (CLIP170) or p150/glued also bind differentially to tubulin, showing a preference for tyrosinated over detyrosinated MTs, which has been linked to MTs stability in recent work [175-177]. Therefore, in view of those controversial data, more work will be needed in order to understand the actual mechanism(s) by which detyrosinated/tyrosinated modifications may regulate MT stability.

Akin to acetylated tubulin, some motor proteins also show increased association to detyrosinated tubulin such as KIF-5, thereby, establishing a guidance for cargo(es) associated with this motor to traffic along detyrosinated MTs [178-180]. Thus,apart from possible effects of the tyrosination/detyrosination cycle on MT stability, these PTMs may act as modulators for intracellular transport events by showing a preferential association with specific motor proteins.

Additional C-terminal glutamate(s) can be further removed, leading to Δ2,3-tubulin, when missing two or three amino acids, respectively. The enzymes responsible for catalyzing these reactions are members of the cytosolic carboxypeptidase family (CCPs), and although no specific consequences have been linked to these two PTMs thus far, Δ2,3-tubulin have been shown to unlock tubulin in a detyrosinated state in an irreversible manner [181].

CCPs are also known to act as deglutamylases, thus cleaving the glutamate residues that are incorporated by Tubulin Tyrosine Ligase-Like (TTLL) proteins, involved in tubulin (poly)glutamylation. In addition, TTLLs can catalyze (poly)glycylation [182, 183] with the deglycylases remaining to be identified [184, 185]. Polyglutamylation is known to induce

higher binding affinity for severing enzymes such as spastin or katanin [186, 187], thus modulating the turnover of MTs. Similarly to other PTMs, certain motors and MAPs display enhanced association with polygutamylated tubulin such as kinesin 2 (KIF-1A), KIF-5, dynein, MAP-2 or MAP1B [188].

Tubulin has been found to undergo palmitoylation, with a preference for the α subunit rather than β, and a suggested role for anchoring tubulin to membranes [189]. β-tubulin has been shown to be phosphorylated by identified kinases, such as Cyclin-dependent kinase 1 (Cdk1) spleen tyrosine kinase (Syk) or LRRK2, with a potential function in regulating MT dynamics during cell division [63, 149, 190]. Polyamination is an irreversible PTM that affects both α and β subunits and has been shown to map near the polymerization sites of MTs, thus conferring MT stability [145]. In conclusion, the huge variability that emerges from distinct PTMs, causing differential protein associations with motor proteins, polymerases/depolymerases or MAPs may impact on both MT stability and vesicular trafficking events [191, 192].

b. Links between MT stability and neurodegeneration

A right balance between dynamic and stable MTs is needed to ensure the proper functioning of the cell. In fact, MT (de)stabilization-related defects have been linked to numerous diseases. For instance, Alzheimer's Disease (AD) is characterized by neurofibrillary tangles (NFTs) mainly composed by modified tau, thus making AD one of the most known tauopathies [193, 194]. Tau modifications, usually hyperphosphorylation, but also its acetylation, result in MT depolymerization, mostly due to the lack of the stabilizing effect induced by MT-bound tau [195, 196]. Similarly, loss of function mutations in Parkin, an E3 ubiquitin ligase linked to PD, are known to prevent Parkin binding to the tubulin heterodimer, thus leading to MTs destabilization, and eventual neurodegeneration [197]. Therefore, MT-stabilizing drugs were proposed to ameliorate various neurodegenerative diseases by reversing the detrimental effects of MT depolymerization. Indeed, the stabilizing drug taxol has been shown to increase axonal diameter and to enlarge growth cones [198-200]. Conversely,

hyperstability may also display negative effects such as axonal swelling or impaired axonal trafficking, as reported when using stabilizing agents or when analyzing the effects of mutations in spastin, linked to hereditary spastic paraplegia (HSP), which may increase the pool of detyrosinated tubulin due to the inability of mutant spastin to process these types of MTs [201-204]. Altogether, the use of MT-regulating agents should be taken with caution, as a fine-tuning of MT dynamics seems to be required, with detrimental effects caused by the presence of either "hyperdynamic" or hyperstable MTs.

c. MTs and vesicular trafficking events

MTs are involved in many key cellular processes such as cell division and differentiation, cytoplasmic organization and polarity, cell shape and motility, vesicular trafficking or as structural components of cilia and flagella [205]. Here, we focus on vesicular trafficking, which is a crucial event in neurons, since MTs act as "roads" for the long-range transport along axons, being essential due to the special neuronal architecture. Indeed, vesicular trafficking deficits associated with impairments in axonal transport represent one of the first pathological signs of most neurodegenerative diseases [206].

Axonal transport can be grouped into either slow (≈0.2–10 mm/day) or fast (≈50–200 mm/day), and the latter can be also classified in terms of its directionality, with two motor proteins, namely kinesin and dynein, regulating the anterograde (away from the soma) and bidirectional transport, and retrograde (back to the soma) trafficking, respectively. The binding of these motor proteins through their tail domain-binding motifs constitutes a very specific process regulated by their differential affinity to distinct types of MTs (see examples in PTMs section). Consequently, cargo transport is a finely modulated process, with slow transport of tubulin and cytosolic proteins, fast transport of synaptic vesicles and organelles in an anterograde fashion, and recycling vesicles, autophagosomes and injury signals in a retrograde fashion, respectively [134, 206].

As previously mentioned, the composition of MTs may play a role in regulating intracellular transport events. Distinct pools of dynamic or stable MTs tagged with specific PTMs or being associated to identified MAPs can modulate the preferential binding of a specific motor protein, and thereby determine cargo destination. Thus, deregulation of MT dynamics and/or PTMs could result in transport-mediated defects such as cargo(es) mislocalization or misfunction.

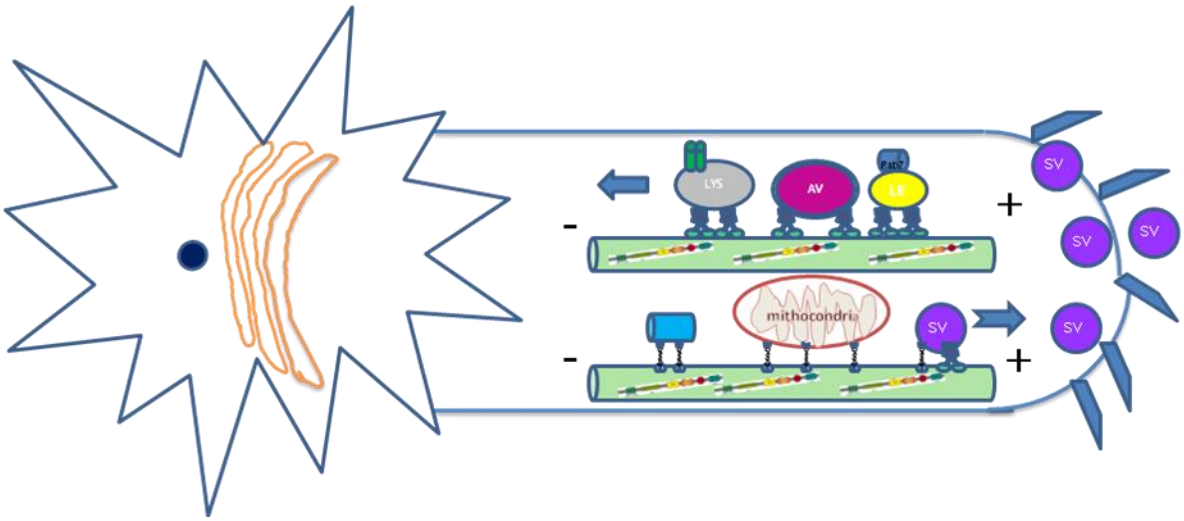

Figure 7: MT-mediated axonal transport. Schematic representation of MT-mediated transport in a neuronal cell. Kinesins ( ) mediate the anterograde transport (from the soma to the dendrites) and dyneins ( ) are responsible for the retrograde transport (from the dendrites to the soma). Fast transport of organelles and synaptic vesicles occurs anterogradely, whereas recycling vesicles, injury signals and used synaptic vesicles are carried backwards. Tubulin and cytosolic proteins are transported anterogradely with a slow movement pattern. Adapted from [127, 207].

Another determinant for the proper functioning of MT-related transport is constituted by the Rab protein family. In their active state, Rabs are known to show preferential association with specific motor proteins by forming complexes with their effectors proteins, which may in turn determine cargo distribution. For instance, Rab5 on early endosomes binds to kinesin like protein 6 (KIF16b) through the Rab5 effector protein phosphatidylinositol-3-OH kinase Vps34

[208], and Rab7 on late endosomes and lysosomes has been shown to bind to the dynein/dynactin motor protein complex via the Rab7-interacting lysosomal protein (RILP), an effector protein for active Rab7 [209, 210]. In this manner, via determining cargo-motor protein association, Rab proteins provide another mechanism for vesicular cargo distribution, thus altering Rab activity may have profound impacts on various intracellular transport events. In agreement with the importance of proper vesicular transport processes for neuronal functioning, deficits thereof comprise the first pathological signs of most neurodegenerative diseases such as Huntington´s disease, amyotrophic lateral sclerosis, Charcot Marie Tooth disease, AD and PD [206, 211].

4. LRRK2 function

LRRK2 has been proposed to be involved in a wide variety of processes within the cell, which are mainly classified into three big groups: **a.** endomembrane trafficking, **b.** signalling pathways and **c.** cytoskeletal dynamics.

a. endomembrane trafficking

Numerous studies have extensively reported an involvement for LRRK2 in endomembrane trafficking by acting at various different steps. For instance, LRRK2 has largely been shown to regulate macroautophagy, a process leading to the degradation of protein aggregates and defunct organelles. The exact mechanism(s) remain currently elusive, with conflicting results suggesting both enhanced or reduced autophagy levels. At first, pathogenic LRRK2 was shown to impair autophagic flux via a pathway involving endolysosomal calcium channels [212]. Additional mechanisms for modulating autophagy were also described, with an mTOR-dependent reduced autophagic response [213], or stimulated autophagic flux induced by Mitogen-activated protein kinase kinase/extracellular signal–regulated kinases (MEK) pathway activation [214]. Importantly, similar results from different studies have been obtained when either inhibiting or enhancing kinase activity [213, 215], which in principle may seem

contradictory. Thus, although it is clear that LRRK2 is a key player in autophagy, important caveats should be considered such as the use of various cell types, endogenous versus overexpressed LRRK2 levels and experiments performed under different *stimuli*, which may stand in the way when trying to elucidate the actual role for LRRK2 in this process.

Further evidence for the involvement of LRRK2 in endomembrane trafficking is the reported link with various Rab proteins. Hence, LRRK2 has been shown to impair synaptic vesicle endocytosis, possibly by phosphorylating Rab5b, a marker for early endosomes, thereby causing its inactivation [216, 217]. Rab7, present on late endosomes and lysosomes, has also been reported to interact with *lrrk*, the LRRK2 Drosophila ortholog, [218], and pathogenic LRRK2 has been recently shown to decrease the amount of active, GTP-bound Rab7, which may underlie various deficits in endolysosomal and autophagic trafficking [219]. In agreement with a role in regulating endolysosomal trafficking, LRRK2 has also been reported to colocalize with multivesicular bodies, which increased upon overexpression of the R1441C mutant [79]. In addition, as mentioned above, a set of Rabs have been recently found to be directly phosphorylated by LRRK2. One of those is Rab12 [54], which likewise to Rab7 is known to mediate autophagosome-lysosome fusion, again suggesting a role for LRRK2 at this step of the pathway. Lastly, LRRK2 has also been reported to impair lysosomal function by alkalinizing their content [212]. Since lysosomes are a point of convergence between autophagy and endocytosis, impairment at this level could impact on both processes, leading to detrimental effects in both pathways.

Apart from Rab12, LRRK2 has also been shown to phosphorylate Rab8 and Rab10 [54], which are known to control polarized vesicle trafficking out of the TGN and to the membrane [220], although no work on this respect has been reported so far. Another interaction at the TGN is the one occurring with Rab7L1, also known as Rab29, which nominates LRRK2 as a possible regulator of the TGN-retromer pathway, with reported alterations in TGN structure upon overexpression of the LRRK2-Rab7L1 complex [221]. In addition, a recently found interaction with the risk factor gene for PD, VPS35, was shown to rescue mutant LRRK2

toxicity in both cells and flies [222]. Likewise, association with other proteins such as Sec16a at the endoplasmic reticulum (ER) [223], or Endophilin A, which has also been shown to be phosphorylated by LRRK2 [224], at the early endosomes, further supports a role for LRRK2 in various endomembrane trafficking steps. Finally, the reported interaction between LRRK2 and MT/MT-related proteins could also be involved in modulating vesicular trafficking steps at many levels.

b. signalling pathways

LRRK2 has been suggested to act as a player in different signalling pathways. First, a role in the mitogen-activated protein kinase (MAPK) cascade has been shown, with *in vitro* phosphorylation of MAP2K, 3, 4, 6 and 7 [225], potentially leading to downstream effects on cell proliferation, apoptosis and a recently described role in neuroinflammation, which has been proposed to contribute to dopaminergic neuron degeneration [226-228]. LRRK2 has further been reported to interact with the main components of the Wingless signalling pathway (Wnt), such as dishevelled proteins 1-3 (DVL1-3), low-density lipoprotein receptor-related protein 6 (LRP6) and β-catenin. Interestingly, upon Wnt ligand stimulation, most pathogenic mutants and two risk factors were shown to decrease the Wnt signalling activity by enhancing repression of β-catenin, while the protective variant, R1398H, seemed to have the opposite effect [229, 230]. Wnt signalling is known to regulate more than 400 genes, amongst which are the ones involved in controlling synaptic function in mature neurons, which could in turn be impaired by pathogenic mutants [231, 232].

An additional role for LRRK2 has been described as a component of the Death Signalling Cascades. Indeed, it has been shown to interact with both TNFR1-associated death domain protein (TRADD) and Fas associated death domain protein (FADD), with the latter exhibiting a higher association with pathogenic LRRK2 [233]. Strikingly, inhibition of the death cascade via either overexpression of dominant-negative FADD or downregulation of caspase-8 was found to prevent cell death in cultured primary cortical neurons transiently overexpressing

LRRK2 PD mutants, thus supporting a role for LRRK2 in the extrinsic cell death pathway [233].

Likewise, LRRK2 has been suggested to be involved in the intrinsic cell death pathway, with reported phosphorylation of both p53[234] and Bcl-2 [235], which could result in either altered mitochondrial function and/or lead to activation of downstream caspases, which ultimately will cause cell death. Collectively, LRRK2 seems to impact upon various signalling pathways, highlighting the importance of a fine regulation of the protein, which when altered, could cause dysfunction of many different cellular processes.

c. cytoskeletal dynamics

Cytoskeletal defects linked to LRRK2-induced pathogenesis have been widely reported. In fact, two of the most recurring pathological aspects described in the literature are axonal transport impairment and deficits in neurite outgrowth, indicating that LRRK2 could be playing a role in cytoskeletal dynamics. While the exact mechanism(s) remain to be elucidated, a lot of effort has been put in order to gain insight into it, even though largely confusing and contradictory data have emerged.

For instance, Cartelli and colleagues analyzed fibroblasts from both sporadic PD patients and from G2019S-mutant LRRK2 PD patients and reported increased levels of unpolymerized tubulin associated with morphological changes when compared to fibroblasts from healthy control patients. Interestingly, both phenotypes were rescued by either treating cells with MT stabilizing drugs like taxol or when overexpressing wildtype LRRK2. Conversely, the deficits were further enhanced when using MT depolymerizing agents such as nocodazole or colchicine. Altogether, these data suggest a role for pathogenic LRRK2 in modulating MT dynamics by inducing MT destabilization. Contradictorily though, they also reported increased acetylated tubulin and enhanced detyrosinated tubulin levels in sporadic and G2019S-LRRK2 PD fibroblasts as compared to control, respectively, which would suggest that pathogenic LRRK2 increases MT stability [197].

Another study reported increased unpolymerized tubulin levels and decreased acetylated tubulin when pharmacologically inhibiting LRRK2 kinase activity in control fibroblasts, although no effect was reported in sporadic PD cells [236]. In apparent contrast, LRRK2 KO mice fibroblasts exhibited high levels of acetylated tubulin, which were reverted when overexpressing wild-type LRRK2 [115]. Thus, further studies in the various cellular systems are required to conclusively determine how wildtype LRRK2, pathogenic LRRK2 mutants or pharmacological LRRK2 kinase inhibitors modulate MT dynamics.

As a potential mechanism for the LRRK2-mediated modulation of MT dynamics, it has been suggested that LRRK2, through its interaction with β-tubulin, could prevent α-TAT1 to access to the K-40 site in α-tubulin, thus keeping α-tubulin in a non-acetylated state. Importantly, pathogenic mutants were shown to alter that interaction, and thus to possibly modify the acetylated tubulin status. However, whereas R1441G and R1441H mutants decreased this interaction, another point mutant at the same site, R1441C, was shown to strengthen it, which may mean that distinct pathogenic mutants can behave differently in controlling MT stability [115].

Godena and others reported that pathogenic R1441C and Y1699C colocalize with "deacetylated" tubulin, which they described as "patches" on acetylated tubulin tracks not stained by an anti-acetylated tubulin antibody. They further described locomotor deficits in flies and alterations in mitochondrial axonal transport, when either of those mutants were overexpressed in motor neurons from *Drosophila* or in cortical neurons from transgenic rats. These effects were reported to be rescued by increasing acetylated tubulin levels either by overexpressing α-TAT1 or by adding the deacetylase inhibitor trichostatin (TSA), again suggesting that pathogenic LRRK2 decreases the levels of stable MTs.

Caesar et al. reported decreased migration of R1441G mouse fibroblasts, but no effect for human G2019S PD patient fibroblasts as compared to controls. The former could be reverted by kinase inhibitors, perhaps indicating that LRRK2 could regulate cytoskeletal dynamics in a kinase activity-dependent manner [114]. However, Choi et al. found retarded or accelerated

microglia motility when using microglia cultured from brains of either *G2019S-LRRK2* or knock-out transgenic mice, respectively [237]. Additionally, another study showed increased myeloid cell chemotaxis of cells derived from G2019S transgenic mice as compared to controls, which correlated with an enhanced and kinase activity-dependent interaction with actin-regulatory proteins [238]. Taken together, whilst there seems ample evidence that LRRK2 modulates cytoskeletal dynamics, the exact mechanism(s) by which it does so, possibly in a cell type-specific manner, remain(s) to be determined. **Figure 8: LRRK2 interactors and**

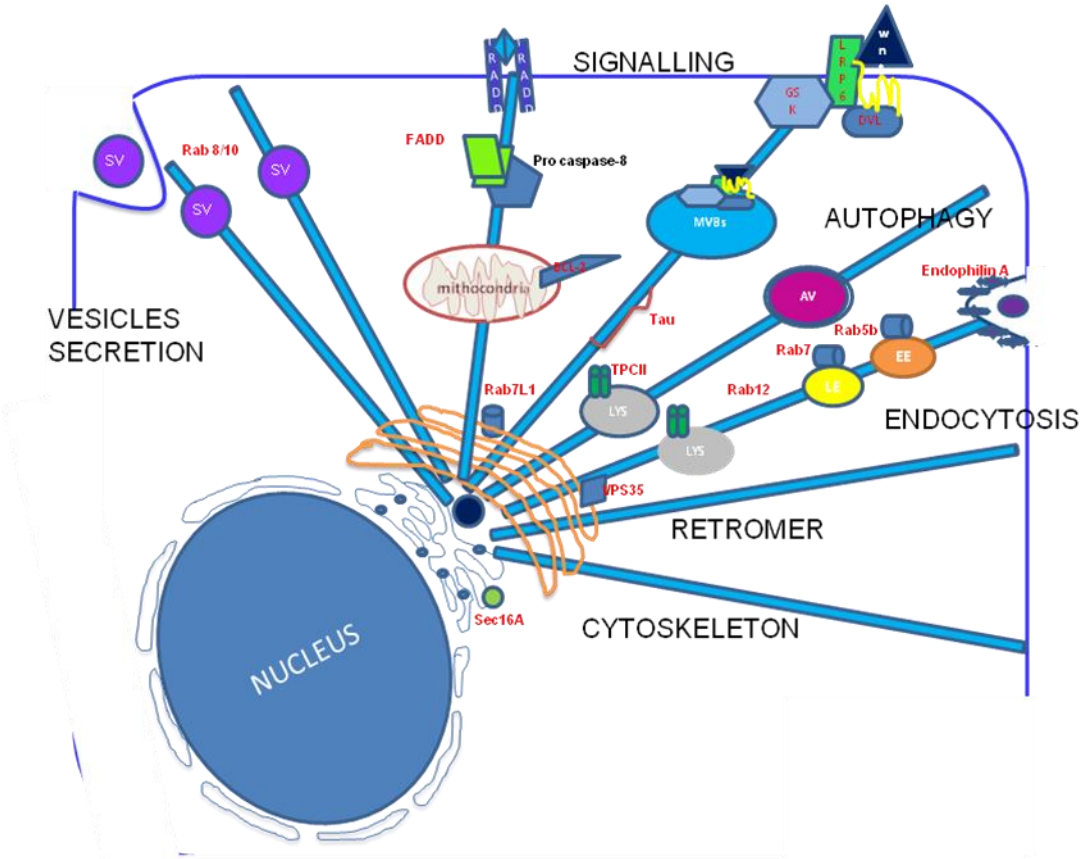

functions. LRRK2 has been shown to interact with numerous proteins involved in a variety of cellular processes, thus linking LRRK2 to several key cellular processes: endomembrane trafficking at distinct steps (autophagy, endocytosis, retromer-mediated trafficking and vesicle secretion); signalling cascades such as Wnt signalling or Death pathways, and cytoskeleton-related processes. Adapted from [239].

IV. Objectives

1. Analyze the subcellular localization of wildtype, pathogenic mutant LRRK2, and of pharmacologically kinase-inhibited LRRK2, with respect to colocalization with microtubules

2. Analyze the preferential association of pathogenic or pharmacologically kinase-inhibited LRRK2 with respect to dynamic versus stable microtubules

3. Determine the effect of kinase activity, as assessed by autophosphorylation, on the subcellular localization of LRRK2

4. Determine the effect of synthetic kinase-dead LRRK2 mutants on the subcellular localization of LRRK2

5. Determine the effect of N-terminal phosphorylation of LRRK2 on subcellular localization

6. Analyze the effect of proposed modulators of LRRK2 GTP binding/GTP hydrolysis on the subcellular localization of LRRK2

7. Determine the effect of synthetic LRRK2 mutants predicted to affect GTP binding/GTP hydrolysis on subcellular localization

8. Analyze the effect of a protective LRRK2 risk variant on the subcellular localization of wildtype and pathogenic LRRK2

9. Determine the effects of all LRRK2 mutants and of pharmacologically kinase-inhibited LRRK2 on GTP binding

10. Determine the effect of all mutants on LRRK2 kinase activity *in vitro*

11. Determine the effect of LRRK2 GTP binding inhibitors on the subcellular localization of pathogenic or pharmacologically kinase-inhibited LRRK2

12. Determine the effect of GTP analogs on the subcellular localization of LRRK2 in permeabilized cells

V. Materials and Methods

Reagents

Trichostatin A, tubacin and nocodazole were from Sigma Aldrich, parthenolide from Eurodiagnostico, LRRK2-IN1, TAE684 and CZC25146 from the Michael J. Fox Foundation, GSK2578215A from Tocris, compound 68 (ID 9108605) and compound 70 (ID 9119202) from Chembridge Corporation (San Diego, USA), and GNE-0877 and GNE-7915 from MedchemExpress (USA), and MLi2 from MRC PPU, Dundee, UK. Natural streptolysin-O was from Abcam (ab63978), non-hydrolyzable GTP test kit from Jena Bioscience (NK-102), and caspase inhibitor Z-VAD-FMK was from Sigma.

DNA constructs and site-directed mutagenesis

GFP-tagged human wildtype, R1441C, Y1699C, G2019S and K1347A LRRK2 constructs were obtained from Addgene. All other constructs were generated by site-directed mutagenesis (QuickChange, Stratagene), and the identity of constructs verified by sequencing of the entire coding region. For transfection purposes, DNA was prepared from bacterial cultures grown at 37 ºC using a midiprep kit (Promega) according to manufacturer´s instructions. GFP-tagged human α-tubulin K40 acetyltransferase (αTAT1) and an enzymatically inactive point mutant (D157N) were from Addgene. Both wildtype and mutant αTAT1 were PCR amplified and subcloned into pDsRED-Express vector using the BaMHI and EcoRI sites to generate C-terminally tagged dsRED-constructs. myc-TRADD, caspase8-DED-EGFP, RICK-EGFP, RIP-(DD)-EYFP and E10-EGFP were kindly provided by H. Wajant (University of Wuerzburg, Germany). GFP-FADD, GFP-caspase8 were kindly provided by R. Siegel (NIH, USA). GFP-tagged human FADD was PCR amplified and subcloned into pCMV-myc-N vector using the XhoI and EcoRI sites to generate N-terminally tagged myc-constructs. GFP-tagged human caspase8 was PCR amplified, previously mutating an EcoRI site, and was then subcloned into pCMV-myc-N vector using the XhoI and EcoRI sites to generate N-terminally myc-tagged

caspase 8. The point mutant caspase-360S construct was generated by site-directed mutagenesis, and identity of the construct verified by sequencing of the entire coding region.

Human flag-tagged ARHGEF7 and the GEF-dead variant (L386R/L387S) were generous gifts from Drs. K. Haebig and M. Bonin (University of Tuebingen, Germany), human V5-tagged ArfGAP1 was a generous gift from Dr. T. Dawson (Johns Hopkins University, Baltimore, USA), human HA-tagged RGS2 was a generous gift from Dr. B. Wolozin (Boston University School of Medicine, Boston, USA), and human flag-HA-tagged 14-3-3β and rat flag-HA-tagged 14-3-3γ were from Addgene. The binding-deficient V181D mutant 14-3-3γ construct was generated by site-directed mutagenesis, and identity of the construct verified by sequencing of the coding region.

Cell culture and transfections

HEK293T/17 cells were cultured as previously described [219] and transfected at 80 % confluence with 2 μg of LRRK2 constructs and 6 μl of LipoD293 (SignaGen Laboratories) per well of a 6 well plate overnight in full medium. Cotransfections were performed with 1.8 μg of LRRK2 constructs and 200 ng of constructs as indicated (400 ng for 14-3-3 constructs). Cells were split onto coverslips the following day at a ratio of 1:4. As indicated, cells were incubated with nocodazole (200 nM), trichostatin A (800 nM), tubacin (10 μM), LRRK2-IN1 (1 μM), TAE684 (200 nM), CZC25146 (200 nM), GSK2578215A (1 μM), GNE-0877 (1 μM), GNE-7915 (1 μM), compound 68 (10 nM - 1 μM), compound 70 (10 nM - 1 μM) for 4 h in full medium, or with parthenolide (5 or 10 μM) for 12 h in full medium, followed by fixation and processing for immunochemistry, or by cell lysis and Western blot analysis as described below. Fibroblasts were cultured as previously described [219] and migration assays were performed as indicated below.

2D and 3D migration assays of human dermal fibroblasts

For 2D migration assays, PD patient fibroblasts harbouring the G2019S mutation and sex- and age-matched controls were seeded at a confluence of $2x10^4$ cells per well on a 12-well plate in IMDM (Iscove's Modified Dulbecco's Medium) medium (Gibco) containing 10 % FBS (Invitrogen). Cells were left to set for at least 4 h, subsequently treated with either 0.5 μM MLi2 or vehicle (DMSO) control as indicated, and imaged for 10 h.

For 3D migration assays, fibroblasts were seeded at a confluence of $1x10^4$ cells on μ-Slide 8 well glass-bottom dishes (IBIDI) coated with a solution containing collagen type I from rat tail at 2mg/ml OPTIMEM, 1 M NaOH, 1 M HEPES and 20 μg/ml fibronectin. They were left to settle for at least 1 h, followed by addition of full medium on top of the solution where the cells were embedded. Subsequently, cells were allowed to expand within the matrix overnight. The following day, cells were treated with either 0.5 μM MLi2 or DMSO vehicle control as indicated and imaged for 10 h.

Live cell imaging of fibroblasts was performed as indicated either for 2D or 3D assays. Live images were acquired on a time lapse microscope using a 20X objective (IX71 Olympus). LRRK2-MLi2 (0.5 μM final concentration) was added at time 0, and images collected using phase contrast. 2 or 4 images at three different Z positions per condition of selected areas were acquired every 15 min for 2D and 3D assays, respectively. Images were analyzed and processed using Fiji software. To track single cells, 30 single cells were measured over time and the resulting velocity data were then exported and analyzed with Chemotaxis and Migration Tool (IBIDI).

Immunofluorescence and laser confocal imaging

MT staining was performed essentially as described [219] Briefly, cells were rinsed twice in PBS, followed by fixation in 3 % formaldehyde, 0.2 % glutaraldehyde, 0.2 % Triton-X100, 10 mM EGTA for 10 min at 37 ºC. Fixed cells were washed twice in PBS for 5 min each, followed by quenching with 50 mM ammonium chloride in PBS for 10 min at RT, and two

washes in PBS for 5 min each. Fixed cells were permeabilized in 0.1 % Triton X-100 in PBS for 10 min, washed in PBS, blocked in 1 % BSA (w/v) in PBS for 20 min, and incubated with primary antibodies in PBS for 1 h. Primary antibodies included mouse monoclonal anti-α-tubulin (Sigma Aldrich, clone DM1A, 1:100), mouse monoclonal anti-β-tubulin (Millipore, clone KMX-1, 1:100), mouse monoclonal anti-acetylated α-tubulin (Sigma, clone 6-11B-1, 1:100), rabbit polyclonal anti-detyrosinated α-tubulin (Abcam, ab48389, 1:200; or Millipore, AB3201, 1:500), rat monoclonal anti-tyrosinated α-tubulin (Abcam, ab6160, 1:100), or rat monoclonal anti-HA (Roche, clone 3F10, 1:500), TRADD from Santa Cruz, FADD from BD Pharmingen, capase 8 from Millipore.

Secondary antibodies included Alexa 647-conjugated goat anti-rabbit, goat anti-mouse or goat anti-rat, or Alexa 488-conjugated goat anti-mouse, goat anti-rabbit or goat anti-rat antibodies (Invitrogen, 1:1000). Coverslips were incubated with secondary antibodies for 1 hr at RT, followed by washes in PBS and mounting using mounting medium containing DAPI (Vector Laboratories).

HEK293/T17 cells images were acquired on a Leica TCS-SP5 confocal microscope using a 63X 1.4 NA oil UV objective (HCX PLAPO CS). Images were collected using single excitation for each wavelength separately and dependent on secondary antibodies (488 nm Argon Laser line and a 510-540 nm emission band pass; 633 HeNe Laser line and a 640-670 nm emission band pass). GFP-tagged proteins were excited with 488 nm Argon Laser line and a 500-530 nm emission band pass, and DAPI was excited with the 405 nm UV diode and a 430-480 nm emission band pass, respectively.

25 image sections of selected areas were acquired with a step size of 0.3 μm, and z-stack images analyzed and processed using Leica Applied Systems (LAS AF6000) image acquisition software. For deconvolution, image sections of selected areas were acquired with a step size of 0.12 μm, and deconvolved using Huygens Essential Deconvolution software.

Quantification of colocalization of mutant or kinase-inhibited LRRK2 with acetylated or detyrosinated α-tubulin was performed essentially as described [240]. For each condition, five

individual cells were analyzed. Eight LRRK2-positive MT tracks were randomly selected from each cell and a line drawn over the length of a straight part of the track. Tracks were scored for the level of colocalization using image calculator and plot profile functions of ImageJ. The percentage of colocalization was subgrouped for each cell, with colocalization 0-50 % (white), 50-90 % (grey) or > 90 % (dark grey).

For determination of the subcellular localization of GFP-tagged LRRK2 proteins, cells were transfected and cultured as described, and fixed 48 h after transfection in 4% paraformaldehyde in PBS for 20 min at RT. Fixed cells were washed twice in PBS, permeabilized in 0.5 % Triton X-100 in PBS for 10 min at RT, washed in PBS, and mounted in mounting medium containing DAPI (Vector Laboratories). Cells were visualized on an inverted microscope (Zeiss) using a 100 x 1.40NA Plan APO oil objective. For each experiment, 100 random cells were scored and assigned to one of three phenotypes (cytosolic: purely diffuse localization; dot-like: presence of at least one dot-like structure (small, usually perinuclear); filamentous: presence of clear filamentous structures). Experiments with RL, TV and RLTV mutants, and experiments involving LRRK2 GTP binding inhibitors were performed and analyzed by two independent observers blind to condition, with comparable results obtained in all cases.

Fibroblast images were acquired on a laser scanning confocal microscope (Nikon AIR) with a 100x or 60x/1.4 Plan-APOCHROMAT oil immersion objective. Images were collected using single excitation for each wavelength separately and dependent on secondary antibodies (488 nm Argon Laser line 488 secondary antibodies were excited with 488 nm Argon Laser line and a 500-530 nm emission band pass, and DAPI was excited with the 405 nm UV diode and a 430-480 nm emission band pass, respectively).

For fibroblast staining cells were rinsed twice in PBS, followed by fixation in ice cold methanol for 3 min at -20 ºC. Fixed cells were washed twice in PBS and blocked in 1 % BSA (w/v) in PBS for 30 min, and incubated with primary antibodies in blocking solution for 1 h. Coverslips were washed twice in PBS and subsequentally incubated with secondary antibodies,

Alexa Fluor 647 phalloidin, and DAPI in blocking solution for 1 hr at RT, followed by washes in PBS and mounting.

Live cell imaging

Live cell imaging of HEK293T/17 cells transfected with GFP-tagged wildtype LRRK2 was performed on cells grown on glass-bottom dishes (IBIDI) in full medium without phenol red. Live images were acquired 48 h after transfection on a Leica TCS-SP5 confocal microscope using a 63X 1.4 NA oil UV objective (HCX PLAPO CS). LRRK2-IN1 (1 μM final concentration) was added at time 0, and images collected using single excitation 488 nm Argon Laser line and a 495-575 nm emission band pass. The 488 nm Argon Laser line was set at 30 %, with pinhole airy at 1. Contrast phase images of single stacks were simultaneously acquired. 15 image sections of selected areas were acquired every 45 sec with a step size of 0.5 μm. Z-stack maximal intensity projection images were analyzed and processed using Leica Applied Systems (LAS AF6000) image acquisition software.

.

MT nucleation assays

Cells were grown and transfected as described above, and split onto poly-L-lysine-coated coverslips 24 hours later. The following day, coverslips in 6-well dishes were placed in an ice-water bath for 1.5 hours to cause cold-induced MT depolymerization. MT regrowth was initiated by placing coverslips at 37 ºC for the indicated time periods, followed by fixation in 4% paraformaldehyde in a buffer containing 60 mM PIPES, 25 mM HEPES, pH 6.9, 10 mM EGTA, 1 mM $MgCl_2$ and 0.5 % Triton-X100 (92) before immunostaining as described above. Cells were visualized on an inverted microscope (Zeiss) using a 100 x 1.40NA Plan APO oil objective. For each timepoint, 100 cells were scored for visible MT staining with antibodies against α-tubulin or acetylated α-tubulin in non-transfected versus transfected cells, and for visible pathogenic LRRK2 filament reformation in transfected cells.

Permeabilization of cells with streptolysin-O

Cells were grown and transfected as described above, and split onto poly-L-lysine-coated coverslips in 24-well plates the following day. Two days after transfection, cells were incubated with or without 500 nM MLi2 for 2 h as indicated. Permeabilization was performed essentially as described previously [241, 242] with slight modifications. Cells were permeabilized in 1 ml of Hank´s balanced salt solution (HBSS; 4.17 mM $NaHCO_3$, 0.34 mM Na_2HPO_4, 0.44 mM KH_2PO_4, 137.9 mM NaCl, 5.3 mM KCl, pH 7.4) containing 16 ng/ml streptolysin-O for 10 min at 37 ºC. This resulted in the permeabilization of around 80 % of cells as independently determined by Trypan blue staining. After 10 min, permeabilization buffer was replaced by 1 ml of resealing buffer (10 mM HEPES, 140 mM NaCl, 5 mM KCl, 1.3 mM $MgCl_2$, 2 mM $CaCl_2$, pH 7.4), and cells were incubated for an additional 10 min at 37 ºC. Buffers contained 500 nM MLi2, 5 μM GTPαS, GPCpp, GppCp, GppNHp or GTPγS as indicated. Amongst the non-hydrolyzable GTP analogs tested, only GTPαS was found to be non-toxic to permeabilized cells up to a concentration of 5 μM, and thus was used for all subsequent experiments. Upon permeabilization and resealing, cells were fixed and stained as described above, and 100 random cells were scored for a filamentous phenotype per condition and experiment. Cells displayed an intact MT network upon 10 min permeabilization and 10 min resealing under all conditions analyzed.

Cell extracts and Western blotting

Cells were collected 48 h after transfection, washed in PBS and resuspended in cell lysis buffer (1 % SDS in PBS containing 1 mM PMSF, 1 mM Na_3VO_4, 5 mM NaF). Extracts were sonicated, boiled and centrifuged at 13,500 rpm for 10 min at 4 °C. Protein concentration of supernatants was estimated using the BCA assay (Pierce), and equal amount of extracts were resolved by SDS-PAGE, transferred to PVDF (in the case of ECL detection) or to nitrocellulose membranes (in the case of detection by Odyssey) and analyzed by Western blotting using a variety of antibodies as indicated, including rabbit polyclonal anti-GFP (Abcam, ab6556,

1:1000), mouse monoclonal anti-myc (Sigma, clone 9E10, 1:1000), rabbit polyclonal anti-V5 (Sigma, V8137, 1:2500), rat monoclonal anti-HA (Roche, clone 3F10, 1:500), mouse monoclonal anti-flag (Sigma, clone M2, 1:500), phospho-S935-LRRK2 antibody (Abcam, 1:1000), mouse monoclonal anti-acetylated α-tubulin (Sigma, clone 6-11B-1, 1:5000), rabbit polyclonal anti-detyrosinated α-tubulin (Millipore, AB3201, 1:500) and mouse monoclonal anti-α-tubulin (Sigma, clone DM1A, 1:10000). Membranes were incubated with primary antibodies in 5% BSA (w/v) in TBS-0.1% Tween-20 for 1.5 h at RT, or overnight at 4 ºC. For ECL detection, membranes were incubated with secondary antibodies in 5% BSA in TBS-0.1% Tween-20 for 1 hr, or with secondary antibodies in PBS (1:10000) for detection by Odyssey, followed by three times 5 min rinses in PBS. Westerns were developed with ECL reagents (Roche), and a series of timed exposures to ensure that densitometric analyses were performed at exposures within the linear range. Most determinations of steady-state protein levels, as well as all GTP binding assays were quantified by ODYSSEY infrared imaging system application software LI-COR Image Studio Lite version 5.2.

GTP binding assays

GTP binding assays were performed essentially as previously described (77). HEK293T/17 cells were cultured in 100 mm diameter dishes and transfected at 70-80% confluence with 12 μg of GFP-tagged LRRK2 DNA and 36 μl of LipoD293 per plate. Cells were split into 100 mm dishes at a ratio of 1:3 the following day, and lysed in 1 ml of lysis buffer per dish (20 mM Tris-HCl, pH 7.4, 1 % Triton X-100, 137 mM NaCl, 3 mM KCl, 10 % (v/v) glycerol, 1 mM EDTA, 1 mM Na_3VO_4, 5 mM NaF, 1 mM PMSF) for 1 h at 4 ºC on a rotary wheel, followed by clarification of extracts by centrifugation at 13,200 rpm for 10 min at 4 ºC. Soluble protein was evenly split into two tubes to a final volume of 500 μl each, and each incubated with 30 μl of 5´-GTP agarose beads (Sigma Aldrich) overnight at 4 ºC on a rotary wheel. One of the two samples was used as control for non-specific binding to GTP-agarose beads by adding a final concentration of 10 mM GTP. The next day, beads were washed twice

with ice-cold lysis buffer, and GTP-bound proteins eluted from beads by incubation with 30 µl ice-cold lysis buffer containing 10 mM GTP for 15 min at 4 ºC on a rotary wheel. Beads were centrifuged at 13,200 rpm for 1 min, eluates were transferred to fresh tubes and resuspended with 5x Laemmli sample buffer containing β-mercaptoethanol. Both eluate and input (5 % total lysate) samples were subjected to SDS-PAGE and Western blotting with an anti-GFP antibody (Abcam, ab6556, 1:1000). GTP binding assays were quantified by ODYSSEY as described above, with GTP-specific binding of each LRRK2 construct normalized to protein input. For experiments determining the effects of GTP binding inhibitors (40,41), the respective compounds were added to the lysis buffer and kept throughout the experiment. For experiments determining the effect of LRRK2 kinase inhibitors, compounds were added to cells 4 h prior to lysis, added to the lysis buffer, and kept throughout the experiment.

In vitro LRRK2 kinase assays

pDEST53-GFP-LRRK2 wildtype and mutants were transiently transfected into HEK293T/17 cells using 20 µg of DNA in 1 ml OPTI-MEM (Thermo Fisher) and 40 µl of linear polyethylenimine (PEI, Polyscience) (20 µM) per 10 cm^2 Petri dish. Cells were harvested 48 h after transfection with 500 µl of lysis buffer (10 mM Tris-HCl pH 7.5, 150 mM NaCl, 5 mM EDTA, 2.5 mM $Na_4P_2O_7$, 1 mM beta-glycerophosphate, 1 mM Na_3VO_4, supplemented with Protease Inhibitor Mixture (Sigma Aldrich) and 1% (v/v) Tween-20). Samples were incubated on ice for 30 min, and centrifuged at 18,000 g for 35 min at 4 °C. Supernatants were incubated overnight with 20 µl of GFP-Trap beads (ChromoTek GmbH, Planegg, Germany) at 4 °C with mild agitation. Beads were sequentially washed with 500 µl of buffer 1 (20 mM Tris-HCl pH 7.5, 500 mM NaCl, 1% (v/v) Tween-20), buffer 2 (20 mM Tris-HCl pH 7.5, 350 mM NaCl, 1% (v/v) Tween-20), buffer 3 (20 mM Tris-HCl pH 7.5, 150 mM NaCl, 1% (v/v) Tween-20), buffer 4 (20 mM Tris-HCl pH 7.5, 150 mM NaCl, 0.1% (v/v) Tween-20) and buffer 5 (20 mM Tris-HCl pH 7.5, 150 mM NaCl, 0.02 % (v/v) Tween-20). GFP-LRRK2-containing beads were resuspended in 100 µl of kinase buffer (25 mM Tris-HCl pH 7.5, 5 mM beta-glycerophosphate,

2 mM DTT, 0.1 mM Na_3VO_4, 10 mM $MgCl_2$ supplemented with 0.007% (v/v) Tween-20) for subsequent *in vitro* kinase assays.

Kinase reactions were started by addition of ATP (200 µM final) and were incubated for 1 h at 30 °C with mild agitation. Samples were centrifuged, supernatants discarded, and proteins eluted from beads by addition of Laemmli sample buffer and boiling for 5 min at 95 °C. Samples (10 µl) were separated by SDS-PAGE, and transferred onto PVDF membranes (Bio-Rad) using the Trans-Blot Turbo Transfer System (Bio-Rad) in semi-dry conditions using 1X Trans-Blot Turbo Transfer Buffer (Bio-Rad) in 20 % (v/v) ethanol at 25 V for 20 min. Membranes were blocked for 40 min in 5 % (w/v) skimmed milk in TBS-T buffer (20 mM Tris-HCl pH 7.4, 150 mM NaCl, 0.1% (v/v) Tween-20), followed by incubation for 1 h with an antibody against the LRRK2 autophosphorylation site T2483 (MJF-R8, Abcam, 1:2000). Membranes were washed 4 times for 10 min with TBS-T buffer, and incubated for 1 h at room temperature with HorseRadish-Peroxidase (HRP)-conjugated rabbit secondary antibodies (1:15000) in 5% (w/v) skimmed milk in TBS-T buffer. Membranes were washed in TBS-T buffer followed by visualization using ECL Western Blotting Detection Reagents (GE Healthcare). Data were normalized to the concentration of the individual proteins on PVDF membranes directly stained with Coomassie (40 % methanol, 10 % acetic acid, 0.1% (w/v) Comassie R-250), and densitometry analysis carried out using ImageJ software, with kinase activities of the various proteins expressed relative wild-type LRRK2, which was present on every gel for comparison.

Statistical analysis

All data are expressed as means ± s.e.m. Data were analyzed by one-way ANOVA with Tukey´s post-hoc test, and $p < 0.05$ was considered significant.

VII. Results

1. LRRK2 and Parkinson´s disease: from lack of structure to gain of function.

FINAL

Send Orders for Reprints to reprints@benthamscience.ae

Current Protein and Peptide Science, 2016, *17*, 1-10

LRRK2 and Parkinson's Disease: From Lack of Structure to Gain of Function

Marian Blanca Ramírez, Jesús Madero-Pérez, Pilar Rivero-Ríos, Mar Martínez-Salvador, Antonio J. Lara Ordóñez, Belén Fernández, Elena Fdez and Sabine Hilfiker*

Institute of Parasitology and Biomedicine "López-Neyra", Consejo Superior de Investigaciones Científicas (CSIC), Avda del Conocimiento s/n, 18016 Granada, Spain

Sabine Hilfiker

Abstract: Mutations in LRRK2 comprise the most common cause for familial Parkinson's disease (PD), and variations increase risk for sporadic disease, implicating LRRK2 in the entire disease spectrum. LRRK2 is a large protein harbouring both GTPase and kinase domains which display measurable catalytic activity. Most pathogenic mutations increase the kinase activity, with increased activity being cytotoxic under certain conditions. These findings have spurred great interest in drug development approaches, and various specific LRRK2 kinase inhibitors have been developed. However, LRRK2 is a largely ubiquitously expressed protein, and inhibiting its function in some non-neuronal tissues has raised safety liability issues for kinase inhibitor approaches. Therefore, understanding the cellular and cell type-specific role(s) of LRRK2 has become of paramount importance. This review will highlight current knowledge on the precise biochemical activities of normal and pathogenic LRRK2, and highlight the most common proposed cellular roles so as to gain a better understanding of the cell type-specific effects of LRRK2 modulators.

Keywords: Autophagy, endocytosis, GTPase, kinase, LRRK2, Parkinson's disease, Rab7, Rab7L1.

1. PARKINSON'S DISEASE

Parkinson's disease (PD) is a devastating and common neurodegenerative disorder affecting 1 - 2% of the population above the age of 65 [1]. It is characterized by the loss of dopaminergic neurons in the substantia nigra, and the presence of Lewy bodies (LBs) in surviving neurons. LBs are composed of fibrillar aggregates of α-synuclein and a variety of ubiquitinated proteins [2], implicating protein aggregation and abnormal protein homeostasis in disease pathomechanism(s). The loss of dopaminergic neurons causes the major clinical hallmarks of PD, which include tremor, bradykinesia, rigidity and postural instability. Treatment options are based on alleviating symptoms, and there are currently no disease-modifying compounds or cures available.

Most PD cases are sporadic or idiopathic in nature. However, around 8 - 10% of all cases are familial and due to mutations in a variety of loci called PARK loci [3]. In addition to the Mendelian inheritance of mutations in genes which cause PD, additional genes with risk effects for disease have been identified by large genome-wide association analyses [4]. Thus, a picture has emerged whereby a combination of genetic predisposition, age and environmental stress seem to contribute to PD pathogenesis.

*Address correspondence to this author at the Institute of Parasitology and Biomedicine "López-Neyra", Consejo Superior de Investigaciones Científicas (CSIC), Avda del Conocimiento s/n, 18016 Granada, Spain; Tel: +34 958 18 16 54; Fax: +34 958 18 16 32; E-mail: sabine.hilfiker@ipb.csic.es

2. PATHOGENIC MUTATIONS IN LRRK2 AND PD

Mutations in LRRK2 comprise the most common cause of familial, late-onset PD, and are found both in hereditary as well as sporadic forms of the disease [5-7]. Indeed, variants around the LRRK2 locus seem to play a major role in disease susceptibility [8]. This is important, as it allows for the reasonable prediction that targeting LRRK2 may be beneficial to the entire spectrum of patients with late-onset PD. Somewhat surprisingly though, pathogenic mutations in LRRK2 display age-dependent but incomplete penetrance, indicating that other factors apart from LRRK2 mutations (e.g. related to genetic background and/or environmental causes) are necessary for the development of PD.

Whilst over 250 amino acid substitutions in LRRK2 have been reported [9], pathogenicity, as defined by the ability to segregate with disease in families, has only been definitely shown for a small set of mutations, including N1437H, R1441C/G/H, Y1699C, G2019S and I2020T (Fig. **1**). LRRK2 belongs to the Roco superfamily of proteins, a multidomain family of Ras-like G proteins characterized by a specific domain structure comprised of a ROC (Ras of complex) and C-terminal of ROC (COR) domain [10-12]. The LRRK2 domain structure includes N-terminal armadillo repeats (ARM), ankyrin repeats (ANK), and leucine-rich repeats (LRR), followed by a ROC, a COR, a kinase and a WD40 domain [13] (Fig. **1**). Interestingly, all identified pathogenic mutations cluster within the central core of the protein. As this central core encodes for domains with putative kinase and GTPase activities, respectively, an obvious

1389-2037/16 $58.00+.00

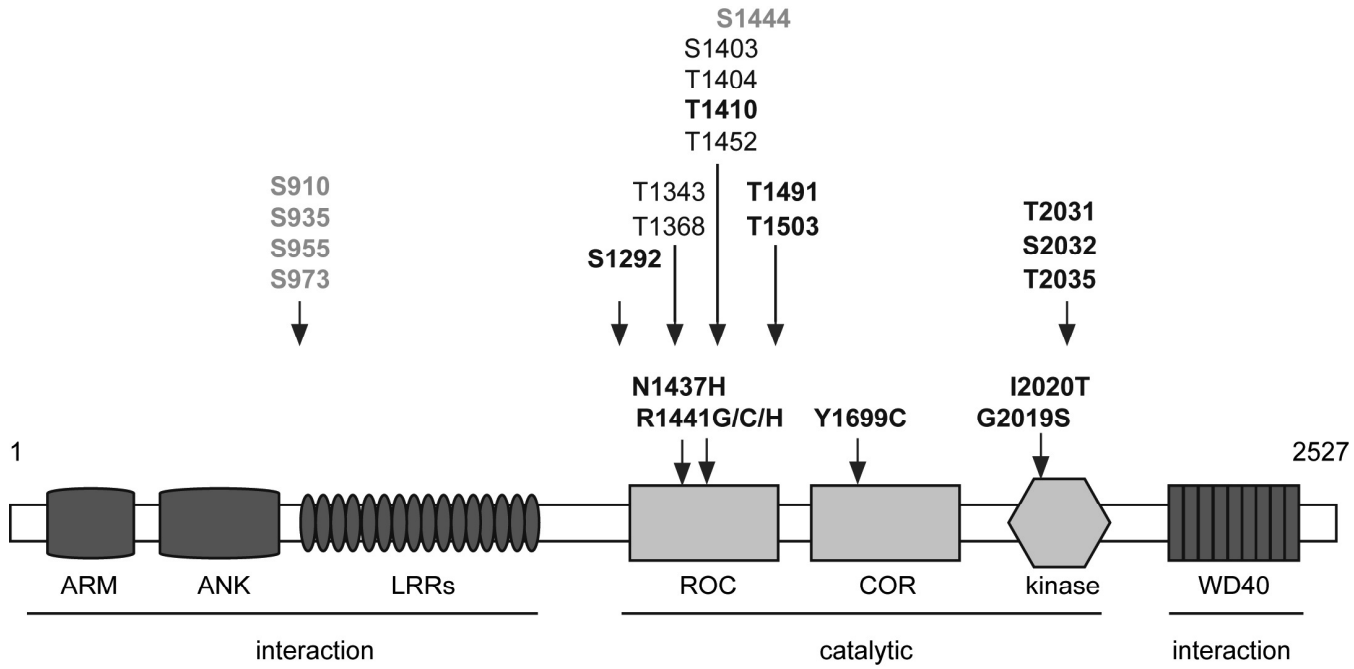

Fig. (1). Schematic representation of LRRK2 domain structure and identified cellular and autophosphorylation sites. LRRK2 domain structure, including armadillo repeats (ARM), ankyrin repeats (ANK), leucine-rich repeats (LRR), followed by a ROC, COR and kinase domain, and a C-terminal WD40 domain. Pathogenic mutations clustered within the central catalytic core are indicated. Phosphorylation sites which have been independently reported at least twice are indicated above the domain structure. Autophosphorylation sites are indicated in black, and cellular phosphorylation sites in grey. Sites which have been detected *in vivo* (with phospho-state-specific antibodies) are depicted in bold. See text for further details.

question in the LRRK2 field has focused on whether these activities are altered by the distinct pathogenic mutations.

3. FROM PECULIAR SEQUENCES TO LACK OF STRUCTURAL INFORMATION

Within the human kinome, LRRK2 belongs to the tyrosine-like kinase family, a set of kinases which phosphorylate serine and/or threonine residues, but bear more primary sequence homology to tyrosine kinases [14]. The LRRK2 kinase harbours unusual sequences in the kinase activation segment, including a DYG hinge motif instead of the DFG motif most commonly observed in kinases [15]. This is further altered by the most common pathogenic LRRK2 mutation (G2019S), which changes the motif to DYS, implicating distinct structural configurations for the ATP-binding pocket of wildtype versus G2019S-mutant LRRK2, respectively [16]. Despite such peculiar sequence differences, LRRK2 has been shown to display kinase activity *in vitro*. Since kinases make for excellent drug targets, LRRK2 has become the most exciting target for therapeutic interventions in PD research to date.

Apart from sequence differences within the kinase domain of LRRK2, the ROC domain which harbours GTPase activity also diverges from other G-protein families [10]. Sequence alignment of the LRRK2 GTPase domain against other GTPases reveals substitutions in residues thought to be important for such activity [17]. This may predict low inherent GTPase activity of LRRK2, which has indeed been determined by biochemical means [18-23]. Similar to the kinase activity, the GTPase activity of LRRK2, whilst largely dormant *in vivo*, may require activation by additional proteins. Alternatively, the relevant molecular feature of the ROC domain of LRRK2 may be related to GTP binding rather than GTP hydrolysis [24, 25]. Indeed, recent studies revealed compounds which reduce LRRK2 GTP binding *in vitro*, associated with decreased kinase activity and attenuated neurodegeneration in cultured cells and *in vivo* [26, 27]. Whilst currently little effort has gone into identifying compounds which modulate GTP binding and/or GTPase activity of LRRK2, such molecules may hold significant therapeutic potential as well.

Structural understanding of LRRK2 is paramount, as it allows for the design of highly specific ATP-competitive as well as non-competitive kinase inhibitors. Furthermore, it allows for insight into the various mechanisms of intra- and inter-molecular regulation, which may aid in the design of additional small molecule modulators, and provides a detailed molecular understanding of the distinct pathogenic mutants. Unfortunately, due to the difficulty in isolating sufficient amounts of pure, soluble protein in its native state, no atomic structures of full-length LRRK2 have been described thus far. Crystal structures have been resolved for the ROC domain of human LRRK2 [28], as well as the ROC-COR bidomain or the kinase domain from related prokaryotic ROCO proteins, respectively [29, 30]. In addition, a variety of modeling studies suggest possible conformational configurations of the various protein-protein interaction domains [31-33]. However, how these domains are positioned with respect to each other and thus able to influence the GTPase and/or kinase activities in a multimeric LRRK2 complex remains unclear.

4. GAIN OF FUNCTION-TYPE BIOCHEMICAL READOUTS FOR PATHOGENIC LRRK2

The most common pathogenic mutation, G2019S, has been consistently shown to upregulate LRRK2 kinase activity [34]. This suggests that this pathogenic mutant may act in a gain of function manner, with enhanced kinase activity reflecting enhanced function. Structural insights from the related kinase domain of ROCO proteins indicate that this mutation may stabilize the activation segment in the active conformation [30]. However, such structural comparison has not been able to predict alterations in the kinase activity of I2020T, another PD-related mutation adjacent to G2019S, even though recent careful phosphorylation studies under both steady-state and pre-steady-state kinetic conditions indicate that this pathogenic mutation may also increase kinase activity by stabilizing the active conformation of LRRK2 [35].

The enhanced kinase activity of G2019S-mutant LRRK2 seems to correlate with neurotoxicity, and pharmacological or genetic inhibition of the kinase activity can rescue the pathogenic mutant-induced phenotypes *in vitro* and *in vivo* [36-41]. These findings indicate that the kinase activity is crucial for LRRK2-mediated cytotoxicity, and that inhibiting this activity may be a valid disease-modifying strategy. However, the extent to which other pathogenic mutations in LRRK2 change this readout remains largely unclear. These mutations cluster in the ROC and COR domains, respectively, and may increase GTP binding and/or decrease GTP hydrolysis. The measurable GTPase activity of LRRK2 is very low, and several studies have shown that it is further decreased by pathogenic mutations in the ROC and COR domains [18-23]. Similarly, introducing the analogous mutations which cause PD into ROCO proteins from lower organisms also decreases their GTPase activity [29]. A decrease in the GTPase activity would result in more GTP-bound LRRK2, which may then perform some downstream role, with pathogenic mutations in the ROC and COR domains enhancing that role in a gain-of-function manner.

The downstream effect(s) of decreased GTPase activity remain unclear. LRRK2 has been proposed to work as a typical GTPase whose activity in intact cells is modulated by GTPase-activating proteins (GAPs) and guanine nucleotide exchange factors (GEFs) [42-45]. Other studies indicate that the GTPase activity may be controlled by dimerization without the need for accessory proteins [46]. Indeed, LRRK2 has been shown to form dimers, with dimers displaying enhanced kinase activity as compared to monomers [47-49]. The latter findings indicate that the GTPase activity of LRRK2 may modulate its kinase activity. However, effects of mutations in the ROC or COR domain on kinase activity have been controversial, with either none or only subtle increases reported [34]. Such differences may relate to protein concentration-dependent differences affecting the amount of LRRK2 dimer present, combined with differences in the co-purification of various factors which may alter inherent kinase activity in those *in vitro* assays [17]. Importantly, introducing pathogenic mutations in the ROC-COR domain on top of the G2019S mutation has been found to cause a significant additional increase in kinase activity [50, 51]. Thus, current data are largely consistent with the idea of a kinase activation mechanism for all pathogenic LRRK2 mutations. Whilst mutations generally only cause subtle increases in kinase activity, this may reflect the late onset of LRRK2-related PD, with slight increases in kinase activity having cumulative negative effects over time. Alternatively, it may pinpoint towards the presence of an additional triggering event which causes activation of LRRK2 in a specific cellular context with resulting downstream pathogenic events.

Few LRRK2 variants which increase PD risk have been analyzed for their effects on kinase activity. The prominent risk variant, G2385R, has been found to either cause no change [19, 52] or a decrease in kinase activity [53, 54], respectively. Whilst the implication of the reported decreased kinase activity for pathogenicity remains unclear, it may suggest that LRRK2 kinase activity needs to be tightly controlled within an acceptable window, as either too much or too little activity may be detrimental for cell viability. Alternatively, the pathogenicity of the G2385R mutation may be unrelated to kinase activity, but mediated by altered protein-protein interactions [54], which would open up the possibility of targeting such interactions as additional therapeutic approaches towards LRRK2-related PD.

5. WHAT LIES DOWNSTREAM OF THAT KINASE ACTIVITY?

Despite significant research efforts, few reproducible substrates for the kinase activity of LRRK2 have been described, amongst those the ERM (ezrin/radixin/moesin) protein family [53, 55]. ERM proteins anchor the actin cytoskeleton to the plasma membrane, and can also regulate the stability of microtubules, suggesting that the kinase activity of LRRK2 may play important roles for correct intracellular organization and vesicular membrane trafficking events. Phospho-ERM levels are altered in neurons from G2019S LRRK2-transgenic mice, with concomitant alterations in actin cytoskeletal dynamics, consistent with the idea that LRRK2 may directly or indirectly regulate the phosphorylation of these proteins [56]. Identification of ERM proteins as LRRK2 kinase substrates has also allowed for the design of efficient model substrate peptides to analyze LRRK2 kinase activity *in vitro* [53, 55]. However, most other currently identified substrates have either not been independently validated, or have been found not to be relevant LRRK2 kinase substrates in intact cells.

At present, possibly the best substrate for the kinase activity of LRRK2 is LRRK2 itself. Autophosphorylation has been described for a large variety of protein kinases, even though it generally does not display stoichiometric features. This may be related to cooperative mechanisms and/or multimeric enzyme complexes resistant to further autophosphorylation, respectively [57]. In addition, whilst autophosphorylation can lead to changes in activity and/or the dependence on activators, it is not always linked to modulation of kinase activity *per se*. Rather, autophosphorylation can regulate the subcellular distribution of protein kinases, resulting in rapid and preferential modulation of specific targets within a defined subcellular microenvironment susceptible to various diffusible second messengers [58].

Several autophosphorylation sites for LRRK2 have been described (Fig. **1**) [47, 50, 51, 59-64]. Whilst largely concentrated in the ROC domain, sites within the kinase domain and the N-terminus have been reported as well [47, 51, 60, 64]. However, in most cases, such autophosphorylation cannot be detected in cell lysates with phospho-state-specific antibodies, indicating that determination of autophosphorylation likely cannot serve as a robust measure for LRRK2 kinase activity. Thus, identification of bona-fide substrates displaying efficient phosphorylation will remain an important issue towards the design of assays measuring changes in kinase activity in distinct pathological and therapeutic settings.

LRRK2 is also phosphorylated by a variety of upstream kinases including cAMP-dependent protein kinase, casein kinase-1 and IKK family members [52, 65-71]. Such cellular phosphorylation (defined as phosphorylation of LRRK2 by other cellular kinases, as opposed to autophosphorylation) occurs mainly, but not exclusively, in the N-terminus of LRRK2, and is decreased by most pathogenic LRRK2 mutants (Fig. **1**). Phosphorylation on these cellular sites is required for 14-3-3 binding, and alterations cause a change in the solubility and/or subcellular localization of LRRK2, highlighting complex additional regulation of LRRK2 by upstream kinases and phosphatases able to dephosphorylate the cellular sites [72]. Interestingly, phosphorylation on those cellular sites also seems to largely correlate with pharmacological inhibition of LRRK2 kinase activity [73-75], and thus has proven to be a useful readout in many kinase inhibitor studies. The precise mechanism behind such correlation remains unclear, but it is possible that inhibitor binding to LRRK2 causes a conformational change which leads to the preferred dephosphorylation of those cellular sites through increased access of phosphatases [75]. Notably, if phosphorylation on those cellular sites correlates with alterations in solubility and/or subcellular localization relevant for pathogenicity, the finding that both pathogenic mutants and pharmacological kinase inhibitors equally cause dephosphorylation of those sites indicates that at least under certain conditions, kinase-inhibited LRRK2 may undergo the same alterations in solubility and/or subcellular localization as pathogenic LRRK2.

A variety of small-molecule kinase inhibitors for LRRK2 have been described. Amongst those, LRRK2-IN-1, GSK2578215A, HG-10-102-01, GNE-0877 and GNE-9605 display high specificity, with minimal and non-overlapping inhibition of few additional off-target kinases [51, 66, 76-78]. Thus, using a variety of those inhibitors in cellular studies allows to predict with reasonable certainty whether observed effects are LRRK2 kinase activity-dependent. In addition, some LRRK2 kinase inhibitor compounds can cross the blood brain barrier, and display attributes which make them suitable for *in vivo* applications [77, 78]. However, a major problem is related to the finding that either pharmacological or genetic inhibition of LRRK2 kinase causes unwanted effects in peripheral tissues, predominantly kidney and lung [40, 78-81]. These seem to be on-target effects, and are likely related to the high endogenous LRRK2 protein levels in those peripheral tissues, reflecting the fact that LRRK2 seems to play important roles for the proper functioning of those peripheral tissues as well [78, 82]. Thus, apart from understanding the pathogenic role of LRRK2 in neuronal tissues related to PD, it has become paramount to understand the normal function of LRRK2 in peripheral tissues, so as to be able to effectively compensate for its loss upon kinase inhibitor treatment approaches.

6. THE CELLULAR ROLES OF LRRK2

Apart from allowing to resolve safety liability issues in peripheral tissues, understanding the cellular role(s) of LRRK2 is also important towards developing pharmacodynamic readouts. Whilst no cellular or animal model system may ever be capable of predicting clinical success, such systems, or a combination thereof, will be essential towards gauging efficacy of target engagement, and will allow for comparisons of dosages which may cause toxicity associated with excessive LRRK2 kinase inhibition. Indeed, whilst genetic ablation of LRRK2 in mice or rats causes phenotypes in peripheral tissues, these are not observed in heterozygous knockdown animals, indicating that proper titration of LRRK2 kinase inhibitors, without fully ablating kinase activity, may achieve the desired effects without impairing the functioning of those peripheral organs.

Various studies employing overexpression approaches of pathogenic LRRK2 in cells as well as animal models have shown that it can cause toxicity in a kinase activity-dependent manner [19, 36-39, 41, 83-85]. However, moderate and transient overexpression of either wildtype or pathogenic mutant LRRK2 does not seem to be toxic, and this allows for cellular phenotypes to be analyzed in detail. A wealth of studies indicate that both endogenous as well as overexpressed pathogenic LRRK2 can regulate various distinct vesicular trafficking pathways including endocytosis, autophagy, the perinuclear positioning of endolysosomes crucial for efficient flux through the endocytic and autophagic systems, respectively, and retromer-mediated trafficking from the late endosome to the Golgi (Fig. **2**) [86-112]. In some cases, several pathogenic LRRK2 mutations have been analyzed side-by-side and found to display the same trafficking deficits. For example, both G2019S and R1441C mutant LRRK2 cause deficits in late endocytic trafficking [91], R1441G, Y1699C and G2019S mutant LRRK2 cause similar alterations in autophagic-lysosomal degradation [104], and R1441C, Y1699C, G2019S and I2020T induce alterations in Golgi morphology further potentiated in the presence of Rab7L1 [110]. In all cases, the extent of cellular deficits in the presence of the various LRRK2 mutants are similar, supporting the idea that they may act by a common mechanism. Furthermore, at least in the context of endocytic trafficking, two structurally distinct kinase inhibitors (LRRK2-IN-1, GSK2578215A) have been shown to revert the observed deficits [91], suggesting that these are indeed kinase activity-dependent.

The distinct trafficking steps mentioned above may not all be simultaneously affected, but rather depend on the precise cellular context. Indeed, effects of LRRK2 on lysosomal positioning or late endocytic deficits have been only observed under conditions favouring high flux through the endocytic system [91, 108]. Similarly, effects of LRRK2 on autophagy have been most prominently observed upon stimulus-triggered autophagy induction [93, 104]. Distinct

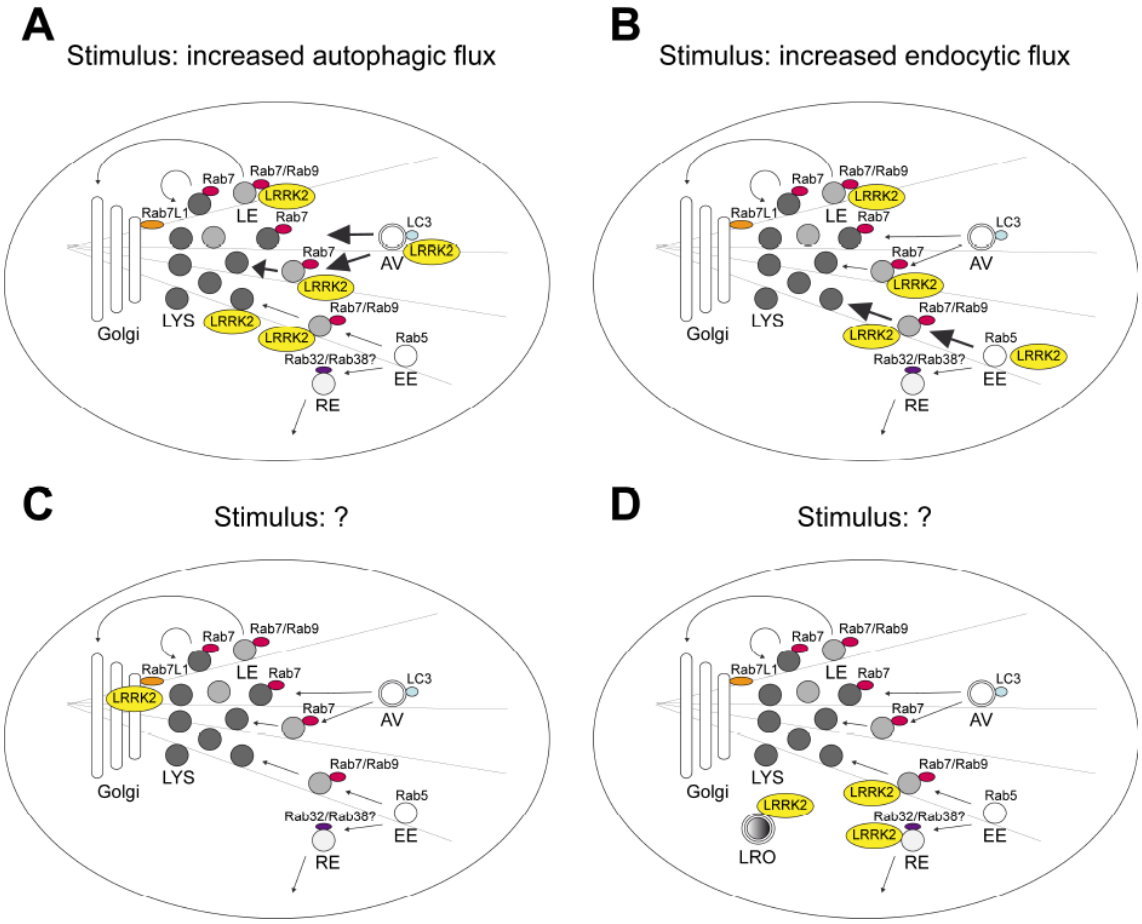

Fig. (2). LRRK2 as a master regulator of various intracellular vesicular trafficking events. Model for differential and stimulus-dependent relocalization of cytosolic LRRK2 to distinct subcellular organelles. **A**) Under conditions of high autophagic demand, LRRK2 may relocalize to autophagosomes as well as late endosomal/lysosomal compartments. **B**) Under conditions of high endocytic demand, LRRK2 may relocalize to early and/or late endosomal structures. **C**) Under conditions yet to be determined, LRRK2 may relocalize to lysosome-related organelles, recycling endosomes and/or late endosomes in a manner dependent on Rab32. **D**) Similarly, under conditions which remain to be determined, LRRK2 may relocalize to the Golgi complex in a manner dependent on Rab7L1. In all cases, it is hypothesized that LRRK2 plays a role in the correct functioning of these organelles which is altered by pathogenic LRRK2 mutants. Cell type-specific differences can be easily superimposed onto this model, either at the level of specific stimuli, subcellular compartmental peculiarities, or cell-type specific expression of downstream targets/binding partners on the distinct organelles. For further details see text. AV, autophagic vacuole; EE, early endosome; LE, late endosome; LRO, lysosome-related organelle; LYS, lysosome; RE, recycling endosome.

stimuli then may differentially impact upon the phosphorylation status of LRRK2 to trigger relocalization of the largely cytosolic protein to a specific subcellular site (see above), and/or may trigger alterations in select LRRK2 interaction partners which then allow for recruitment of LRRK2 to distinct subcellular localizations (Fig. **2**). In either case, the idea that distinct stimuli may recruit LRRK2 to different intracellular membranes where it may then act upon a small, localized set of targets to bring about alterations in defined trafficking steps is further supported by recent findings that LRRK2 can interact and/or modulate a set of Rab proteins localized to different subcellular localizations, including Rab7, Rab9, Rab32 and Rab7L1. Rab GTPases are critical regulators of membrane traffic, organelle biogenesis and maturation. They display distinct or partially overlapping subcellular distributions, and regulate distinct or partially overlapping subcellular trafficking steps [113, 114]. For example, both Rab7 and Rab9 are known to regulate trafficking from early to late endosomes as well as retromer-mediated trafficking from late endosomes to the Golgi complex. Rab7 is also required for trafficking from late endosomes to lysosomes, trafficking from autophagosomes to late endosomes and/or lysosomes, for the proper perinuclear positioning of late endosomes and lysosomes, and for lysosome biogenesis [113, 114]. The function of Rab32 is characterized to a lesser degree, but this Rab protein seems to be involved in the biogenesis of lysosome-related organelles in specific cell types [115], as well as in various additional trafficking steps involving recycling endosomes and/or late endosomes [116], and Rab7L1 seems involved in retromer-mediated trafficking between the Golgi and late endosomes [113, 114]. Interestingly, LRRK2 has been reported to interact with Rab7, and to regulate both Rab7- and Rab9-mediated trafficking events, as well as proper endolysosomal positioning which is important for appropriate flux through the endosomal degradative system [108, 109]. Consistent with the observed trafficking deficits, pathogenic LRRK2 has been found to decrease the GTPase activity of Rab7 [91].

In addition, LRRK2 has been shown to interact with Rab32, which seems to cause relocalization of LRRK2 to a variety of intracellular organelles including recycling endosomes and/or late endosomes [116], even though possible effects of LRRK2 on the GTPase activity of Rab32, or the downstream cellular consequences of the Rab32-mediated relocalization of LRRK2 to these organelles remain to be determined (Fig. **2**). Finally, LRRK2 has been reported to interact with Rab7L1 [110, 111]. Rab7L1 is part of the PARK16 locus associated with PD risk, and increased expression seems to be associated with increased risk [8, 110]. Rab7L1 is localized to the Golgi network [117, 118], and its expression causes relocalization of LRRK2 to the Golgi, with concomitant defects in retromer-mediated trafficking between the Golgi and the late endosome as well as altered Golgi morphology [110, 111], whilst it remains unknown whether LRRK2 modulates the GTPase activity of Rab7L1 (Fig. **2**). Therefore, more work is needed to elucidate the set of precise cellular signals which trigger relocalization of LRRK2, possible LRRK2-induced alterations in the GTPase activity of the distinct Rab proteins, and the detailed cellular consequences of such differential relocalization for the proper functioning of the various intracellular organelles and vesicular trafficking steps.

Altogether, a picture is emerging whereby distinct stimuli may cause recruitment of LRRK2 to different subcellular sites, where it may then modulate specific vesicular trafficking pathways by acting on a subset of proteins (Fig. **2**). These proteins may be compartment-specific and/or shared between distinct subcellular compartments, and some of them may further be tissue-specific. Thus, albeit a large amount of LRRK2 protein interactors have been described, with the strength of evidence for each of these interactions carefully analyzed [119, 120], only a small subset of interactions are likely to take place in a cell-type and stimulus-dependent manner. If so, this would make LRRK2 a ubiquitous master regulator of various vesicular membrane trafficking events, with implicit challenges for therapeutic applications into its regulation.

CONCLUSIONS AND PERSPECTIVES

LRRK2 plays a crucial role in the pathomechanism(s) underlying both sporadic and familial PD. Most pathogenic mutants seem to increase the kinase activity of LRRK2, and kinase activity seems to correlate with neurotoxicity. These findings form the basis for the hypothesis that LRRK2 kinase inhibition should be a valid therapeutic drug development strategy. Indeed, kinase inhibition has been shown to have beneficial effects in various *in vivo* model systems where pathogenic LRRK2 is overexpressed. However, inhibition of LRRK2 in peripheral tissues raises safety liability issues. Therefore, it is of paramount importance to understand the cellular function(s) and dysfunction(s) associated with normal and pathogenic LRRK2, respectively. The vast majority of data indicate that LRRK2 regulates a variety of intracellular vesicular trafficking steps in a stimulus-dependent manner. Some of those cellular assays may allow for pharmacodynamic readouts of target engagement of kinase inhibitors, and help in defining appropriate dosing regimens whilst avoiding cellular toxicity. In addition, a detailed cell biological understanding of those steps, and their cell type-specific modulation will be crucial for any future attempt to move LRRK2 kinase inhibitors into a clinical setup. Whilst much remains to be done, there is great hope that some of these LRRK2-specific compounds may comprise future treatment options for people with PD.

CONFLICT OF INTEREST

The authors confirm that this article content has no conflict of interest.

ACKNOWLEDGEMENTS

Work in the laboratory is funded by FEDER, the Spanish Ministry of Economy and Competitiveness (SAF2014-58653-R), the Junta de Andalucia (CTS-6816), the BBVA Foundation and the Michael J. Fox Foundation. B.F. was funded by a Juan de la Cierva Fellowship (MINECO; JCI2010-07703).

REFERENCES

[1] Lees, A.J.; Hardy, J.; Revesz, T. Parkinson's disease. *Lancet,* **2009**, *373*(9680), 2055-2066.

[2] Wakabayashi, K.; Tanji, K.; Odagiri, S.; Miki, Y.; Mori, F.; Takahashi, H. The Lewy body in Parkinson's disease and related neurodegenerative disorders. *Mol. Neurobiol.,* **2013**, *47*(2), 495-508.

[3] Singleton, A.B.; Farrer, M.J.; Bonifati, V. The genetics of Parkinson's disease: progress and therapeutic implications. *Mov. Disord.,* **2013**, *28*(1), 14-23.

[4] Clarimón, J.; Kulisevsky, J. Parkinson's disease: from genetics to clinical practice. *Curr. Genomics,* **2013**, *14*(8), 560-567.

[5] Paisán-Ruíz, C.; Jain, S.; Evans, E.W.; Gilks, W.P.; Simón, J.; van der Brug, M.; López de Munain, A.; Aparicio, S.; Gil, A.M.; Khan, N.; Johnson, J.; Martinez, J.R.; Nicholl, D.; Carrera, I.M.; Pena, A.S.; de Silva, R.; Lees, A.; Martí-Massó, J.F.; Pérez-Tur, J.; Wood, N.W.; Singleton, A.B. Cloning of the gene containing mutations that cause PARK8-linked Parkinson's disease. *Neuron,* **2004**, *44*(4), 595-600.

[6] Zimprich, A.; Biskup, S.; Leitner, P.; Lichtner, P.; Farrer, M.; Lincoln, S.; Kachergus, J.; Hulihan, M.; Uitti, R.J.; Calne, D.B.; Stoessl, A.J.; Pfeiffer, R.F.; Patenge, N.; Carbajal, I.C.; Vieregge, P.; Asmus, F.; Müller-Myhsok, B.; Dickson, D.W.; Meitinger, T.; Strom, T.M.; Wszolek, Z.K.; Gasser, T. Mutations in LRRK2 cause autosomal-dominant parkinsonism with pleomorphic pathology. *Neuron,* **2004**, *44*(4), 601-607.

[7] Lesage, S.; Brice, A. Role of mendelian genes in "sporadic" Parkinson's disease. *Parkinsonism Relat. Disord.,* **2012**, *Suppl 1*, S66-S70.

[8] Nalls, M.A.; Pankratz, N.; Lill, C.M.; Do, C.B.; Hernandez, D.G.; Saad, M.; DeStefano, A.L.; Kara, E.; Bras, J.; Sharma, M.; Schulte, C.; Keller, M.F.; Arepalli, S.; Letson, C.; Edsall, C.; Stefansson, H.; Liu, X.; Pliner, H.; Lee, J.H.; Cheng, R.; International Parkinson's Disease Genomics Consortium (IPDGC); Parkinson's Study Group (PSG) Parkinson's Research: The Organized GENetics Initiative (PROGENI); 23andMe; GenePD; NeuroGenetics Research Consortium (NGRC); Hussman Institute of Human Genomics (HIHG); Ashkenazi Jewish Dataset Investigator; Cohorts for Health and Aging Research in Genetic Epidemiology (CHARGE); North American Brain Expression Consortium (NABEC); United Kingdom Brain Expression Consortium (UKBEC); Greek Parkinson's Disease Consortium; Alzheimer Genetic Analysis Group, Ikram, M.A.; Ioannidis, J-P.; Hadjigeorgiou, G.M.; Bis, J.C.; Martinez, M.; Perlmutter, J.S.; Goate, A.; Marder, K.; Fiske, B.; Sutherland, M.; Xiromerisiou, G.; Myers, R.H.; Clark, L.N.; Stefansson, K.; Hardy, J.A.; Heutink, P.; Chen, H.; Wood, N.W.; Houlden, H.; Payami, H.; Brice, A.; Scott, W.K.; Gasser, T.; Bertram, L.; Eriksson, N.; Foroud, T.; Singleton, A.B. Large-scale meta-analysis of genome-wide association data identifies six new risk loci for Parkinson's disease. *Nat. Genet.,* **2014**, *46*(9), 989-993.

[9] Rubio, J.P.; Topp, S.; Warren, L.; St Jean, P.L.; Wegmann, D.; Kessner, D.; Novembre, J.; Shen, J.; Fraser, D.; Aponte, J.; Nangle,

K.; Cardon, L.R.; Ehm, M.G.; Chissoe, S.L.; Whittaker, J.C.; Nelson, M.R.; Mooser, V.E. Deep sequencing of the LRRK2 gene in 14,002 individuals reveals evidence of purifying selection and independent origin of the p.Arg1628Pro mutation in Europe. *Hum. Mutat.,* **2012**, *33*(7), 1087-1098.

[10] Bosgraaf, L.; Van Haastert, P.J. Roc, a Ras/GTPase domain in complex proteins. *Biochim. Biophys. Acta.,* **2003**, *1643*(1-3), 5-10.

[11] Marín, I.; van Egmond, W.N.; van Haastert, P.J. The Roco protein family: a functional perspective. *FASEB J.,* **2008**, *22*(9), 3103-3110.

[12] Gilsbach, B.K.; Kortholt, A. Structural biology of the LRRK2 GTPase and kinase domains: implications for regulation. *Front. Mol. Neurosci.,* **2014**, *7*, 32.

[13] Mills, R.D.; Mulhern, T.D.; Liu, F.; Culvenor, J.G.; Cheng, H.C. Prediction of the repeat domain structures and impact of parkinsonism-associated variations on structure and function of all functional domains of leucine-rich repeat kinase 2 (LRRK2). *Hum. Mutat.,* **2014**, *35*(4), 395-412.

[14] Manning, G.; Whyte, D.B.; Martinez, R.; Hunter, T.; Sudarsanam, S. The protein kinase complement of the human genome. *Science,* **2002**, *298*(5600), 1912-1934.

[15] Nolen, B., Taylor, S., Ghosh, G. Regulation of protein kinases: controlling activity through activation segment conformation. *Mol. Cell,* **2004**, *15*(5), 661-675.

[16] Liu, Z.; Galemmo, R.A. Jr.; Fraser, K.B.; Moehle, M.S.; Sen, S.; Volpicelli-Daley, L.A.; DeLucas, L.J.; Ross, L.J.; Valiyaveettil, J.; Moukha-Chafiq, O.; Pathak, A.K.; Ananthan, S.; Kezar, H.; White, E.L.; Gupta. V.; Maddry, J.A.; Suto, M.J.; West, A.B. Unique functional and structural properties of the LRRK2 protein ATP-binding pocket. *J. Biol. Chem.,* **2014**, *289*(47), 32937-32951.

[17] West, A.B. Ten years and counting: moving leucine-rich repeat kinase 2 inhibitors to the clinic. *Mov. Disord*., **2015**, *30*(2), 180-189.

[18] Lewis, P.A.; Greggio, E.; Beilina, A.; Jain, S.; Baker, A.; Cookson, M.R. The R1441C mutation of LRRK2 disrupts GTP hydrolysis. *Biochem. Biophys. Res. Commun*., **2007**, *357*(3), 668-671.

[19] West, A.B.; Moore, D.J.; Choi, C.; Andrabi, S.A.; Li, X.; Dikeman, D.; Biskup, S.; Zhang, Z., Lim, K.L.; Dawson, V.L.; Dawson, T.M. Parkinson's disease-associated mutations in LRRK2 link enhanced GTP-binding and kinase activities to neuronal toxicity. *Hum. Mol. Genet*., **2007**, *16*(2), 223-232.

[20] Li, X.; Tan, Y.C.; Poulose, S.; Olanow, C.W.; Huang, X.Y.; Yue, Z. Leucine-rich repeat kinase 2 (LRRK2)/PARK8 possesses GTPase activity that is altered in familial Parkinson's disease R1441C/G mutants. *J. Neurochem.,* **2007**, *103*(1), 238-247.

[21] Guo, L.; Gandhi, P.N.; Wang, W.; Petersen, R.B.; Wilson-Delfosse, A.L.; Chen, S.G.; The Parkinson's disease-associated protein, leucine-rich repeat kinase 2 (LRRK2), is an authentic GTPase that stimulates kinase activity. *Exp. Cell Res*., **2007**, *313*(16), 3658-3670.

[22] Daniëls, V.; Vancraenenbroeck, R.; Law, B.M.; Greggio, E.; Lobbestael, E.; Gao, F.; De Maeyer, M.; Cookson, M.R.; Harvey, K.; Baekelandt, V.; Taymans, J.M. Insight into the mode of action of the LRRK2 Y1699C pathogenic mutant. *J. Neurochem.,* **2011**, *116*(2), 304-315.

[23] Liao, J.; Wu, CX.; Burlak, C.; Zhang, S.; Sahm, H.; Wang, M.; Zhang, Z.Y.; Vogel, K.W.; Federici, M.; Riddle, S.M.; Nichols, R.J.; Liu, D.; Cookson, M.R.; Stone, T.A.; Hoang, Q.Q. Parkinson disease-associated mutation R1441H in LRRK2 prolongs the "active state" of its GTPase domain. *Proc. Natl. Acad. Sci. U. S. A*., **2014**, *111*(11), 4055-4060.

[24] Ito, G.; Okai, T.; Fujino, G.; Takeda, K.; Ichijo, H.; Katada, T.; Iwatsubo, T. GTP binding is essential to the protein kinase activity of LRRK2, a causative gene product for familial Parkinson's disease. *Biochemistry*, **2007**, *46*(5), 1380-1388.

[25] Taymans, J.M.; Vancraenenbroeck, R.; Ollikainen, P.; Beilina, A.; Lobbestael, E.; De Maeyer, M.; Baekelandt, V.; Cookson, M.R. LRRK2 kinase activity is dependent on LRRK2 GTP binding capacity but independent of LRRK2 GTP binding. *PLoS One*, **2011**, *6*(8), e23207.

[26] Li, T.; Yang, D.; Zhong, S.; Thomas, J.M.; Xue, F.; Liu, J.; Kong, L.; Voulalas, P.; Hassan, H.E.; Park, J.S.; MacKerell, A.D.; Jr, Smith, W.W. Novel LRRK2 GTP-binding inhibitors reduced degeneration in Parkinson's disease cell and mouse models. *Hum. Mol. Genet.*, **2014**, *23*(23), 6212-6222.

[27] Li, T.; He, X.; Thomas, J.M.; Yang, D.; Zhong, S.; Xue, F., Smith, W.W. A novel GTP-binding inhibitor, FX2149, attenuates LRRK2 toxicity in Parkinson's disease models. *PLoS One*, **2015**, *10*(3), e0122461.

[28] Deng, J.; Lewis, P.A.; Greggio, E.; Sluch, E.; Beilina, A.; Cookson, M.R. Structure of the ROC domain from the Parkinson's disease-associated leucine-rich repeat kinase 2 reveals a dimeric GTPase. *Proc. Natl. Acad. Sci. U. S. A.*, **2008**, *105*(5), 1499-1504.

[29] Gotthardt, K.; Weyand, M.; Kortholt, A.; Van Haastert, P.J.; Wittinghofer, A. Structure of the Roc-COR domain tandem of C. tepidum, a prokaryotic homologue of the human LRRK2 Parkinson kinase. *EMBO J.,* **2008**, *27*(16), 2239-2249.

[30] Gilsbach, B.K.; Ho, F.Y.; Vetter, I.R.; van Haastert, P.J.; Wittinghofer, A.; Kortholt, A. Roco kinase structures give insights into the mechanism of Parkinson disease-related leucine-rich-repeat kinase 2 mutations. *Proc. Natl. Acad. Sci. U. S. A.*, **2012**, *109*(26), 10322-10327.

[31] Cardona, F.; Tormos-Pérez, M.; Pérez-Tur, J. Structural and functional in silico analysis of LRRK2 missense substitutions. *Mol. Biol. Rep*., **2014**, *41*(4), 2529-2542.

[32] Mills, R.D.; Mulhern, T.D.; Liu, F.; Culvenor, J.G.; Cheng, H.C. Prediction of the repeat domain structures and impact of parkinsonism-associated variations on structure and function of all functional domains of leucine-rich repeat kinase 2 (LRRK2). *Hum. Mutat.,* **2014**, *35*(4), 395-412.

[33] Mills, R.D.; Mulhern, T.D.; Cheng, H.C.; Culvenor, J.G. Analysis of LRRK2 accessory repeat domains: prediction of repeat length, number and sites of Parkinson's disease mutations. *Biochem. Soc. Trans.,* **2012**, *40*(5), 1086-1089.

[34] Greggio, E.; Cookson, M.R. Leucine-rich repeat kinase 2 mutations and Parkinson's disease: three questions. *ASN Neuro.,* **2009**, *1*(1), pii: e00002.

[35] Ray, S.; Bender, S.; Kang, S.; Lin, R.; Glicksman M.A.; Liu M. The Parkinson disease-linked LRRK2 protein mutation I2020T stabilizes an active state conformation leading to increased kinase activity. *J. Biol. Chem.,* **2014**, *289*(19), 13042-13053.

[36] Greggio, E.; Jain, S.; Kingsbury, A.; Bandopadhyay, R.; Lewis, P.; Kaganovich, A.; van der Brug, M.P.; Beilina, A.; Blackinton, J.; Thomas, K.J.; Ahmad, R.; Miller, D.W.; Kesavapany, S.; Singleton, A.; Lees, A.; Harvey, R.J.; Harvey. K.; Cookson, M.R. Kinase activity is required for the toxic effects of mutant LRRK2/dardarin. *Neurobiol. Dis.,* **2006**, *23*(2), 329-341.

[37] Smith, W.W.; Pei, Z.; Jiang, H.; Dawson, V.L.; Dawson, T.M.; Ross, C.A. Kinase activity of mutant LRRK2 mediates neuronal toxicity. *Nat. Neurosci.,* **2006**, *9*(10), 1231-1233.

[38] Lee, B.D.; Shin, J.H.; VanKampen, J.; Petrucelli, L.; West, A.B.; Ko, H.S.; Lee, Y.I.; Maguire-Zeiss, K.A.; Bowers, W.J.; Federoff, H.J.; Dawson, V.L.; Dawson, T.M. Inhibitors of leucine-rich repeat kinase-2 protect against models of Parkinson's disease. *Nat. Med.,* **2010**, *16*(9), 998-1000.

[39] MacLeod, D.; Dowman, J.; Hammond, R.; Leete, T.; Inoue, K.; Abeliovich, A. The familial Parkinsonism gene LRRK2 regulates neurite process morphology. *Neuron,* **2006**, *52*(4), 587-593.

[40] Herzig, M.C.; Kolly, C.; Persohn, E.; Theil, D.; Schweizer, T.; Hafner, T.; Stemmelen, C.; Troxler, T.J.; Schmid, P.; Danner, S.; Schnell, C.R.; Mueller, M.; Kinzel, B.; Grevot, A.; Bolognani, F.; Stirn, M.; Kuhn, R.R.; Kaupmann, K.; van der Putten, P.H.; Rovelli, G.; Shimshek, D.R. LRRK2 protein levels are determined by kinase function and are crucial for kidney and lung homeostasis in mice. *Hum. Mol. Genet.*, **2011**, *20*(21), 4209-4223.

[41] Yao, C.; Johnson, W.M.; Gao, Y.; Wang, W.; Zhang, J.; Deak, M.; Alessi, D.R.; Zhu, X.; Mieyal, J.J.; Roder, H.; Wilson-Delfosse, A.L.; Chen, S.G. Kinase inhibitors arrest neurodegeneration in cell and C. elegans models of LRRK2 toxicity. *Hum. Mol. Genet.*, **2013**, *22*(2), 328-344.

[42] Stafa, K.; Trancikova, A.; Webber, P.J.; Glauser, L.; West, A.B.; Moore, D.J. GTPase activity and neuronal toxicity of Parkinson's disease-associated LRRK2 is regulated by ArfGAP1. *PLoS Genet*., **2012**, *8*(2), e1002526.

[43] Xiong, Y.; Yuan, C.; Chen, R.; Dawson, T.M.; Dawson, V.L. ArfGAP1 is a GTPase activating protein for LRRK2: reciprocal regulation of ArfGAP1 by LRRK2. *J. Neurosci*., **2012**, *32*(11), 3877-3886.

[44] Dusonchet, J.; Li, H.; Guillily, M.; Liu, M.; Stafa, K.; Derada, Troletti C.; Boon, J.Y.; Saha, S.; Glauser, L.; Mamais, A.; Citro, A.; Youmans, KL.; Liu, L.; Schneider, BL.; Aebischer, P.; Yue, Z.;

Bandopadhyay, R.; Glicksman, M.A.; Moore, D.J.; Collins, JJ.; Wolozin, B. A Parkinson's disease gene regulatory network identifies the signaling protein RGS2 as a modulator of LRRK2 activity and neuronal toxicity. *Hum. Mol. Genet*., **2014**, *23*(18), 4887-4905.

[45] Haebig, K.; Gloeckner, C.J.; Miralles, M.G.; Gillardon, F.; Schulte, C.; Riess, O.; Ueffing, M.; Biskup, S.; Bonin, M. ARHGEF7 (Beta-PIX) acts as guanine nucleotide exchange factor for leucine-rich repeat kinase 2. *PLoS One*, **2010**, *5*(10), e13762.

[46] Gasper, R.; Meyer, S.; Gotthardt, K.; Sirajuddin, M.; Wittinghofer, A. It takes two to tango: regulation of G proteins by dimerization. *Nat. Rev. Mol. Cell. Biol*., **2009**, *10*(6), 423-429.

[47] Greggio, E.; Zambrano, I.; Kaganovich, A.; Beilina, A.; Taymans, J.M.; Daniëls, V.; Lewis, P.; Jain, S.; Ding, J.; Syed, A.; Thomas, K.J.; Baekelandt, V.; Cookson, M.R. The Parkinson disease-associated leucine-rich repeat kinase 2 (LRRK2) is a dimer that undergoes intramolecular autophosphorylation. *J. Biol. Chem.,* **2008**, *283*(24), 16906-16914.

[48] Sen, S.; Webber, P.J.; West, A.B. Dependence of leucine-rich repeat kinase 2 (LRRK2) kinase activity on dimerization. *J. Biol. Chem.,* **2009**, *284*(52), 36346-36356.

[49] Berger, Z.; Smith, K.A.; Lavoie, M.J. Membrane localization of LRRK2 is associated with increased formation of the highly active LRRK2 dimer and changes in its phosphorylation. *Biochemistry,* **2010**, *49*(26), 5511-5523.

[50] Webber, P.J.; Smith, A.D.; Sen, S.; Renfrow, M.B.; Mobley, J.A.; West, A.B. Autophosphorylation in the leucine-rich repeat kinase 2 (LRRK2) GTPase domain modifies kinase and GTP-binding activities. *J. Mol. Biol*., **2011**, *412*(1), 94-110.

[51] Sheng, Z.; Zhang, S.; Bustos, D.; Kleinheinz, T.; Le Pichon, C.E.; Dominguez, S.L.; Solanoy, H.O.; Drummond, J.; Zhang, X.; Ding, X.; Cai, F.; Song, Q.; Li, X.; Yue, Z.; van der Brug, M.P.; Burdick, D.J.; Gunzner-Toste, J.; Chen, H.; Liu, X.; Estrada, A.A.; Sweeney, Z.K.; Scearce-Levie, K.; Moffat, J.G.; Kirkpatrick, D.S.; Zhu, H. Ser1292 autophosphorylation is an indicator of LRRK2 kinase activity and contributes to the cellular effects of PD mutations. *Sci. Transl. Med*., **2012**, *4*(164), 164ra161.

[52] Nichols, R.J.; Dzamko, N.; Morrice, N.A.; Campbell, D.G.; Deak, M.; Ordureau, A.; Macartney, T.; Tong, Y.; Shen, J.; Prescott, A.R.; Alessi, D.R. 14-3-3 binding to LRRK2 is disrupted by multiple Parkinson's disease-associated mutations and regulates cytoplasmic localization. *Biochem. J.,* **2010**, *430*(3), 393-404.

[53] Jaleel, M.; Nichols, R.J.; Deak, M.; Campbell, D.G.; Gillardon, F.; Knebel, A.; Alessi, D.R. LRRK2 phosphorylates moesin at threonine-558: characterization of how Parkinson's disease mutants affect kinase activity. *Biochem. J.*, **2007**, *405*(2), 307-317.

[54] Rudenko, I.N.; Kaganovich, A.; Hauser, D.N.; Beylina, A.; Chia, R.; Ding, J.; Maric, D.; Jaffe, H.; Cookson, M.R. The G2385R variant of leucine-rich repeat kinase 2 associated with Parkinson's disease is a partial loss-of-function mutation. *Biochem. J.*, **2012**, *446*(1), 99-111.

[55] Nichols, R.J.; Dzamko, N.; Hutti, J.E.; Cantley, L.C.; Deak, M.; Moran, J.; Bamborough, P.; Reith, A.D.; Alessi, D.R. Substrate specificity and inhibitors of LRRK2, a protein kinase mutated in Parkinson's disease. *Biochem. J.*, **2009**, *424*(1), 47-60.

[56] Parisiadou, L.; Xie, C.; Cho, H.J.; Lin, X.; Gu, X.L.; Long, C.X.; Lobbestael, E.; Baekelandt, V.; Taymans, J.M.; Sun, L.; Cai, H. Phosphorylation of ezrin/radixin/moesin proteins by LRRK2 promotes the rearrangement of actin cytoskeleton in neuronal morphogenesis. *J. Neurosci.*, **2009**, *29*(44), 13971-13980.

[57] Kwiatkowski, A.P.; Shell, D.J.; King, M.M. The role of autophosphorylation in activation of the type II calmodulin-dependent protein kinase. *J. Biol. Chem.,* **1988**; *263*(14), 6484-6486.

[58] Saitoh, T.; Schwartz, J.H. Phosphorylation-dependent subcellular translocation of a Ca2+/calmodulin-dependent protein kinase produces an autonomous enzyme in Aplysia neurons. *J. Cell Biol.,* **1985**, *100*(3), 835-842.

[59] Pungaliya, P.P.; Bai, Y.; Lipinski, K.; Anand, V.S.; Sen, S.; Brown, E.L.; Bates, B.; Reinhart, P.H.; West, A.B.; Hirst, W.D.; Braithwaite, S.P. Identification and characterization of a leucine-rich repeat kinase 2 (LRRK2) consensus phosphorylation motif. *PLoS One*, **2010**, *5*(10), e13672.

[60] Li, X.; Moore, D.J.; Xiong, Y.; Dawson, T.M.; Dawson, V.L. Re-evaluation of phosphorylation sites in the Parkinson disease-associated leucine-rich repeat kinase 2. *J. Biol. Chem*., **2010**, *285*(38), 29569-29576.

[61] Gloeckner, C.J.; Boldt, K.; von Zweydorf, F.; Helm, S.; Wiesent, L.; Sarioglu, H.; Ueffing, M. Phosphopeptide analysis reveals two discrete clusters of phosphorylation in the N-terminus and the Roc domain of the Parkinson-disease associated protein kinase LRRK2. *J. Proteome Res.,* **2010**, *9*(4), 1738-1745.

[62] Kamikawaji, S.; Ito, G.; Iwatsubo, T. Identification of the autophosphorylation sites of LRRK2. *Biochemistry*, **2009**, *48*(46), 10963-10975.

[63] Greggio, E.; Taymans, J.M.; Zhen, E.Y.; Ryder, J.; Vancraenenbroeck, R.; Beilina, A.; Sun, P.; Deng, J.; Jaffe, H.; Baekelandt, V.; Merchant, K.; Cookson, M.R. The Parkinson's disease kinase LRRK2 autophosphorylates its GTPase domain at multiple sites. *Biochem. Biophys. Res. Commun*., **2009**, *389*(3), 449-454.

[64] Luzón-Toro, B.; Rubio de la Torre, E.; Delgado, A.; Pérez-Tur, J.; Hilfiker, S. Mechanistic insight into the dominant mode of the Parkinson's disease-associated G2019S LRRK2 mutation. *Hum. Mol. Genet*., **2007**, *16*(17), 2031-2039.

[65] Dzamko, N.; Deak, M.; Hentati, F.; Reith, A.D.; Prescott, A.R.; Alessi, D.R.; Nichols, R.J. Inhibition of LRRK2 kinase activity leads to dephosphorylation of Ser(910)/Ser(935), disruption of 14-3-3 binding and altered cytoplasmic localization. *Biochem. J.,* **2010**, *430*(3), 405-413.

[66] Deng, X.; Dzamko, N.; Prescott, A.; Davies, P.; Liu, Q.; Yang, Q.; Lee, J.D.; Patricelli, M.P.; Nomanbhoy, T.K.; Alessi, D.R.; Gray, N.S. Characterization of a selective inhibitor of the Parkinson's disease kinase LRRK2. *Nat. Chem. Biol.,* **2011**, *7*(4), 203-205.

[67] Li, X.; Wang, Q.J.; Pan, N.; Lee, S.; Zhao, Y.; Chait, B.T.; Yue, Z. Phosphorylation-dependent 14-3-3 binding to LRRK2 is impaired by common mutations of familial Parkinson's disease. *PLoS One*, **2011**, *6*(3), e17153.

[68] Doggett, E.A.; Zhao, J.; Mork, C.N.; Hu, D.; Nichols, R.J. Phosphorylation of LRRK2 serines 955 and 973 is disrupted by Parkinson's disease mutations and LRRK2 pharmacological inhibition. *J. Neurochem*., **2012**, *120*(1), 37-45.

[69] Dzamko, N.; Inesta-Vaquera, F.; Zhang, J.; Xie, C.; Cai, H.; Arthur, S.; Tan, L., Choi, H.; Gray, N.; Cohen, P.; Pedrioli, P.; Clark, K.; Alessi, D.R. The IkappaB kinase family phosphorylates the Parkinson's disease kinase LRRK2 at Ser935 and Ser910 during Toll-like receptor signaling. *PLoS One*, **2012**, *7*(6), e39132.

[70] Muda, K.; Bertinetti, D.; Gesellchen, F.; Hermann, J.S.; von Zweydorf, F.; Geerlof, A.; Jacob, A.; Ueffing, M.; Gloeckner, C.J.; Herberg, F.W. Parkinson-related LRRK2 mutation R1441C/G/H impairs PKA phosphorylation of LRRK2 and disrupts its interaction with 14-3-3. *Proc. Natl. Acad. Sci. U. S. A.*, **2014**, *111*(1), 34-43.

[71] Chia R.; Haddock S.; Beilina A.; Rudenko I.N.; Mamais A.; Kaganovich A.; Li Y.; Kumaran R.; Nalls M.A.; Cookson M.R. Phosphorylation of LRRK2 by casein kinase 1α regulates trans-Golgi clustering via differential interaction with ARHGEF7. *Nat. Commun*., **2014**, *5*, 5827.

[72] Lobbestael, E.; Zhao, J.; Rudenko, I.N.; Beylina, A.; Gao, F.; Wetter, J.; Beullens, M.; Bollen, M.; Cookson, M.R.; Baekelandt, V.; Nichols, R.J.; Taymans, J.M. Identification of protein phosphatase 1 as a regulator of the LRRK2 phosphorylation cycle. *Biochem. J.*, **2013**, *456*(1), 119-128.

[73] Reynolds, A.; Doggett, E.A.; Riddle, S.M.; Lebakken, C.S.; Nichols, R.J. LRRK2 kinase activity and biology are not uniformly predicted by its autophosphorylation and cellular phosphorylation site status. *Front. Mol. Neurosci.*, **2014**, *7*, 54.

[74] Vancraenenbroeck, R.; De Raeymaecker, J.; Lobbestael, E.; Gao, F.; De Maeyer, M.; Voet, A.; Baekelandt, V.; Taymans, J.M. In silico, *in vitro* and cellular analysis with a kinome-wide inhibitor panel correlates cellular LRRK2 dephosphorylation to inhibitor activity on LRRK2. *Front. Mol. Neurosci.*, **2014**, 7, 51. doi: 10.3389/fnmol.2014.00051.

[75] Ito, G.; Fujimoto, T.; Kamikawaji, S.; Kuwahara, T.; Iwatsubo, T. Lack of correlation between the kinase activity of LRRK2 harboring kinase-modifying mutations and its phosphorylation at Ser910, 935, and Ser955. *PLoS One*, **2014**, *9*(5), e97988.

[76] Reith, A.D.; Bamborough, P.; Jandu, K.; Andreotti, D.; Mensah, L.; Dossang, P.; Choi, H.G.; Deng, X.; Zhang, J.; Alessi, D.R.; Gray, N.S. GSK2578215A; a potent and highly selective 2-arylmethyloxy-5-substitutent-N-arylbenzamide LRRK2 kinase inhibitor. *Bioorg. Med. Chem. Lett.*, **2012**, *22*(17), 5625-5629.

[77] Estrada, A.A.; Chan, B.K.; Baker-Glenn, C.; Beresford, A.; Burdick, D.J.; Chambers, M.; Chen, H.; Dominguez, S.L.; Dotson, J.; Drummond, J.; Flagella, M.; Fuji, R.; Gill, A.; Halladay, J.; Har-

ris, S.F.; Heffron, T.P.; Kleinheinz, T.; Lee, D.W.; Le Pichon, C.E.; Liu, X.; Lyssikatos, J.P.; Medhurst, A.D.; Moffat, J.G.; Nash, K.; Scearce-Levie, K.; Sheng, Z.; Shore, D.G.; Wong, S.; Zhang, S.; Zhang, X.; Zhu, H.; Sweeney, Z.K. Discovery of highly potent, selective, and brain-penetrant aminopyrazole leucine-rich repeat kinase 2 (LRRK2) small molecule inhibitors. *J. Med. Chem.*, **2014**, *57*(3), 921-936.

[78] Fuji, R.N.; Flagella, M.; Baca, M.; S Baptista, M.A.; Brodbeck, J.; Chan, B.K.; Fiske, B.K.; Honigberg, L.; Jubb, A.M.; Katavolos, P.; Lee, D.W.; Lewin-Koh, S.C.; Lin, T.; Liu, X.; Liu, S.; Lyssikatos, J.P.; O'Mahony, J.; Reichelt, M.; Roose-Girma, M.; Sheng, Z.; Sherer, T.; Smith, A.; Solon, M.; Sweeney, Z.K.; Tarrant, J.; Urkowitz, A.; Warming, S.; Yaylaoglu, M.; Zhang, S.; Zhu, H.; Estrada, A.A.; Watts, R.J. Effect of selective LRRK2 kinase inhibition on nonhuman primate lung. *Sci. Transl. Med.*, **2015**, *7*(273), 273ra15.

[79] Tong, Y.; Giaime, E.; Yamaguchi, H.; Ichimura, T.; Liu, Y.; Si, H.; Cai, H.; Bonventre, J.V.; Shen, J. Loss of leucine-rich repeat kinase 2 causes age-dependent bi-phasic alterations of the autophagy pathway. *Mol. Neurodegener.*, **2012**, *7*, 2.

[80] Ness, D.; Ren, Z.; Gardai, S.; Sharpnack, D.; Johnson, V.J.; Brennan, R.J.; Brigham, E.F.; Olaharski, A.J. Leucine-rich repeat kinase 2 (LRRK2)-deficient rats exhibit renal tubule injury and perturbations in metabolic and immunological homeostasis. *PLoS One*, **2013**, *8*(6), e66164.

[81] Baptista, M.A.; Dave, K.D.; Frasier, M.A.; Sherer, T.B.; Greeley, M.; Beck, M.J.; Varsho, J.S.; Parker, G.A.; Moore, C.; Churchill, M.J.; Meshul, C.K.; Fiske, B.K. Loss of leucine-rich repeat kinase 2 (LRRK2) in rats leads to progressive abnormal phenotypes in peripheral organs. *PLoS One*, **2013**, *8*(11), e80705.

[82] Westerlund, M.; Belin, A.C.; Anvret, A.; Bickford, P.; Olson, L.; Galter, D. Developmental regulation of leucine-rich repeat kinase 1 and 2 expression in the brain and other rodent and human organs: Implications for Parkinson's disease. *Neuroscience*, **2008**, *152*(2), 429-436.

[83] Iaccarino, C.; Crosio, C.; Vitale, C.; Sanna, G.; Carrì, M.T.; Barone, P. Apoptotic mechanisms in mutant LRRK2-mediated cell death. *Hum. Mol. Genet.*, **2007**, *16*(11), 1319-1326.

[84] Skibinski, G.; Nakamura, K.; Cookson, M.R.; Finkbeiner, S. Mutant LRRK2 toxicity in neurons depends on LRRK2 levels and synuclein but not kinase activity or inclusion bodies. *J. Neurosci.*, **2014**, *34*(2), 418-433.

[85] Tsika, E.; Nguyen, A.P.; Dusonchet, J.; Colin, P.; Schneider, B.L.; Moore, D.J. Adenoviral-mediated expression of G2019S LRRK2 induces striatal pathology in a kinase-dependent manner in a rat model of Parkinson's disease. *Neurobiol. Dis.*, **2015**, *77*, 49-61.

[86] Shin, N.; Jeong, H.; Kwon, J.; Heo, H.Y.; Kwon, J.J.; Yun, H.J.; Kim, C.H.; Han, B.S.; Tong, Y.; Shen, J.; Hatano, T.; Hattori, N.; Kim, K.S.; Chang, S.; Seol, W. LRRK2 regulates synaptic vesicle endocytosis. *Exp. Cell Res.*, **2008**, *314*(10), 2055-2065.

[87] Piccoli, G.; Condliffe, S.B.; Bauer, M.; Giesert, F.; Boldt, K.; De Astis, S.; Meixner, A.; Sarioglu, H.; Vogt-Weisenhorn, D.M.; Wurst, W.; Gloeckner, C.J.; Matteoli, M.; Sala, C.; Ueffing, M. LRRK2 controls synaptic vesicle storage and mobilization within the recycling pool. *J. Neurosci.*, **2011**, *31*(6), 2225-2237.

[88] Matta, S.; Van Kolen, K.; da Cunha, R.; van den Bogaart, G.; Mandemakers, W.; Miskiewicz, K.; De Bock, P.J.; Morais, V.A.; Vilain, S.; Haddad, D.; Delbroek, L.; Swerts, J.; Chávez-Gutiérrez, L.; Esposito, G.; Daneels, G.; Karran, E.; Holt, M.; Gevaert, K.; Moechars, D.W.; De Strooper, B.; Verstreken, P. LRRK2 controls an EndoA phosphorylation cycle in synaptic endocytosis. *Neuron*, **2012**, *75*(6), 1008-1021.

[89] Arranz, A.M.; Delbroek, L.; Van Kolen, K.; Guimarães, M.R.; Mandemakers, W.; Daneels, G.; Matta, S.; Calafate, S.; Shaban, H.; Baatsen, P.; De Bock, P.J.; Gevaert, K.; Vanden Berghe, P.; Verstreken P.; De Strooper, B.; Moechars, D. LRRK2 functions in synaptic vesicle endocytosis through a kinase-dependent mechanism. *J. Cell Sci.*, **2015**, *128*(3), 541-552.

[90] Schreij, A.M.; Chaineau, M.; Ruan, W.; Lin, S.; Barker, P.A.; Fon, E.A.; McPherson, P.S. LRRK2 localizes to endosomes and interacts with clathrin-light chains to limit Rac1 activation. *EMBO Rep.*, **2015**, *16*(1), 79-86.

[91] Gómez-Suaga, P.; Rivero-Ríos, P.; Fdez, E.; Blanca Ramírez, M.; Ferrer, I.; Aiastui, A.; López De Munain, A.; Hilfiker, S. LRRK2 delays degradative receptor trafficking by impeding late endosomal budding through decreasing Rab7 activity. *Hum. Mol. Genet.*, **2014**, *23*(25), 6779-6796.

[92] Plowey, E.D.; Cherra, S.J. 3rd; Liu, Y.J.; Chu, C.T. Role of autophagy in G2019S-LRRK2-associated neurite shortening in differentiated SH-SY5Y cells. *J. Neurochem.*, **2008**, *105*(3), 1048-1056.

[93] Alegre-Abarrategui, J.; Christian, H.; Lufino, M.M.; Mutihac, R.; Venda, L.L.; Ansorge, O.; Wade-Martins, R. LRRK2 regulates autophagic activity and localizes to specific membrane microdomains in a novel human genomic reporter cellular model. *Hum. Mol. Genet.,* **2009**, *18*(21), 4022-4034.

[94] Ramonet, D.; Daher, J.P.; Lin, B.M.; Stafa, K.; Kim, J.; Banerjee, R.; Westerlund, M.; Pletnikova, O.; Glauser, L.; Yang, L.; Liu, Y.; Swing, D.A.; Beal, M.F.; Troncoso, J.C.; McCaffery, J.M.; Jenkins, N.A.; Copeland, N.G.; Galter, D.; Thomas, B.; Lee, M.K.; Dawson, T.M.; Dawson, V.L.; Moore, D.J. Dopaminergic neuronal loss, reduced neurite complexity and autophagic abnormalities in transgenic mice expressing G2019S mutant LRRK2. *PLoS One,* **2011**, *6*(4), e18568.

[95] Gómez-Suaga, P.; Luzón-Toro, B.; Churamani, D.; Zhang, L.; Bloor-Young, D.; Patel, S.; Woodman, P.G.; Churchill, G.C.; Hilfiker, S. Leucine-rich repeat kinase 2 regulates autophagy through a calcium-dependent pathway involving NAADP. *Hum. Mol. Genet.,* **2012**, *21*(3), 511-525.

[96] Sánchez-Danés, A.; Richaud-Patin, Y.; Carballo-Carbajal, I.; Jiménez-Delgado, S.; Caig, C.; Mora, S.; Di Guglielmo, C.; Ezquerra, M.; Patel, B.; Giralt, A.; Canals, J.M.; Memo, M.; Alberch, J.; López-Barneo, J.; Vila, M.; Cuervo, A.M.; Tolosa, E.; Consiglio, A.; Raya, A. Disease-specific phenotypes in dopamine neurons from human iPS-based models of genetic and sporadic Parkinson's disease. *EMBO Mol. Med.*, **2012**, *4*(5), 380-395.

[97] Bravo-San Pedro, J.M.; Niso-Santano, M.; Gómez-Sánchez, R.; Pizarro-Estrella, E.; Aiastui-Pujana, A.; Gorostidi, A.; Climent, V.; López de Maturana, R.; Sanchez-Pernaute, R.; López de Munain, A.; Fuentes, J.M.; González-Polo, R.A. The LRRK2 G2019S mutant exacerbates basal autophagy through activation of the MEK/ERK pathway. *Cell. Mol. Life Sci.,* **2013**, *70*(1), 121-136.

[98] Cherra, S.J. 3rd; Steer, E.; Gusdon, A.M.; Kiselyov, K.; Chu, C.T. Mutant LRRK2 elicits calcium imbalance and depletion of dendritic mitochondria in neurons. *Am. J. Pathol.,* **2013**, *182*(2), 474-484.

[99] Hindle, S.; Afsari, F.; Stark, M.; Middleton, C.A.; Evans, G.J.; Sweeney, S.T.; Elliott, C.J. Dopaminergic expression of the Parkinsonian gene LRRK2-G2019S leads to non-autonomous visual neurodegeneration, accelerated by increased neural demands for energy. *Hum. Mol. Genet.,* **2013**, *22*(11), 2129-2140.

[100] Orenstein, S.J.; Kuo, S.H.; Tasset, I.; Arias, E.; Koga, H.; Fernandez-Carasa, I.; Cortes, E.; Honig, L.S.; Dauer, W.; Consiglio, A.; Raya, A.; Sulzer, D.; Cuervo, A.M. Interplay of LRRK2 with chaperone-mediated autophagy. *Nat. Neurosci.,* **2013**, *16*(4), 394-406.

[101] Su, Y.C.; Qi, X. Inhibition of excessive mitochondrial fission reduced aberrant autophagy and neuronal damage caused by LRRK2 G2019S mutation. *Hum. Mol. Genet.*, **2013**, *22*(22), 4545-4561.

[102] Manzoni, C.; Mamais, A.; Dihanich, S.; Abeti, R.; Soutar, M.P.; Plun-Favreau, H.; Giunti, P.; Tooze, S.A.; Bandopadhyay, R.; Lewis, P.A. Inhibition of LRRK2 kinase activity stimulates macroautophagy. *Biochim. Biophys. Acta*, **2013**, *1833*(12), 2900-2910.

[103] Saha, S.; Liu-Yesucevitz, L.; Wolozin, B. Regulation of autophagy by LRRK2 in Caenorhabditis elegans. *Neurodegener. Dis.*, **2014**, *13*(2-3), 110-113.

[104] Manzoni, C.; Mamais, A.; Dihanich, S.; McGoldrick, P.; Devine, M.J.; Zerle, J.; Kara, E.; Taanman, J.W.; Healy, D.G.; Marti-Masso, J.F.; Schapira, A.H.; Plun-Favreau, H.; Tooze, S.; Hardy, J.; Bandopadhyay, R.; Lewis, P.A. Pathogenic Parkinson's disease mutations across the functional domains of LRRK2 alter the autophagic/lysosomal response to starvation. *Biochem. Biophys. Res. Commun.*, **2013**, *441*(4), 862-866.

[105] Yakhine-Diop, S.M.; Bravo-San Pedro, J.M.; Gómez-Sánchez, R.; Pizarro-Estrella, E.; Rodríguez-Arribas, M.; Climent, V.; Aiastui, A.; López de Munain, A.; Fuentes, J.M.; González-Polo, R.A. G2019S LRRK2 mutant fibroblasts from Parkinson's disease patients show increased sensitivity to neurotoxin 1-methyl-4-phenylpyridinium dependent of autophagy. *Toxicology*, **2014**, *324*, 1-9.

[106] Saez-Atienzar, S.; Bonet-Ponce, L.; Blesa, J.R.; Romero, F.J.; Murphy, M.P.; Jordan, J.; Galindo, M.F. The LRRK2 inhibitor GSK2578215A induces protective autophagy in SH-SY5Y cells:

involvement of Drp-1-mediated mitochondrial fission and mitochondrial-derived ROS signaling. *Cell Death Dis.,* **2014**, *5*, e1368.

[107] Schapansky, J.; Nardozzi, J.D.; Felizia, F.; LaVoie, M.J. Membrane recruitment of endogenous LRRK2 precedes its potent regulation of autophagy. *Hum. Mol. Genet.,* **2014**, *23*(16), 4201-4214.

[108] Dodson, M.W.; Zhang, T.; Jiang, C.; Chen, S.; Guo, M. Roles of the Drosophila LRRK2 homolog in Rab7-dependent lysosomal positioning. *Hum. Mol. Genet.,* **2012**, *21*(6), 1350-1363.

[109] Dodson, M.W.; Leung, L.K.; Lone, M.; Lizzio, M.A.; Guo, M.; Novel ethyl methanesulfonate (EMS)-induced null alleles of the Drosophila homolog of LRRK2 reveal a crucial role in endolysosomal functions and autophagy *in vivo*. *Dis. Model Mech.,* **2014**, *7*(12), 1351-1363.

[110] Beilina, A.; Rudenko, I.N.; Kaganovich, A.; Civiero, L.; Chau, H.; Kalia, S.K.; Kalia, L.V.; Lobbestael, E.; Chia, R.; Ndukwe, K.; Ding, J.; Nalls, M.A. International Parkinson's Disease Genomics Consortium. North American Brain Expression Consortium; Olszewski, M.; Hauser, D.N.; Kumaran, R.; Lozano, A.M.; Baekelandt, V.; Greene, L.E.; Taymans, J.M.; Greggio, E.; Cookson, M.R. Unbiased screen for interactors of leucine-rich repeat kinase 2 supports a common pathway for sporadic and familial Parkinson disease. *Proc. Natl. Acad. Sci. U. S. A.*, **2014**, *111*(7), 2626-2631.

[111] MacLeod, D.A.; Rhinn, H.; Kuwahara, T.; Zolin, A.; Di Paolo, G.; McCabe, B.D.; Marder, K.S.; Honig, L.S.; Clark, L.N.; Small, S.A.; Abeliovich, A. RAB7L1 interacts with LRRK2 to modify intraneuronal protein sorting and Parkinson's disease risk. *Neuron*, **2013**, *77*(3), 425-439.

[112] Gómez-Suaga, P.; Fdez, E.; Fernández, B.; Martínez-Salvador, M.; Blanca Ramírez, M.; Madero-Pérez, J.; Rivero-Ríos, P.; Fuentes, J.M.; Hilfiker, S. Novel insights into the neurobiology underlying LRRK2-linked Parkinson's disease. *Neuropharmacology,* **2014**, 85, 45-56.

[113] Hutagalung, A.H.; Novick, P.J. Role of Rab GTPases in membrane traffic and cell physiology. *Physiol. Rev.*, **2011**, *91*(1), 119-149.

[114] Stenmark, H. Rab GTPases as coordinators of vesicle traffic. *Nat. Rev. Mol. Cell. Biol.*, **2009**, *10*(8), 513-525.

[115] Bultema, J.J.; Di Pietro, S.M. Cell type-specific Rab32 and Rab38 cooperate with the ubiquitous lysosome biogenesis machinery to synthesize specialized lysosome-related organelles. *Small GTPases*, **2013**, *4*(1), 16-21.

[116] Waschbüsch D.; Michels H.; Strassheim S.; Ossendorf E.; Kessler D.; Gloeckner C.J.; Barnekow A. LRRK2 transport is regulated by its novel interacting partner Rab32. *PLoS One*, **2014**, *9*(10), e111632.

[117] Helip-Wooley, A.; Thoene, J.G. Sucrose-induced vacuolation results in increased expression of cholesterol biosynthesis and lysosomal genes. *Exp. Cell Res.,* **2004**, *292*(1), 89-100.

[118] Wang, S.; Ma, Z.; Xu, X.; Wang, Z.; Sun, L.; Zhou, Y.; Lin, X.; Hong, W.; Wang, T. A role of Rab29 in the integrity of the trans-Golgi network and retrograde trafficking of mannose-6-phosphate receptor. *PLoS One*, **2014**, *9*(5), e96242.

[119] Manzoni, C.; Denny, P.; Lovering, R.C.; Lewis, P.A. Computational analysis of the LRRK2 interactome. *PeerJ.*, **2015**, *3*, e778.

[120] Porras, P.; Duesbury, M.; Fabregat, A.; Ueffing, M.; Orchard, S.; Gloeckner, C.J.; Hermjakob, H. A visual review of the interactome of LRRK2: Using deep-curated molecular interaction data to represent biology. *Proteomics,* **2015**, *15*(8), 1390-1404.

Received: December 02, 2015 Revised: January 08, 2016 Accepted: January 08, 2016

2. LRRK2: from kinase to GTPase to microtubules and back.

Biochemical Society Transactions (2017) **45** 141–146
DOI: 10.1042/BST20160333

Review Article

LRRK2: from kinase to GTPase to microtubules and back

Marian Blanca Ramírez, Antonio Jesús Lara Ordóñez, Elena Fdez and Sabine Hilfiker

Institute of Parasitology and Biomedicine 'López-Neyra', Consejo Superior de Investigaciones Científicas (CSIC), Avda del Conocimiento s/n, 18016 Granada, Spain

Correspondence: Sabine Hilfiker (sabine.hilfiker@ipb.csic.es)

Mutations in the *Leucine-Rich Repeat Kinase 2* (*LRRK2*) gene are intimately linked to both familial and sporadic Parkinson's disease. LRRK2 is a large protein kinase able to bind and hydrolyse GTP. A wealth of *in vitro* studies have established that the distinct pathogenic LRRK2 mutants differentially affect those enzymatic activities, either causing an increase in kinase activity without altering GTP binding/GTP hydrolysis, or displaying no change in kinase activity but increased GTP binding/decreased GTP hydrolysis. Importantly, recent studies have shown that all pathogenic LRRK2 mutants display increased kinase activity towards select kinase substrates when analysed in intact cells. To understand those apparently discrepant results, better insight into the cellular role(s) of normal and pathogenic LRRK2 is crucial. Various studies indicate that LRRK2 regulates numerous intracellular vesicular trafficking pathways, but the mechanism(s) by which the distinct pathogenic mutants may equally interfere with such pathways has largely remained elusive. Here, we summarize the known alterations in the catalytic activities of the distinct pathogenic LRRK2 mutants and propose a testable working hypothesis by which the various mutants may affect membrane trafficking events in identical ways by culminating in increased phosphorylation of select substrate proteins known to be crucial for membrane trafficking between specific cellular compartments.

Introduction

Parkinson's disease (PD) is a common neurodegenerative disorder of largely unknown aetiology, with ageing as a major risk factor [1]. Over a decade ago, mutations in the *Leucine-Rich Repeat kinase 2* (*LRRK2*) gene were reported to cause autosomal-dominant PD [2,3]. Subsequent reports revealed that mutations in LRRK2 comprise the most common cause for familial PD and that several LRRK2 variants either positively or negatively correlate with PD risk [4,5], highlighting the importance of LRRK2 in disease pathogenesis.

The LRRK2 protein comprises various domains implicated in protein–protein interactions and a central region consisting of a Ras-of-complex (ROC) GTPase domain and a kinase domain connected via a C-terminal of ROC (COR) domain (Figure 1). All currently identified pathogenic mutations cluster in this central region, suggesting that targeting those activities may allow for the development of disease-modifying therapies. Towards this end, highly selective, potent and brain-permeable LRRK2 kinase inhibitors have been developed [6], and our understanding of the alterations in the catalytic activities of the various pathogenic LRRK2 mutants has greatly increased over the past years. However, there remain big gaps in our understanding of the cellular role(s) of LRRK2 in neuronal as well as non-neuronal cells, even though such understanding is critical for successfully bringing LRRK2-related drugs into the clinic.

LRRK2 is expressed in many tissues, suggesting that it regulates events common to various distinct cell types. Indeed, pathogenic LRRK2 has been reported to have an impact upon several conserved vesicular trafficking steps related to endocytic uptake, endosome–lysosome and autophagosome–lysosome trafficking as well as retromer-mediated trafficking to and from the Golgi complex [7]. Mechanistically,

Received: 16 September 2016
Revised: 14 October 2016
Accepted: 18 October 2016

Version of Record published:
15 February 2017

Biochemical Society Transactions (2017) **45** 141–146
DOI: 10.1042/BST20160333

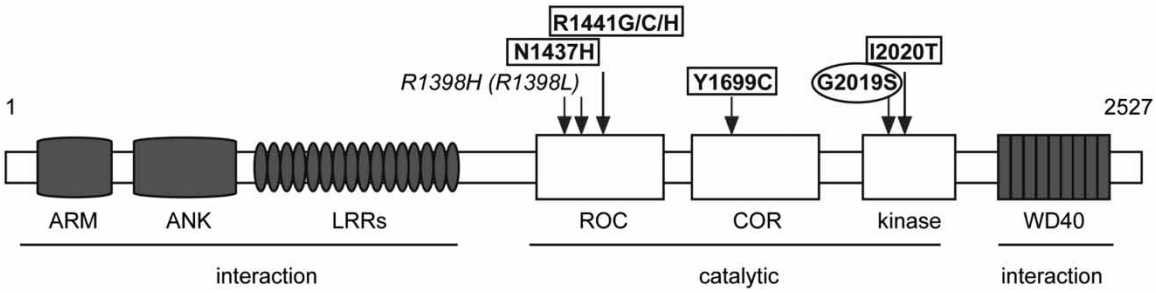

Figure 1. Schematic representation of the domain structure of LRRK2, including armadillo repeats (ARM), ankyrin repeats (ANK), leucine-rich repeats (LRRs), a ROC domain, a COR domain, a kinase domain and a C-terminal WD40 domain.

Pathogenic mutations are indicated in bold. The mutation which increases kinase activity *in vitro* without altering GTP binding/GTP hydrolysis is circled; the mutations which do not alter kinase activity *in vitro* but cause increased GTP binding/decreased GTP hydrolysis are boxed. The protective R1398H variant (or synthetic R1398L mutation) is shown in italics. For further details, see text.

this may involve direct and/or indirect regulation of several distinct Rab proteins [7–14]. Rab proteins comprise a family of over 60 small GTPases which function as molecular switches, alternating between a GTP-bound active form and a GDP-bound inactive form. They are reversibly localized to distinct intracellular membranes where they interact with coat components, motor proteins and SNARE proteins to control vesicle budding, microtubule (MT)-dependent vesicle motility and vesicle fusion [15]. Interestingly, a subset of Rab proteins have recently been found to serve as LRRK2 kinase substrates, with phosphorylation thought to inactivate Rab protein function and thus the specific vesicular transport steps which these Rab proteins are regulating [14]. Since LRRK2 has also been described to bind to MT and may regulate their dynamics [16], alterations in MT stability may result in (additional) downstream effects on a vast array of vesicular trafficking routes. Here, we review current knowledge and propose a testable working model by which the distinct altered catalytic activities of the pathogenic LRRK2 mutants may have an impact upon multiple MT-mediated vesicular trafficking steps through a common mechanism.

The LRRK2 kinase and GTPase activities

A set of pathogenic LRRK2 mutations have been described, including the R1441C/G/H and N1437H mutations in the ROC domain, the Y1699C mutation in the COR domain, and the G2019S and I2020T mutations in the kinase domain (Figure 1). The most prominent G2019S mutation in the kinase domain has been consistently shown to increase LRRK2 kinase activity as assessed using *in vitro* phosphorylation assays [14,17,18]. Thus, the G2019S mutant may act in a gain-of-function manner, with enhanced kinase activity towards defined substrates detrimental to cell survival. Indeed, the enhanced kinase activity of the G2019S mutant has been shown to correlate with neurotoxicity which can be reverted by either pharmacological or genetic kinase inhibition [19–21]. However, none of the other pathogenic mutations in the ROC or COR domain seem associated with increased inherent LRRK2 kinase activity *in vitro* [14,17,18].

LRRK2 is also able to bind GTP and displays inherent GTPase activity. Pathogenic mutations in the ROC and COR domain (R1441C/G, Y1699C) have been found to display increased GTP binding and decreased GTPase activity [22–24], with no changes observed with the G2019S mutation [23,25–27]. Interestingly, a R1398H polymorphism in the ROC domain of LRRK2 associated with decreased PD risk [5] has recently been reported to display decreased GTP binding and increased GTP hydrolysis, opposite to that reported for pathogenic mutants in the ROC and COR domain [28], and similar results have been described for an artificial R1398L mutation [25–27]. These data suggest that pathogenic mutations in the ROC and COR domain increase the amount of GTP-bound LRRK2, and that such a GTP-bound form of LRRK2 may be pathogenic. In support of this view, decreasing the GTP-bound state of pathogenic LRRK2 seems beneficial to cell survival in *in vitro* and animal models [29], indicating that specific and brain-permeable LRRK2 GTP-binding inhibitors may provide an alternative therapeutic strategy for at least some PD cases due to mutations in the ROC and the COR domain.

Biochemical Society Transactions (2017) **45** 141–146
DOI: 10.1042/BST20160333

Altogether, a picture has emerged whereby LRRK2-mediated pathogenicity results either from mutations which increase kinase activity without altering the GTP-bound state of LRRK2, or from mutations which increase the GTP-bound state without altering kinase activity. However, a recent seminal study found that all pathogenic LRRK2 mutants analysed (R1441C/G/H, Y1699C, G2019S, I2020T) increase the phosphorylation of a set of bona fide LRRK2 kinase substrate proteins in intact cells, whilst at the same time corroborating that only the G2019S mutant increases substrate phosphorylation when measured in *in vitro* phosphorylation assays using purified components [14]. Whilst awaiting independent validation by other laboratories, this is a crucially important finding, as it suggests that the distinct pathogenic LRRK2 mutants may all act through a common pathogenic mechanism by increasing the phosphorylation of LRRK2 kinase substrates in intact cells, and thus that LRRK2 kinase inhibitors may be beneficial to the entire LRRK2-linked PD spectrum.

The LRRK2 MT connection

How may pathogenic LRRK2 mutants with unaltered inherent kinase activity *in vitro* cause increased substrate phosphorylation in a cellular context? A wide variety of scenarios are possible. For example, the distinct pathogenic LRRK2 mutants may differentially regulate other kinases and/or phosphatases which also impinge upon the Rab substrates or their respective regulatory proteins [30] (Figure 2A,B). Indeed, various kinases and phosphatases have been reported to modulate the phosphorylation status of some Rab proteins. Whilst this is most prominently observed during mitosis [31], non-mitotic alterations in Rab phosphorylation at sites distinct from or identical to those predicted and/or shown to be phosphorylated by LRRK2 have been reported as well [32–34]. However, there is currently no evidence that all pathogenic LRRK2 mutants except for the G2019S

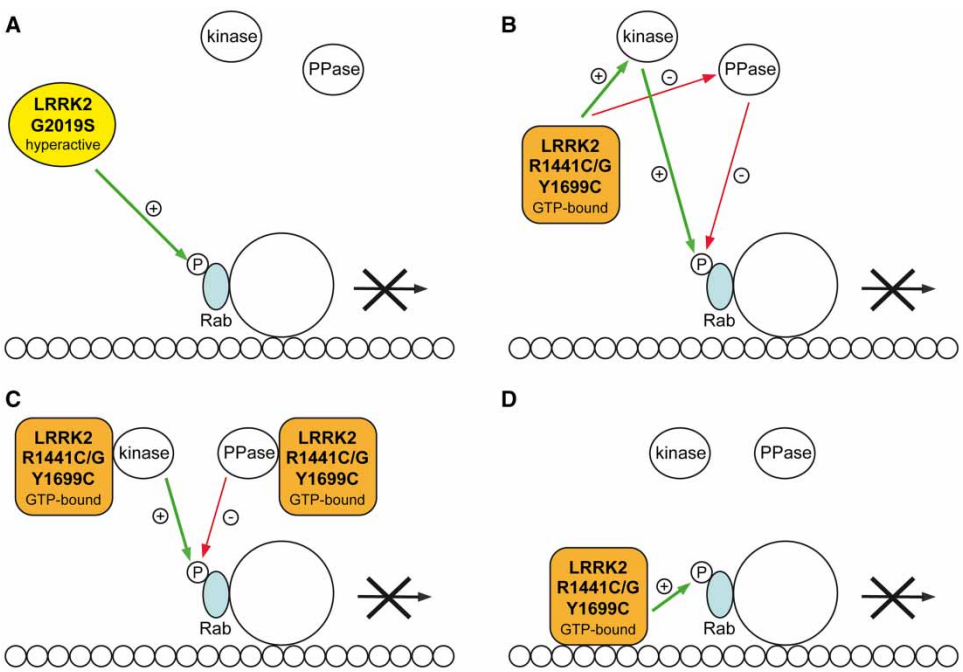

Figure 2. Possible models for how all pathogenic LRRK2 mutants may cause increased Rab protein phosphorylation in intact cells.

(**A**) The G2019S mutant causes increased Rab protein phosphorylation due to an inherent increase in kinase activity. (**B**) The other pathogenic LRRK2 mutants may positively regulate kinase(s) which phosphorylate the Rab protein at the equivalent residue phosphorylated by LRRK2, or negatively regulate phosphatase(s) (PPase) which dephosphorylate the phosphorylated residue in the Rab protein. (**C**) Regulation of such kinases and/or phosphatases by the pathogenic LRRK2 mutants may involve direct protein–protein interactions. (**D**) Pathogenic LRRK2 mutants, due to enhanced GTP binding, may preferentially associate with (stable) MTs, and such increased molecular proximity may cause increased phosphorylation of Rab proteins bound to transport vesicles as they move along the MT tracks. In all cases, Rab protein phosphorylation is hypothesized to interfere with vesicular trafficking steps by currently unknown molecular mechanism(s).

Biochemical Society Transactions (2017) **45** 141–146
DOI: 10.1042/BST20160333

mutant regulate the activities of other kinases and/or phosphatases which have an impact upon the phosphorylation status of the select Rab proteins which are LRRK2 kinase substrates.

Along similar lines, the distinct pathogenic LRRK2 mutants may differentially interact with Rab kinases and/or phosphatases, altering their activities and/or substrate specificities towards the Rab substrates, thereby causing changes in the overall phosphorylation status of these proteins in intact cells (Figure 2C). Indeed, select pathogenic LRRK2 mutants have been shown to display altered interactions with various protein kinases and phosphatases [33–38], but a careful side-by-side analysis of all pathogenic LRRK2 mutants with respect to those interactions, as well as the identification of the precise kinases and/or phosphatase(s) responsible for further modulating the phosphorylation status of the Rab proteins which serve as LRRK2 kinase substrates is currently missing.

Another scenario depends on differences in the subcellular localization of the distinct pathogenic LRRK2 mutant proteins. If all pathogenic LRRK2 mutants except the G2019S mutant display altered intracellular localization overlapping with that of the identified LRRK2 kinase substrate(s), such increased molecular proximity may lead to enhanced substrate protein phosphorylation similar to that mediated by the kinase-activating G2019S mutation, even though not associated with an increase in *in vitro* kinase activity *per se* (Figure 2D). Such alterations in the subcellular localization of pathogenic mutant LRRK2 proteins may further be due to GTP-binding-mediated differences in protein–protein interactions. Indeed, the large number of reported LRRK2 interactors [39,40] suggests an important role for protein interactors in regulating the cellular biology of LRRK2, even though there is currently no evidence for interactions which are selectively enhanced by all pathogenic LRRK2 mutants except for G2019S.

Since MT are required for many intracellular cargo transport processes, the reported interactions of LRRK2 with MTs warrant particular attention. Endogenous LRRK2 has been consistently shown to physically interact and co-localize with MTs [41–44]. Such interactions may alter MT dynamics, with expected downstream effects on many distinct MT-mediated vesicular transport events [16]. Alternatively, MT binding may increase the amount of LRRK2 in molecular proximity to various transport vesicles which carry distinct Rab proteins, thereby locally increasing their phosphorylation status. Thus, an enhanced MT association of select pathogenic LRRK2 mutants may result in increased Rab substrate protein phosphorylation in the absence of increased inherent kinase activity, with downstream effects on vesicular trafficking steps governed by those Rab proteins.

This model predicts that all pathogenic mutants with the exception of G2019S display increased MT association, and this indeed has been described for several LRRK2 mutants when compared with G2019S [45], consistent with observations from our laboratory (unpublished). The dynamics of MT are modulated by post-translational tubulin modifications which seem to be recognized by different molecular motor proteins, thereby further contributing to the establishment and maintenance of polarized vesicular trafficking. Given that many vesicular transport events occur preferentially along stable MT tracks [16,46–48], the model further predicts a preferential association of pathogenic LRRK2 with a subpopulation of stable MTs, which has been reported at least for the pathogenic R1441C and Y1699C mutants [49]. In this manner, just a few strategically placed pathogenic LRRK2 molecules, with equal inherent kinase activity when compared with the wild-type molecule, may be able to phosphorylate significant amounts of Rab proteins bound to various transport vesicles which move up and down MT tracks to their respective destinations. Interestingly, R1441C/G, Y1699C, G2019S and I2020T mutants have all been shown to enhance trans-Golgi network clustering when co-expressed with Rab7L1 [11], and primary fibroblasts from R1441C, Y1699C and G2019S LRRK2 PD patients all display the same autophagic alterations [50]. These observations suggest that all pathogenic LRRK2 mutants may converge onto the same functional outputs, even though the precise links between differential Rab phosphorylation and MT binding underlying the cellular phenotypes currently remain unknown.

Corroborating the proposed working model will require careful and correlative side-by-side analysis of all pathogenic LRRK2 mutants with respect to MT interactions, kinase activity and GTP binding. A testable prediction of this model is that the subcellular localization of all pathogenic LRRK2 mutants except for G2019S should be altered when decreasing LRRK2 GTP binding either by introducing the protective R1398H variant or by pharmacologically interfering with LRRK2 GTP binding, and decreasing GTP binding should result in decreased phosphorylation of the Rab substrate proteins mediated by all pathogenic LRRK2 mutants except for the G2019S mutant. The model further predicts that any LRRK2-mediated Rab protein phosphorylation causes deficits in vesicular trafficking, and future studies are required to determine whether LRRK2-mediated phosphorylation causes alterations in the GTP-bound (active) state of the Rab proteins, or changes in their interactions with select motor proteins, either one of which would interfere with vesicle mobility [15].

Concluding remarks

Over the past decade, significant progress has been made in our understanding of how distinct pathogenic LRRK2 mutations alter the catalytic activities of this enzyme. A picture has emerged whereby either aberrant kinase activity or an increase in the amount of GTP-bound LRRK2 may confer pathogenicity, even though the underlying mechanism(s) have remained elusive. The recent identification of Rab proteins as LRRK2 interactors and/or kinase substrates, together with the well-established role(s) of LRRK2 in MT-related processes allows for the proposal of a simple and testable working model by which all pathogenic LRRK2 mutants may culminate in identical changes in Rab-related membrane trafficking events relevant to disease pathogenesis and in a manner dependent on kinase activity. Whilst much work remains to be done to understand the cell biology underlying LRRK2-related PD, studies of this type will greatly aid in translating LRRK2 kinase inhibitors into the clinic, with a positive impact upon the life of millions of people currently suffering from this debilitating neurodegenerative disease.

Abbreviations

COR, C-terminal of Roc; LRRK2, leucine-rich repeat kinase 2; MT, microtubule; PD, Parkinson's disease; ROC, Ras-of-complex

Funding

Work in the laboratory is supported by FEDER, grants from the Spanish Ministry of Economy and Competitiveness [grant number SAF2014-58653-R], the BBVA Foundation and the Michael J. Fox Foundation (MJFF).

Competing Interests

The Authors declare that there are no competing interests associated with the manuscript.

References

1 Lesage, S. and Brice, A. (2009) Parkinson's disease: from monogenic forms to genetic susceptibility factors. *Hum. Mol. Genet.* **18**, R48–R59 doi:10.1093/hmg/ddp012
2 Paisán-Ruíz, C., Jain, S., Evans, E.W., Gilks, W.P., Simón, J., van der Brug, M. et al. (2004) Cloning of the gene containing mutations that cause PARK8-linked Parkinson's disease. *Neuron* **44**, 595–600 doi:10.1016/j.neuron.2004.10.023
3 Zimprich, A., Biskup, S., Leitner, P., Lichtner, P., Farrer, M., Lincoln, S. et al. (2004) Mutations in LRRK2 cause autosomal-dominant parkinsonism with pleomorphic pathology. *Neuron* **44**, 601–607 doi:10.1016/j.neuron.2004.11.005
4 Bardien, S., Lesage, S., Brice, A. and Carr, J. (2011) Genetic characteristics of leucine-rich repeat kinase 2 (LRRK2) associated Parkinson's disease. *Parkinsonism Relat. Disord.* **17**, 501–508 doi:10.1016/j.parkreldis.2010.11.008
5 Chen, L., Zhang, S., Liu, Y., Hong, H., Wang, H., Zheng, Y. et al. (2011) LRRK2 R1398H polymorphism is associated with decreased risk of Parkinson's disease in a Han Chinese population. *Parkinsonism Relat. Disord.* **17**, 291–292 doi:10.1016/j.parkreldis.2010.11.012
6 Taymans, J.-M. and Greggio, E. (2015) LRRK2 kinase inhibition as a therapeutic strategy for Parkinson's disease, where do we stand? *Curr. Neuropharmacol.* **14**, 214–225 doi:10.2174/1570159X13666151030102847
7 Gómez-Suaga, P., Fdez, E., Fernández, B., Martínez-Salvador, M., Blanca Ramírez, M., Madero-Pérez, J. et al. (2014) Novel insights into the neurobiology underlying LRRK2-linked Parkinson's disease. *Neuropharmacology* **85**, 45–56 doi:10.1016/j.neuropharm.2014.05.020
8 Shin, N., Jeong, H., Kwon, J., Heo, H.Y., Kwon, J.J., Yun, H.J. et al. (2008) LRRK2 regulates synaptic vesicle endocytosis. *Exp. Cell Res.* **314**, 2055–2065 doi:10.1016/j.yexcr.2008.02.015
9 Gomez-Suaga, P., Rivero-Rios, P., Fdez, E., Blanca Ramirez, M., Ferrer, I., Aiastui, A. et al. (2014) LRRK2 delays degradative receptor trafficking by impeding late endosomal budding through decreasing Rab7 activity. *Hum. Mol. Genet.* **23**, 6779–6796 doi:10.1093/hmg/ddu395
10 MacLeod, D.A., Rhinn, H., Kuwahara, T., Zolin, A., Di Paolo, G., McCabe, B.D. et al. (2013) RAB7L1 interacts with LRRK2 to modify intraneuronal protein sorting and Parkinson's disease risk. *Neuron* **77**, 425–439 doi:10.1016/j.neuron.2012.11.033
11 Beilina, A., Rudenko, I.N., Kaganovich, A., Civiero, L., Chau, H., Kalia, S.K. et al. (2014) Unbiased screen for interactors of leucine-rich repeat kinase 2 supports a common pathway for sporadic and familial Parkinson disease. *Proc. Natl Acad. Sci. U.S.A.* **111**, 2626–2631 doi:10.1073/pnas.1318306111
12 Dodson, M.W., Zhang, T., Jiang, C., Chen, S. and Guo, M. (2012) Roles of the Drosophila LRRK2 homolog in Rab7-dependent lysosomal positioning. *Hum. Mol. Genet.* **21**, 1350–1363 doi:10.1093/hmg/ddr573
13 Waschbüsch, D., Michels, H., Strassheim, S., Ossendorf, E., Kessler, D., Gloeckner, C.J. et al. (2014) LRRK2 transport is regulated by its novel interacting partner Rab32. *PLoS One* **9**, e111632 doi:10.1371/journal.pone.0111632
14 Steger, M., Tonelli, F., Ito, G., Davies, P., Trost, M., Vetter, M. et al. (2016) Phosphoproteomics reveals that Parkinson's disease kinase LRRK2 regulates a subset of Rab GTPases. *Elife* **5**. pii: e12813 doi:10.7554/eLife.12813
15 Stenmark, H. (2009) Rab GTPases as coordinators of vesicle traffic. *Nat. Rev. Mol. Cell Biol.* **10**, 513–525 doi:10.1038/nrm2728
16 Pellegrini, L., Wetzel, A., Grannó, S., Heaton, G. and Harvey, K. (2016) Back to the tubule: microtubule dynamics in Parkinson's disease. *Cell. Mol. Life Sci.* PMID:27600680
17 Jaleel, M., Nichols, R.J., Deak, M., Campbell, D.G., Gillardon, F., Knebel, A. et al. (2007) LRRK2 phosphorylates moesin at threonine-558: characterization of how Parkinson's disease mutants affect kinase activity. *Biochem. J.* **405**, 307–317 doi:10.1042/BJ20070209

Biochemical Society Transactions (2017) **45** 141–146
DOI: 10.1042/BST20160333

18 Greggio, E. and Cookson, M.R. (2009) Leucine-rich repeat kinase 2 mutations and Parkinson's disease: three questions. *ASN Neuro* **1**, pii: e00002 doi:10.1042/AN20090007

19 Greggio, E., Jain, S., Kingsbury, A., Bandopadhyay, R., Lewis, P., Kaganovich, A. et al. (2006) Kinase activity is required for the toxic effects of mutant LRRK2/dardarin. *Neurobiol. Dis.* **23**, 329–341 doi:10.1016/j.nbd.2006.04.001

20 Smith, W.W., Pei, Z., Jiang, H., Dawson, V.L., Dawson, T.M. and Ross, C.A. (2006) Kinase activity of mutant LRRK2 mediates neuronal toxicity. *Nat. Neurosci.* **9**, 1231–1233 doi:10.1038/nn1776

21 Lee, B.D., Shin, J.-H., VanKampen, J., Petrucelli, L., West, A.B., Ko, H.S. et al. (2010) Inhibitors of leucine-rich repeat kinase-2 protect against models of Parkinson's disease. *Nat. Med.* **16**, 998–1000 doi:10.1038/nm.2199

22 Lewis, P.A., Greggio, E., Beilina, A., Jain, S., Baker, A. and Cookson, M.R. (2007) The R1441C mutation of LRRK2 disrupts GTP hydrolysis. *Biochem. Biophys. Res. Commun.* **357**, 668–671 doi:10.1016/j.bbrc.2007.04.006

23 West, A.B., Moore, D.J., Choi, C., Andrabi, S.A., Li, X., Dikeman, D. et al. (2006) Parkinson's disease-associated mutations in LRRK2 link enhanced GTP-binding and kinase activities to neuronal toxicity. *Hum. Mol. Genet.* **16**, 223–232 doi:10.1093/hmg/ddl471

24 Daniëls, V., Vancraenenbroeck, R., Law, B.M.H., Greggio, E., Lobbestael, E., Gao, F. et al. (2011) Insight into the mode of action of the LRRK2 Y1699C pathogenic mutant. *J. Neurochem.* **116**, 304–315 doi:10.1111/j.1471-4159.2010.07105.x

25 Xiong, Y., Coombes, C.E., Kilaru, A., Li, X., Gitler, A.D., Bowers, W.J. et al. (2010) GTPase activity plays a key role in the pathobiology of LRRK2. *PLoS Genet.* **6**, e1000902 doi:10.1371/journal.pgen.1000902

26 Stafa, K., Trancikova, A., Webber, P.J., Glauser, L., West, A.B. and Moore, D.J. (2012) GTPase activity and neuronal toxicity of Parkinson's disease-associated LRRK2 is regulated by ArfGAP1. *PLoS Genet.* **8**, e1002526 doi:10.1371/journal.pgen.1002526

27 Biosa, A., Trancikova, A., Civiero, L., Glauser, L., Bubacco, L., Greggio, E. et al. (2013) GTPase activity regulates kinase activity and cellular phenotypes of Parkinson's disease-associated LRRK2. *Hum. Mol. Genet.* **22**, 1140–1156 doi:10.1093/hmg/dds522

28 Nixon-Abell, J., Berwick, D.C., Grannó, S., Spain, V.A., Blackstone, C. and Harvey, K. (2016) Protective LRRK2 R1398H variant enhances GTPase and Wnt signaling activity. *Front. Mol. Neurosci.* **9**, 18 doi:10.3389/fnmol.2016.00018

29 Li, T., Yang, D., Zhong, S., Thomas, J.M., Xue, F., Liu, J. et al. (2014) Novel LRRK2 GTP-binding inhibitors reduced degeneration in Parkinson's disease cell and mouse models. *Hum. Mol. Genet.* **23**, 6212–6222 doi:10.1093/hmg/ddu341

30 Barr, F.A. (2013) Rab GTPases and membrane identity: causal or inconsequential? *J. Cell Biol.* **202**, 191–199 doi:10.1083/jcb.201306010

31 Stenmark, H. (2009) Rab GTPases as coordinators of vesicle traffic. *Nat. Rev. Mol. Cell Biol.* **10**, 513–525 doi:10.1038/nrm2728

32 Levin, R.S., Hertz, N.T., Burlingame, A.L., Shokat, K.M. and Mukherjee, S. (2016) Innate immunity kinase TAK1 phosphorylates Rab1 on a hotspot for posttranslational modifications by host and pathogen. *Proc. Natl Acad. Sci. U.S.A.* **113**, E4776–E4783 doi:10.1073/pnas.1608355113

33 Shinde, S.R. and Maddika, S. (2016) PTEN modulates EGFR late endocytic trafficking and degradation by dephosphorylating Rab7. *Nat. Commun.* **7**, 10689 doi:10.1038/ncomms10689

34 Lai, Y.-C., Kondapalli, C., Lehneck, R., Procter, J.B., Dill, B.D., Woodroof, H.I. et al. (2015) Phosphoproteomic screening identifies Rab GTPases as novel downstream targets of PINK1. *EMBO J.* **34**, 2840–2861 doi:10.15252/embj.201591593

35 Civiero, L., Cirnaru, M.D., Beilina, A., Rodella, U., Russo, I., Belluzzi, E. et al. (2015) Leucine-rich repeat kinase 2 interacts with p21-activated kinase 6 to control neurite complexity in mammalian brain. *J. Neurochem.* **135**, 1242–1256 doi:10.1111/jnc.13369

36 Parisiadou, L., Yu, J., Sgobio, C., Xie, C., Liu, G., Sun, L. et al. (2014) LRRK2 regulates synaptogenesis and dopamine receptor activation through modulation of PKA activity. *Nat. Neurosci.* **17**, 367–376 doi:10.1038/nn.3636

37 Lobbestael, E., Zhao, J., Rudenko, I.N., Beilina, A., Gao, F., Wetter, J. et al. (2013) Identification of protein phosphatase 1 as a regulator of the LRRK2 phosphorylation cycle. *Biochem. J.* **456**, 119–128 doi:10.1042/BJ20121772

38 Athanasopoulos, P.S., Jacob, W., Neumann, S., Kutsch, M., Wolters, D., Tan, E.K. et al. (2016) Identification of protein phosphatase 2A as an interacting protein of leucine-rich repeat kinase 2. *Biol. Chem.* **397**, 541–554 doi:10.1515/hsz-2015-0189

39 Manzoni, C., Denny, P., Lovering, R.C. and Lewis, P.A. (2015) Computational analysis of the LRRK2 interactome. *PeerJ* **3**, e778 doi:10.7717/peerj.778

40 Porras, P., Duesbury, M., Fabregat, A., Ueffing, M., Orchard, S., Gloeckner, C.J. et al. (2015) A visual review of the interactome of LRRK2: using deep-curated molecular interaction data to represent biology. *Proteomics* **15**, 1390–1404 doi:10.1002/pmic.201400390

41 Gandhi, P.N., Wang, X., Zhu, X., Chen, S.G. and Wilson-Delfosse, A.L. (2008) The Roc domain of leucine-rich repeat kinase 2 is sufficient for interaction with microtubules. *J. Neurosci. Res.* **86**, 1711–1720 doi:10.1002/jnr.21622

42 Gillardon, F. (2009) Leucine-rich repeat kinase 2 phosphorylates brain tubulin-beta isoforms and modulates microtubule stability — a point of convergence in parkinsonian neurodegeneration? *J. Neurochem.* **110**, 1514–1522 doi:10.1111/j.1471-4159.2009.06235.x

43 Caesar, M., Zach, S., Carlson, C.B., Brockmann, K., Gasser, T. and Gillardon, F. (2013) Leucine-rich repeat kinase 2 functionally interacts with microtubules and kinase-dependently modulates cell migration. *Neurobiol. Dis.* **54**, 280–288 doi:10.1016/j.nbd.2012.12.019

44 Law, B.M.H., Spain, V.A., Leinster, V.H.L., Chia, R., Beilina, A., Cho, H.J. et al. (2014) A direct interaction between leucine-rich repeat kinase 2 and specific β-tubulin isoforms regulates tubulin acetylation. *J. Biol. Chem.* **289**, 895–908 doi:10.1074/jbc.M113.507913

45 Kett, L.R., Boassa, D., Ho, C.C.-Y., Rideout, H.J., Hu, J., Terada, M. et al. (2012) LRRK2 Parkinson disease mutations enhance its microtubule association. *Hum. Mol. Genet.* **21**, 890–899 doi:10.1093/hmg/ddr526

46 Cai, D., McEwen, D.P., Martens, J.R., Meyhofer, E. and Verhey, K.J. (2009) Single molecule imaging reveals differences in microtubule track selection between kinesin motors. *PLoS Biol.* **7**, e1000216 doi:10.1371/journal.pbio.1000216

47 Jacobson, C., Schnapp, B. and Banker, G.A. (2006) A change in the selective translocation of the kinesin-1 motor domain marks the initial specification of the axon. *Neuron* **49**, 797–804 doi:10.1016/j.neuron.2006.02.005

48 Kaul, N., Soppina, V. and Verhey, K.J. (2014) Effects of α-tubulin K40 acetylation and detyrosination on kinesin-1 motility in a purified system. *Biophys. J.* **106**, 2636–2643 doi:10.1016/j.bpj.2014.05.008

49 Godena, V.K., Brookes-Hocking, N., Moller, A., Shaw, G., Oswald, M., Sancho, R.M. et al. (2014) Increasing microtubule acetylation rescues axonal transport and locomotor deficits caused by LRRK2 Roc-COR domain mutations. *Nat. Commun.* **5**, 5245 doi:10.1038/ncomms6245

50 Manzoni, C., Mamais, A., Dihanich, S., McGoldrick, P., Devine, M.J., Zerle, J. et al. (2013) Pathogenic Parkinson's disease mutations across the functional domains of LRRK2 alter the autophagic/lysosomal response to starvation. *Biochem. Biophys. Res. Commun.* **441**, 862–866 doi:10.1016/j.bbrc.2013.10.159

3. GTP binding regulates cellular localization of Parkinsońs disease-associated LRRK2.

OXFORD

Human Molecular Genetics, 2017, Vol. 0, No. 0 1–21

doi: 10.1093/hmg/ddx161
Advance Access Publication Date: 26 April 2017
Original Article

ORIGINAL ARTICLE

GTP binding regulates cellular localization of Parkinson's disease-associated LRRK2

Marian Blanca Ramírez[1], Antonio Jesús Lara Ordóñez[1], Elena Fdez[1], Jesús Madero-Pérez[1], Adriano Gonnelli[2], Matthieu Drouyer[3,4], Marie-Christine Chartier-Harlin[3,4], Jean-Marc Taymans[3,4], Luigi Bubacco[2] Elisa Greggio[2] and Sabine Hilfiker[1,*]

[1]Institute of Parasitology and Biomedicine 'López-Neyra', Consejo Superior de Investigaciones Científicas (CSIC), 18016 Granada, Spain, [2]Department of Biology, University of Padova, Padova 35121, Italy, [3]Univ. Lille, Inserm, CHU Lille, UMR-S 1172 - JPArc - Centre de Recherche Jean-Pierre AUBERT Neurosciences et Cancer, F-59000 Lille, France and [4]Inserm, UMR-S 1172 Early Stages of Parkinson's Disease Team, F-59000 Lille, France

*To whom correspondence should be addressed. Tel: +34 958 18 16 54; Fax: +34 958 18 16 32; Email: sabine.hilfiker@ipb.csic.es

Abstract

Mutations in leucine-rich repeat kinase 2 (LRRK2) comprise the most common cause of familial Parkinson's disease (PD), and sequence variants modify risk for sporadic PD. Previous studies indicate that LRRK2 interacts with microtubules (MTs) and alters MT-mediated vesicular transport processes. However, the molecular determinants within LRRK2 required for such interactions have remained unknown. Here, we report that most pathogenic LRRK2 mutants cause relocalization of LRRK2 to filamentous structures which colocalize with a subset of MTs, and an identical relocalization is seen upon pharmacological LRRK2 kinase inhibition. The pronounced colocalization with MTs does not correlate with alterations in LRRK2 kinase activity, but rather with increased GTP binding. Synthetic mutations which impair GTP binding, as well as LRRK2 GTP-binding inhibitors profoundly interfere with the abnormal localization of both pathogenic mutant as well as kinase-inhibited LRRK2. Conversely, addition of a non-hydrolyzable GTP analog to permeabilized cells enhances the association of pathogenic or kinase-inhibited LRRK2 with MTs. Our data elucidate the mechanism underlying the increased MT association of select pathogenic LRRK2 mutants or of pharmacologically kinase-inhibited LRRK2, with implications for downstream MT-mediated transport events.

Introduction

Parkinson's disease (PD) is a common neurodegenerative disease with incompletely understood etiology, affecting around 1–2% of the elderly (1). Mutations in the leucine-rich repeat kinase 2 (LRRK2) gene cause PD inherited in an autosomal-dominant fashion (2,3). Additionally, various variants have been identified which either positively or negatively correlate with PD risk (4–9), highlighting the general importance of LRRK2 for disease pathogenesis. The LRRK2 protein contains various domains implicated in protein–protein interactions, as well as a central region comprised of a Ras-of-complex (ROC) GTPase domain and a kinase domain, connected via a C-terminal of ROC

Received: February 19, 2017. **Revised:** April 17, 2017. **Accepted:** April 21, 2017

(COR) domain (10,11). All currently identified pathogenic mutants localize to this central region, and seem associated either with enhanced kinase activity (e.g. G2019S) (12–14), increased GTP binding (15–18) or reduced GTPase activity (19,20), suggesting that abnormal kinase and/or GTP-domain activities may cause neurodegeneration in LRRK2-linked PD (21). Indeed, pathogenic mutations in LRRK2 can promote cellular deficits through both GTP-dependent and kinase-dependent mechanisms (13,16,22–26), raising hopes that selective LRRK2 kinase inhibitors (27–29), GTP-binding competitors or GTPase modulators may delay the onset of LRRK2-related PD.

The precise mechanism(s) underlying LRRK2-linked PD remain largely unknown, but a variety of studies suggest underlying cytoskeletal alterations which may impact upon various vesicular trafficking steps (30). Endogenous LRRK2 protein can physically interact and colocalize with microtubules (MTs) (31–33). Such colocalization has also been observed with overexpressed LRRK2, and is profoundly enhanced with certain pathogenic LRRK2 mutants (34,35) as well as by several LRRK2 kinase inhibitors (36–38). Finally, pathogenic LRRK2 has been reported to impair MT-mediated axonal transport in a manner correlated with enhanced MT association (35,39). Thus, an increased interaction of LRRK2 with MTs seems to have detrimental effects on MT-mediated vesicular transport events. However, the molecular determinant(s) within LRRK2 required for such interaction are largely unknown.

Here, we have analyzed the subcellular localization of all pathogenic LRRK2 mutants as well as of pharmacologically kinase-inhibited LRRK2. We find that both mutant and kinase-inhibited LRRK2 preferentially interact with stable MTs. This interaction does not correlate with altered LRRK2 autophosphorylation status or kinase activity, but with enhanced GTP binding. Synthetic mutations in LRRK2 which reduce GTP binding, as well as two recently described GTP-binding inhibitors that attenuate LRRK2-mediated toxicity in cell and animal models (40,41) potently decrease this interaction, whilst a non-hydrolyzable GTP analog enhances the interaction. Thus, GTP-binding inhibitors may be useful for treating select forms of pathogenic LRRK2-linked PD.

Results

Kinase-inhibited LRRK2 and most pathogenic LRRK2 mutants display altered cellular localization

As previously described (34–38), GFP-tagged wild-type LRRK2 protein was found to adopt a purely cytosolic localization in the majority of transfected HEK293T cells (Fig. 1A). A small percentage of cells displayed additional dot-like localization in the form of one or several small, usually perinuclear structures, and a small percentage displayed a filamentous phenotype (Fig. 1A). Such localization was not tag-dependent, as also observed with myc-tagged LRRK2 constructs (not shown) (34).

The subcellular localization of LRRK2 may be modulated by either extrinsic and/or intrinsic factors. In support of the latter, pharmacological inhibition of LRRK2 kinase activity by either H1152 (36) or LRRK2-IN1 (37) has been reported to cause relocalization of LRRK2 to filamentous structures. Indeed, application of a whole set of specific and structurally distinct LRRK2 kinase inhibitors (37,42–46) triggered a profound relocalization of wild-type LRRK2 to filamentous structures (Fig. 1B) without causing alterations in steady-state protein levels (Fig. 1C). Relocalization was dose-dependent (Fig. 1D) and fast (Fig. 1E), being detectable within minutes after application of kinase inhibitor. Thus, pharmacological kinase inhibition invariably causes alterations in the subcellular localization of LRRK2.

We next evaluated the localization of all currently identified pathogenic LRRK2 mutants (N1437H, R1441C/G, Y1699C, I2012T, G2019S, I2020T) (2,3,17,47,48), as well as of two synthetic mutants known to either impair kinase activity (K1906M) or guanine nucleotide binding (K1347A), respectively. When compared with wild-type LRRK2, the filamentous phenotype was profoundly enhanced by all pathogenic LRRK2 mutants except for G2019S and I2012T (Fig. 1F and G). Both kinase-inactive and GTP-binding-deficient mutants displayed a primarily cytosolic localization (Fig. 1F and G), and all mutants with the exception of K1347A (26) were expressed to similar degrees (Fig. 1H), indicating that the observed differences in subcellular localization were not due to alterations in steady-state protein levels. Application of a LRRK2 kinase inhibitor (LRRK2-IN1) caused a further increase in filament formation of wild-type and all mutant LRRK2 proteins analyzed, but had no effect on synthetic kinase-inactive or GTP-binding-deficient mutants (Fig. 1G), suggesting that the latter two may be in a conformation incompatible with inhibitor binding (49,50). Thus, most pathogenic LRRK2 mutants display a profoundly altered subcellular localization, and pharmacological kinase inhibition further potentiates such relocalization for both wild-type as well as all currently identified pathogenic LRRK2 mutants.

LRRK2 filaments preferentially decorate stable MTs

The filamentous LRRK2 structures described here have been previously reported to colocalize with MTs (34,36). MTs are heterogeneous structures subject to distinct posttranslational modifications including acetylation and detyrosination (51–53), with the latter shown to cause increased MT stability (54). In non-transfected cells, the majority of the total MT array contained predominantly tyrosinated α-tubulin, indicative of dynamic MTs. Only a small subset of MTs was positive for acetylated and/or detyrosinated α-tubulin, with both posttranslational modifications frequently observed on the same MT tracks in a patchy, alternating fashion (Fig. 2A and B). Pathogenic as well as kinase inhibitor-induced LRRK2 filaments extensively colocalized with acetylated and/or detyrosinated α-tubulin, thus indicating a preference for association with stable MTs (Fig. 2A–C).

When compared with dynamic MTs, stable MTs display increased resistance to nocodazole, but are effectively disrupted upon cold treatment (55). Indeed, LRRK2 filaments were significantly disrupted upon cold treatment, with nocodazole being less effective (Fig. 3A). MT nucleation assays further revealed a delay between MT regrowth as assayed by staining against α-tubulin, the reformation of acetylated MTs, and the reformation of mutant LRRK2 filaments, in agreement with the preferential association of LRRK2 with stable MTs (Fig. 3B).

To examine whether modulating the acetylation and/or detyrosination status of MTs may influence the filamentous localization of pathogenic and kinase-inhibited LRRK2, we treated cells with two distinct α-tubulin deacetylase inhibitors (56) which increased the extent of tubulin acetylation and caused a modest decrease in the LRRK2 filamentous phenotype (Fig. 3C and D). As an alternative approach, we overexpressed αTAT1, the major α-tubulin acetyltransferase (57), which caused an increase in α-tubulin acetylation and a profound decrease in the pathogenic LRRK2 filamentous phenotype (Fig. 3E and F). An enzymatically inactive point mutant (D157N) (57) displayed

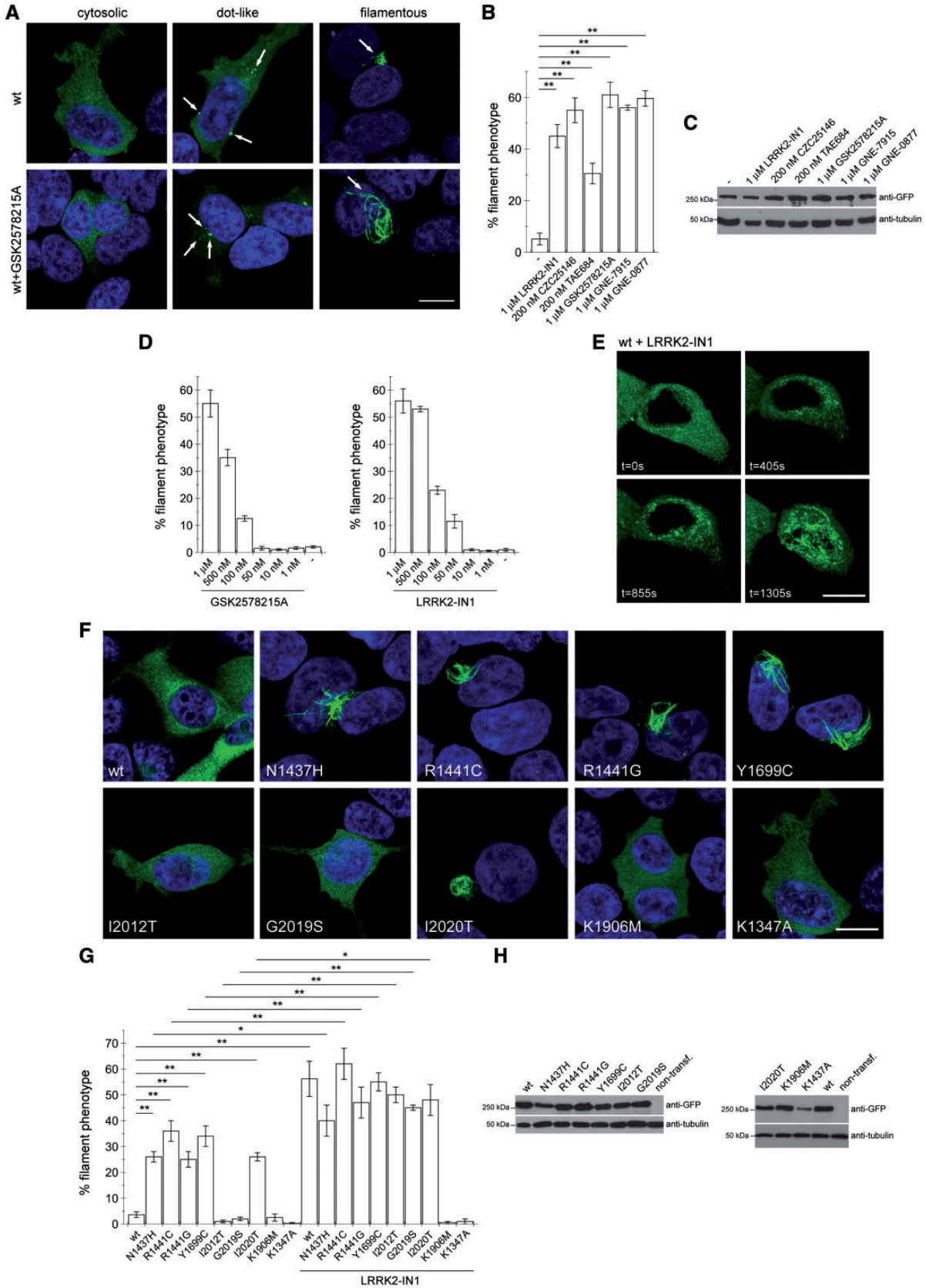

Figure 1. Effects of pharmacological kinase inhibitors and pathogenic mutations on LRRK2 subcellular localization. (**A**) Example of subcellular localization of wild-type GFP-tagged LRRK2 (wt) in the absence or presence of LRRK2 kinase inhibitor as indicated. Scale bar, 10 µm. (**B**) Quantification of the percentage of transfected cells displaying a filamentous phenotype in the absence of treatment (–), or upon 4 h incubation with distinct LRRK2 kinase inhibitors as indicated. Bars represent mean ± SEM

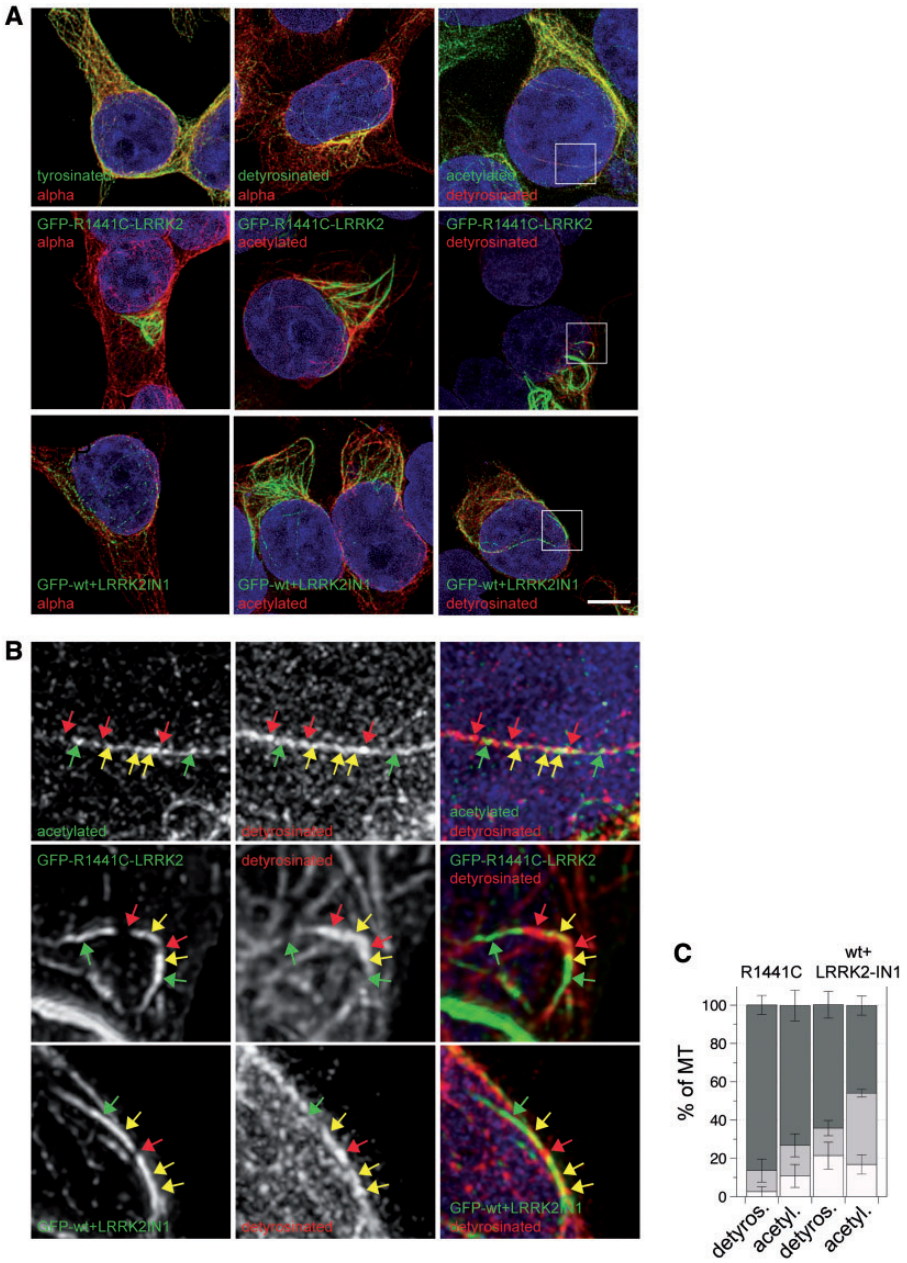

Figure 2. Pathogenic mutant and kinase-inhibited LRRK2 preferentially decorate stable MTs. (**A**) Example of non-transfected cells stained with antibodies against tyrosinated, detyrosinated, acetylated or α-tubulin (alpha) as indicated, or cells transfected with GFP-tagged R1441C-mutant LRRK2 and stained with antibodies as indicated, or cells transfected with GFP-tagged wild-type LRRK2, treated for 1 h with 1 μM LRRK2-IN1 and stained with antibodies as indicated. All images were deconvolved as described in Materials and Methods. Scale bar, 10 μm. (**B**) Magnification of squares as indicated in (A). Colored arrows indicate preferential staining with one antibody (red and green, respectively), or colocalization (yellow). (**C**) Quantification of colocalization of pathogenic mutant LRRK2 or wild-type LRRK2 in the presence of kinase inhibitor with either acetylated or detyrosinated MTs was performed as described in Materials and Methods. The percentage of colocalization was subgrouped for each cell, with colocalization 0–50% (white), 50–90% (gray) or > 90% (dark gray). Bars represent mean ± SEM ($n = 5$ cells).

Figure 1. Continued

($n = 3$; $^{**}P < 0.005$). (**C**) Cells were transfected with GFP-tagged wild-type LRRK2, treated with distinct kinase inhibitors for 4 h as indicated, and extracts analyzed for protein levels by western blotting using an anti-GFP antibody, and alpha-tubulin as loading control. (**D**) Quantification of the percentage of transfected cells displaying a filamentous phenotype in the absence (–) or presence of distinct concentrations of kinase inhibitors as indicated. Bars represent mean ± SEM ($n = 3$). (**E**) Live images of cells expressing wild-type GFP-tagged LRRK2 at distinct times after adding 1 μM LRRK2-IN1. Scale bar, 10 μm. (**F**) Examples of cells depicting the prominent subcellular localization of the various GFP-tagged LRRK2 constructs as indicated. Scale bar, 10 μm. (**G**) Quantification of the filamentous phenotype of various GFP-tagged LRRK2 constructs from the type of experiments as depicted in (F), in either the absence or presence of 1 μM LRRK2-IN1 for 4 h as indicated. Bars represent mean ± SEM ($n = 4$; $^{*}P < 0.05$; $^{**}P < 0.005$). (**H**) Cells were transfected with GFP-tagged LRRK2 constructs as indicated, and extracts analyzed for protein levels by western blotting using an anti-GFP antibody, and tubulin as loading control.

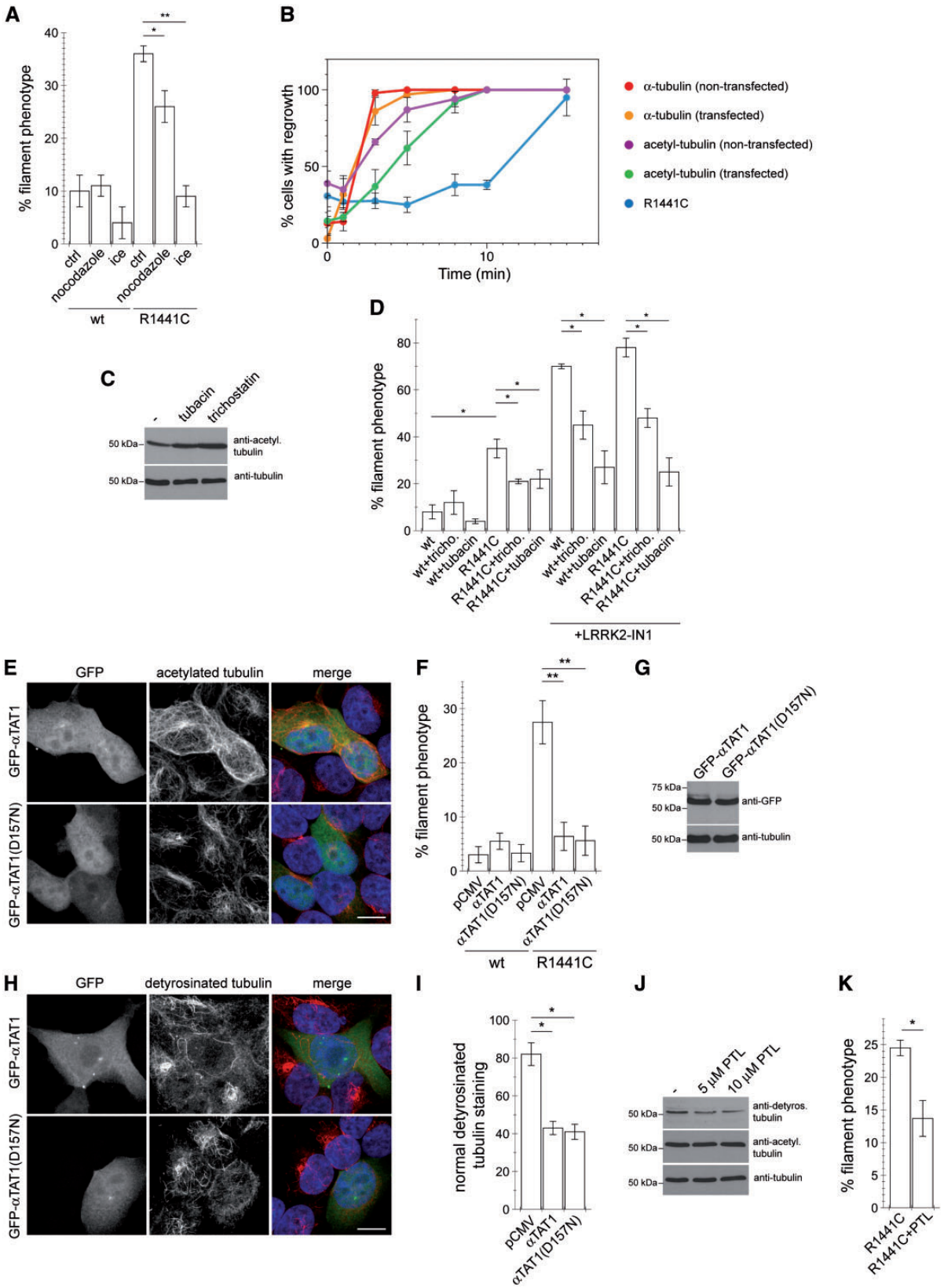

Figure 3. Effects of modulating the acetylation or detyrosination status of MTs on filament formation of pathogenic LRRK2. (**A**) Cells were transfected with constructs as indicated, and either left untreated (ctrl), or incubated with nocodazole or on ice, followed by quantification of the percentage of cells displaying a filamentous LRRK2 phenotype. Bars represent mean ± SEM ($n = 4$; *$P < 0.05$; **$P < 0.01$). (**B**) Cells were transfected with pathogenic LRRK2, incubated on ice for 1.5 h to disrupt MTs, and MT nucleation/regrowth performed for the indicated times at 37 °C. Cells were stained for α-tubulin or acetylated α-tubulin, and the percentage of non-transfected or transfected cells displaying visible MT regrowth and reformation of the filamentous pathogenic LRRK2 phenotype quantified as indicated. Bars represent

steady-state protein levels similar to wild-type αTAT1 (Fig. 3G), and was without effect on the acetylation status of α-tubulin (Fig. 3E). However, overexpression of the αTAT1 mutant defective in acetyltransferase activity also interfered with pathogenic LRRK2 filament formation, indicating that the observed effects were independent of MT acetylation status (Fig. 3F). Importantly, and as previously reported (58), expression of active and inactive αTAT1 both caused a decrease in detyrosinated α-tubulin (Fig. 3H and I), suggesting that LRRK2 filament formation may be largely modulated by the detyrosination status of MTs. Whilst the tubulin carboxypeptidase catalyzing the detyrosination of α-tubulin remains to be identified (53), parthenolide (PTL), a sesquiterpene lactone, has been shown to inhibit the activity of this enzyme (59,60). Indeed, treatment of cells with PTL caused a decrease in detyrosinated α-tubulin associated with a reduction in the filamentous phenotype of pathogenic mutant LRRK2 (Fig. 3J and K). Altogether, these results indicate that both pathogenic and kinase-inhibited LRRK2 preferentially associate with a subset of stable MTs in a manner mainly dependent on their detyrosination status.

LRRK2 filament formation does not correlate with kinase activity or autophosphorylation status

We next set out to identify the determinants within LRRK2 necessary for the observed MT interactions. Autophosphorylation of kinases is often used as a readout of enhanced kinase activity. LRRK2 has been shown to be autophosphorylated at various sites (61–65), with phosphorylation of one particular site (S1292) detectable *in vivo* and increased in the context of various pathogenic mutants (38). As previously reported (38), when introduced into a combined pathogenic mutant background (R1441C-Y1699C-G2019S), the S1292A mutation decreased the LRRK2 filamentous phenotype (Fig. 4A). However, when introduced into constructs bearing the individual pathogenic LRRK2 mutations, no change in their subcellular localization was observed (Fig. 4B), with all mutants expressed to similar degrees (Fig. 4C). Thus, enhanced S1292 autophosphorylation does not seem to comprise a relevant molecular determinant required for the observed filamentous phenotype of pathogenic LRRK2 mutants.

A series of distinct pharmacological kinase inhibitors caused filament formation, whilst a kinase-inactive point mutant (K1906M) did not (Fig. 1). Pharmacological kinase inhibition has been suggested to induce a conformational change in LRRK2 associated with dephosphorylation of the cellular N-terminal phosphorylation sites including S935, which was not observed with kinase-dead point mutants (50). Indeed, two distinct kinase-dead point mutants (K1906M and T2035A) displayed N-terminal phosphorylation levels similar to wild-type LRRK2 (Fig. 5A and B). Pharmacological kinase inhibition of wild-typEe LRRK2 caused dephosphorylation of the N-terminal S935 residue, which was also observed when adding pharmacological kinase inhibitor to kinase-dead T2035A, but not to the K1906M mutant, respectively (Fig. 5A and B). The changes in N-terminal dephosphorylation correlated with filament formation in pharmacologically kinase-inhibited wild-type and T2035A mutant LRRK2, with K1906M mutant LRRK2 not showing dephosphorylation neither filament formation upon pharmacological kinase inhibition (Fig. 5C). Therefore, synthetic kinase-dead LRRK2 mutants do not seem to properly mimick the features of pharmacologically kinase-inhibited LRRK2, with the latter being accompanied by a change associated with dephosphorylation of the N-terminal cellular phosphorylation sites.

The filamentous localization of LRRK2 is modulated by 14-3-3

Interestingly, N-terminal phosphorylation is also decreased in pathogenic LRRK2 mutants which display a filamentous phenotype, but not in the G2019S mutant which is largely cytosolic (36,66,67) (Fig. 5D). Since dephosphorylation of the cellular N-terminal phosphorylation sites causes disruption of 14-3-3 binding (66,67), and since overexpression of 14-3-3 proteins has been found to ameliorate the effects of pathogenic LRRK2 on neurite length (68), we next wondered whether 14-3-3 protein overexpression may alter the filamentous phenotype and N-terminal phosphorylation status of LRRK2. Overexpression of either 14-3-3β or 14-3-3γ, both reported to interact with LRRK2 (69,70), decreased the filamentous phenotype of pathogenic LRRK2 without altering its dot-like localization (Fig. 6A and B). In addition, expression of either 14-3-3 protein decreased the filamentous phenotype of wild-type or pathogenic LRRK2 induced upon pharmacological kinase inhibition (Fig. 6B). In contrast, whilst expressed to a similar degree (Fig. 6C), a loss-of-function point mutant (V181D) of 14-3-3γ (70) was without effect (Fig. 6B). Overexpression of wild-type but not mutant 14-3-3γ was associated with an increase in N-terminal phosphorylation of pathogenic mutant LRRK2 similar to that observed with wild-type LRRK2 (Fig. 6D). Therefore, modulating cellular 14-3-3 levels with concomitant effects on the N-terminal phosphorylation status of LRRK2 seems to modulate filament formation.

We next wondered whether abolishing N-terminal phosphorylation may be sufficient to cause the observed filamentous phenotype of pathogenic and pharmacologically kinase-inhibited LRRK2. Preventing N-terminal phosphorylation by mutating S935 or S910/S935, either in the presence or absence of additional mutations in S955 and S973 caused increased dot-like localization (66,67) (Fig. 7A), but had no effect on the filamentous phenotype in either the absence or presence of LRRK2 kinase inhibitor (Fig. 7B), with all mutants expressed to similar degrees (Fig. 7C). Similarly, mutating another phosphorylation

Figure 3. Continued

mean ± SEM ($n = 4$ experiments). (**C**) Cells were left either untreated (–) or treated with tubacin or trichostatin A as indicated, and extracts analyzed for levels of acetylated α-tubulin and total α-tubulin as loading control. (**D**) Cells were transfected with the indicated constructs, left untreated or incubated with trichostatin A (tricho.) or tubacin either in the presence or absence of 1 μM LRRK2-IN1 for 4 h, and the percentage of cells displaying a filamentous phenotype quantified. Bars represent mean ± SEM ($n = 3$; $^*P < 0.05$). (**E**) Cells were transfected with GFP-tagged wild-type αTAT1 or an inactive point mutant (D157N) as indicated, followed by staining with an antibody against acetylated α-tubulin. Scale bar, 10 μm. (**F**) Cells were co-transfected with either GFP-tagged wild-type or R1441C-mutant LRRK2 and empty control vector (pCMV) or RFP-tagged wild-type or mutant αTAT1 as indicated, followed by quantification of the percentage of cells displaying a filamentous LRRK2 phenotype. Bars represent mean ± SEM ($n = 3$; $^{**}P < 0.01$). (**G**) Cells were transfected with GFP-tagged wild-type or mutant αTAT1 as indicated, and extracts analyzed for protein levels with α-tubulin as loading control. (**H**) Cells were transfected with GFP-tagged wild-type αTAT1 or an inactive point mutant (D157N) as indicated, followed by staining with an antibody against detyrosinated α-tubulin. Scale bar, 10 μm. (**I**) Cells were transfected with wild-type or mutant αTAT1 as indicated, and the percentage of transfected cells with visibly abnormal detyrosinated α-tubulin staining quantified. Bars represent mean ± SEM ($n = 3$; $^*P < 0.05$). (**J**) Cells were left either untreated (–), or treated with different concentrations of parthenolide (PTL) for 12 h as indicated, and extracts analyzed for levels of detyrosinated, acetylated and total α-tubulin. (**K**) Cells were transfected with R1441C-mutant LRRK2, treated for 12 h with PTL as indicated, followed by quantification of the percentage of cells displaying a filamentous LRRK2 phenotype. Bars represent mean ± SEM ($n = 3$; $^*P < 0.05$).

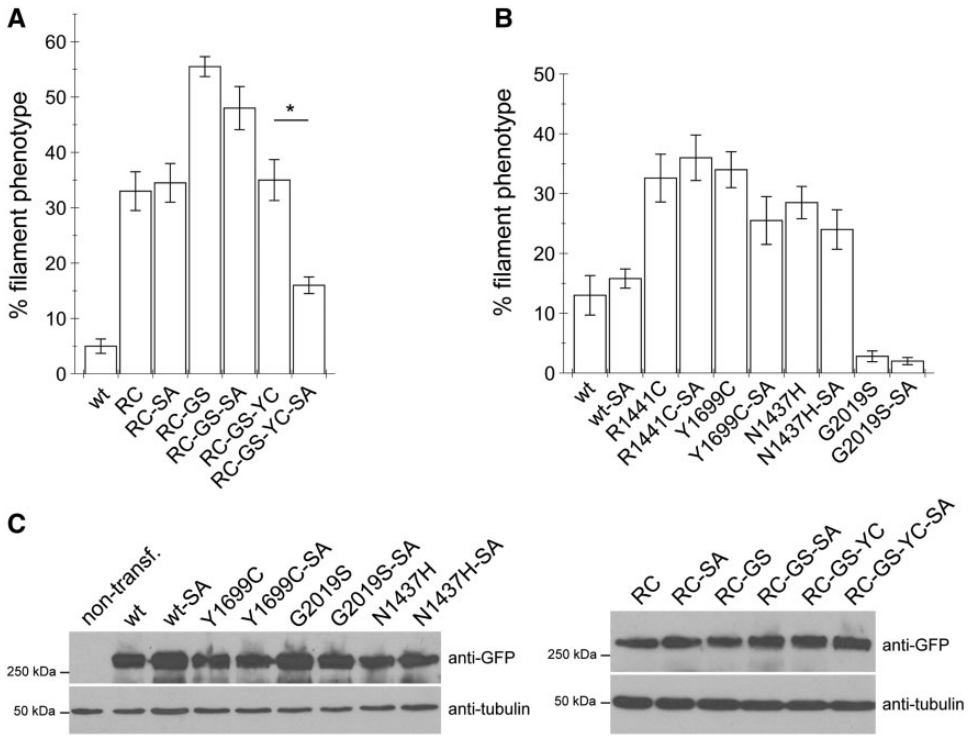

Figure 4. Alterations in autophosphorylation status of LRRK2 on S1292 does not correlate with filamentous phenotype. (**A**) Cells were transfected with the indicated constructs, followed by quantification of the percentage of cells displaying a filamentous phenotype. Bars represent mean ± SEM ($n = 5$; $^*P < 0.05$). (**B**) Cells were transfected with the indicated constructs, followed by quantification of the percentage of cells displaying a filamentous phenotype. Bars represent mean ± SEM ($n = 5$). (**C**) Cells were transfected with GFP-tagged LRRK2 constructs as indicated, and extracts analyzed for protein levels by western blotting using an anti-GFP antibody, and tubulin as loading control.

site in the ROC domain in conjunction with S910, both previously reported to be important for 14-3-3 binding (71) caused increased dot-like localization of wild-type LRRK2 (Fig. 7D), but had no effect on the filament phenotype (Fig. 7E), with similar steady-state protein levels of all mutants examined (Fig. 7C). Thus, mimicking lack of phosphorylation of sites involved in 14-3-3 binding is not sufficient to mimick the filamentous phenotype observed with mutant or pharmacologically kinase-inhibited LRRK2.

Mutations within the catalytic switch II motif of the ROC GTPase domain impair the filamentous localization of pathogenic and kinase-inhibited LRRK2

Apart from altered kinase activity, altered GTP binding and/or GTPase activity have been implicated in LRRK2-related pathogenesis (16,23–26,40,41,72,73). The GTPase activity of LRRK2 has been reported to be modulated by GTPase activating proteins (GAPs) including ArfGAP1 and RGS2, and guanine nucleotide exchange factors (GEFs) such as ARHGEF7 (24,25,74,75). Co-expression of either ArfGAP1 or RGS2 with wild-type or pathogenic R1441C-mutant LRRK2 was without effect on the filamentous phenotype of LRRK2 in the absence or presence of kinase inhibitors (Fig. 8A and B). ARHGEF7 significantly decreased wild-type LRRK2 filament formation triggered by pharmacological kinase inhibition, and also decreased filament formation of pathogenic LRRK2 in the absence or presence of kinase inhibitors (Fig. 8C). However, an inactive GEF-dead variant (L386R/L387S) (75), expressed to similar degrees, also effectively interfered with filament formation (Fig. 8C and D). As the binding of ARHGEF7 to LRRK2 is independent on the guanine nucleotide exchange activity of ARHGEF7 (75), the observed effects of both active and inactive ARHGEF7 are likely due to competing for the same binding site(s) on LRRK2 as those required for MT interactions, rather than due to effects related to ARGEF7-mediated alterations of the GTPase activity of LRRK2.

As an alternative approach to probe for the effect of LRRK2 GTP binding on filament formation, we generated a set of synthetic mutations. Previous structural studies have suggested that two residues in the ROC domain of LRRK2 (R1398 and T1343) may be important for interaction with the γ-phosphate of GTP (76). In addition, mutating R1398 has been described to decrease LRRK2 GTP binding, with a further decrease observed when additionally mutating T1343 (23), and both R1398L and R1398L/T1343V mutations have been reported to largely revert the effects of pathogenic LRRK2 on neurite outgrowth, all whilst having no detrimental effects on protein stability and/or structure (26). We thus wondered whether these mutations may alter the pathogenic LRRK2 filamentous phenotype. When introduced into wild-type or G2019S-mutant LRRK2, no effect on filament formation was observed with either R1398L (RL), T1343V (TV) or R1398L/T1343V (RLTV) mutations (Fig. 8E). However, the RL mutation caused a significant decrease in filament formation in the context of all pathogenic filament-forming LRRK2 mutants (N1437H, R1441C, Y1699C and I2020T) (Fig. 8F and G). Whilst the TV mutation was not displaying an effect on its own when introduced into wild-type or the various pathogenic LRRK2 mutants, the combination of both synthetic mutations (RLTV) drastically decreased the filamentous phenotype of pathogenic N1437H, R1441C, Y1699C and I2020T LRRK2, with all the various proteins expressed to similar degrees (Fig. 8F–H).

Importantly, the RLTV mutation also decreased filament formation of wild-type and pathogenic LRRK2 mutants upon pharmacological kinase inhibition (Fig. 8E–G), indicating a shared mechanism underlying the altered localization of pathogenic mutant and kinase-inhibited LRRK2.

Various reports indicate that an R1398H polymorphism in LRRK2 is associated with decreased PD risk (6–9). Similar to the R1398L mutation, the protective R1398H (RH) mutation reduced the filamentous phenotype of pathogenic LRRK2 in the absence or presence of kinase inhibitors, and this effect was not due to altered steady-state protein levels (Fig. 9A and B). Thus, select mutations in the switch II region of the ROC domain of LRRK2, including a protective risk variant, profoundly decrease the filamentous localization of pathogenic as well as kinase-inhibited LRRK2.

Altered subcellular localization of pathogenic and kinase-inhibited LRRK2 correlates with increased GTP binding and can be reverted by select LRRK2 GTP-binding inhibitors

As the synthetic mutations in the ROC domain are predicted to interfere with GTP binding (76), we measured steady-state GTP binding capacity of pathogenic mutant or pharmacologically kinase-inhibited LRRK2. As previously reported, addition of LRRK2 kinase inhibitors caused a significant increase in GTP binding of wild-type LRRK2 (77) (Fig. 10A and B), whilst the K1347A mutation, known to disrupt the guanine nucleotide-binding P-loop motif, almost completely abolished GTP binding (16,26) (Fig. 10C and D). All filament-forming pathogenic mutants displayed enhanced GTP binding when compared with wild-type LRRK2 (Fig. 10C and D), whilst the RL mutation, and to a larger degree the RLTV mutation, caused a drastic decrease in steady-state GTP binding of wild-type and all pathogenic mutants (Fig. 10E and F). Similarly to the RL mutation, and as previously described in the context of wild-type LRRK2 (78), the protective R1398H variant also displayed a decrease in GTP binding of wild-type and all pathogenic LRRK2 mutants (Fig. 10G).

The capacity for GTP binding may be important for LRRK2 kinase activity (79). Therefore, we next tested the effects of the RL and RLTV mutations on LRRK2 kinase activity. Of all mutants analyzed, only G2019S caused a significant, around 3-fold increase in LRRK2 kinase activity, in agreement with previous studies (80,81) (Fig. 11A and B). The RLTV mutation significantly decreased kinase activity of wild-type and most pathogenic LRRK2 mutants, whilst the RL mutation showed little effect on kinase activity (Fig. 11A and B), even though both RL and RLTV mutants interfered with the filamentous LRRK2 phenotype (Fig. 8E–G). These results indicate that the altered subcellular localization of mutant or pharmacologically kinase-inhibited LRRK2 correlates with enhanced GTP binding rather than with alterations in LRRK2 kinase activity.

Recent studies have described the identification of several LRRK2 GTP-binding inhibitors able to attenuate LRRK2 toxicity, and able to rescue vesicular transport deficits associated with impaired neurite outgrowth (39–41). Both compound 68 and compound 70 significantly reduced LRRK2 GTP binding *in vitro* (Fig. 12A and B). Importantly, these compounds also reverted the filamentous phenotype of both pathogenic and pharmacologically kinase-inhibited LRRK2 (Fig. 12C and D). Conversely, addition of a non-hydrolyzable GTP analog to transiently permeabilized cells enhanced the filamentous phenotype of pathogenic or kinase-inhibited LRRK2 (Fig. 12E), providing further and direct evidence for the importance of GTP binding as a crucial molecular determinant for LRRK2 filament formation.

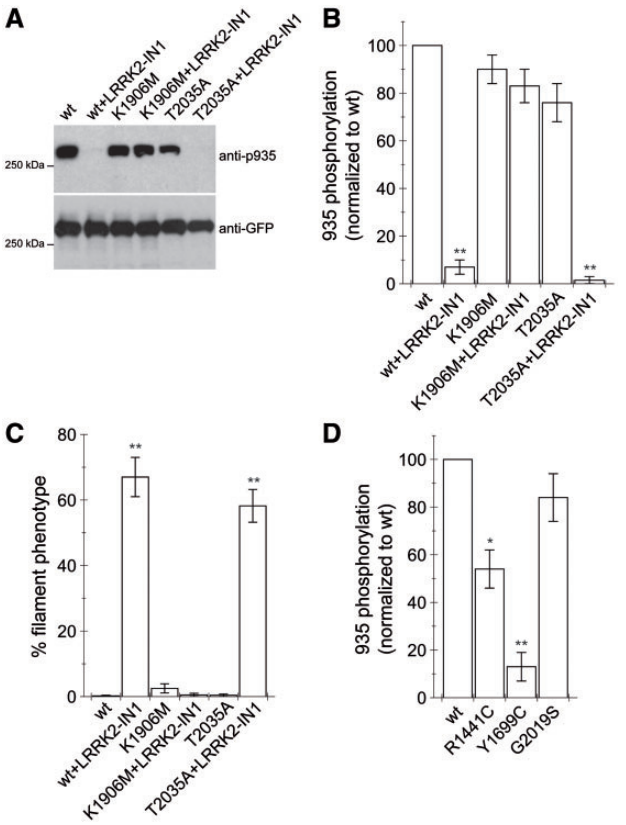

Figure 5. Differential dephosphorylation of cellular N-terminal phosphorylation sites correlates with filamentous phenotype in pharmacologically kinase-inhibited, synthetic kinase-dead and pathogenic mutant LRRK2. (**A**) Cells were transfected with the indicated constructs, and either left untreated or incubated with 1 μM LRRK2-IN1 for 4 h as indicated, and extracts analyzed for phosphorylated (S935) or total (GFP) GFP-tagged LRRK2 as indicated. (**B**) Quantification of the type of experiments depicted in A, with phospho-S935 signals normalized to those found in wild-type LRRK2. Bars represent mean ± SEM ($n = 3$; $^{**}P < 0.01$). (**C**) Cells were transfected with the indicated constructs, and either left untreated or incubated with 1 μM LRRK2-IN1 for 4 h as indicated, followed by quantification of the percentage of transfected cells displaying a filamentous phenotype. Bars represent mean ± SEM ($n = 4$; $^{**}P < 0.001$). (**D**) Cells were transfected with the indicated constructs, extracts analyzed for phosphorylated (S935) or total (GFP) GFP-tagged LRRK2 as indicated, and phospho-S935 signals normalized to wild-type LRRK2. Bars represent mean ± SEM ($n = 3$; $^{**}P < 0.01$; $^{*}P < 0.05$).

Finally, to determine the relative importance of altered N-terminal phosphorylation to the observed filamentous phenotype, we analyzed the phosphorylation of the N-terminal S935 residue in wild-type or pathogenic mutant LRRK2 in the absence or presence of the RL, the RLTV, or the protective RH mutation (Fig. 13A and B). The presence of mutations shown to cause a decrease in GTP binding and filament formation did not display altered S935 phosphorylation when compared with their respective non-mutant counterparts (Fig. 13A and B). Similarly, GTP-binding inhibitors which decrease GTP binding and partially revert the filamentous phenotype caused no effect on S935 phosphorylation of pharmacologically kinase-inhibited or pathogenic mutant LRRK2, respectively (Fig. 13C), and GTP analogs which increase filament formation did not change S935 phosphorylation of either pathogenic or pharmacologically kinase-inhibited LRRK2 (Fig. 13D). Since increasing cellular 14-3-

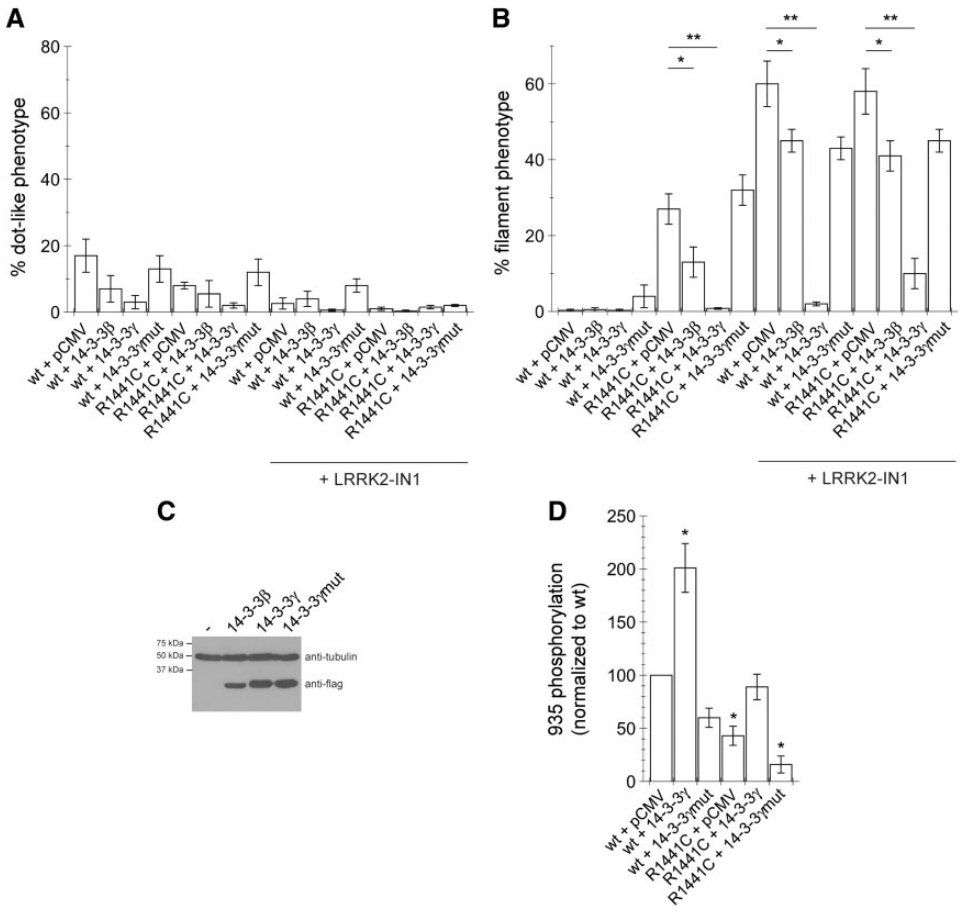

Figure 6. Overexpression of 14-3-3 alters filamentous LRRK2 phenotype and N-terminal phosphorylation status. (**A**) Cells were transfected with the indicated constructs, and either left untreated or incubated with 1 μM LRRK2-IN1 for 4 h, followed by quantification of the percentage of transfected cells displaying a dot-like LRRK2 phenotype. (**B**) Same as in (A), but quantifying the percentage of cells displaying a filamentous phenotype. Bars represent mean ± SEM ($n = 3$; $^*P < 0.05$; $^{**}P < 0.005$). (**C**) Cells were transfected with flag-HA-tagged constructs as indicated, and extracts analyzed for protein levels by western blotting using an anti-flag antibody, and tubulin as loading control. (**D**) Cells were transfected with the indicated constructs, extracts analyzed for phosphorylated (S935) or total (GFP) GFP-tagged LRRK2 as indicated, and phospho-S935 signals normalized to wild-type LRRK2. Bars represent mean ± SEM ($n = 3$; $^*P < 0.05$).

3 levels with a concomitant increase in the N-terminal phosphorylation status of pathogenic LRRK2 was found to decrease the filamentous phenotype of pathogenic LRRK2 (Fig. 6), we analyzed whether this correlated with altered GTP binding. Indeed, the presence of wild-type, but not of loss-of-function mutant 14-3-3γ, caused a decrease in LRRK2 GTP binding (Fig. 13E). Therefore, whilst changes in the N-terminal phosphorylation status can parallel the observed alterations in the subcellular localization of pathogenic or pharmacologically kinase-inhibited LRRK2, they do not seem to be necessary to cause such phenotype. Rather, the key molecular determinant underlying the filamentous phenotype of pathogenic or pharmacologically kinase-inhibited LRRK2 relates to altered GTP binding.

Discussion

Various independent studies have reported that LRRK2 interacts with MTs, even though a preferential association with dynamic versus stable MTs has remained unclear (31,33–35). Whilst the presence of LRRK2 in growth cones has been taken to indicate that it may preferentially interact with dynamic MTs (39), such localization may be contributed to by additional factors. Furthermore, the previously reported alternating nature between the presence of pathogenic LRRK2 and acetylated α-tubulin staining has been taken as evidence that it interacts with dynamic MTs (35), but our data suggest this to be an unlikely interpretation for several reasons. Firstly, only a small subset of all MTs display posttranslational modifications including detyrosination and acetylation, and compared with colocalization with α-tubulin or tyrosinated α-tubulin, we observed a high degree of colocalization of mutant and kinase-inhibited LRRK2 with only the small subset of detyrosinated and/or acetylated MTs. Furthermore, detyrosination and acetylation can often be observed on the same tracks in a 'patchy' fashion (82), reminiscent of the colocalization of LRRK2 with MT tracks which are either detyrosinated and/or acetylated. Finally, decreasing detyrosination by various means interfered with the filamentous LRRK2 phenotype. Whilst some of the data have to be interpreted with care due to the likely lack of compound selectivity (53), they are consistent with the idea that modulation of posttranslational tubulin modifications can impact upon the interaction of mutant and kinase-inhibited LRRK2 with stable MTs.

Both acetylation and detyrosination are generally enriched on stable MTs, but the contribution of acetylation to MT stability remains unclear (53), whilst detyrosination has been clearly reported to protect MTs from the depolymerizing activity of certain motor proteins, thereby increasing their longevity (54).

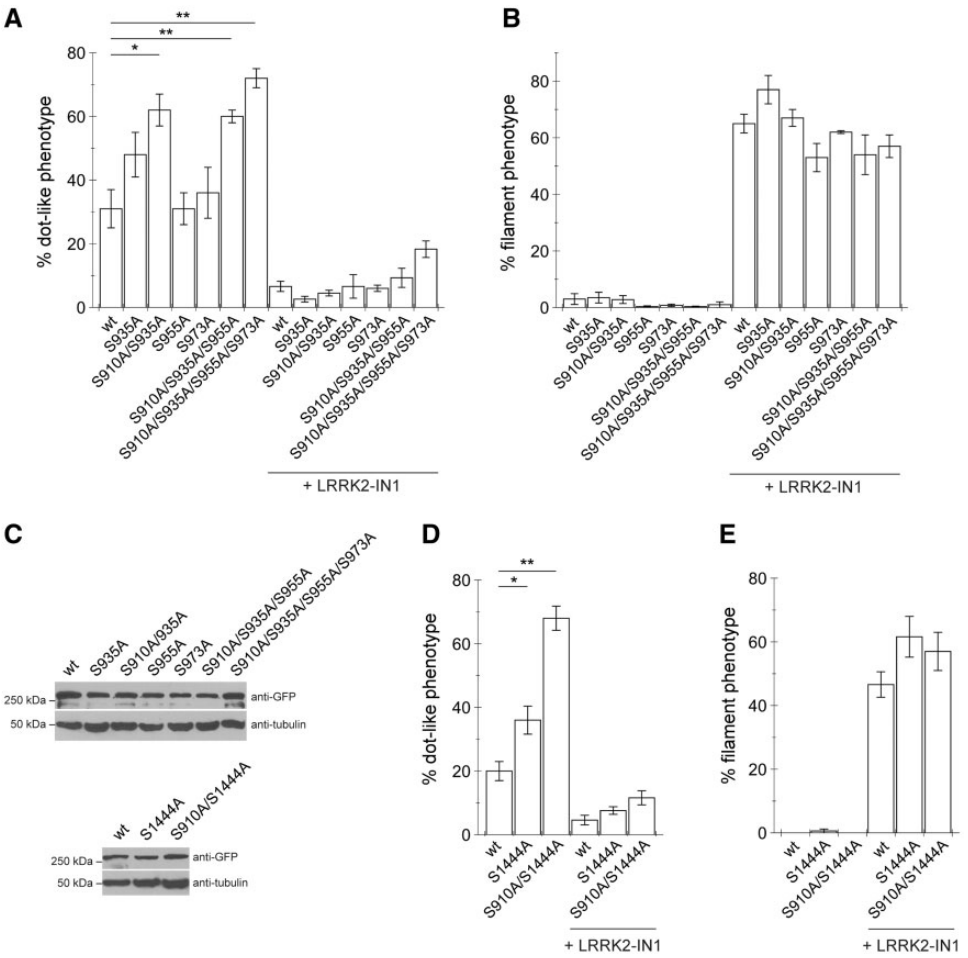

Figure 7. Mutations of the LRRK2 cellular phosphorylation sites do not cause a filamentous phenotype. (**A**) Cells were transfected with the indicated constructs, and either left untreated or incubated with 1 μM LRRK2-IN1 for 4 h as indicated, followed by quantification of the percentage of transfected cells displaying a dot-like LRRK2 phenotype. Bars represent mean ± SEM ($n = 4$; $^{*}P < 0.01$; $^{**}P < 0.005$). (**B**) Same as in (A), but quantifying the percentage of cells displaying a filamentous phenotype. (**C**) Cells were transfected with GFP-tagged LRRK2 constructs as indicated, and extracts analyzed for protein levels by western blotting using an anti-GFP antibody, and tubulin as loading control. (**D**) Cells were transfected with the indicated constructs, and either left untreated or incubated with 1 μM LRRK2-IN1 for 4 h as indicated, followed by quantification of the percentage of transfected cells displaying a dot-like LRRK2 phenotype. Bars represent mean ± SEM ($n = 4$; $^{*}P < 0.05$; $^{**}P < 0.005$). (**E**) Same as in (D), but quantifying the percentage of cells displaying a filamentous phenotype.

Apart from contributing to MT stability, posttranslational tubulin modifications are also recognized by different molecular motor proteins, and this contributes to the establishment and maintenance of polarized vesicular trafficking (83–85). Therefore, enhanced interactions of pathogenic and kinase-inhibited LRRK2 with stable MTs may interfere with select vesicular trafficking events such as the kinesin-mediated transport along stable axonal MTs (85,86). In support of this possibility, pathogenic LRRK2-mediated axonal vesicular transport deficits have been consistently reported in various experimental model systems (35,39,87,88), and synaptic and axonal degeneration are observed in postmortem brains of PD patients (89). In sum, currently available data are consistent with the LRRK2-MT interaction occurring on a subpopulation of stable MTs, with possible downstream effects on MT-mediated vesicular transport events.

The precise molecular determinants within LRRK2 required for MT interactions have remained unknown. Here, we found that all pathogenic LRRK2 mutants with the exception of G2019S and I2012T showed enhanced colocalization with MTs. When assayed *in vitro*, only G2019S has been consistently reported to display increased kinase activity (80,81), with I2012T showing a decrease (14), and pathogenic mutants in the ROC–COR domain showing no change when compared with wild-type LRRK2, respectively. Thus, the altered subcellular localization of the various pathogenic LRRK2 mutants does not seem to correlate with their inherent differences in kinase activity as determined *in vitro*.

As another means to gauge for a possible correlation between altered kinase activity and filament formation, we determined the impact of abolishing autophosphorylation on this cellular readout. Like many other protein kinases, LRRK2 is subject to autophosphorylation (38,61–65). Amongst a variety of identified sites, autophosphorylation at S1292 has been detected *in vivo*, and a S1292A mutation has been reported to substantially reduce the filamentous localization of a LRRK2 variant harboring two distinct pathogenic mutations within the same molecule (38). Whilst we did corroborate a decrease in the filamentous phenotype of a LRRK2 variant harboring multiple pathogenic mutations, abolishing this autophosphorylation site in the context of the individual pathogenic mutants was without effect on their subcellular localization. We cannot exclude

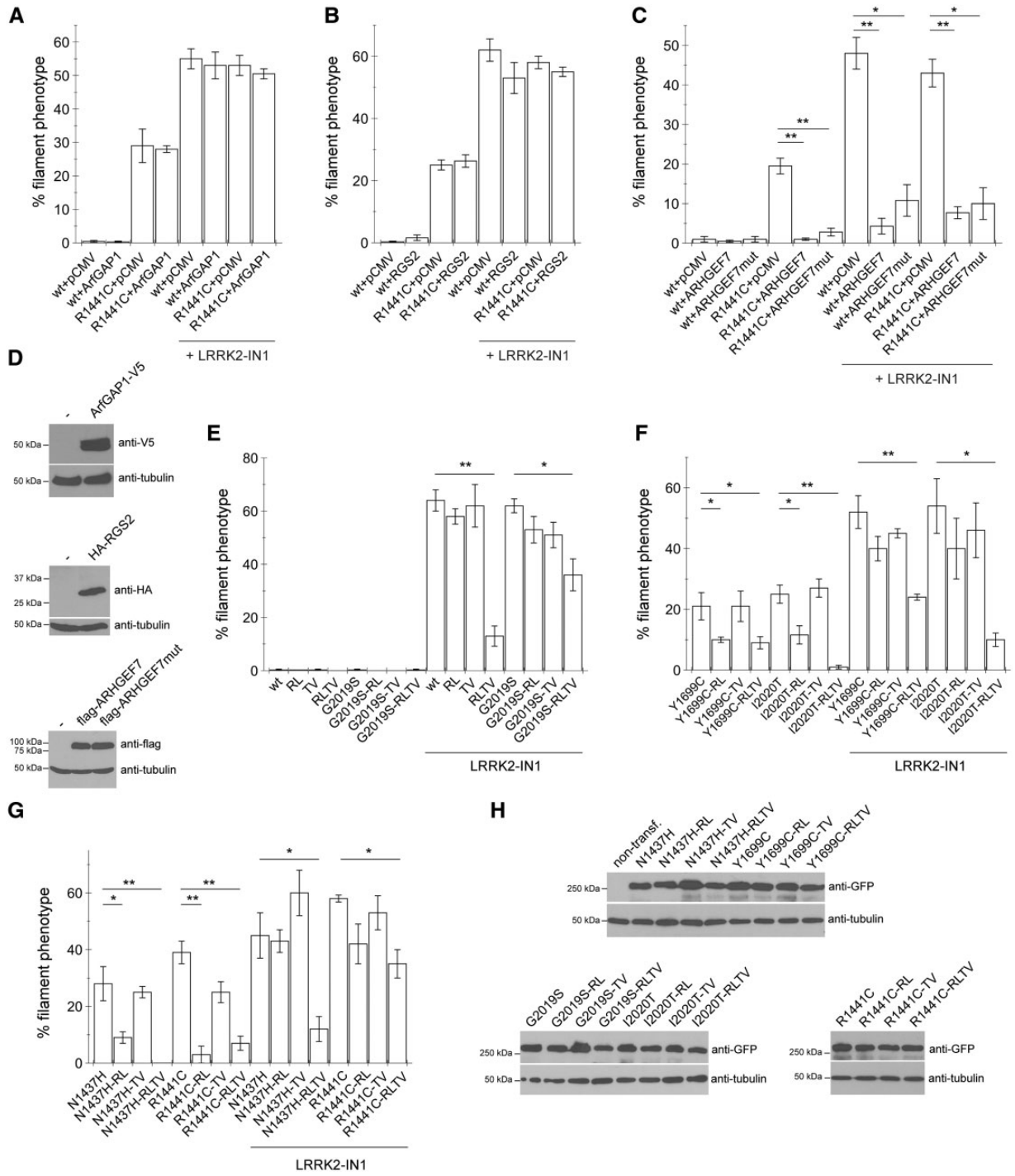

Figure 8. Mutations in the catalytic switch II motif impair the filamentous phenotype of pathogenic and kinase-inhibited LRRK2. (**A**) Cells were transfected with either wild-type or pathogenic LRRK2 along with ArfGAP1, left untreated or incubated in the presence of 1 μM LRRK2-IN1 for 4 h as indicated, and the percentage of cells displaying a filamentous phenotype quantified. Bars represent mean ± SEM ($n = 3$). (**B**) Cells were transfected with either wild-type or pathogenic LRRK2 along with RGS2, left untreated or incubated in the presence of 1 μM LRRK2-IN1 for 4 h as indicated, and the percentage of cells displaying a filamentous phenotype quantified. Bars represent mean ± SEM ($n = 4$). (**C**) Cells were transfected with either wild-type or pathogenic LRRK2 along with ARHGEF7 or inactive variant (ARHGEF7mut), left untreated or incubated in the presence of 1 μM LRRK2-IN1 for 4 h as indicated, and the percentage of cells displaying a filamentous phenotype quantified. Bars represent mean ± SEM ($n = 3$; *$P < 0.05$; **$P < 0.01$). (**D**) Cells were transfected with tagged constructs as indicated, and extracts analyzed for protein levels by western blotting, with tubulin as loading control. (**E**) Cells were transfected with the indicated LRRK2 variants, left untreated or incubated in the presence of 1 μM LRRK2-IN1 for 4 h, and the percentage of cells displaying a filamentous phenotype quantified. Bars represent mean ± SEM ($n = 3$; *$P < 0.05$; **$P < 0.01$). (**F**) As in (**E**). Bars represent mean ± SEM ($n = 3$; *$P < 0.05$; **$P < 0.01$). (**G**) As in (**E**). Bars represent mean ± SEM ($n = 3$; *$P < 0.05$; **$P < 0.01$). (**H**) Cells were transfected with the indicated GFP-tagged constructs, and extracts analyzed for protein levels by western blotting, with tubulin as loading control.

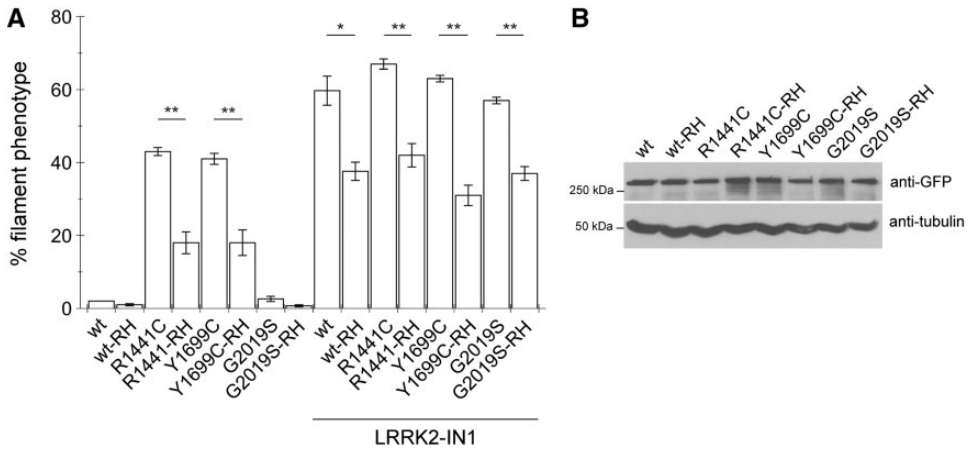

Figure 9. The protective R1398H PD risk variant decreases the filamentous LRRK2 phenotype. (**A**) Cells were transfected with the indicated constructs, left untreated or incubated in the presence of 1 μM LRRK2-IN1 for 4 h, and the percentage of cells displaying a filamentous phenotype quantified. Bars represent mean ± SEM ($n = 3$; $^{*}P < 0.05$; $^{**}P < 0.005$). (**B**) Cells were transfected with the indicated GFP-tagged constructs, and extracts analyzed for protein levels by western blotting, with tubulin as loading control.

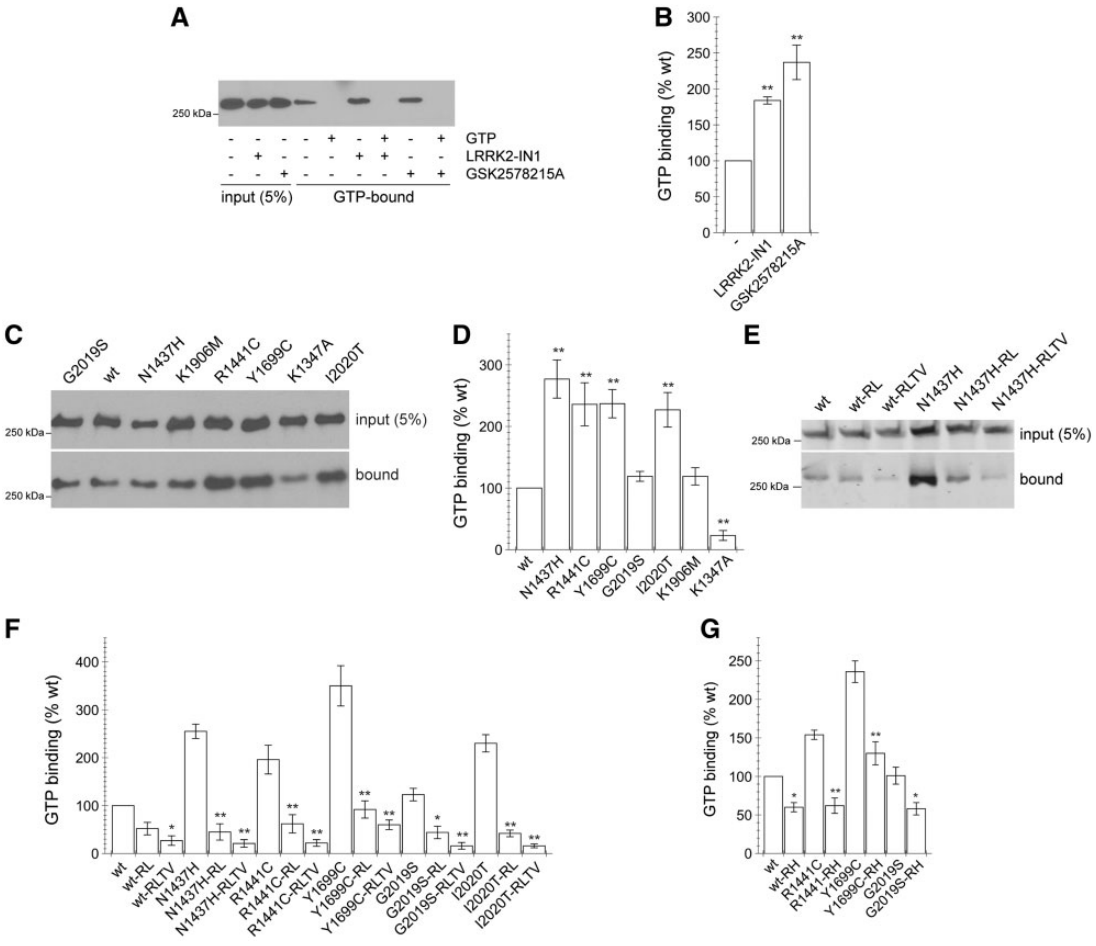

Figure 10. Pathogenic mutant or pharmacologically kinase-inhibited LRRK2 display enhanced GTP binding, and both RL and RLTV mutations cause a decrease in LRRK2 GTP binding. (**A**) Transfected HEK293T cells were incubated with either 1 μM LRRK2-IN1 or 1 μM GSK2578215A for 4 h as indicated, LRRK2 was affinity-purified from lysates using GTP-agarose in the presence of kinase inhibitors, and input (5%) and GTP-bound protein subjected to western blot analysis using an anti-GFP antibody. (**B**) Quantification of the type of experiments depicted in (A). Bars represent mean ± SEM ($n = 4$; $^{**}P < 0.005$). (**C**) Cells were transfected with various constructs as indicated, LRRK2 variants were affinity-purified using GTP-agarose beads, and input and GTP-bound protein subjected to western blot analysis using an anti-GFP antibody. (**D**) Quantification of the type of experiments depicted in (C). Bars represent mean ± SEM ($n = 4$; $^{**}P < 0.005$). (**E**) Cells were transfected with various constructs as indicated, and LRRK2 variants affinity-purified and subjected to western blot analysis as described above. (**F**) Quantification of the type of experiments depicted in (E). Bars represent mean ± SEM ($n = 5$; $^{*}P < 0.05$; $^{**}P < 0.005$). (**G**) Cells were transfected with the various constructs as indicated, and LRRK2 variants affinity-purified and subjected to western blot analysis followed by quantification as described above. Bars represent mean ± SEM ($n = 4$; $^{*}P < 0.05$; $^{**}P < 0.01$).

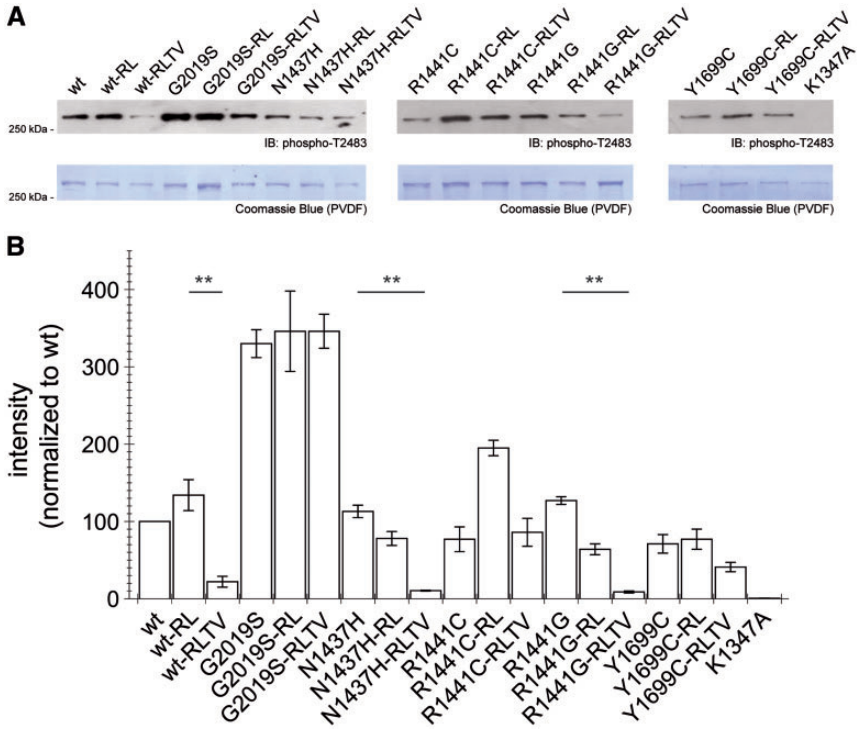

Figure 11. Effects of RL and RLTV mutations on LRRK2 kinase activity. (A) Example of autophosphorylation of distinct LRRK2 proteins as indicated. Autophosphorylation was detected with an antibody against phospho-Thr2483 (top) and was normalized to protein input as measured by Coomassie Blue staining (bottom). (B) Quantification of the type of experiments as depicted in (A), with values normalized to autophosphorylation of wild-type LRRK2. Bars represent mean ± SEM ($n = 4$; $^{**}P < 0.001$).

that autophosphorylation at multiple distinct sites within LRRK2 may contribute toward modulating the enhanced localization of most pathogenic LRRK2 to MTs, but the generally low stoichiometry of such autophosphorylation events (61) makes this an unlikely possibility. Altogether, our data indicate that the altered subcellular localization of the various pathogenic LRRK2 mutants does not correlate with alterations in inherent LRRK2 kinase activity.

However, and in an apparently contradictory manner, various structurally distinct and specific LRRK2 kinase inhibitors all triggered the relocalization of wild-type and mutant LRRK2 to MTs, whilst such relocalization was not observed with two distinct kinase-dead point mutants (K1906M and T2035A). LRRK2 is phosphorylated by a variety of upstream cellular kinases at distinct sites within the N-terminus, including S910, S935, S955 and S973, and phosphorylation at these sites is important for 14-3-3 binding (36,61,66,67). Pharmacological kinase inhibition has been suggested to be associated with a conformational change associated with dephosphorylation of the N-terminal phosphorylation sites, and such dephosphorylation was not found with two distinct synthetic kinase-dead mutants, suggesting that these mutants may not properly mimick the features of pharmacologically kinase-inhibited LRRK2 (50). We corroborated these findings, and further found that dephosphorylation of the N-terminal phosphorylation sites was observed in the presence of pharmacological kinase inhibitor in the case of the T2035A, but not the K1906M mutant. Thus, and in contrast to the T2035A mutant, the K1906M mutant may not be able to bind kinase inhibitor and/or may not be able to undergo an inhibitor-mediated conformational change. The differential dephosphorylation of the N-terminal sites correlated with the differential ability of those mutants to form a filamentous phenotype in the presence of pharmacological kinase inhibition, indicating that N-terminal dephosphorylation parallels the altered subcellular localization of pharmacologically kinase-inhibited LRRK2.

Apart from pharmacologically kinase-inhibited LRRK2, all pathogenic mutants which displayed enhanced filament formation are known to show decreased N-terminal phosphorylation and 14-3-3 binding (36,61,66,67). Increasing cellular 14-3-3 levels reverted the filamentous phenotype of both pathogenic and kinase-inhibited LRRK2, which correlated with increased N-terminal phosphorylation and decreased GTP binding. To determine whether dephosphorylation of the N-terminus of LRRK2 is sufficient to cause a filamentous phenotype, we mutated all currently known N-terminal phosphorylation sites implicated in 14-3-3 binding. As previously described, Ala mutations of S910 and S935, but not of S955 or S973 were without effect on the filamentous phenotype, but caused a relocalization of LRRK2 into the dot-like phenotype. Mutating two distinct residues (S910 and S1444) also implicated in 14-3-3 binding (71) caused a similar subcellular relocalization. Whilst the identity of those dot-like structures remains unclear, the observation that a pharmacological kinase inhibitor was able to relocalize those mutant proteins back into a filamentous phenotype suggests that these structures are not irreversible protein aggregates. Our data suggest that N-terminal dephosphorylation is not sufficient to cause the filamentous phenotype of pathogenic or pharmacologically kinase-inhibited LRRK2. In addition, no significant changes in N-terminal phosphorylation were observed when altering the GTP-binding status of LRRK2 by either mutational or pharmacological means, even though such

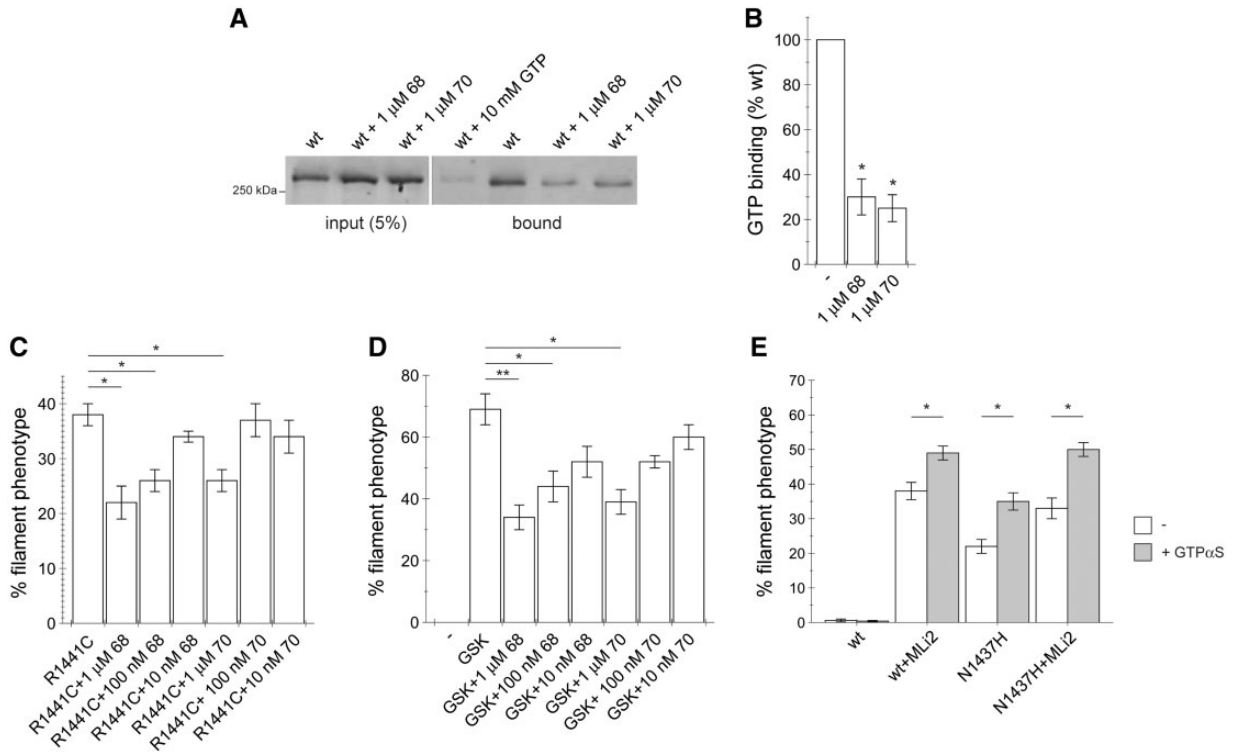

Figure 12. LRRK2 GTP-binding inhibitors decrease, and GTP analogs increase the filamentous phenotype. (**A**) Example of GTP binding of wild-type LRRK2 in the absence or presence of two distinct GTP-binding inhibitors as indicated. Inhibitors were added during cell lysis, and were present throughout binding. Input (5%) and GTP-bound proteins were subjected to western blot analysis using an anti-GFP antibody. (**B**) Quantification of the type of experiments depicted in (A). Bars represent mean ± SEM ($n = 3$; *$P < 0.005$). (**C**) Cells were transfected with R1441C-pathogenic LRRK2, and treated for 3 h with the respective concentration of GTP-binding inhibitors as indicated prior to analysis for LRRK2 subcellular localization. Bars represent mean ± SEM ($n = 3$; *$P < 0.05$). (**D**) Cells were transfected with wild-type LRRK2, treated for 1 h with GTP-binding inhibitors as indicated, followed by addition of 1 μM GSK2578215A and incubation for another 2 h before fixation and analysis for LRRK2 subcellular localization. Bars represent mean ± SEM ($n = 3$; **$P < 0.01$; *$P < 0.05$). (**E**) Cells were transfected as indicated and treated with 500 nM MLi2 for 2 h before permeabilization as indicated. Cells were permeabilized with streptolysin-O for 10 min, and incubated in resealing buffer for another 10 min both in the presence or absence of GTPαS or 500 nM MLi2 as indicated, followed by fixation and analysis for LRRK2 subcellular localization. Bars represent mean ± SEM ($n = 3$; *$P < 0.05$).

manipulations profoundly affected the subcellular localization of LRRK2. Therefore, N-terminal dephosphorylation also does not seem to be necessary for the observed changes in subcellular localization.

To further understand the shared mechanism underlying the filamentous phenotype of both pathogenic mutant and pharmacologically kinase-inhibited LRRK2, we probed for possible effects related to GTP binding. The GTP domain has been shown to exhibit important roles for the biological functions of LRRK2 (16,23–26,40,41,72,73), even though the precise mechanism(s) of action remain unclear. We observed a perfect correlation between increased steady-state levels of GTP binding of mutant as well as of pharmacologically kinase-inhibited LRRK2 with the enhanced colocalization with MTs, indicating that increased steady-state GTP binding may explain the convergence onto a common cellular readout. We next used both molecular as well as pharmacological approaches to determine whether interfering with LRRK2 GTP binding would revert the altered subcellular localization. Residues R1398 and T1343 have been implicated in GTP binding according to structural and biochemical studies (23,37), and careful biochemical analysis has shown that mutating these residues has no impact on protein stability and/or macromolecular structure (26). In agreement with the importance of those residues for LRRK2 function (26), mutations of RL or RLTV caused a drastic decrease in steady-state levels of GTP binding of all pathogenic LRRK2 mutants, which was paralleled by a decrease in the filamentous phenotype in the absence as well as presence of kinase inhibitors. Interestingly, the RH substitution reported to confer protection against PD (6–9) also decreased the filamentous phenotype of mutant or pharmacologically kinase-inhibited LRRK2, which was associated with a decrease in steady-state GTP binding. Whilst the precise mechanism by which this variant protects against PD risk remains to be further elucidated, it is tempting to speculate that GTP-binding-mediated alterations in the subcellular localization may play a contributing role.

Previous studies reported either increased (RL) or decreased (RLTV) GTP hydrolysis activity of wild-type and G2019S-mutant LRRK2, with no changes observed in GTP binding (26). Such opposing effects on GTP hydrolysis do not parallel the observed decrease in filament formation with both mutants as found here. In addition, a recent study also reported a decrease in steady-state GTP binding of the protective RH variant when compared with wild-type LRRK2 (78). Whilst the lack of altered GTP binding of RL and RLTV mutants as reported previously (26) remains unclear, it may be due to subtle assay differences combined with the inherently low GTP binding affinity of LRRK2 *per se*. In either case, the reported decrease in GTP binding of the protective RH variant (78), together with our current data highlight the importance of the R1398 residue for steady-state GTP binding.

As proof-of-concept, we analyzed the effects of two recently identified small-molecule LRRK2 GTP-binding inhibitors (40,41). Both compounds interfered with steady-state GTP binding *in*

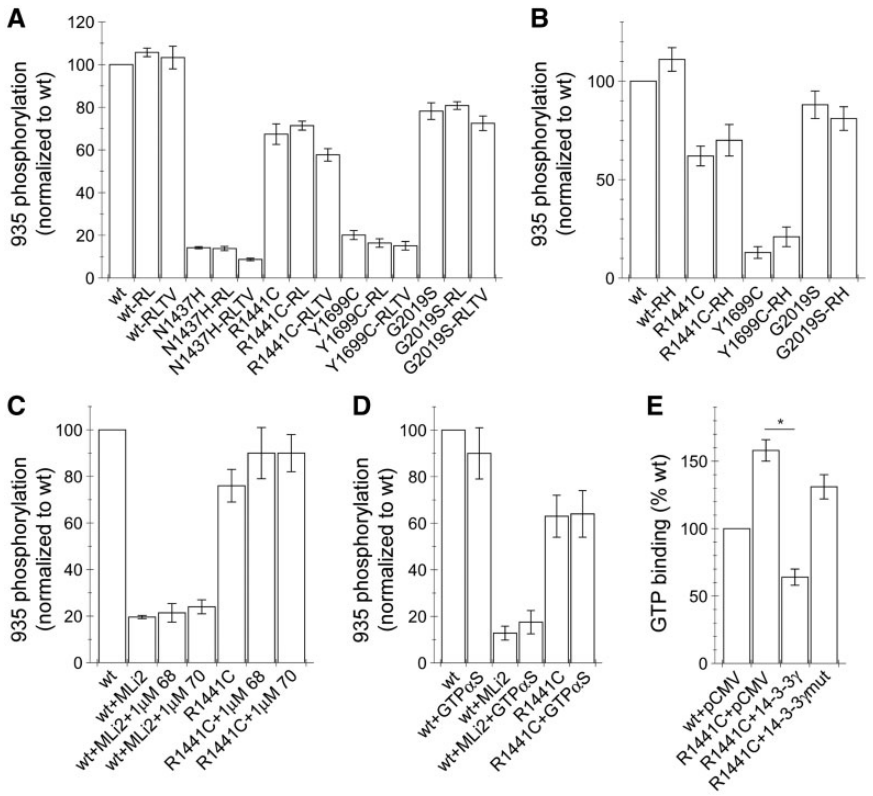

Figure 13. Alterations in the N-terminal phosphorylation status of LRRK2 are not necessary to cause a filamentous phenotype. (**A**) Cells were transfected with the indicated constructs, extracts analyzed for phosphorylated (S935) or total LRRK2 as indicated, and phospho-S935 signals normalized to wild-type LRRK2. Bars represent mean ± SEM ($n = 4$). (**B**) Cells were transfected with the indicated constructs, and extracts analyzed as described in (A). Bars represent mean ± SEM ($n = 5$). (**C**) Cells were transfected with the indicated constructs, treated with 500 nM MLi2 and/or with 1 μM GTP-binding inhibitors as indicated, and extracts analyzed for phospho-S935 signals as described in (A). Bars represent mean ± SEM ($n = 5$). (**D**) Cells were transfected with the indicated constructs, treated with 500 nM MLi2 for 2 h before permeabilization in the absence or presence of GTPαS as indicated, and analysis of extracts performed as described in (A). Bars represent mean ± SEM ($n = 5$). (**E**) Cells were transfected with the indicated constructs, LRRK2 variants were affinity-purified using GTP-agarose beads, and GTP-bound protein subjected to analysis for phospho-S935 signals as described in A. Bars represent mean ± SEM ($n = 3$; *$P < 0.05$).

vitro, and significantly reduced the enhanced colocalization of mutant or pharmacologically kinase-inhibited LRRK2 with MTs. These GTP-binding inhibitors have also been reported to reduce LRRK2 kinase activity in serum-starved cells (40). However, since all pharmacological LRRK2 kinase inhibitors analyzed here were found to increase the filamentous phenotype, the main mechanism of action of the GTP inhibitor compounds is most likely related to interfering with LRRK2 GTP binding rather than with kinase activity. Whilst promising lead compounds, they are unlikely to be highly specific for LRRK2-mediated GTP binding, but may modulate GTP binding of many other proteins. Thus, future studies in intact animal models using synthetic mutations which interfere with GTP binding (e.g. the protective RH risk variant) will be required to determine whether modulating GTP binding can abolish the detrimental effects of pathogenic LRRK2, as this would warrant further efforts to develop specific GTP-binding inhibitors to treat LRRK2-related PD due to ROC–COR mutations.

To obtain direct evidence that GTP binding is required for filament formation, we transiently permeabilized cells in the presence or absence of a non-hydrolyzable GTP analog. Addition of a non-hydrolyzable GTP analog did not induce filament formation of wild-type LRRK2, which may be due to differences in the conformational state of both pathogenic and pharmacologically kinase-inhibited LRRK2 versus wild-type LRRK2, in conjunction with the low inherent GTP binding affinity of wild-type LRRK2. However, addition of a non-hydrolyzable GTP analog increased the filamentous phenotype of both pathogenic and kinase-inhibited LRRK2, providing formal proof that GTP binding is crucial for the altered subcellular localization of pathogenic and pharmacologically kinase-inhibited LRRK2.

Amongst all pathogenic LRRK2 mutants, only the G2019S mutation has been consistently shown to display increased kinase activity when measured *in vitro* (80,81), whilst not displaying increased GTP binding or association with MTs when compared with wild-type. In contrast, all ROC–COR mutants showed unaltered kinase activity *in vitro*, but increased GTP binding and a filamentous phenotype. Conversely, both G2019S and filament-forming LRRK2 mutants were found to cause increased phosphorylation of certain Rab proteins when measured from intact cells (81). Rab proteins are associated with distinct vesicular structures moving along MT tracks. Therefore, the enhanced MT association of ROC–COR mutants may cause increased substrate phosphorylation due to enhanced 'molecular proximity', without an inherent increase in kinase activity. Whilst further studies will be necessary to corroborate the detailed downstream effects of the pathogenic LRRK2-mediated MT interactions, our results suggest a model whereby the distinct pathogenic LRRK2 mutants may impact upon the same intracellular MT-mediated vesicular trafficking events, albeit doing so by distinct means.

Materials and Methods

Reagents

Trichostatin A, tubacin and nocodazole were from Sigma Aldrich, PTL from Eurodiagnostico, LRRK2-IN1, TAE684 and CZC25146 from the Michael J. Fox Foundation, GSK2578215A from Tocris, compound 68 (ID 9108605) and compound 70 (ID 9119202) from Chembridge Corporation (San Diego, USA), and GNE-0877 and GNE-7915 from MedchemExpress (USA), and MLi2 from MRC PPU, Dundee, UK. Natural streptolysin-O was from Abcam (ab63978), and non-hydrolyzable GTP test kit from Jena Bioscience (NK-102).

DNA constructs and site-directed mutagenesis

GFP-tagged human wild-type, R1441C, Y1699C, G2019S and K1347A LRRK2 constructs were obtained from Addgene. All other constructs were generated by site-directed mutagenesis (QuickChange, Stratagene), and the identity of constructs verified by sequencing of the entire coding region. For transfection purposes, DNA was prepared from bacterial cultures grown at 37 °C using a midiprep kit (Promega) according to the manufacturer's instructions. GFP-tagged human α-tubulin K40 acetyltransferase (αTAT1) and an enzymatically inactive point mutant (D157N) (62) were from Addgene. Both wild-type and mutant αTAT1 were PCR amplified and subcloned into pDsRED-Express vector using the *Ba*MHI and *Eco*RI sites to generate C-terminally tagged dsRED-constructs. Human flag-tagged ARHGEF7 and the GEF-dead variant (L386R/L387S) were generous gifts from Drs K. Haebig and M. Bonin (University of Tuebingen, Germany), human V5-tagged ArfGAP1 was a generous gift from Dr T. Dawson (Johns Hopkins University, Baltimore, USA), human HA-tagged RGS2 was a generous gift from Dr. B. Wolozin (Boston University School of Medicine, Boston, USA), and human flag-HA-tagged 14-3-3β and rat flag-HA-tagged 14-3-3γ were from Addgene. The binding-deficient V181D mutant 14-3-3γ construct was generated by site-directed mutagenesis, and identity of the construct verified by sequencing of the coding region.

Cell culture and transfections

HEK293T/17 cells were cultured as previously described (90) and transfected at 80% confluence with 2 μg of LRRK2 constructs and 6 μl of LipoD293 (SignaGen Laboratories) per well of a six-well plate overnight in full medium. Cotransfections were performed with 1.8 μg of LRRK2 constructs and 200 ng of constructs as indicated (400 ng for 14-3-3 constructs). Cells were split onto coverslips the following day at a ratio of 1:4. As indicated, cells were incubated with nocodazole (200 nM), trichostatin A (800 nM), tubacin (10 μM), LRRK2-IN1 (1 μM), TAE684 (200 nM), CZC25146 (200 nM), GSK2578215A (1 μM), GNE-0877 (1 μM), GNE-7915 (1 μM), compound 68 (10 nM to 1 μM), compound 70 (10 nM to 1 μM) for 3 h in full medium, or with PTL (5 or 10 μM) for 12 h in full medium, followed by fixation and processing for immunochemistry, or by cell lysis and western blot analysis as described in following sections.

Immunofluorescence and laser confocal imaging

MT staining was performed essentially as described (91). Briefly, cells were rinsed twice in PBS, followed by fixation in 3% formaldehyde, 0.2% glutaraldehyde, 0.2% Triton X-100, 10 mM EGTA for 10 min at 37 °C. Fixed cells were washed two times in PBS for 5 min each, followed by quenching with 50 mM ammonium chloride in PBS for 10 min at RT, and two washes in PBS for 5 min each. Fixed cells were permeabilized in 0.1% Triton X-100 in PBS for 10 min, washed in PBS, blocked in 1% BSA (w/v) in PBS for 20 min, and incubated with primary antibodies in PBS for 1 h. Primary antibodies included mouse monoclonal anti-α-tubulin (Sigma Aldrich, clone DM1A, 1:100), mouse monoclonal anti-β-tubulin (Millipore, clone KMX-1, 1:100), mouse monoclonal anti-acetylated α-tubulin (Sigma, clone 6-11B-1, 1:100), rabbit polyclonal anti-detyrosinated α-tubulin (Abcam, ab48389, 1:200; or Millipore, AB3201, 1:500), rat monoclonal anti-tyrosinated α-tubulin (Abcam, ab6160, 1:100), or rat monoclonal anti-HA (Roche, clone 3F10, 1:500).

Secondary antibodies included Alexa 647-conjugated goat anti-rabbit, goat anti-mouse or goat anti-rat, or Alexa 488-conjugated goat anti-mouse, goat anti-rabbit or goat anti-rat antibodies (Invitrogen, 1:1000). Coverslips were incubated with secondary antibodies for 1 h at RT, followed by washes in PBS and mounting using mounting medium containing DAPI (Vector Laboratories).

Images were acquired on a Leica TCS-SP5 confocal microscope using a 63× 1.4 NA oil UV objective (HCX PLAPO CS). Images were collected using single excitation for each wavelength separately and dependent on secondary antibodies (488 nm Argon Laser line and a 510–540 nm emission band pass; 633 HeNe Laser line and a 640–670 nm emission band pass). GFP-tagged proteins were excited with 488 nm Argon Laser line and a 500–530 nm emission band pass, and DAPI was excited with the 405 nm UV diode and a 430–480 nm emission band pass, respectively.

Twenty-five image sections of selected areas were acquired with a step size of 0.3 μm, and z-stack images analyzed and processed using Leica Applied Systems (LAS AF6000) image acquisition software. For deconvolution, image sections of selected areas were acquired with a step size of 0.12 μm, and deconvolved using Huygens Essential Deconvolution software.

Quantification of colocalization of mutant or kinase-inhibited LRRK2 with acetylated or detyrosinated α-tubulin was performed essentially as described (82). For each condition, five individual cells were analyzed. Eight LRRK2-positive MT tracks were randomly selected from each cell and a line drawn over the length of a straight part of the track. Tracks were scored for the level of colocalization using image calculator and plot profile functions of ImageJ. The percentage of colocalization was subgrouped for each cell, with colocalization 0–50% (white), 50–90% (gray) or >90% (dark gray).

For the determination of the subcellular localization of GFP-tagged LRRK2 proteins, cells were transfected and cultured as described, and fixed 48 h after transfection in 4% paraformaldehyde in PBS for 20 min at RT. Fixed cells were washed two times in PBS, permeabilized in 0.5% Triton X-100 in PBS for 10 min at RT, washed in PBS, and mounted in mounting medium containing DAPI (Vector Laboratories). Cells were visualized on an inverted microscope (Zeiss) using a 100× 1.40 NA Plan APO oil objective. For each experiment, 100 random cells were scored and assigned to one of three phenotypes [cytosolic: purely diffuse localization; dot-like: presence of at least one dot-like structure (small, usually perinuclear); filamentous: presence of clear filamentous structures]. Experiments with RL, TV and RLTV mutants, and experiments involving LRRK2 GTP-binding inhibitors were performed and analyzed by two independent observers blind to condition, with comparable results obtained in all cases.

Live cell imaging

Live cell imaging of HEK293T/17 cells transfected with GFP-tagged wild-type LRRK2 was performed on cells grown on glass-bottom dishes (IBIDI) in full medium without phenol red. Live images were acquired 48 h after transfection on a Leica TCS-SP5 confocal microscope using a 63× 1.4 NA oil UV objective (HCX PLAPO CS). LRRK2-IN1 (1 μM final concentration) was added at time 0, and images collected using single excitation 488 nm Argon Laser line and a 495–575 nm emission band pass. The 488 nm Argon Laser line was set at 30%, with pinhole airy at 1. Contrast phase images of single stacks were simultaneously acquired. Fifteen image sections of selected areas were acquired every 45 s with a step size of 0.5 μm. Z-stack maximal intensity projection images were analyzed and processed using Leica Applied Systems (LAS AF6000) image acquisition software.

MT nucleation assays

Cells were grown and transfected as described above, and split onto poly-L-lysine-coated coverslips 24 h later. The following day, coverslips in six-well dishes were placed in an ice-water bath for 1.5 h to cause cold-induced MT depolymerization. MT regrowth was initiated by placing coverslips at 37 °C for the indicated time periods, followed by fixation in 4% paraformaldehyde in a buffer containing 60 mM PIPES, 25 mM HEPES, pH 6.9, 10 mM EGTA, 1 mM $MgCl_2$ and 0.5% Triton X-100 (92) before immunostaining as described above. Cells were visualized on an inverted microscope (Zeiss) using a 100× 1.40 NA Plan APO oil objective. For each timepoint, 100 cells were scored for visible MT staining with antibodies against α-tubulin or acetylated α-tubulin in non-transfected versus transfected cells, and for visible pathogenic LRRK2 filament reformation in transfected cells.

Permeabilization of cells with streptolysin-O

Cells were grown and transfected as described above, and split onto poly-L-lysine-coated coverslips in 24-well plates the following day. Two days after transfection, cells were incubated with or without 500 nM MLi2 for 2 h as indicated. Permeabilization was performed essentially as described previously (93,94) with slight modifications. Cells were permeabilized in 1 ml of Hank's balanced salt solution (HBSS; 4.17 mM $NaHCO_3$, 0.34 mM Na_2HPO_4, 0.44 mM KH_2PO_4, 137.9 mM NaCl, 5.3 mM KCl, pH 7.4) containing 16 ng/ml streptolysin-O for 10 min at 37 °C. This resulted in the permeabilization of around 80% of cells as independently determined by Trypan blue staining. After 10 min, permeabilization buffer was replaced by 1 ml of resealing buffer (10 mM HEPES, 140 mM NaCl, 5 mM KCl, 1.3 mM $MgCl_2$, 2 mM $CaCl_2$, pH 7.4), and cells were incubated for an additional 10 min at 37 °C. Buffers contained 500 nM MLi2, 5 μM GTPαS, GPCpp, GppCp, GppNHp or GTPγS as indicated. Amongst the non-hydrolyzable GTP analogs tested, only GTPαS was found to be non-toxic to permeabilized cells up to a concentration of 5 μM, and thus was used for all subsequent experiments. Upon permeabilization and resealing, cells were fixed and stained as described above, and 100 random cells were scored for a filamentous phenotype per condition and experiment. Cells displayed an intact MT network upon 10 min permeabilization and 10 min resealing under all conditions analyzed.

Cell extracts and western blotting

Cells were collected 48 h after transfection, washed in PBS and resuspended in cell lysis buffer (1% SDS in PBS containing 1 mM PMSF, 1 mM Na_3VO_4, 5 mM NaF). Extracts were sonicated, boiled and centrifuged at 13 500 rpm for 10 min at 4 °C. Protein concentration of supernatants was estimated using the BCA assay (Pierce), and equal amount of extracts were resolved by SDS-PAGE, transferred to PVDF (in the case of ECL detection) or to nitrocellulose membranes (in the case of detection by Odyssey) and analyzed by western blotting using a variety of antibodies as indicated, including rabbit polyclonal anti-GFP (Abcam, ab6556, 1:1000), mouse monoclonal anti-myc (Sigma, clone 9E10, 1:1000), rabbit polyclonal anti-V5 (Sigma, V8137, 1:2500), rat monoclonal anti-HA (Roche, clone 3F10, 1:500), mouse monoclonal anti-flag (Sigma, clone M2, 1:500), phospho-S935-LRRK2 antibody (Abcam, 1:1000), mouse monoclonal anti-acetylated α-tubulin (Sigma, clone 6-11B-1, 1:5000), rabbit polyclonal anti-detyrosinated α-tubulin (Millipore, AB3201, 1:500) and mouse monoclonal anti-α-tubulin (Sigma, clone DM1A, 1:10 000). Membranes were incubated with primary antibodies in 5% BSA (w/v) in TBS–0.1% Tween-20 for 1.5 h at RT, or overnight at 4 °C. For ECL detection, membranes were incubated with secondary antibodies in 5% BSA in TBS–0.1% Tween-20 for 1 h, or with secondary antibodies in PBS (1:10 000) for detection by Odyssey, followed by three times 5 min rinses in PBS. Westerns were developed with ECL reagents (Roche), and a series of timed exposures to ensure that densitometric analyses were performed at exposures within the linear range. Most determinations of steady-state protein levels, as well as all GTP-binding assays were quantified by ODYSSEY infrared imaging system application software LI-COR Image Studio Lite version 5.2.

For determination of S935-phosphorylation status, HEK293T cells were transiently transfected with the indicated constructs to express wild-type or mutant LRRK2 using 1 μg of DNA in 50 μl OPTI-MEM (Thermo Fisher) and 2 μg of linear polyethylenimine (PEI, Polyscience) per P24 well. Cells were lysed 48 h after transfection with 100 μl of lysis buffer [20 mM Tris–HCl, pH 7.5, 150 mM NaCl, 1 mM EDTA, 1% Triton, 10% glycerol, supplemented with Protease and Phosphatase Inhibitor Mixture (Roche)]. Samples were incubated on ice for 30 min and cleared by centrifugation at 18 000*g* for 30 min at 4 °C. Protein concentration of supernatants was estimated using the BCA assay (Pierce), and equal amount of protein (10 μg) were resolved on 3–8% SDS-PAGE, transferred onto PVDF membranes (Bio-Rad) and analyzed by immunofluorescence western blotting using antibodies against total-LRRK2 antibody (N241 A/34, NeuroNab, 1:1000) or anti-GFP antibody (Abcam, ab6556, 1:1000), phospho-S935-LRRK2 antibody [UDD2 10(12), Abcam, 1:1000] and mouse monoclonal anti-beta-actin (Sigma, 1:10 000). Membranes were incubated with primary antibodies in 5% BSA (w/v) in TBS–0.1% Tween-20 overnight at 4 °C. Membranes were washed three times for 10 min with TBS–Tween buffer, and incubated for 1.5 h at room temperature with anti-mouse Alexa-488 and anti-rabbit Alexa-568 secondary antibodies (1:1000) in 5% BSA (w/v) in TBS-T buffer. Membranes were washed in TBS-T buffer followed by visualization on Typhoon FLA9500 (GE Healthcare) and densitometry analysis carried out using ImageJ software. In some cases, analysis was performed as described above by ODYSSEY infrared imaging system application software LI-COR Image Studio Lite version 5.2. In all cases, total LRRK2 protein levels were comparable amongst the different mutants analyzed.

GTP-binding assays

GTP-binding assays were performed essentially as previously described (77). HEK293T/17 cells were cultured in 100 mm diameter dishes and transfected at 70–80% confluence with 12 μg of GFP-tagged LRRK2 DNA and 36 μl of LipoD293 per plate. Cells were split into 100 mm dishes at a ratio of 1:3 the following day, and lysed in 1 ml of lysis buffer per dish [20 mM Tris–HCl, pH 7.4, 1% Triton X-100, 137 mM NaCl, 3 mM KCl, 10% (v/v) glycerol, 1 mM EDTA, 1 mM Na_3VO_4, 5 mM NaF, 1 mM PMSF] for 1 h at 4 °C on a rotary wheel, followed by clarification of extracts by centrifugation at 13 200 rpm for 10 min at 4 °C. Soluble protein was evenly split into two tubes to a final volume of 500 μl each, and each incubated with 30 μl of 5'-GTP agarose beads (Sigma Aldrich) overnight at 4 °C on a rotary wheel. One of the two samples was used as control for non-specific binding to GTP-agarose beads by adding a final concentration of 10 mM GTP. The next day, beads were washed two times with ice-cold lysis buffer, and GTP-bound proteins eluted from beads by incubation with 30 μl ice-cold lysis buffer containing 10 mM GTP for 15 min at 4 °C on a rotary wheel. Beads were centrifuged at 13 200 rpm for 1 min, eluates were transferred to fresh tubes and resuspended with 5× Laemmli sample buffer containing β-mercaptoethanol. Both eluate and input (5% total lysate) samples were subjected to SDS-PAGE and western blotting with an anti-GFP antibody (Abcam, ab6556, 1:1000). GTP-binding assays were quantified by ODYSSEY as described above, with GTP-specific binding of each LRRK2 construct normalized to protein input. For experiments determining the effects of GTP-binding inhibitors (40,41), the respective compounds were added to the lysis buffer and kept throughout the experiment. For experiments determining the effect of LRRK2 kinase inhibitors, compounds were added to cells 4 h prior to lysis, added to the lysis buffer, and kept throughout the experiment.

In vitro LRRK2 kinase assays

pDEST53-GFP-LRRK2 wild-type and mutants were transiently transfected into HEK293T/17 cells using 20 μg of DNA in 1 ml OPTI-MEM (Thermo Fisher) and 40 μl of linear PEI (Polyscience) (20 μM) per 10 cm^2 Petri dish. Cells were harvested 48 h after transfection with 500 μl of lysis buffer [10 mM Tris–HCl, pH 7.5, 150 mM NaCl, 5 mM EDTA, 2.5 mM $Na_4P_2O_7$, 1 mM β-glycerophosphate, 1 mM Na_3VO_4, supplemented with Protease Inhibitor Mixture (Sigma Aldrich) and 1% (v/v) Tween-20]. Samples were incubated on ice for 30 min, and centrifuged at 18 000*g* for 35 min at 4 °C. Supernatants were incubated overnight with 20 μl of GFP-Trap beads (ChromoTek GmbH, Planegg, Germany) at 4 °C with mild agitation. Beads were sequentially washed with 500 μl of buffer 1 [20 mM Tris–HCl, pH 7.5, 500 mM NaCl, 1% (v/v) Tween-20], buffer 2 [20 mM Tris–HCl, pH 7.5, 350 mM NaCl, 1% (v/v) Tween-20], buffer 3 [20 mM Tris–HCl, pH 7.5, 150 mM NaCl, 1% (v/v) Tween-20], buffer 4 [20 mM Tris–HCl, pH 7.5, 150 mM NaCl, 0.1% (v/v) Tween-20] and buffer 5 [20 mM Tris–HCl, pH 7.5, 150 mM NaCl, 0.02% (v/v) Tween-20]. GFP-LRRK2-containing beads were resuspended in 100 μl of kinase buffer [25 mM Tris–HCl, pH 7.5, 5 mM β-glycerophosphate, 2 mM DTT, 0.1 mM Na_3VO_4, 10 mM $MgCl_2$ supplemented with 0.007% (v/v) Tween-20] for subsequent *in vitro* kinase assays.

Kinase reactions were started by addition of ATP (200 μM final) and were incubated for 1 h at 30 °C with mild agitation. Samples were centrifuged, supernatants discarded and proteins eluted from beads by addition of Laemmli sample buffer and boiling for 5 min at 95 °C. Samples (10 μl) were separated by SDS-PAGE, and transferred onto PVDF membranes (Bio-Rad) using the Trans-Blot Turbo Transfer System (Bio-Rad) in semi-dry conditions using 1× Trans-Blot Turbo Transfer Buffer (Bio-Rad) in 20% (v/v) ethanol at 25 V for 20 min. Membranes were blocked for 40 min in 5% (w/v) skimmed milk in TBS-T buffer [20 mM Tris–HCl, pH 7.4, 150 mM NaCl, 0.1% (v/v) Tween-20], followed by incubation for 1 h with an antibody against the LRRK2 autophosphorylation site T2483 (MJF-R8, Abcam, 1:2000). Membranes were washed four times for 10 min with TBS-T buffer, and incubated for 1 h at room temperature with horseradish peroxidase-conjugated rabbit secondary antibodies (1:15 000) in 5% (w/v) skimmed milk in TBS-T buffer. Membranes were washed in TBS-T buffer followed by visualization using ECL Western Blotting Detection Reagents (GE Healthcare). Data were normalized to the concentration of the individual proteins on PVDF membranes directly stained with Coomassie [40% methanol, 10% acetic acid, 0.1% (w/v) Comassie R-250], and densitometry analysis carried out using ImageJ software, with kinase activities of the various proteins expressed relative wild-type LRRK2, which was present on every gel for comparison.

Statistical analysis

All data are expressed as means ± SEM. Data were analyzed by one-way ANOVA with Tukey's post hoc test, and $P < 0.05$ was considered significant.

Acknowledgements

We thank Laura Montosa for excellent technical assistance with microscopy, and Drs T. Dawson, B. Wolozin, K. Haebig and M. Bonin for generously providing a variety of constructs used in the present study.

Conflict of Interest statement. None declared.

Funding

S.H. is supported by the Michael J. Fox Foundation, the BBVA Foundation, FEDER, and the Spanish Ministry of Economy and Competitiveness (SAF2014-58653-R). Funding to pay the Open Access publication charges for this article was provided by SAF2014-58653-R.

References

1. Lees, A.J., Hardy, J. and Revesz, T. (2009) Parkinson's disease. *Lancet*, **373**, 2055–2066.
2. Zimprich, A., Biskup, S., Leitner, P., Lichtner, P., Farrer, M., Lincoln, S., Kachergus, J., Hulihan, M., Uitti, R.J., Calne, D.B. *et al.* (2004) Mutations in LRRK2 cause autosomal-dominant Parkinsonism with pleomorphic pathology. *Neuron*, **44**, 601–607.
3. Paisán-Ruíz, C., Jain, S., Evans, E.W., Gilks, W.P., Simón, J., van der Brug, M., López de Munaín, A., Aparicio, S., Gil, A.M., Khan, N. *et al.* (2004) Cloning of the gene containing mutations that cause PARK8-linked Parkinson's disease. *Neuron*, **44**, 595–600.
4. Simón-Sánchez, J., Schulte, C., Bras, J.M., Sharma, M., Gibbs, J.R., Berg, D., Paisan-Ruiz, C., Lichtner, P., Scholz, S.W., Hernandez, D.G. *et al.* (2009) Genome-wide association study reveals genetic risk underlying Parkinson's disease. *Nat. Genet.*, **41**, 1308–1312.
5. Satake, W., Nakabayashi, Y., Mizuta, I., Hirota, Y., Ito, C., Kubo, M., Kawaguchi, T., Tsunoda, T., Watanabe, M., Takeda, A. *et al.* (2009) Genome-wide association study identifies

common variants at four loci as genetic risk factors for Parkinson's disease. *Nat. Genet.*, **41**, 1303–1307.
6. Tan, E.K., Peng, R., Teo, Y.Y., Tan, L.C., Angeles, D., Ho, P., Chen, M.L., Lin, C.H., Mao, X.Y., Chang, X.L. *et al.* (2010) Multiple LRRK2 variants modulate risk of Parkinson disease: a Chinese multicenter study. *Hum. Mutat.*, **31**, 561–568.
7. Ross, O.A., Soto-Ortolaza, A.I., Heckman, M.G., Aasly, J.O., Abahuni, N., Annesi, G., Bacon, J.A., Bardien, S., Bozi, M., Brice, A. *et al.* (2011) Association of LRRK2 exonic variants with susceptibility to Parkinson's disease: a case-control study. *Lancet Neurol.*, **10**, 898–908.
8. Chen, L., Zhang, S., Liu, Y., Hong, H., Wang, H., Zheng, Y., Zhou, H., Chen, J., Xian, W., He, Y. *et al.* (2011) LRRK2 R1398H polymorphism is associated with decreased risk of Parkinson's disease in a Han Chinese population. *Parkinsonism Relat. Disord.*, **17**, 291–292.
9. Heckman, M.G., Elbaz, A., Soto-Ortolaza, A.I., Serie, D.J., Aasly, J.O., Annesi, G., Augurger, G., Bacon, J.A., Boczarka-Jedynak, M., Bozi, M. *et al.* (2014) Protective effect of LRRK2 p.R1398H on risk of Parkinson's disease is independent of MAPT and SNCA variants. *Neurobiol. Aging*, **35**, 266.e5–214.
10. Mata, I.F., Wedemeyer, W.J., Farrer, M.J., Taylor, J.P. and Gallo, K.A. (2006) LRRK2 in Parkinson's disease: protein domains and functional insights. *Trends Neurosci.*, **29**, 286–293.
11. Cardona, F., Tormos-Pérez, M. and Pérez-Tur, J. (2014) Structural and functional *in silico* analysis of LRRK2 missense substitutions. *Mol. Biol. Rep.*, **41**, 2529–2542.
12. West, A.B., Moore, D.J., Biskup, S., Bugayenko, A., Smith, W.W., Ross, C.A., Dawson, V.L. and Dawson, T.M. (2005) Parkinson's disease-associated mutations in leucine-rich repeat kinase 2 augment kinase activity. *Proc. Natl. Acad. Sci. U.S.A.*, **102**, 16842–16847.
13. Greggio, E., Jain, S., Kingsbury, A., Bandopadhyay, R., Lewis, P., Kaganovich, A., van der Brug, M.P., Beilina, A., Blackinton, J., Thomas, K.J. *et al.* (2006) Kinase activity is required for the toxic effects of mutant LRRK2/dardarin. *Neurobiol. Dis.*, **23**, 329–341.
14. Jaleel, M., Nichols, R.J., Deak, M., Campbell, D.G., Gillardon, F., Knebel, A. and Alessi, D.R. (2007) LRRK2 phosphorylates moesin at threonine-558: characterization of how Parkinson's disease mutants affect kinase activity. *Biochem. J.*, **405**, 307–317.
15. Ito, G., Okai, T., Fujino, G., Takeda, K., Ichijo, H., Katada, T. and Iwatsubo, T. (2007) GTP binding is essential to the protein kinase activity of LRRK2, a causative gene product for familial Parkinson's disease. *Biochemistry*, **46**, 1380–1388.
16. West, A.B., Moore, D.J., Choi, C., Andrabi, S.A., Li, X., Dikeman, D., Biskup, S., Zhang, Z., Lim, K.L., Dawson, V.L. and Dawson, T.M. (2007) Parkinson's disease-associated mutations in LRRK2 link enhanced GTP-binding and kinase activities to neuronal toxicity. *Hum. Mol. Genet.*, **16**, 223–232.
17. Aasly, J.O., Vilariño-Guell, C., Dachsel, J.C., Webber, P.J., West, A.B., Haugarvoll, K., Johansen, K.K., Toft, M., Nutt, J.G., Payami, H. *et al.* (2010) Novel pathogenic LRRK2 p.Asn1437His substitution in familial Parkinson's disease. *Mov. Disord.*, **25**, 2156–2163.
18. Liao, J., Wu, C.W., Burlak, C., Zhang, S., Sahm, H., Wang, M., Zhang, Z.Y., Vogel, K.W., Federici, M., Riddle, S.M. *et al.* (2014) Parkinson disease-associated mutation R1441H in LRRK2 prolongs the "active state" of its GTPase domain. *Proc. Natl. Acad. Sci. U.S.A.*, **111**, 4055–4060.
19. Lewis, P.A., Greggio, E., Beilina, A., Jain, S., Baker, A. and Cookson, M.R. (2007) The R1441C mutation of LRRK2 disrupts GTP hydrolysis. *Biochem. Biophys. Res. Commun.*, **357**, 668–671.
20. Li, X., Tan, Y.C., Poulose, S., Olanow, C.W., Huang, X.Y. and Yue, Z. (2007) Leucine-rich repeat kinase 2 (LRRK2)/PARK8 possesses GTPase activity that is altered in familial Parkinson's disease R1441C/G mutants. *J. Neurochem.*, **103**, 238–247.
21. Cookson, M.R. (2015) LRRK2 pathways leading to neurodegeneration. *Curr. Neurol. Neurosci. Rep.*, **15**, 42.
22. Smith, W.W., Pei, Z., Jiang, H., Dawson, V.L., Dawson, T.M. and Ross, C.A. (2006) Kinase activity of mutant LRRK2 mediates neuronal toxicity. *Nat. Neurosci.*, **9**, 1231–1233.
23. Xiong, Y., Coombes, C.E., Kilaru, A., Li, X., Gitler, A.D., Bowers, W.J., Dawson, V.L., Dawson, T.M. and Moore, D.J. (2010) GTPase activity plays a key role in the pathobiology of LRRK2. *PLoS Genet*, **6**, e1000902.
24. Stafa, K., Trancikova, A., Webber, P.J., Glauser, L., West, A.B. and Moore, D.J. (2012) GTPase activity and neuronal toxicity of Parkinson's disease-associated LRRK2 is regulated by ArfGAP1. *PLoS Genet.*, **8**, e1002526.
25. Xiong, Y., Yuan, C., Chen, R., Dawson, T.M. and Dawson, T.L. (2012) ArfGAP1 is a GTPase activating protein for LRRK2: reciprocal regulation of ArfGAP1 by LRRK2. *J. Neurosci.*, **32**, 3877–3886.
26. Biosa, A., Trancikova, A., Civiero, L., Glauser, L., Bubacco, L., Greggio, E. and Moore, D.J. (2013) GTPase activity regulates kinase activity and cellular phenotypes of Parkinsons's disease-associated LRRK2. *Hum. Mol. Genet.*, **22**, 1140–1156.
27. Fuji, R.N., Flagella, M., Baca, M., Baptista, M.A., Brodbeck, J., Chan, B.K., Fiske, B.K., Honigberg, L., Jubb, A.M., Katavolos, P. *et al.* (2015) Effect of selective LRRK2 kinase inhibition in nonhuman primate lung. *Sci. Transl. Med.*, **7**, 273ra15.
28. Fell, M.J., Mirescu, C., Basu, K., Cheewatrakoolpong, B., DeMong, D.E., Ellis, J.M., Hyde, L.A., Lin, Y., Markgraf, C.G., Mei, H. *et al.* (2015) MLi-2, a potent, selective and centrally active compound for exploring the therapeutic potential and safety of LRRK2 kinase inhibition. *J. Pharmacol. Exp. Ther.*, **355**, 397–409.
29. Taymans, J.M. and Greggio, E. (2016) LRRK2 kinase inhibition as a therapeutic strategy for Parkinson's disease, where do we stand? *Curr. Neuropharmacol.*, **14**, 214–225.
30. Gómez-Suaga, P., Fdez, E., Fernández, B., Martínez-Salvador, M., Blanca Ramírez, M., Madero-Pérez, J., Rivero-Ríos, P., Fuentes, J.M. and Hilfiker, S. (2014) Novel insights into the neurobiology underlying LRRK2-linked Parkinson's disease. *Neuropharmacology*, **85**, 45–56.
31. Gandhi, P.N., Wang, X., Zhu, X., Chen, S.G. and Wilson-Delfosse, A.L. (2008) The Roc domain of leucine-rich repeat kinase 2 is sufficient for interaction with microtubules. *J. Neurosci. Res.*, **86**, 1711–1720.
32. Caesar, M., Zach, S., Carlson, C.B., Brockmann, K., Gasser, T. and Gillardon, F. (2013) Leucine-rich repeat kinase 2 functionally interacts with microtubules and kinase-dependently modulates cell migration. *Neurobiol. Dis.*, **54**, 280–288.
33. Gillardon, F. (2009) Leucine-rich repeat kinase 2 phosphorylates brain tubulin-beta isoforms and modulates microtubule stability-a point of convergence in Parkinsonian neurodegeneration? *J. Neurochem.*, **110**, 1514–1522.
34. Kett, L.R., Boassa, D., Ho, C.C., Rideout, H.J., Hu, J., Terada, M., Ellisman, M. and Dauer, W.T. (2012) LRRK2 Parkinson disease mutations enhance its microtubule association. *Hum. Mol. Genet.*, **21**, 890–899.
35. Godena, V.K., Brookes-Hocking, N., Moller, A., Shaw, G., Oswald, M., Sancho, R.M., Miller, C.C., Whitworth, A.J. and De Vos, K.J. (2014) Increasing microtubule acetylation

rescues axonal transport and locomotor deficits caused by LRRK2 ROC–COR domain mutations. *Nat. Commun.*, **5**, 5245.
36. Dzamko, N., Deak, M., Hentati, F., Reith, A.D., Prescott, A.R., Alessi, D.R. and Nichols, R.J. (2010) Inhibition of LRRK2 kinase activity leads to dephosphorylation of Ser(910)/Ser(935), disruption of 14-3-3 binding and altered cytoplasmic localization. *Biochem. J.*, **430**, 405–413.
37. Deng, X., Dzamko, N., Prescott, A., Davies, P., Liu, Q., Yang, Q., Lee, J.D., Patricelli, M.P., Nomanbhoy, T.K., Alessi, D.R. and Gray, N.S. (2011) Characterization of a selective inhibitor of the Parkinson's disease kinase LRRK2. *Nat. Chem. Biol.*, **7**, 203–205.
38. Sheng, Z., Zhang, S., Bustos, D., Kleinheinz, T., Le Pichon, C.E., Dominguez, S.L., Solanoy, H.O., Drummond, J., Zhang, X., Ding, X. *et al.* (2012) Ser1292 autophosphorylation is an indicator of LRRK2 kinase activity and contributes to the cellular effects of PD mutations. *Sci. Trans. Med.*, **4**, 164ra161.
39. Thomas, J.M., Li, T., Yang, W., Xue, F., Fishman, P.S. and Smith, W.W. (2017) 68 and FX2149 attenuate mutant LRRK2-R1441C-induced neural transport impairment. *Front. Aging Neurosci.*, **8**, 337.
40. Li, T., Yang, D., Zhong, S., Thomas, J.M., Xue, F., Liu, J., Kong, L., Voulalas, P., Hassan, H.E., Park, J.S. *et al.* (2014) Novel LRRK2 GTP-binding inhibitors reduced degeneration in Parkinson's disease cell and mouse models. *Hum. Mol. Genet.*, **23**, 6212–6222.
41. Li, T., He, X., Thomas, J.M., Yang, D., Zhong, S., Xue, F. and Smith, W.W. (2015) A novel GTP-binding inhibitor, FX2149, attenuates LRRK2 toxicity in Parkinson's disease models. *PLoS ONE*, **10**, e0122461.
42. Zhang, J., Deng, X., Choi, H.G., Alessi, D.R. and Gray, N.S. (2012) Characterization of TAE684 as a potent LRRK2 kinase inhibitor. *Bioorg. Med. Chem. Lett.*, **22**, 1864–1869.
43. Ramsden, N., Perrin, J., Ren, Z., Lee, B.D., Zinn, N., Dawson, V.L., Tam, D., Bova, M., Lang, M., Drewes, G. *et al.* (2011) Chemoproteomics-based design of potent LRRK2-selective lead compounds that attenuate Parkinson's disease-related toxicity in human neurons. *ACS Chem. Biol.*, **6**, 1021–1028.
44. Reith, A.D., Bamborough, P., Jandu, K., Andreotti, D., Mensah, L., Dossang, P., Choi, H.G., Deng, X., Zhang, J., Alessi, D.R. and Gray, N.S. (2012) GSK2578215A; A potent and highly selective 2-arylmethyloxy-5-substituent-N-arylbenzamide LRRK2 kinase inhibitor. *Bioorg. Med. Chem. Lett.*, **22**, 5625–5629.
45. Estrada, A.A., Liu, X., Baker-Glenn, C., Beresford, A., Burdick, D.J., Chambers, M., Chan, B.K., Chen, H., Ding, X., DiPasquale, A.G. *et al.* (2012) Discovery of highly potent, selective, and brain-penetrable leucine-rich repeat kinase 2 (LRRK2) small molecular inhibitors. *J. Med. Chem.*, **55**, 9416–9433.
46. Estrada, A.A., Chan, B.K., Baker-Glenn, C., Beresford, A., Burdick, D.J., Chambers, M., Chen, H., Dominguez, S.L., Dotson, J., Drummond, J. *et al.* (2014) Discovery of highly potent, selective, and brain-penetrant aminopyrazole leucine-rich repeat kinase 2 (LRRK2) small molecule inhibitors. *J. Med. Chem.*, **57**, 921–936.
47. Tomiyama, H., Li, Y., Funayama, M., Hasegawa, K., Yoshino, H., Kubo, S., Sato, K., Hattori, T., Lu, C.S., Inzelberg, R. *et al.* (2006) Clinicogenetic study of mutations in LRRK2 exon 41 in Parkinson's disease patients from 18 countries. *Mov. Disord.*, **21**, 1102–1108.
48. Funayama, M., Hasegawa, K., Ohta, E., Kawashima, N., Komiyama, M., Kowa, H., Tsuji, S. and Obata, F. (2005) An LRRK2 mutation as a cause for the parkinsonism in the original PARK8 family. *Ann. Neurol.*, **57**, 918–921.
49. Greggio, E., Zambrano, I., Kaganovich, A., Beilina, A., Taymans, J.M., Daniels, V., Lewis, P., Jain, S., Ding, J., Syed, A. *et al.* (2008) The Parkinson's disease-associated leucine-rich repeat kinase 2 (LRRK2) is a dimer that undergoes intramolecular autophosphorylation. *J. Biol. Chem.*, **283**, 16906–16914.
50. Ito, G., Fujimoto, T., Kamikawaji, S., Kuwahara, T. and Iwatsubo, T. (2014) Lack of correlation between the kinase activity of LRRK2 harboring kinase-modifying mutations and its phosphorylation at Ser910, 935, and Ser955. *PLoS ONE*, **9**, e97988.
51. Wloga, D. and Gaertig, J. (2010) Post-translational modifications of microtubules. *J. Cell Sci.*, **123**, 3447–3455.
52. Song, Y. and Brady, S.T. (2015) Post-translational modifications of tubulins: pathways to functional diversity of microtubules. *Trends Cell Biol.*, **25**, 125–136.
53. Janke, C. (2014) The tubulin code: molecular components, readout mechanisms, and functions. *J. Cell Biol.*, **206**, 461–472.
54. Peris, L., Wagenbach, M., Lafanechère, L., Brocard, J., Moore, A.T., Kozielski, F., Job, D., Wordeman, L. and Andrieux, A. (2009) Motor-dependent microtubule disassembly driven by tubulin tyrosination. *J. Cell Biol.*, **185**, 1159–1166.
55. Matsuyama, A., Shimazu, T., Sumida, Y., Saito, A., Yoshimatsu, Y., Seigneurin-Berny, D., Osada, H., Komatsu, Y., Nishino, N., Khochbin, S. *et al.* (2002) *In vivo* destabilization of dynamic microtubules by HDAC6-mediated deacetylation. *EMBO J.*, **21**, 6820–6831.
56. Haggarty, S.J., Koeller, K.M., Wong, J.C., Grozinger, C.M. and Schreiber, S.L. (2003) Domain-selective small-molecule inhibitor of histone deacetylase 6 (8HDAC6)-mediated tubulin deacetylation. *Proc. Natl. Acad. Sci. U.S.A.*, **100**, 4389–4394.
57. Shida, T., Cueva, J.G., Xu, Z., Goodman, M.B. and Nachury, M.V. (2010) The major a-tubulin K40 acetyltransferase aTAT1 promotes rapid ciliogenesis and efficient mechanosensation. *Proc. Natl. Acad. Sci. U.S.A.*, **107**, 21517–21522.
58. Kalebic, N., Martinez, C., Perlas, E., Hublitz, P., Bilbao-Cortes, D., Fiedorczuk, K., Andolfo, A. and Heppenstall, P.A. (2013) Tubulin acetyltransferase aTAT1 destabilizes microtubules independently of its acetylation activity. *Mol. Cell Biol.*, **33**, 1114–1123.
59. Fonrose, X., Ausseil, F., Soleilhac, E., Masson, V., David, B., Pouny, I., Cintrat, J.C., Rousseau, B., Barette, C., Massiot, G. and Lafanechère, L. (2007) Parthenolide inhibits tubulin carboxypeptidase activity. *Cancer Res.*, **67**, 3371–3378.
60. Barisic, M., Silva e Sousa, R., Tripathy, S.K., Magiera, M.M., Zaytsev, A.V., Pereira, A.L., Janke, C., Grishchuk, E.L. and Maiato, H. (2015) Mitosis. Microtubule detyrosination guides chromosomes during mitosis. *Science*, **348**, 799–803.
61. Gloeckner, C.J., Boldt, K., von Zweydorf, F., Helm, S., Wiesent, L., Sarioglu, H. and Ueffing, M. (2010) Phosphopeptide analysis reveals two discrete clusters of phosphorylation in the N-terminus and the Roc domain of the Parkinson-disease associated protein kinase LRRK2. *J. Proteome Res.*, **9**, 1738–1745.
62. Greggio, E., Taymans, J.M., Zhen, E.Y., Ryder, J., Vancraenenbroeck, R., Beilina, A., Sun, P., Deng, J., Jaffe, H., Baekelandt, V., Merchant, K. and Cookson, M.R. (2009) The Parkinson's disease kinase LRRK2 autophosphorylates its GTPase domain at multiple sites. *Biochem. Biophys. Res. Commun.*, **389**, 449–454.
63. Kamikawaji, S., Ito, G. and Iwatsubo, T. (2009) Identification of the autophosphorylation sites of LRRK2. *Biochemistry*, **48**, 10963–10975.

64. Pungaliya, P.P., Bai, Y., Lipinski, K., Anand, V.S., Sen, S., Brown, E.L., Bates, B., Reinhart, P.H., West, A.B., Hirst, W.D. and Braithwaite, S.P. (2010) Identification and characterization of a leucine-rich repeat kinase 2 (LRRK2) consensus phosphorylation motif. *PLoS ONE*, **5**, e13672.
65. Webber, P.J., Smith, A.D., Sen, S., Renfrow, M.B., Mobley, J.A. and West, A.B. (2011) Autophosphorylation in the leucine-rich repeat kinase 2 (LRRK2) GTPase domain modifies kinase and GTP-binding activities. *J. Mol. Biol.*, **412**, 94–110.
66. Nichols, R.J., Dzamko, N., Morrice, N.A., Campbell, D.G., Deak, M., Ordureau, A., Macartney, T., Tong, Y., Shen, J., Prescott, A.R. and Alessi, D.R. (2010) 14-3-3 binding to LRRK2 is disrupted by multiple Parkinson's disease-associated mutations and regulates cytoplasmic localization. *Biochem. J.*, **430**, 393–404.
67. Doggett, E.A., Zhao, J., Mork, C.N., Hu, D. and Nichols, R.J. (2012) Phosphorylation of LRRK2 serines 955 and 973 is disrupted by Parkinson's disease mutations and LRRK2 pharmacological inhibition. *J. Neurochem.*, **120**, 37–45.
68. Lavalley, N.J., Slone, S.R., Ding, H., West, A.B. and Yacoubian, A.T. (2016) 14-3-3 proteins regulate mutant LRRK2 kinase activity and neurite shortening. *Hum. Mol. Genet.*, **25**, 109–122.
69. Li, X., Wang, Q.J., Pan, N., Lee, S., Zhao, Y., Chait, B.T. and Yue, X. (2011) Phosphorylation-dependent 14-3-3 binding to LRRK2 is impaired by common mutations of familial Parkinson's disease. *PLoS One*, **6**, e17153.
70. Darling, D.L., Yingling, J. and Wynshaw-Boris, A. (2005) Role of 14-3-3 proteins in eukaryotic signaling and development. *Curr. Top. Dev. Biol.*, **68**, 281–315.
71. Muda, K., Bertinetti, D., Besellchen, F., Hermann, J.S., von Zweydorf, F., Geerlof, A., Jacob, A., Ueffing, M., Gloeckner, C.F. and Herberg, F.W. (2014) Parkinson-related LRRK2 mutation R1441C/G/H impairs PKA phosphorylation of LRRK2 and disrupts its interaction with 14-3-3. *Proc. Natl. Acad. Sci. U.S.A.*, **111**, E34–E43.
72. Xiong, Y., Dawson, V.L. and Dawson, T.M. (2012) LRRK2 GTPase dysfunction in the pathogenesis of Parkinson's disease. *Biochem. Soc. Trans.*, **40**, 1074–1079.
73. Tsika, E. and Moore, D.J. (2013) Contribution of GTPase activity to LRRK2-associated Parkinson disease. *Small GTPases*, **4**, 164–170.
74. Dusonchet, J., Li, H., Guillily, M., Liu, M., Stafa, K., Derada Troletti, C., Boon, J.Y., Saha, S., Glauser, L., Mamais, A. *et al.* (2014) A Parkinson's disease gene regulatory network identifies the signaling protein RGS2 as a modulator of LRRK2 activity and neuronal toxicity. *Hum. Mol. Genet.*, **23**, 4887–4905.
75. Haebig, K., Gloeckner, C.J., Miralles, M.G., Gillardon, F., Schulte, C., Riess, O., Ueffing, M., Biskup, S. and Bonin, B. (2010) ARHGEF7 (BETA-PIX) acts as guanine nucleotide exchange factor for leucine-rich repeat kinase 2. *PLoS One*, **5**, e13762.
76. Deng, J., Lewis, P.A., Greggio, E., Sluch, E., Beilina, A. and Cookson, M.R. (2008) Structure of the ROC domain from the Parkinson's disease-associated leucine-rich repeat kinase 2 reveals a dimeric GTPase. *Proc. Natl. Acad. Sci. U.S.A.*, **105**, 1499–1504.
77. Chia, R., Haddock, S., Beilina, A., Rudenko, I.N., Mamais, A., Kaganovich, A., Li, Y., Kumaran, R., Nalls, M.A. and Cookson, M.R. (2014) Phosphorylation of LRRK2 by casein kinase 1a regulates trans-Golgi clustering via differential interaction with ARHGEF7. *Nat. Commun.*, **5**, 5827.
78. Nixon-Abell, J., Berwick, D.C., Grannó, S., Spain, V.A., Blackstone, C. and Harvey, K. (2016) Protective LRRK2 R1398H variant enhances GTPase and Wnt signaling activity. *Front. Mol. Neurosci.*, **8**, 9:18.
79. Taymans, J.M., Vancraenenbroeck, R., Ollikainen, P., Beilina, A., Lobbestael, E., De Maeyer, M., Baekelandt, V. and Cookson, M.R. (2011) LRRK2 kinase activity is dependent on LRRK2 GTP binding capacity but independent of LRRK2 GTP binding. *PLoS ONE*, **6**, e23207.
80. Greggio, E. and Cookson, M.R. (2009) Leucine-rich repeat kinase 2 mutations and Parkinson's disease: three questions. *ASN Neuro*, **1**, e00002.
81. Steger, M., Tonelli, F., Ito, G., Davies, P., Trost, M., Vetter, M., Wachter, S., Lorentzen, E., Duddy, G., Wilson, S. *et al.* (2016) Phosphoproteomics reveals that Parkinson's disease kinase LRRK2 regulates a subset of Rab GTPases. *Elife*, **5**, e12813.
82. Dunn, S., Morrison, E.E., Liverpool, T.B., Molina-París, C., Cross, R.A., Alonso, M.C. and Peckham, M. (2008) Differential trafficking of Kif5c on tyrosinated and detyrosinated microtubules in live cells. *J. Cell Sci.*, **121**, 1085–1095.
83. Jacobson, C., Schnapp, B. and Banker, G.A. (2006) A change in the selective translocation of the kinesin-1 motor domain marks the initial specification of the axon. *Neuron*, **49**, 797–804.
84. Konishi, Y. and Setou, M. (2009) Tubulin tyrosination navigates the kinesin-1 motor domain to axons. *Nat. Neurosci.*, **12**, 559–567.
85. Kaul, N., Soppina, V. and Verhey, K.J. (2014) Effects of a-tubulin K40 acetylation and detyrosination on kinesin-1 motility in a purified system. *Biophys. J.*, **106**, 2636–2643.
86. Cambray-Deakin, M.A. and Burgoyne, R.D. (1987) Posttranslational modifications of a-tubulin: acetylated and detyrosinated forms in axons of rat cerebellum. *J. Cell Biol.*, **104**, 1569–1574.
87. Sakaguchi-Nakashima, A., Meir, J.Y., Jin, Y., Matsumoto, K. and Hisamoto, N. (2007) LRK-1, a *C. elegans* PARK8-related kinase, regulates axonal-dendritic polarity of SV proteins. *Curr. Biol.*, **17**, 592–598.
88. Cirnaru, M.D., Marte, A., Belluzzi, E., Russo, I., Gabrielli, M., Longo, F., Arcuri, L., Murru, L., Bubacco, L., Matteoli, M. *et al.* (2014) LRRK2 kinase activity regulates synaptic vesicle trafficking and neurotransmitter release through modulation of LRRK2 macro-molecular complex. *Front. Mol. Neurosci.*, **7**, 49.
89. Goldstein, A.Y., Wang, X. and Schwarz, T.L. (2008) Axonal transport and the delivery of pre-synaptic components. *Curr. Opin. Neurobiol.*, **18**, 495–503.
90. Gómez-Suaga, P., Rivero-Ríos, P., Fdez, E., Blanca Ramírez, M., Ferrer, I., Aiastui, A., López de Munain, A. and Hilfiker, S. (2014) LRRK2 delays degradative receptor trafficking by impeding late endosomal budding through decreasing Rab7 activity. *Hum. Mol. Genet.*, **23**, 6779–6796.
91. Ciani, L. and Salinas, P.C. (2007) c-Jun N-terminal kinase (JNK) cooperates with Gsk3beta to regulate Dishevelled-mediated microtubule stability. *BMC Cell Biol.*, **8**, 27.
92. Choi, Y.K., Liu, P., Sze, S.K., Dai, C. and Qi, R.Z. (2010) CDK5RAP2 stimulates microtubule nucleation by the gamma-tubulin ring complex. *J. Cell Biol.*, **191**, 1089–1095.
93. Walev, I., Bhakdi, S.C., Hofmann, F., Djonder, N., Valeva, A., Aktories, K. and Bhakdi, S. (2001) Delivery of proteins into living cells by reversible membrane permeabilization with streptolysin-O. *Proc. Natl. Acad. Sci. U.S.A.*, **98**, 3185–3190.
94. Kano, F., Nakatsu, D., Noguchi, Y., Yamamoto, A. and Murata, M. (2012) A resealed-cell system for analyzing pathogenic intracellular events: perturbation of endocytic pathways under diabetic conditions. *PLoS ONE*, **7**, e44127.

4. LRRK2: a death effector filament protein?

As previously mentioned in the introduction, LRRK2 has been involved in the Death Signalling Cascades, consistent with its reported association with the main components of this pathway. Indeed, an interaction with Fas associated death domain protein (FADD) and LRRK2 has been described, with pathogenic mutants having shown to enhance this association, thus suggesting that pathogenic LRRK2 could play a role in the extrinsic cell death pathway. In agreement with these findings, inhibition of this cascade via either overexpressing dominant-negative FADD or downregulating caspase-8 could prevent cell death in cultured primary cortical neurons transiently overexpressing pathogenic LRRK2 mutants. Additional indication for the involvement of LRRK2 in this pathway is suggested by the finding that LRRK2 can interact with the TNFR1-associated death domain protein (TRADD), although the strength of this interaction seems minor compared to the one reported with FADD [233].

FADD and TRADD are characterized by containing a death effector domain (DED), thus acting as a scaffold for the recruitment of caspases, and eventually leading to apoptosis. Interestingly, DED-containing proteins have been shown to undergo a filamentous conformation, forming the so-called death-effector filaments, which have been described to mediate the recruitment and sequential activation of the death pathway components, thereby triggering cell death [243]. These proteins assemble into a multiprotein complex termed death-inducing signalling complex (DISC), which recruits and activates caspase-8, thereby triggering cell death [244].

Since we found that pathogenic and kinase-inhibited LRRK2 formed filamentous intracellular structures, we initially wondered whether these structures may reflect death effector filaments, thus recruiting caspase-8 and inducing cell death.

First, we analyzed the localization of different DED-containing proteins shown to be involved in this death signalling pathway. We overexpressed the following constructs (myc-TRADD, myc-FADD, myc-caspase-8, GFP-RICK, GFP-RIP) and observed that all of them,

with the exception of caspase-8, exhibited a filamentous distribution, consistent with the previously reported DED-mediated death effector filament formation (Figure 9A) .

In order to determine whether LRRK2 might be involved in the death signalling pathway, we analyzed the colocalization of pathogenic LRRK2 with FADD or TRADD by co-expressing GFP-R1441C-LRRK2 and myc-FADD or myc-TRADD, respectively. Whilst pathogenic LRRK2 only partially colocalized with TRADD, more colocalization was observed with FADD, consistent with previous work [243]. Importantly though, while FADD and TRADD displayed a typical death-effector-type filamentous phenotype, GFP-R1441C distribution seemed to be similar when coexpressed with either FADD or TRADD, but distinct when overexpressed on its own, thus suggesting that the altered pathogenic LRRK2 localization in the presence of FADD or TRADD may reflect its recruitment to death effector filaments (Figure 9B).

As another approach to determine whether the pathogenic LRRK2 filaments reflected death-effector filaments, we analyzed whether they would be able to recruit caspase-8. For this purpose, we co-expressed GFP-R1441C-LRRK2 and myc-caspase-8. Whilst pathogenic LRRK2 displayed its typical filamentous distribution, those filaments were not able to recruit caspase-8. Similar results were observed when pharmacologically inhibiting the LRRK2 kinase activity, suggesting that pathogenic or pharmacologically kinase-inhibited LRRK2 filaments are not death effector filaments (Figure 9C). Finally, we also analyzed the percentage of apoptosis either when overexpressing GFP-R1441C-LRRK2 or upon pharmacological kinase inhibition, as compared to GFP-wildtype LRRK2. No significant differences in cell death were observed when quantifying apoptosis by DAPI staining (data not shown), further supporting the idea that the pathogenic or kinase-inhibited LRRK2 filaments are not death-effector filaments.

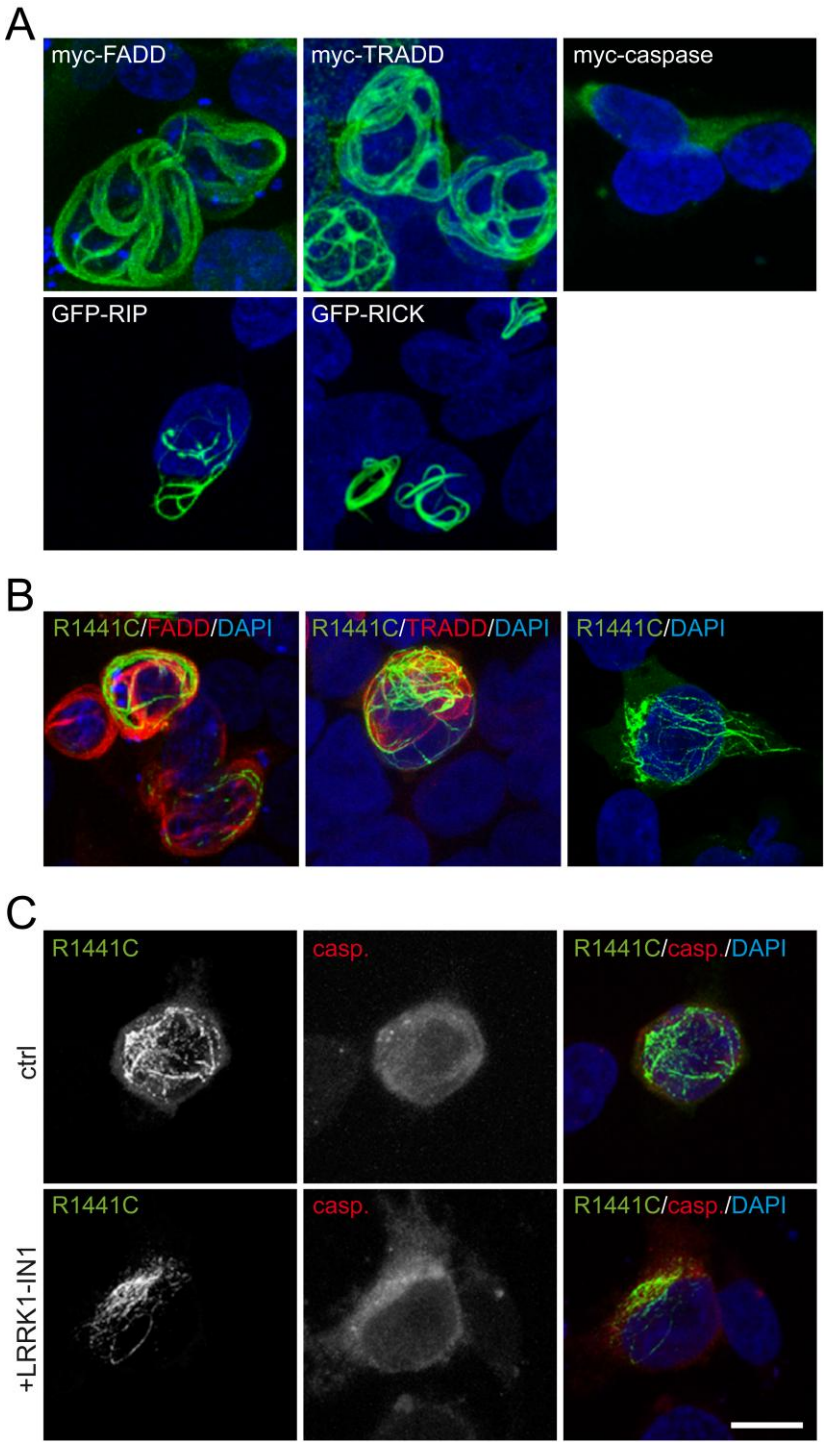

Figure 9: LRRK2 filaments are not death effector filaments. (A) Cells were transfected with the indicated constructs, they were subsequently stained for myc, when necessary, and representative pictures for each condition were acquired. (**B)** Cells were cotransfected with GFP-tagged R1441C-mutant LRRK2 and either myc-FADD or myc-TRADD, as indicated, they

were subsequently stained for myc, and representative pictures of each condition were acquired. **(C)** Cells were cotransfected with GFP-tagged R1441C-mutant LRRK2 and myc-caspase-8, and were either left untreated (ctrl) or incubated with 1µM LRRK2-IN1 for 4h as indicated. Cells were then stained for myc, and representative pictures of each condition were acquired.

5. Alterations in motility as a cellular readout for pathogenic LRRK2 in Parkinson's Disease.

Previous work suggests that LRRK2 could play a role in MT dynamics [114, 115, 197, 238]. Thus, in order to asses that in a physiological model, we used age-sex-passage-matched fibroblasts that express endogenous LRRK2 and used cell motility as a cellular readout. We first evaluated the effect of kinase inhibition by treating control cells with Mli2, which has been recently described to be the most specific LRRK2 kinase inhibitor [60]. However, no change on cell migration speed was found, as measured by time lapse microscopy. We then analyzed fibroblasts derived from skin biopsies taken from Parkinson's Disease (PD) patients carrying the G2019S mutation, and found that there was a trend to display higher speed as compared to control cells. However, more work will be required in order to further prove this effect, and define the exact mechanism by which G2019S mutants could induce faster motility, such as treatment with kinase inhibitors which would determine whether this might be a kinase activity mediated effect.

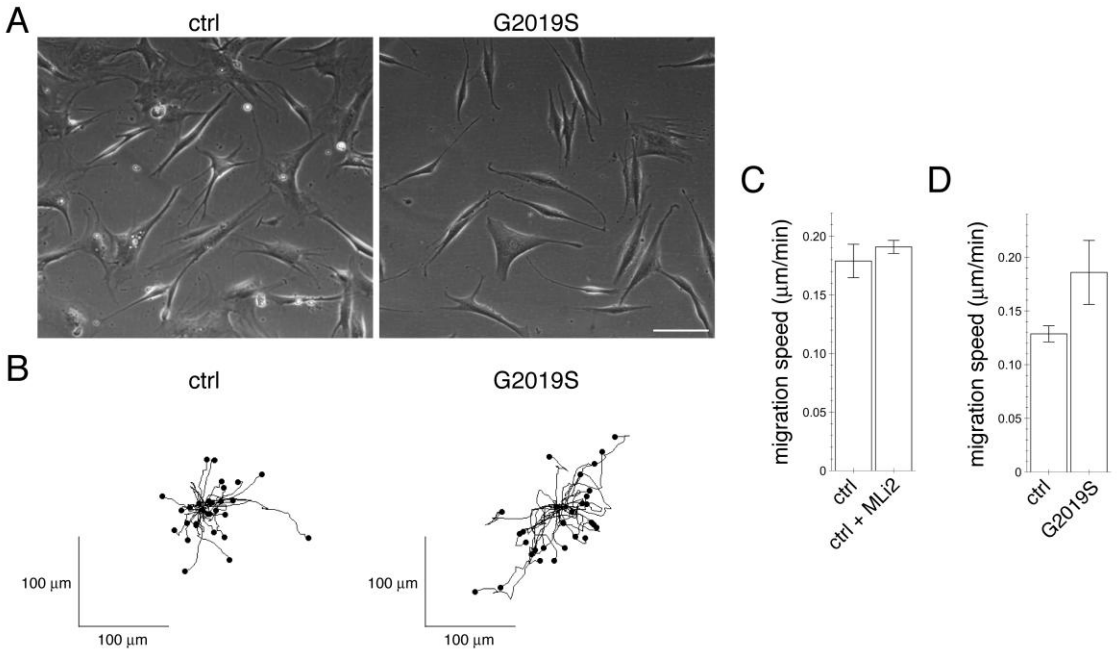

Figure 10: Pathogenic and kinase inhibited LRRK2 effect on MT dynamics. (A) Example of a phase contrast picture of control and G2019S mutant fibroblasts. **(B)** Plot of speed in control versus G2019S mutant cells. **(C)** Quantification of migration speed of either untreated (control) or in the presence of 0.5µM Mli2 for 10h, as indicated. **(D)** Quantification of migration speed of either control or G2019S mutant for 10h, as indicated.

VIII. Discussion

The interaction of LRRK2 with MTs has been widely validated by several studies from different labs, although whether LRRK2 displays higher affinity for stable versus dynamic MTs remains controversial [63, 82, 83, 113, 115, 245]. Our data corroborate this interaction and provide evidence for a preferential association of pathogenic or pharmacologically kinase-inhibited LRRK2 with stable MTs. First, we describe significant colocalization of pathogenic and kinase-inhibited LRRK2 with MT markers, which contrasts the absence of colocalization with other markers for various organelles such as EEA1, LAMP2, GM130 or LC3 (data not shown). Second, and consistent with previous work [82], we show that this association can be partially reduced by nocodazole, but much more profoundly so by cold treatment. This is reminiscent of the differential behaviour of stable MTs towards those distinct treatments, as dynamic MTs are equally disrupted by both treatments. Third, we could also partially revert the MT association of LRRK2 by deacetylase inhibitors, which in principle would point to the acetylation status of tubulin being a determinant for altering LRRK2 localization, as suggested by Godena et al. [83]. However, when overexpressing either wildtype or catalytically inactive point-mutant α-TAT-1, this association was equally rescued, thus discarding the previous hypothesis. Strikingly, recent work shows a shared role for both α-TAT-1 and its inactive mutant in destabilizing MTs, as indicated by a decrease in detyrosinated tubulin staining [164]. Indeed, we also observed a decrease in detyrosinated tubulin staining upon wildtype or inactive mutant α-TAT-1 overexpression. To modulate MT detyrosination status, given the lack of knowledge about the identity of the carboxypeptidase catalyzing this detyrosination process, we used parthenolide, an identified inhibitor for this enzyme activity [246, 247], which reduced the LRRK2-MT association. Altogether, our data suggest that LRRK2 preferentially interacts with stable MTs, and that this interation is modulated by detyrosinated, rather than acetylated tubulin levels.

Detyrosinated tubulin has been shown to play a role in modulating vesicular trafficking through preferentially associating with motor proteins [178-180], and differential interactions

with depolymerizing and severing enzymes suggest further regulatory roles for this PTM in regulating MT stability [172-174]. In addition, several studies have shown LRRK2-mediated organellar transport defects [54, 83, 115, 239], Thus, the enhanced association between pathogenic LRRK2 and stable MTs could result in trafficking deficits in a kinase activity-mediated manner.

Whilst the precise mechanism(s) remain unknown, several scenarios are possible. On the one hand, LRRK2 may directly impact upon MT stability by regulating the levels of detyrosinated (and acetylated) tubulin and/or by altering the recruitment of motor proteins, with downstream effects on vesicular trafficking events. Indeed, there is published work suggesting that LRRK2 may act as a destabilizer for stable MTs, with deficits being rescued by deacetylase inhibitors [83] or stabilizing drugs such as taxol [245]. Additionally, LRRK2 KO MEFs have been found to display higher levels of acetylated tubulin, further supporting a destabilizing role for LRRK2. In agreement with these findings, our data indicate that overexpression of pathogenic LRRK2 causes enhanced disruption of acetylated MTs upon cold treatment. Whilst tantalizing, more work will be needed in order to fully understand the effect(s) of LRRK2 on MT stability.

Alternatively, the association of pathogenic LRRK2 with stable MTs may impact on Rab8a phosphorylation, since it has recently been found that all pathogenic LRRK2 mutants cause an increase in Rab8a phosphorylation, when assayed in intact cells [54]. Importantly, and since only the G2019S mutant displays increased kinase activity *in vitro* [30, 31, 50], our findings allows us to propose a working model by which the pathogenic mutants which display unaltered kinase activity *in vitro* (the filament-forming mutants) may increase Rab8a phosphorylation in intact cells, as they display enhanced association with MTs, thereby causing enhanced Rab8a phosphorylation via "molecular proximity", as vesicles carrying Rab8a traffic along MTs [248]. Interestingly, this could as well result in vesicular trafficking alterations, since Rab8a phosphorylation has been proposed to cause a loss-of-function protein [54], which may

cause disruption of the interaction of Rab8a and its motor protein, as such interactions generally only occur when Rabs are in their active, GTP-bound state [5].

In order to test this hypothesis, Rab8a phosphorylation could be assayed in both the absence and presence of MTs destabilizing agents (especially those which modulate the detyrosination status of MTs). If this model is valid, the increase in Rab8a phosphorylation as compared to wildtype LRRK2 should be abolished by the pathogenic LRRK2 mutants that are known to display enhanced association with stable MTs, but not by the inherently kinase-hyperactive G2019S mutant. Taken together, this model would for the first time allow us to propose a common mechanism for all pathogenic mutants.

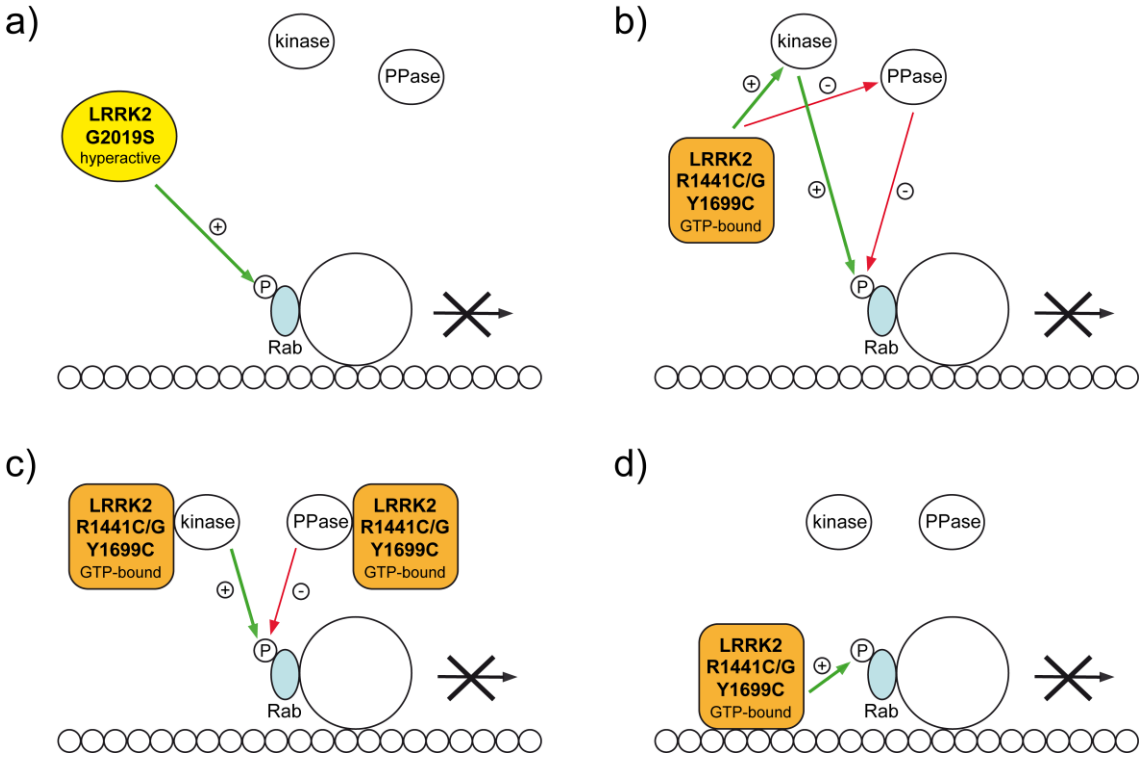

Figure 11: Possible models for how all pathogenic LRRK2 mutants may cause increased Rab protein phosphorylation in intact cells. **(A)** The G2019S mutant causes increased Rab protein phosphorylation due to an inherent increase in kinase activity. **(B)** The other pathogenic LRRK2 mutants may positively regulate kinase(s) which phosphorylate the Rab protein at the equivalent residue phosphorylated by LRRK2, or negatively regulate phosphatase(s) (PPase) which dephosphorylate the phosphorylated residue in the Rab protein.

(C) Regulation of such kinases and/or phosphatases by the pathogenic LRRK2 mutants may involve direct protein–protein interactions. **(D)** Pathogenic LRRK2 mutants, due to enhanced GTP binding, may preferentially associate with (stable) MTs, and such increased molecular proximity may cause increased phosphorylation of Rab proteins bound to transport vesicles as they move along the MT tracks. In all cases, Rab protein phosphorylation is hypothesized to interfere with vesicular trafficking steps by currently unknown molecular mechanism(s). Adapted from [5]

Having described that pathogenic and pharmacologically kinase-inhibited LRRK2 preferentially interact with stable, detyrosinated MTs, we next aimed to define the molecular determinant(s) within LRRK2 responsible for such interaction. All pathogenic LRRK2 mutants relocalized onto stable MTs (filamentous phenotype) with the exception of G2019S and I2012T mutants, which displayed a mainly cytosolic distribution pattern identical to that observed with wildtype LRRK2. Two artificial mutants which inhibit GTP binding (K1347A) or kinase activity (K1906M), respectively, also did not display altered subcellular localization. When measured *in vitro*, G2019S has been consistently reported to increase kinase activity [47, 51, 249, 250], with I2012T being shown to decrease kinase activity, the pathogenic ROC-COR mutants displaying no change, and K1906M being a synthetic kinase-dead mutant [44-48, 251]. Thus, the reported differences in kinase activity amongst the various pathogenic mutants do not seem to correlate with the enhanced association with stable MTs.

To test for the importance of kinase activity for such altered subcellular localization, we also made a point mutation in an autophosphorylation site (S1292) which had been previously validated both *in vivo* and *in vitro* [66]. Whilst a partial effect in reducing the stable MT association was found when abolishing this autophosphorylation site within the context of a triple pathogenic mutant (R1441C, Y1669C, G2019S), no change was observed in the context of single pathogenic LRRK2 mutations. Autophosphorylation events in protein kinases are generally of low stoichiometry. Therefore, altered kinase activity *per se*, as reflected by an

altered autophosphorylation status, is unlikely to contribute to the enhanced association of pathogenic LRRK2 mutants with stable MTs [66, 252] .

However, and in apparent contrast, when pharmacologically inhibiting LRRK2 kinase activity by various specific and structurally distinct kinase inhibitors [55-60], wildtype as well as all pathogenic LRRK2 underwent filament formation. As another means to test whether filament formation could be due a kinase activity-mediated event, we analyzed the localization of two different kinase-dead mutants (K1906M and T2035A). Neither of those mutants displayed enhanced filament formation, suggesting that they cannot properly mimic the effect of pharmacological kinase inhibitors. Indeed, pharmacological kinase inhibition, thought to cause a conformational change within LRRK2, caused dephosphorylation of the N-terminal phosphorylation sites, which was not observed with the kinase-dead mutants, consistent with previous work [58, 74, 75, 251]. In summary, both pharmacological kinase inhibition as well as most kinase-active pathogenic LRRK2 mutants displayed enhanced colocalization with stable MTs, indicating that such altered localization does not correlate with the kinase activity of LRRK2.

Apart from pharmacological kinase inhibition, most pathogenic mutants have been also shown to display reduced N-terminal phosphorylation [48, 74]. We thus wondered whether dephosphorylation of the N-terminus could correlate with the filamentous phenotype. Indeed, the pathogenic filament-forming LRRK2 mutants showed significantly decreased levels of S935 phosphorylation, whereas a mutant displaying a cytosolic distribution, G2019S, showed no change. Additionally, in the presence of pharmacological kinase inhibitors, K1906M did not undergo filament formation and presented no change in S935 phosphorylation levels, whereas T2035A displayed a filamentous phenotype and showed completely abolished S935 phosphorylation, which supports a correlation between N-terminal LRRK2 phosphorylation and filament formation.

Since phosphorylation at the N-terminus has been shown to be required for the interaction of LRRK2 with 14-3-3 proteins [48, 72, 75], we tested whether 14-3-3 could

modulate filament formation. Thus, we coexpressed 14-3-3β, 14-3-3γ, or a loss-of-function point-mutant version of 14-3-3γ with either wildtype or pathogenic LRRK2 and analyzed the subcellular localization of LRRK2. Interestingly, whereas no effect was found with 14-3-3β, we reported an almost complete reversal of filament formation, with a concomitant decrease in S935 phosphorylation levels when overexpressing wildtype but not binding-deficient mutant 14-3-3γ. This suggests that binding of 14-3-3γ to the cluster of cellular phosphorylation sites may maintain these sites in a phosphorylated state, which in turn may prevent the altered subcellular localization of LRRK2. Our data are also consistent with previous work showing the preferential association of LRRK2 with 14-3-3γ, as compared to other 14-3-3 isoforms [72, 73].

Based on the above findings, we next evaluated whether abolishing N-terminal phosphorylation is sufficient for inducing the relocalization of LRRK2. However, when making S/A substitutions at the cellular phosphorylation sites as well as at one additional site that has been equally described to be involved in the interaction of LRRK2 with 14-3-3 [73], we did not find any change in filament formation, thus suggesting that an additional mechanism should be involved in this process.

Interestingly, pharmacological kinase inhibitors have been reported to cause an increase in steady-state GTP binding of LRRK2 [77]. In addition, most pathogenic LRRK2 mutants which cause enhanced filament formation have been described to display increased GTP binding [33, 71, 89, 101, 102, 105-108]. Therefore, we next wondered whether enhanced GTP binding may play a role in filament formation.

In other to modulate steady-state GTP binding, we co-expressed LRRK2 with its identified GEF (ArhGEF7) [100] or with its two reported GAPs (RGS2 and ArfGAP1), respectively [101-103]. However, the presence of GAPs did not alter the subcellular localization of LRRK2. Interestingly, whilst ArfGAP1 has been reported to alter the GTPase activity of LRRK2, this was not associated with changes in GTP binding [102]. Furthermore, both active and inactive ArhGEF7 interfered with the filamentous LRRK2 phenotype. The similar effects induced by both wildtype and catalytically inactive ArhGEF7 suggest that since they both have

been shown to equally bind to LRRK2 through the ROC domain [100, 124], the reversal in filament formation may be due to ArfGEF7 competing with the MT binding site of LRRK2, which is also located in the ROC domain [113], rather than by altering steady-state GTP binding.

As another means to gauge for GTP binding regulation, we overexpressed synthetic LRRK2 mutants which cluster in the ROC domain and which have been shown to alter GTP hydrolysis/GTP binding [91]. Remarkably, we saw a significant decrease of the filamentous phenotype upon introducing either the R1398L (RL) or the R1398L/T1343V (RL/TV) mutations in the context of the filament-forming pathogenic mutants, whereas the T1343V (TV) mutation on its own showed no effect. Such rescue was also observed in the context of pharmacologically kinase-inhibited LRRK2, suggesting a common mechanism for filament formation. To shed more light into this, we analyzed the GTP binding capacity of both pathogenic as well as pharmacologically kinase-inhibited LRRK2 in the context of the RL and RLTV mutations. Both pathogenic as well as pharmacologically kinase-inhibited LRRK2 displayed enhanced steady-state GTP binding which was reduced by either RL or RLTV mutations, correlating with the alterations in subcellular localization.

Another amino acid substitution at the R1398 residue, R1398H, which also decreased the filamentous phenotype, was also found to reduce GTP binding capacity, consistent with previous work [253]. Interestingly, this mutant has been found to be a protective variant for PD [38-40], raising the possibility that at least part of its protective effect may be due to inhibiting alterations in the subcellular localization of LRRK2. *In vitro* kinase assays with the various pathogenic LRRK2 mutants in the context of the RL or RLTV mutations showed no correlation between kinase activity and filament formation, again indicating that the effects were not mediated by altered kinase activity, but rather perfectly correlating with alterations in GTP binding.

We next employed two novel compounds that have been shown to decrease LRRK2 GTP binding, namely 68 and 70 [110, 111], and we found that they reduced filament formation

induced by either pathogenic or kinase-inhibited LRRK2. Whilst compounds 68 and 70 have also been described to alter LRRK2 kinase activity [110], the observed absence of correlation of the filamentous phenotype with kinase activity indicates that the effect of these compounds in regulating LRRK2 localization is mediated by altering the steady-state GTP binding status of LRRK2, rather than through modulating its kinase activity. Furthermore, modifying GTP binding by either of these compounds or by the synthetic RL or RLTV mutants failed to alter N-terminal phosphorylation, and overexpression of 14-3-3γ, which decreased the filamentous phenotype, caused a reduction in GTP binding. Therefore, whilst the N-terminal phosphorylation status can correlate with altered subcellular localization, it is not necessary for such altered localization. Finally, increasing GTP levels upon treatment of permeabilized cells with a non-hydrolysable GTP analog, GTPαS, was found to enhance filament formation, providing formal proof-of-concept that such altered localization is mediated by altered GTP binding of LRRK2.

Taken together, our findings highlight the mechanism by which most pathogenic mutants and as well as kinase-inhibited LRRK2 undergo abnormal localization to a subset of stable MTs, thereby impacting upon vesicular trafficking events known to be crucial for the proper functioning of neuronal cells. In agreement with this, a recent study has described that GTP binding inhibitors can rescue the organellar transport deficits induced by R1441C mutant LRRK2 [111]. Although more work will be needed to validate the relevance of GTP binding for the pathogenicity of LRRK2 *in vivo*, such as by introducing an R1398H/L mutation in the context of the pathogenic R1441C mutation in transgenic mice, our results provide strong evidence for an important role for GTP binding in LRRK2-mediated pathogenicity.

IX. Conclusions/Conclusiones

1. Wildtype LRRK2 is largely cytosolic, whilst most pathogenic LRRK2 mutants, as well as pharmacologically kinase-inhibited LRRK2, colocalize with microtubules

2. Pathogenic and pharmacologically kinase-inhibited LRRK2 preferentially associate with stable, detyrosinated microtubules

3. Abolishing a prominent autophosphorylation site in LRRK2 has no effect on its subcellular localization

4. Synthetic kinase-dead LRRK2 mutants do not mimic pharmacologically kinase-inhibited LRRK2 in terms of cellular phosphorylation or subcellular localization

5. N-terminal dephosphorylation of LRRK2 correlates with altered subcellular localization, but is neither necessary nor sufficient for it

6. Neither identified GTPase activating proteins (GAPs) nor GTP/GTP exchange factors (GEFs) for LRRK2 modulate the subcellular localization of pathogenic or pharmacologically kinase-inhibited LRRK2

7. Synthetic mutants predicted to affect GTP binding potently impair the altered subcellular localization of pathogenic or pharmacologically kinase-inhibited LRRK2

8. A protective LRRK2 risk variant largely reverts the altered subcellular localization of pathogenic or pharmacologically kinase-inhibited LRRK2

9. Pathogenic LRRK2 mutations and pharmacologically kinase-inhibited LRRK2 display increased GTP binding which correlates with altered subcellular localization, and synthetic mutants which decrease the altered subcellular localization, or the protective LRRK2 risk variant, decrease GTP binding

10. There is no correlation between altered kinase activity of pathogenic LRRK2 mutants, or synthetic mutants impairing GTP binding, with the observed alterations in subcellular localization

11. Two distinct LRRK2 GTP binding inhibitors rescue the altered subcellular localization of pathogenic or pharmacologically kinase-inhibited LRRK2

12. Non-hydrolysable GTP analogs increase the altered subcellular localization of pathogenic or pharmacologically kinase-inhibited LRRK2, providing formal proof that modified GTP binding correlates with altered localization

Conclusiones

1. Wildtype LRRK2 tiene una localización principalmente citosólica, mientras que la mayoría de los mutantes patógenicos de LRRK2, así como su versión farmacológicamente inhibida de la actividad kinasa, colocalizan con microtúbulos

2. Mutantes patógenicos de LRRK2, así como su versión farmacológicamente inhibida de la actividad kinasa se asocian preferentemente con microtúbulos estables con tinción positiva de tubulina destirosinada

3. La eliminación de un sitio prominente de autofosforilación en LRRK2 no afecta a su localización celular

4. Mutantes artificiales que inactivan la actividad kinasa de LRRK2 no mimetizan su inhibición farmacológica, ni en función de su localización celular ni tampoco en la localización celular de LRRK2

5. La desfosforilación del dominio N-terminal de LRRK2 correlaciona con la alteración en la localización celular de LRRK2, pero no es necesario ni suficiente para inducirla

6. La sobreexpresión de GAPs o GEFs para LRRK2 no modula la localización celular ni de LRRK2 patogénico ni de su versión inactiva de la actividad kinasa mediante inhibición farmacológica

7. Mutantes sintéticos que afectan a la unión de GTP interfieren con la localización celular de LRRK2 patogénico, así como de su versión farmacológicamente inhibida de la actividad kinasa

8. Un mutante protectivo de LRRK2 revierte la localización celular de LRRK2 patogénico y de su versión farmacológicamente inhibida de la actividad kinasa

9. LRRK2 patogénico y su versión farmacológicamente inhibida de la actividad kinasa presentan un aumento en unión a GTP, lo cual se correlaciona con una alteración en la

localización celular de LRRK2, mientras que tanto los mutantes sintéticos del dominio GTPasa como el mutante protectivo que revierten esta localización celular alterada, disminuyen la unión a GTP

10. La actividad kinasa de LRRK2 no se correlaciona con la alteración en la localización celular vista con los mutantes patógenicos de LRRK2 o con los mutantes sintéticos del dominio GTPasa

11. Dos inhibidores de unión a GTP son capaces de rescatar la alteración en la localización celular inducida por LRRK2 patogénico y por su versión farmacológicamente inhibida de la actividad kinasa

12. Análogos no hidrolizables de GTP alteran en mayor manera la localización celular inducida por LRRK2 patogénico y por su versión farmacológicamente inhibida de la actividad kinasa, lo cual supone una prueba formal de que un cambio en GTP correlaciona con la alteración de la localización celular de LRRK2

X. References

1. Jost, W.H. and H. Reichmann, *"An essay on the shaking palsy" 200 years old.* J Neural Transm (Vienna), 2017.
2. Halliday, G., A. Lees, and M. Stern, *Milestones in Parkinson's disease--clinical and pathologic features.* Mov Disord, 2011. **26**(6): p. 1015-21.
3. Ledoux, M.S., W.T. Dauer, and T.T. Warner, *Emerging common molecular pathways for primary dystonia.* Mov Disord, 2013. **28**(7): p. 968-81.
4. Belin, A.C. and M. Westerlund, *Parkinson's disease: a genetic perspective.* FEBS J, 2008. **275**(7): p. 1377-83.
5. Blanca Ramirez, M., et al., *LRRK2: from kinase to GTPase to microtubules and back.* Biochem Soc Trans, 2017. **45**(1): p. 141-146.
6. Dauer, W. and S. Przedborski, *Parkinson's disease: mechanisms and models.* Neuron, 2003. **39**(6): p. 889-909.
7. Sveinbjornsdottir, S., *The clinical symptoms of Parkinson's disease.* J Neurochem, 2016. **139 Suppl 1**: p. 318-324.
8. Bellucci, A., et al., *Review: Parkinson's disease: from synaptic loss to connectome dysfunction.* Neuropathol Appl Neurobiol, 2016. **42**(1): p. 77-94.
9. Pont-Sunyer, C., et al., *The prodromal phase of leucine-rich repeat kinase 2-associated Parkinson disease: Clinical and imaging Studies.* Mov Disord, 2017.
10. Surmeier, D.J., et al., *What causes the death of dopaminergic neurons in Parkinson's disease?* Prog Brain Res, 2010. **183**: p. 59-77.
11. Ferrazzoli, D., et al., *Does Cognitive Impairment Affect Rehabilitation Outcome in Parkinson's Disease?* Front Aging Neurosci, 2016. **8**: p. 192.
12. Singleton, A.B., M.J. Farrer, and V. Bonifati, *The genetics of Parkinson's disease: progress and therapeutic implications.* Mov Disord, 2013. **28**(1): p. 14-23.

13. Polymeropoulos, M.H., et al., *Linkage of the locus for cerebral cavernous hemangiomas to human chromosome 7q in four families of Mexican-American descent.* Neurology, 1997. **48**(3): p. 752-7.

14. Kruger, R., et al., *Ala30Pro mutation in the gene encoding alpha-synuclein in Parkinson's disease.* Nat Genet, 1998. **18**(2): p. 106-8.

15. Zarranz, J.J., et al., *The new mutation, E46K, of alpha-synuclein causes Parkinson and Lewy body dementia.* Ann Neurol, 2004. **55**(2): p. 164-73.

16. Chartier-Harlin, M.C., et al., *Alpha-synuclein locus duplication as a cause of familial Parkinson's disease.* Lancet, 2004. **364**(9440): p. 1167-9.

17. Kann, M., et al., *Role of parkin mutations in 111 community-based patients with early-onset parkinsonism.* Ann Neurol, 2002. **51**(5): p. 621-5.

18. Gouider-Khouja, N., et al., *Autosomal recessive parkinsonism linked to parkin gene in a Tunisian family. Clinical, genetic and pathological study.* Parkinsonism Relat Disord, 2003. **9**(5): p. 247-51.

19. Farrer, M., et al., *Lewy bodies and parkinsonism in families with parkin mutations.* Ann Neurol, 2001. **50**(3): p. 293-300.

20. hValente, E.M., et al., *Hereditary early-onset Parkinson's disease caused by mutations in PINK1.* Science, 2004. **304**(5674): p. 1158-60.

21. Kalinderi, K., S. Bostantjopoulou, and L. Fidani, *The genetic background of Parkinson's disease: current progress and future prospects.* Acta Neurol Scand, 2016. **134**(5): p. 314-326.

22. Polymeropoulos, M.H., et al., *Mapping of a gene for Parkinson's disease to chromosome 4q21-q23.* Science, 1996. **274**(5290): p. 1197-9.

23. Farrer, M., et al., *A chromosome 4p haplotype segregating with Parkinson's disease and postural tremor.* Hum Mol Genet, 1999. **8**(1): p. 81-5.

24. Matsumine, H., et al., *Localization of a gene for an autosomal recessive form of juvenile Parkinsonism to chromosome 6q25.2-27.* Am J Hum Genet, 1997. **60**(3): p. 588-96.

25. Valente, E.M., et al., *Localization of a novel locus for autosomal recessive early-onset parkinsonism, PARK6, on human chromosome 1p35-p36.* Am J Hum Genet, 2001. **68**(4): p. 895-900.

26. van Duijn, C.M., et al., *Park7, a novel locus for autosomal recessive early-onset parkinsonism, on chromosome 1p36.* Am J Hum Genet, 2001. **69**(3): p. 629-34.

27. Funayama, M., et al., *A new locus for Parkinson's disease (PARK8) maps to chromosome 12p11.2-q13.1.* Ann Neurol, 2002. **51**(3): p. 296-301.

28. Satake, W., et al., *Genome-wide association study identifies common variants at four loci as genetic risk factors for Parkinson's disease.* Nat Genet, 2009. **41**(12): p. 1303-7.

29. Vilarino-Guell, C., et al., *VPS35 mutations in Parkinson disease.* Am J Hum Genet, 2011. **89**(1): p. 162-7.

30. Zimprich, A., et al., *Mutations in LRRK2 cause autosomal-dominant parkinsonism with pleomorphic pathology.* Neuron, 2004. **44**(4): p. 601-7.

31. Paisan-Ruiz, C., et al., *Cloning of the gene containing mutations that cause PARK8-linked Parkinson's disease.* Neuron, 2004. **44**(4): p. 595-600.

32. Lesage, S. and A. Brice, *Parkinson's disease: from monogenic forms to genetic susceptibility factors.* Hum Mol Genet, 2009. **18**(R1): p. R48-59.

33. Aasly, J.O., et al., *Novel pathogenic LRRK2 p.Asn1437His substitution in familial Parkinson's disease.* Mov Disord, 2010. **25**(13): p. 2156-63.

34. Funayama, M., et al., *An LRRK2 mutation as a cause for the parkinsonism in the original PARK8 family.* Ann Neurol, 2005. **57**(6): p. 918-21.

35. Tomiyama, H., et al., *Clinicogenetic study of mutations in LRRK2 exon 41 in Parkinson's disease patients from 18 countries.* Mov Disord, 2006. **21**(8): p. 1102-8.

36. Ross, O.A., et al., *Analysis of Lrrk2 R1628P as a risk factor for Parkinson's disease.* Ann Neurol, 2008. **64**(1): p. 88-92.

37. Funayama, M., et al., *Leucine-rich repeat kinase 2 G2385R variant is a risk factor for Parkinson disease in Asian population.* Neuroreport, 2007. **18**(3): p. 273-5.

38. Chen, L., et al., *LRRK2 R1398H polymorphism is associated with decreased risk of Parkinson's disease in a Han Chinese population.* Parkinsonism Relat Disord, 2011. **17**(4): p. 291-2.

39. Tan, E.K., et al., *Multiple LRRK2 variants modulate risk of Parkinson disease: a Chinese multicenter study*. Hum Mutat, 2010. **31**(5): p. 561-8.

40. Heckman, M.G., et al., *Protective effect of LRRK2 p.R1398H on risk of Parkinson's disease is independent of MAPT and SNCA variants.* Neurobiol Aging, 2014. **35**(1): p. 266 e5-14.

41. Luzon-Toro, B., et al., *Mechanistic insight into the dominant mode of the Parkinson's disease-associated G2019S LRRK2 mutation.* Hum Mol Genet, 2007. **16**(17): p. 2031-9.

42. Huse, M. and J. Kuriyan, *The conformational plasticity of protein kinases.* Cell, 2002. **109**(3): p. 275-82.

43. Kornev, A.P., et al., *Surface comparison of active and inactive protein kinases identifies a conserved activation mechanism.* Proc Natl Acad Sci U S A, 2006. **103**(47): p. 17783-8.

44. Ray, S., et al., *The Parkinson disease-linked LRRK2 protein mutation I2020T stabilizes an active state conformation leading to increased kinase activity.* J Biol Chem, 2014. **289**(19): p. 13042-53.

45. Gloeckner, C.J., et al., *The Parkinson disease causing LRRK2 mutation I2020T is associated with increased kinase activity.* Hum Mol Genet, 2006. **15**(2): p. 223-32.

46. Ho, D.H., et al., *G2385R and I2020T Mutations Increase LRRK2 GTPase Activity.* Biomed Res Int, 2016. **2016**: p. 7917128.

47. Jaleel, M., et al., *LRRK2 phosphorylates moesin at threonine-558: characterization of how Parkinson's disease mutants affect kinase activity.* Biochem J, 2007. **405**(2): p. 307-17.

48. Nichols, R.J., et al., *14-3-3 binding to LRRK2 is disrupted by multiple Parkinson's disease-associated mutations and regulates cytoplasmic localization.* Biochem J, 2010. **430**(3): p. 393-404.

49. Rudenko, I.N., et al., *The G2385R variant of leucine-rich repeat kinase 2 associated with Parkinson's disease is a partial loss-of-function mutation.* Biochem J, 2012. **446**(1): p. 99-111.

50. Bonifati, V., *LRRK2 low-penetrance mutations (Gly2019Ser) and risk alleles (Gly2385Arg)-linking familial and sporadic Parkinson's disease.* Neurochem Res, 2007. **32**(10): p. 1700-8.

51. Greggio, E., et al., *Kinase activity is required for the toxic effects of mutant LRRK2/dardarin.* Neurobiol Dis, 2006. **23**(2): p. 329-41.

52. Smith, W.W., et al., *Kinase activity of mutant LRRK2 mediates neuronal toxicity.* Nat Neurosci, 2006. **9**(10): p. 1231-3.

53. Lee, B.D., et al., *Inhibitors of leucine-rich repeat kinase-2 protect against models of Parkinson's disease.* Nat Med, 2010. **16**(9): p. 998-1000.

54. Steger, M., et al., *Phosphoproteomics reveals that Parkinson's disease kinase LRRK2 regulates a subset of Rab GTPases.* Elife, 2016. **5**.

55. Ramsden, N., et al., *Chemoproteomics-based design of potent LRRK2-selective lead compounds that attenuate Parkinson's disease-related toxicity in human neurons.* ACS Chem Biol, 2011. **6**(10): p. 1021-8.

56. Zhang, J., et al., *Characterization of TAE684 as a potent LRRK2 kinase inhibitor.* Bioorg Med Chem Lett, 2012. **22**(5): p. 1864-9.

57. Estrada, A.A., et al., *Discovery of highly potent, selective, and brain-penetrant aminopyrazole leucine-rich repeat kinase 2 (LRRK2) small molecule inhibitors.* J Med Chem, 2014. **57**(3): p. 921-36.

58. Deng, X., et al., *Characterization of a selective inhibitor of the Parkinson's disease kinase LRRK2.* Nat Chem Biol, 2011. **7**(4): p. 203-5.

59. Najafov, A., et al., *Characterization of GSK2334470, a novel and highly specific inhibitor of PDK1.* Biochem J, 2011. **433**(2): p. 357-69.

60. Fell, M.J., et al., *MLi-2, a Potent, Selective, and Centrally Active Compound for Exploring the Therapeutic Potential and Safety of LRRK2 Kinase Inhibition.* J Pharmacol Exp Ther, 2015. **355**(3): p. 397-409.

61. Kumar, A., et al., *The Parkinson's disease associated LRRK2 exhibits weaker in vitro phosphorylation of 4E-BP compared to autophosphorylation.* PLoS One, 2010. **5**(1): p. e8730.

62. Bailey, R.M., et al., *LRRK2 phosphorylates novel tau epitopes and promotes tauopathy.* Acta Neuropathol, 2013. **126**(6): p. 809-27.

63. Gillardon, F., *Leucine-rich repeat kinase 2 phosphorylates brain tubulin-beta isoforms and modulates microtubule stability--a point of convergence in parkinsonian neurodegeneration?* J Neurochem, 2009. **110**(5): p. 1514-22.

64. Pungaliya, P.P., et al., *Identification and characterization of a leucine-rich repeat kinase 2 (LRRK2) consensus phosphorylation motif.* PLoS One, 2010. **5**(10): p. e13672.

65. Li, X., et al., *Reevaluation of phosphorylation sites in the Parkinson disease-associated leucine-rich repeat kinase 2.* J Biol Chem, 2010. **285**(38): p. 29569-76.

66. Sheng, Z., et al., *Ser1292 autophosphorylation is an indicator of LRRK2 kinase activity and contributes to the cellular effects of PD mutations.* Sci Transl Med, 2012. **4**(164): p. 164ra161.

67. Gloeckner, C.J., et al., *Phosphopeptide analysis reveals two discrete clusters of phosphorylation in the N-terminus and the Roc domain of the Parkinson-disease associated protein kinase LRRK2.* J Proteome Res, 2010. **9**(4): p. 1738-45.

68. Greggio, E., et al., *The Parkinson's disease kinase LRRK2 autophosphorylates its GTPase domain at multiple sites.* Biochem Biophys Res Commun, 2009. **389**(3): p. 449-54.

69. Kamikawaji, S., G. Ito, and T. Iwatsubo, *Identification of the autophosphorylation sites of LRRK2.* Biochemistry, 2009. **48**(46): p. 10963-75.

70. Webber, P.J., et al., *Autophosphorylation in the leucine-rich repeat kinase 2 (LRRK2) GTPase domain modifies kinase and GTP-binding activities.* J Mol Biol, 2011. **412**(1): p. 94-110.

71. West, A.B., et al., *Parkinson's disease-associated mutations in LRRK2 link enhanced GTP-binding and kinase activities to neuronal toxicity.* Hum Mol Genet, 2007. **16**(2): p. 223-32.

72. Li, X., et al., *Phosphorylation-dependent 14-3-3 binding to LRRK2 is impaired by common mutations of familial Parkinson's disease.* PLoS One, 2011. **6**(3): p. e17153.

73. Muda, K., et al., *Parkinson-related LRRK2 mutation R1441C/G/H impairs PKA phosphorylation of LRRK2 and disrupts its interaction with 14-3-3.* Proc Natl Acad Sci U S A, 2014. **111**(1): p. E34-43.

74. Doggett, E.A., et al., *Phosphorylation of LRRK2 serines 955 and 973 is disrupted by Parkinson's disease mutations and LRRK2 pharmacological inhibition.* J Neurochem, 2012. **120**(1): p. 37-45.

75. Dzamko, N., et al., *Inhibition of LRRK2 kinase activity leads to dephosphorylation of Ser(910)/Ser(935), disruption of 14-3-3 binding and altered cytoplasmic localization.* Biochem J, 2010. **430**(3): p. 405-13.

76. Dzamko, N., et al., *The IkappaB kinase family phosphorylates the Parkinson's disease kinase LRRK2 at Ser935 and Ser910 during Toll-like receptor signaling.* PLoS One, 2012. **7**(6): p. e39132.

77. Chia, R., et al., *Phosphorylation of LRRK2 by casein kinase 1alpha regulates trans-Golgi clustering via differential interaction with ARHGEF7.* Nat Commun, 2014. **5**: p. 5827.

78. Lobbestael, E., et al., *Identification of protein phosphatase 1 as a regulator of the LRRK2 phosphorylation cycle.* Biochem J, 2013. **456**(1): p. 119-28.

79. Alegre-Abarrategui, J., et al., *LRRK2 regulates autophagic activity and localizes to specific membrane microdomains in a novel human genomic reporter cellular model.* Hum Mol Genet, 2009. **18**(21): p. 4022-34.

80. Deng, X., et al., *Leucine-rich repeat kinase 2 inhibitors: a patent review (2006 - 2011).* Expert Opin Ther Pat, 2012. **22**(12): p. 1415-26.

81. Lavalley, N.J., et al., *14-3-3 Proteins regulate mutant LRRK2 kinase activity and neurite shortening.* Hum Mol Genet, 2016. **25**(1): p. 109-22.

82. Kett, L.R., et al., *LRRK2 Parkinson disease mutations enhance its microtubule association.* Hum Mol Genet, 2012. **21**(4): p. 890-9.

83. Godena, V.K., et al., *Increasing microtubule acetylation rescues axonal transport and locomotor deficits caused by LRRK2 Roc-COR domain mutations.* Nat Commun, 2014. **5**: p. 5245.

84. Tsika, E. and D.J. Moore, *Mechanisms of LRRK2-mediated neurodegeneration.* Curr Neurol Neurosci Rep, 2012. **12**(3): p. 251-60.

85. Tsika, E. and D.J. Moore, *Contribution of GTPase activity to LRRK2-associated Parkinson disease.* Small GTPases, 2013. **4**(3): p. 164-70.

86. Vetter, I.R. and A. Wittinghofer, *The guanine nucleotide-binding switch in three dimensions.* Science, 2001. **294**(5545): p. 1299-304.

87. Gotthardt, K., et al., *Structure of the Roc-COR domain tandem of C. tepidum, a prokaryotic homologue of the human LRRK2 Parkinson kinase.* EMBO J, 2008. **27**(16): p. 2239-49.

88. Ito, G., et al., *GTP binding is essential to the protein kinase activity of LRRK2, a causative gene product for familial Parkinson's disease.* Biochemistry, 2007. **46**(5): p. 1380-8.

89. Liao, J., et al., *Parkinson disease-associated mutation R1441H in LRRK2 prolongs the "active state" of its GTPase domain.* Proc Natl Acad Sci U S A, 2014. **111**(11): p. 4055-60.

90. Liu, M., et al., *Kinetic mechanistic studies of wild-type leucine-rich repeat kinase 2: characterization of the kinase and GTPase activities.* Biochemistry, 2010. **49**(9): p. 2008-17.

91. Biosa, A., et al., *GTPase activity regulates kinase activity and cellular phenotypes of Parkinson's disease-associated LRRK2.* Hum Mol Genet, 2013. **22**(6): p. 1140-56.

92. Webber, P.J. and A.B. West, *LRRK2 in Parkinson's disease: function in cells and neurodegeneration.* FEBS J, 2009. **276**(22): p. 6436-44.

93. Greggio, E., et al., *The Parkinson disease-associated leucine-rich repeat kinase 2 (LRRK2) is a dimer that undergoes intramolecular autophosphorylation.* J Biol Chem, 2008. **283**(24): p. 16906-14.

94. Civiero, L., et al., *Biochemical characterization of highly purified leucine-rich repeat kinases 1 and 2 demonstrates formation of homodimers.* PLoS One, 2012. **7**(8): p. e43472.

95. Sen, S., P.J. Webber, and A.B. West, *Dependence of leucine-rich repeat kinase 2 (LRRK2) kinase activity on dimerization.* J Biol Chem, 2009. **284**(52): p. 36346-56.

96. Ito, G. and T. Iwatsubo, *Re-examination of the dimerization state of leucine-rich repeat kinase 2: predominance of the monomeric form.* Biochem J, 2012. **441**(3): p. 987-94.

97. Guaitoli, G., et al., *Structural model of the dimeric Parkinson's protein LRRK2 reveals a compact architecture involving distant interdomain contacts.* Proc Natl Acad Sci U S A, 2016. **113**(30): p. E4357-66.

98. Jorgensen, N.D., et al., *The WD40 domain is required for LRRK2 neurotoxicity.* PLoS One, 2009. **4**(12): p. e8463.

99. Deng, J., et al., *Structure of the ROC domain from the Parkinson's disease-associated leucine-rich repeat kinase 2 reveals a dimeric GTPase.* Proc Natl Acad Sci U S A, 2008. **105**(5): p. 1499-504.

100. Haebig, K., et al., *ARHGEF7 (Beta-PIX) acts as guanine nucleotide exchange factor for leucine-rich repeat kinase 2.* PLoS One, 2010. **5**(10): p. e13762.

101. Xiong, Y., et al., *GTPase activity plays a key role in the pathobiology of LRRK2.* PLoS Genet, 2010. **6**(4): p. e1000902.

102. Stafa, K., et al., *GTPase activity and neuronal toxicity of Parkinson's disease-associated LRRK2 is regulated by ArfGAP1.* PLoS Genet, 2012. **8**(2): p. e1002526.

103. Dusonchet, J., et al., *A Parkinson's disease gene regulatory network identifies the signaling protein RGS2 as a modulator of LRRK2 activity and neuronal toxicity.* Hum Mol Genet, 2014. **23**(18): p. 4887-905.

104. Xiong, Y., et al., *ArfGAP1 is a GTPase activating protein for LRRK2: reciprocal regulation of ArfGAP1 by LRRK2.* J Neurosci, 2012. **32**(11): p. 3877-86.

105. Daniels, V., et al., *Insight into the mode of action of the LRRK2 Y1699C pathogenic mutant.* J Neurochem, 2011. **116**(2): p. 304-15.

106. Li, X., et al., *Leucine-rich repeat kinase 2 (LRRK2)/PARK8 possesses GTPase activity that is altered in familial Parkinson's disease R1441C/G mutants.* J Neurochem, 2007. **103**(1): p. 238-47.

107. Lewis, P.A., et al., *The R1441C mutation of LRRK2 disrupts GTP hydrolysis.* Biochem Biophys Res Commun, 2007. **357**(3): p. 668-71.

108. Guo, L., et al., *The Parkinson's disease-associated protein, leucine-rich repeat kinase 2 (LRRK2), is an authentic GTPase that stimulates kinase activity*. Exp Cell Res, 2007. **313**(16): p. 3658-70.

109. West, A.B., V.L. Dawson, and T.M. Dawson, *To die or grow: Parkinson's disease and cancer*. Trends Neurosci, 2005. **28**(7): p. 348-52.

110. Li, T., et al., *Novel LRRK2 GTP-binding inhibitors reduced degeneration in Parkinson's disease cell and mouse models.* Hum Mol Genet, 2014. **23**(23): p. 6212-22.

111. Thomas, J.M., et al., *68 and FX2149 Attenuate Mutant LRRK2-R1441C-Induced Neural Transport Impairment.* Front Aging Neurosci, 2016. **8**: p. 337.

112. Manzoni, C., *The LRRK2-macroautophagy axis and its relevance to Parkinson's disease*. Biochem Soc Trans, 2017. **45**(1): p. 155-162.

113. Gandhi, P.N., et al., *The Roc domain of leucine-rich repeat kinase 2 is sufficient for interaction with microtubules*. J Neurosci Res, 2008. **86**(8): p. 1711-20.

114. Caesar, M., et al., *Leucine-rich repeat kinase 2 functionally interacts with microtubules and kinase-dependently modulates cell migration.* Neurobiol Dis, 2013. **54**: p. 280-8.

115. Law, B.M., et al., *A direct interaction between leucine-rich repeat kinase 2 and specific beta-tubulin isoforms regulates tubulin acetylation.* J Biol Chem, 2014. **289**(2): p. 895-908.

116. Kawakami, F., et al., *LRRK2 phosphorylates tubulin-associated tau but not the free molecule: LRRK2-mediated regulation of the tau-tubulin association and neurite outgrowth.* PLoS One, 2012. **7**(1): p. e30834.

117. Kawakami, F., et al., *Leucine-rich repeat kinase 2 regulates tau phosphorylation through direct activation of glycogen synthase kinase-3beta.* FEBS J, 2014. **281**(1): p. 3-13.

118. Khan, N.L., et al., *Mutations in the gene LRRK2 encoding dardarin (PARK8) cause familial Parkinson's disease: clinical, pathological, olfactory and functional imaging and genetic data.* Brain, 2005. **128**(Pt 12): p. 2786-96.

119. Rajput, A., et al., *Parkinsonism, Lrrk2 G2019S, and tau neuropathology.* Neurology, 2006. **67**(8): p. 1506-8.

120. Ujiie, S., et al., *LRRK2 I2020T mutation is associated with tau pathology.* Parkinsonism Relat Disord, 2012. **18**(7): p. 819-23.

121. Li, Y., et al., *Mutant LRRK2(R1441G) BAC transgenic mice recapitulate cardinal features of Parkinson's disease.* Nat Neurosci, 2009. **12**(7): p. 826-8.

122. Melrose, H.L., et al., *Impaired dopaminergic neurotransmission and microtubule-associated protein tau alterations in human LRRK2 transgenic mice.* Neurobiol Dis, 2010. **40**(3): p. 503-17.

123. Chan, S.L., et al., *MAP1B rescues LRRK2 mutant-mediated cytotoxicity.* Mol Brain, 2014. **7**: p. 29.

124. Habig, K., et al., *LRRK2 guides the actin cytoskeleton at growth cones together with ARHGEF7 and Tropomyosin 4.* Biochim Biophys Acta, 2013. **1832**(12): p. 2352-67.

125. Civiero, L., et al., *Leucine-rich repeat kinase 2 interacts with p21-activated kinase 6 to control neurite complexity in mammalian brain.* J Neurochem, 2015. **135**(6): p. 1242-56.

126. Hattula, K., et al., *A Rab8-specific GDP/GTP exchange factor is involved in actin remodeling and polarized membrane transport.* Mol Biol Cell, 2002. **13**(9): p. 3268-80.

127. Li, R. and G.G. Gundersen, *Beyond polymer polarity: how the cytoskeleton builds a polarized cell.* Nat Rev Mol Cell Biol, 2008. **9**(11): p. 860-73.

128. Amos, L.A. and D. Schlieper, *Microtubules and maps.* Adv Protein Chem, 2005. **71**: p. 257-98.

129. Mitchison, T. and M. Kirschner, *Dynamic instability of microtubule growth.* Nature, 1984. **312**(5991): p. 237-42.

130. Westermann, S. and K. Weber, *Post-translational modifications regulate microtubule function.* Nat Rev Mol Cell Biol, 2003. **4**(12): p. 938-47.

131. Verhey, K.J. and J. Gaertig, *The tubulin code.* Cell Cycle, 2007. **6**(17): p. 2152-60.

132. Conde, C. and A. Caceres, *Microtubule assembly, organization and dynamics in axons and dendrites.* Nat Rev Neurosci, 2009. **10**(5): p. 319-32.

133. Chakraborti, S., et al., *The emerging role of the tubulin code: From the tubulin molecule to neuronal function and disease.* Cytoskeleton (Hoboken), 2016. **73**(10): p. 521-550.

134. Dubey, J., N. Ratnakaran, and S.P. Koushika, *Neurodegeneration and microtubule dynamics: death by a thousand cuts.* Front Cell Neurosci, 2015. **9**: p. 343.

135. Baas, P.W., et al., *Stability properties of neuronal microtubules.* Cytoskeleton (Hoboken), 2016. **73**(9): p. 442-60.

136. Arce, C.A., et al., *Incorporation of L-tyrosine, L-phenylalanine and L-3,4-dihydroxyphenylalanine as single units into rat brain tubulin.* Eur J Biochem, 1975. **59**(1): p. 145-9.

137. Hallak, M.E., et al., *Release of tyrosine from tyrosinated tubulin. Some common factors that affect this process and the assembly of tubulin.* FEBS Lett, 1977. **73**(2): p. 147-50.

138. Paturle-Lafanechere, L., et al., *Characterization of a major brain tubulin variant which cannot be tyrosinated.* Biochemistry, 1991. **30**(43): p. 10523-8.

139. Aillaud, I., et al., *A synthetic entry to furo[2,3-b]pyridin-4(1H)-ones and related furoquinolinones via iodocyclization.* Org Lett, 2006. **8**(6): p. 1113-6.

140. Edde, B., et al., *Posttranslational glutamylation of alpha-tubulin.* Science, 1990. **247**(4938): p. 83-5.

141. Alexander, J.E., et al., *Characterization of posttranslational modifications in neuron-specific class III beta-tubulin by mass spectrometry.* Proc Natl Acad Sci U S A, 1991. **88**(11): p. 4685-9.

142. Redeker, V., et al., *Polyglycylation of tubulin: a posttranslational modification in axonemal microtubules.* Science, 1994. **266**(5191): p. 1688-91.

143. Caron, J.M., *Posttranslational modification of tubulin by palmitoylation: I. In vivo and cell-free studies.* Mol Biol Cell, 1997. **8**(4): p. 621-36.

144. L'Hernault, S.W. and J.L. Rosenbaum, *Chlamydomonas alpha-tubulin is posttranslationally modified by acetylation on the epsilon-amino group of a lysine.* Biochemistry, 1985. **24**(2): p. 473-8.

145. Song, Y., et al., *Transglutaminase and polyamination of tubulin: posttranslational modification for stabilizing axonal microtubules.* Neuron, 2013. **78**(1): p. 109-23.

146. Eipper, B.A., *Rat brain microtubule protein: purification and determination of covalently bound phosphate and carbohydrate.* Proc Natl Acad Sci U S A, 1972. **69**(8): p. 2283-7.

147. Matten, W.T., et al., *Tubulin is phosphorylated at tyrosine by pp60c-src in nerve growth cone membranes.* J Cell Biol, 1990. **111**(5 Pt 1): p. 1959-70.

148. Faruki, S., R.L. Geahlen, and D.J. Asai, *Syk-dependent phosphorylation of microtubules in activated B-lymphocytes.* J Cell Sci, 2000. **113 (Pt 14)**: p. 2557-65.

149. Fourest-Lieuvin, A., et al., *Microtubule regulation in mitosis: tubulin phosphorylation by the cyclin-dependent kinase Cdk1*. Mol Biol Cell, 2006. **17**(3): p. 1041-50.

150. Chu, C.W., et al., *A novel acetylation of beta-tubulin by San modulates microtubule polymerization via down-regulating tubulin incorporation.* Mol Biol Cell, 2011. **22**(4): p. 448-56.

151. Ren, Y., J. Zhao, and J. Feng, *Parkin binds to alpha/beta tubulin and increases their ubiquitination and degradation.* J Neurosci, 2003. **23**(8): p. 3316-24.

152. Wong, C.C., et al., *Global analysis of posttranslational protein arginylation.* PLoS Biol, 2007. **5**(10): p. e258.

153. Walgren, J.L., et al., *High glucose and insulin promote O-GlcNAc modification of proteins, including alpha-tubulin.* Am J Physiol Endocrinol Metab, 2003. **284**(2): p. E424-34.

154. Xiao, H., et al., *Post-translational modifications to Toxoplasma gondii alpha- and beta-tubulins include novel C-terminal methylation.* J Proteome Res, 2010. **9**(1): p. 359-72.

155. Jaffrey, S.R., et al., *Protein S-nitrosylation: a physiological signal for neuronal nitric oxide.* Nat Cell Biol, 2001. **3**(2): p. 193-7.

156. Rosas-Acosta, G., et al., *A universal strategy for proteomic studies of SUMO and other ubiquitin-like modifiers.* Mol Cell Proteomics, 2005. **4**(1): p. 56-72.

157. Janke, C. and J.C. Bulinski, *Post-translational regulation of the microtubule cytoskeleton: mechanisms and functions.* Nat Rev Mol Cell Biol, 2011. **12**(12): p. 773-86.

158. Magiera, M.M. and C. Janke, *Investigating tubulin posttranslational modifications with specific antibodies.* Methods Cell Biol, 2013. **115**: p. 247-67.

159. Song, Y. and S.T. Brady, *Post-translational modifications of tubulin: pathways to functional diversity of microtubules.* Trends Cell Biol, 2015. **25**(3): p. 125-36.

160. Shida, T., et al., *The major alpha-tubulin K40 acetyltransferase alphaTAT1 promotes rapid ciliogenesis and efficient mechanosensation.* Proc Natl Acad Sci U S A, 2010. **107**(50): p. 21517-22.

161. Hubbert, C., et al., *HDAC6 is a microtubule-associated deacetylase.* Nature, 2002. **417**(6887): p. 455-8.

162. North, B.J., et al., *The human Sir2 ortholog, SIRT2, is an NAD+-dependent tubulin deacetylase.* Mol Cell, 2003. **11**(2): p. 437-44.

163. Szyk, A., et al., *Molecular basis for age-dependent microtubule acetylation by tubulin acetyltransferase.* Cell, 2014. **157**(6): p. 1405-15.

164. Kalebic, N., et al., *Tubulin acetyltransferase alphaTAT1 destabilizes microtubules independently of its acetylation activity.* Mol Cell Biol, 2013. **33**(6): p. 1114-23.

165. Kaul, N., V. Soppina, and K.J. Verhey, *Effects of alpha-tubulin K40 acetylation and detyrosination on kinesin-1 motility in a purified system.* Biophys J, 2014. **106**(12): p. 2636-43.

166. Ersfeld, K., et al., *Characterization of the tubulin-tyrosine ligase.* J Cell Biol, 1993. **120**(3): p. 725-32.

167. Szyk, A., et al., *Tubulin tyrosine ligase structure reveals adaptation of an ancient fold to bind and modify tubulin.* Nat Struct Mol Biol, 2011. **18**(11): p. 1250-8.

168. Prota, A.E., et al., *Structural basis of tubulin tyrosination by tubulin tyrosine ligase.* J Cell Biol, 2013. **200**(3): p. 259-70.

169. Khawaja, S., G.G. Gundersen, and J.C. Bulinski, *Enhanced stability of microtubules enriched in detyrosinated tubulin is not a direct function of detyrosination level.* J Cell Biol, 1988. **106**(1): p. 141-9.

170. Webster, D.R., et al., *Detyrosination of alpha tubulin does not stabilize microtubules in vivo.* J Cell Biol, 1990. **111**(1): p. 113-22.

171. Cook, T.A., T. Nagasaki, and G.G. Gundersen, *Rho guanosine triphosphatase mediates the selective stabilization of microtubules induced by lysophosphatidic acid.* J Cell Biol, 1998. **141**(1): p. 175-85.

172. Peris, L., et al., *Motor-dependent microtubule disassembly driven by tubulin tyrosination.* J Cell Biol, 2009. **185**(7): p. 1159-66.

173. Sirajuddin, M., L.M. Rice, and R.D. Vale, *Regulation of microtubule motors by tubulin isotypes and post-translational modifications.* Nat Cell Biol, 2014. **16**(4): p. 335-44.

174. Roll-Mecak, A. and R.D. Vale, *Structural basis of microtubule severing by the hereditary spastic paraplegia protein spastin.* Nature, 2008. **451**(7176): p. 363-7.

175. Peris, L., et al., *Tubulin tyrosination is a major factor affecting the recruitment of CAP-Gly proteins at microtubule plus ends.* J Cell Biol, 2006. **174**(6): p. 839-49.

176. Bieling, P., et al., *CLIP-170 tracks growing microtubule ends by dynamically recognizing composite EB1/tubulin-binding sites.* J Cell Biol, 2008. **183**(7): p. 1223-33.

177. Gundersen, G.G., *Evolutionary conservation of microtubule-capture mechanisms.* Nat Rev Mol Cell Biol, 2002. **3**(4): p. 296-304.

178. Konishi, Y. and M. Setou, *Tubulin tyrosination navigates the kinesin-1 motor domain to axons.* Nat Neurosci, 2009. **12**(5): p. 559-67.

179. Liao, G. and G.G. Gundersen, *Kinesin is a candidate for cross-bridging microtubules and intermediate filaments. Selective binding of kinesin to detyrosinated tubulin and vimentin.* J Biol Chem, 1998. **273**(16): p. 9797-803.

180. Kreitzer, G., G. Liao, and G.G. Gundersen, *Detyrosination of tubulin regulates the interaction of intermediate filaments with microtubules in vivo via a kinesin-dependent mechanism.* Mol Biol Cell, 1999. **10**(4): p. 1105-18.

181. Kalinina, E., et al., *A novel subfamily of mouse cytosolic carboxypeptidases.* FASEB J, 2007. **21**(3): p. 836-50.

182. Janke, C., et al., *Tubulin polyglutamylase enzymes are members of the TTL domain protein family.* Science, 2005. **308**(5729): p. 1758-62.

183. Regnard, C., et al., *Characterisation of PGs1, a subunit of a protein complex co-purifying with tubulin polyglutamylase.* J Cell Sci, 2003. **116**(Pt 20): p. 4181-90.

184. Kimura, Y., et al., *Identification of tubulin deglutamylase among Caenorhabditis elegans and mammalian cytosolic carboxypeptidases (CCPs).* J Biol Chem, 2010. **285**(30): p. 22936-41.

185. Rogowski, K., et al., *A family of protein-deglutamylating enzymes associated with neurodegeneration.* Cell, 2010. **143**(4): p. 564-78.

186. Sharma, N., et al., *Katanin regulates dynamics of microtubules and biogenesis of motile cilia.* J Cell Biol, 2007. **178**(6): p. 1065-79.

187. Lacroix, B., et al., *Tubulin polyglutamylation stimulates spastin-mediated microtubule severing.* J Cell Biol, 2010. **189**(6): p. 945-54.

188. Garnham, C.P. and A. Roll-Mecak, *The chemical complexity of cellular microtubules: tubulin post-translational modification enzymes and their roles in tuning microtubule functions.* Cytoskeleton (Hoboken), 2012. **69**(7): p. 442-63.

189. Zambito, A.M. and J. Wolff, *Palmitoylation of tubulin.* Biochem Biophys Res Commun, 1997. **239**(3): p. 650-4.

190. Peters, J.D., et al., *Syk, activated by cross-linking the B-cell antigen receptor, localizes to the cytosol where it interacts with and phosphorylates alpha-tubulin on tyrosine.* J Biol Chem, 1996. **271**(9): p. 4755-62.

191. Qiang, L., et al., *Tau protects microtubules in the axon from severing by katanin.* J Neurosci, 2006. **26**(12): p. 3120-9.

192. Yu, W., et al., *The microtubule-severing proteins spastin and katanin participate differently in the formation of axonal branches.* Mol Biol Cell, 2008. **19**(4): p. 1485-98.

193. Kosik, K.S., et al., *Developmentally regulated expression of specific tau sequences.* Neuron, 1989. **2**(4): p. 1389-97.

194. Shin, R.W., et al., *Massive accumulation of modified tau and severe depletion of normal tau characterize the cerebral cortex and white matter of Alzheimer's disease. Demonstration using the hydrated autoclaving method.* Am J Pathol, 1992. **140**(4): p. 937-45.

195. Cohen, T.J., et al., *The acetylation of tau inhibits its function and promotes pathological tau aggregation.* Nat Commun, 2011. **2**: p. 252.

196. Cook, C., et al., *Acetylation of the KXGS motifs in tau is a critical determinant in modulation of tau aggregation and clearance.* Hum Mol Genet, 2014. **23**(1): p. 104-16.

197. Cappelletti, G., et al., *Linking microtubules to Parkinson's disease: the case of parkin.* Biochem Soc Trans, 2015. **43**(2): p. 292-6.

198. Ferrari-Toninelli, G., et al., *Microtubule stabilizing effect of notch activation in primary cortical neurons.* Neuroscience, 2008. **154**(3): p. 946-52.

199. Chuckowree, J.A. and J.C. Vickers, *Cytoskeletal and morphological alterations underlying axonal sprouting after localized transection of cortical neuron axons in vitro.* J Neurosci, 2003. **23**(9): p. 3715-25.

200. Letourneau, P.C., T.A. Shattuck, and A.H. Ressler, *Branching of sensory and sympathetic neurites in vitro is inhibited by treatment with taxol.* J Neurosci, 1986. **6**(7): p. 1912-7.

201. Hazan, J., et al., *Spastin, a new AAA protein, is altered in the most frequent form of autosomal dominant spastic paraplegia.* Nat Genet, 1999. **23**(3): p. 296-303.

202. Fassier, C., et al., *Microtubule-targeting drugs rescue axonal swellings in cortical neurons from spastin knockout mice.* Dis Model Mech, 2013. **6**(1): p. 72-83.

203. Scuteri, A., et al., *Paclitaxel toxicity in post-mitotic dorsal root ganglion (DRG) cells.* Anticancer Res, 2006. **26**(2A): p. 1065-70.

204. Gornstein, E. and T.L. Schwarz, *The paradox of paclitaxel neurotoxicity: Mechanisms and unanswered questions.* Neuropharmacology, 2014. **76 Pt A**: p. 175-83.

205. Esteves, A.R. and S.M. Cardoso, *LRRK2 at the Crossroad Between Autophagy and Microtubule Trafficking: Insights into Parkinson's Disease.* Neuroscientist, 2016.

206. Pellegrini, L., et al., *Back to the tubule: microtubule dynamics in Parkinson's disease.* Cell Mol Life Sci, 2017. **74**(3): p. 409-434.

207. Pasinelli, P. and R.H. Brown, *Molecular biology of amyotrophic lateral sclerosis: insights from genetics.* Nat Rev Neurosci, 2006. **7**(9): p. 710-23.

208. Hoepfner, S., et al., *Modulation of receptor recycling and degradation by the endosomal kinesin KIF16B.* Cell, 2005. **121**(3): p. 437-50.

209. Cantalupo, G., et al., *Rab-interacting lysosomal protein (RILP): the Rab7 effector required for transport to lysosomes.* EMBO J, 2001. **20**(4): p. 683-93.

210. Jordens, I., et al., *The Rab7 effector protein RILP controls lysosomal transport by inducing the recruitment of dynein-dynactin motors.* Curr Biol, 2001. **11**(21): p. 1680-5.

211. Millecamps, S. and J.P. Julien, *Axonal transport deficits and neurodegenerative diseases.* Nat Rev Neurosci, 2013. **14**(3): p. 161-76.

212. Gomez-Suaga, P., et al., *Leucine-rich repeat kinase 2 regulates autophagy through a calcium-dependent pathway involving NAADP.* Hum Mol Genet, 2012. **21**(3): p. 511-25.

213. Manzoni, C., et al., *Pathogenic Parkinson's disease mutations across the functional domains of LRRK2 alter the autophagic/lysosomal response to starvation.* Biochem Biophys Res Commun, 2013. **441**(4): p. 862-6.

214. Bravo-San Pedro, J.M., et al., *The LRRK2 G2019S mutant exacerbates basal autophagy through activation of the MEK/ERK pathway.* Cell Mol Life Sci, 2013. **70**(1): p. 121-36.

215. Manzoni, C., et al., *Inhibition of LRRK2 kinase activity stimulates macroautophagy.* Biochim Biophys Acta, 2013. **1833**(12): p. 2900-10.

216. Yun, H.J., et al., *An early endosome regulator, Rab5b, is an LRRK2 kinase substrate.* J Biochem, 2015. **157**(6): p. 485-95.

217. Shin, N., et al., *LRRK2 regulates synaptic vesicle endocytosis.* Exp Cell Res, 2008. **314**(10): p. 2055-65.

218. Dodson, M.W., et al., *Roles of the Drosophila LRRK2 homolog in Rab7-dependent lysosomal positioning.* Hum Mol Genet, 2012. **21**(6): p. 1350-63.

219. Gomez-Suaga, P., et al., *LRRK2 delays degradative receptor trafficking by impeding late endosomal budding through decreasing Rab7 activity.* Hum Mol Genet, 2014. **23**(25): p. 6779-96.

220. Ito, G., et al., *Phos-tag analysis of Rab10 phosphorylation by LRRK2: a powerful assay for assessing kinase function and inhibitors.* Biochem J, 2016. **473**(17): p. 2671-85.

221. MacLeod, D.A., et al., *RAB7L1 interacts with LRRK2 to modify intraneuronal protein sorting and Parkinson's disease risk.* Neuron, 2013. **77**(3): p. 425-39.

222. Linhart, R., et al., *Vacuolar protein sorting 35 (Vps35) rescues locomotor deficits and shortened lifespan in Drosophila expressing a Parkinson's disease mutant of Leucine-Rich Repeat Kinase 2 (LRRK2).* Mol Neurodegener, 2014. **9**: p. 23.

223. Cho, H.J., et al., *Leucine-rich repeat kinase 2 regulates Sec16A at ER exit sites to allow ER-Golgi export.* EMBO J, 2014. **33**(20): p. 2314-31.

224. Matta, S., et al., *LRRK2 controls an EndoA phosphorylation cycle in synaptic endocytosis.* Neuron, 2012. **75**(6): p. 1008-21.

225. Gloeckner, C.J., et al., *The Parkinson disease-associated protein kinase LRRK2 exhibits MAPKKK activity and phosphorylates MKK3/6 and MKK4/7, in vitro.* J Neurochem, 2009. **109**(4): p. 959-68.

226. Karunakaran, S., et al., *Selective activation of p38 mitogen-activated protein kinase in dopaminergic neurons of substantia nigra leads to nuclear translocation of p53 in 1-methyl-4-phenyl-1,2,3,6-tetrahydropyridine-treated mice.* J Neurosci, 2008. **28**(47): p. 12500-9.

227. Gardet, A., et al., *LRRK2 is involved in the IFN-gamma response and host response to pathogens.* J Immunol, 2010. **185**(9): p. 5577-85.

228. Russo, I., L. Bubacco, and E. Greggio, *LRRK2 and neuroinflammation: partners in crime in Parkinson's disease?* J Neuroinflammation, 2014. **11**: p. 52.

229. Sancho, R.M., B.M. Law, and K. Harvey, *Mutations in the LRRK2 Roc-COR tandem domain link Parkinson's disease to Wnt signalling pathways.* Hum Mol Genet, 2009. **18**(20): p. 3955-68.

230. Berwick, D.C., et al., *Pathogenic LRRK2 variants are gain-of-function mutations that enhance LRRK2-mediated repression of beta-catenin signaling.* Mol Neurodegener, 2017. **12**(1): p. 9.

231. MacDonald, B.T., K. Tamai, and X. He, *Wnt/beta-catenin signaling: components, mechanisms, and diseases.* Dev Cell, 2009. **17**(1): p. 9-26.

232. Inestrosa, N.C. and E. Arenas, *Emerging roles of Wnts in the adult nervous system.* Nat Rev Neurosci, 2010. **11**(2): p. 77-86.

233. Ho, C.C., et al., *The Parkinson disease protein leucine-rich repeat kinase 2 transduces death signals via Fas-associated protein with death domain and caspase-8 in a cellular model of neurodegeneration.* J Neurosci, 2009. **29**(4): p. 1011-6.

234. Ho, D.H., et al., *Leucine-Rich Repeat Kinase 2 (LRRK2) phosphorylates p53 and induces p21(WAF1/CIP1) expression.* Mol Brain, 2015. **8**: p. 54.

235. Su, Y.C., X. Guo, and X. Qi, *Threonine 56 phosphorylation of Bcl-2 is required for LRRK2 G2019S-induced mitochondrial depolarization and autophagy.* Biochim Biophys Acta, 2015. **1852**(1): p. 12-21.

236. Esteves, A.R., R.H. Swerdlow, and S.M. Cardoso, *LRRK2, a puzzling protein: insights into Parkinson's disease pathogenesis.* Exp Neurol, 2014. **261**: p. 206-16.

237. Choi, I., et al., *LRRK2 G2019S mutation attenuates microglial motility by inhibiting focal adhesion kinase.* Nat Commun, 2015. **6**: p. 8255.

238. Moehle, M.S., et al., *The G2019S LRRK2 mutation increases myeloid cell chemotactic responses and enhances LRRK2 binding to actin-regulatory proteins.* Hum Mol Genet, 2015. **24**(15): p. 4250-67.

239. Cookson, M.R., *Cellular functions of LRRK2 implicate vesicular trafficking pathways in Parkinson's disease.* Biochem Soc Trans, 2016. **44**(6): p. 1603-1610.

240. Dunn, S., et al., *Differential trafficking of Kif5c on tyrosinated and detyrosinated microtubules in live cells.* J Cell Sci, 2008. **121**(Pt 7): p. 1085-95.

241. Walev, I., et al., *Delivery of proteins into living cells by reversible membrane permeabilization with streptolysin-O.* Proc Natl Acad Sci U S A, 2001. **98**(6): p. 3185-90.

242. Kano, F., et al., *A resealed-cell system for analyzing pathogenic intracellular events: perturbation of endocytic pathways under diabetic conditions.* PLoS One, 2012. **7**(8): p. e44127.

243. Siegel, R.M., et al., *Death-effector filaments: novel cytoplasmic structures that recruit caspases and trigger apoptosis.* J Cell Biol, 1998. **141**(5): p. 1243-53.

244. Dickens, L.S., et al., *A death effector domain chain DISC model reveals a crucial role for caspase-8 chain assembly in mediating apoptotic cell death.* Mol Cell, 2012. **47**(2): p. 291-305.

245. Cartelli, D., et al., *Microtubule dysfunction precedes transport impairment and mitochondria damage in MPP+ -induced neurodegeneration.* J Neurochem, 2010. **115**(1): p. 247-58.

246. Fonrose, X., et al., *Parthenolide inhibits tubulin carboxypeptidase activity.* Cancer Res, 2007. **67**(7): p. 3371-8.

247. Barisic, M., et al., *Mitosis. Microtubule detyrosination guides chromosomes during mitosis.* Science, 2015. **348**(6236): p. 799-803.

248. Kaplan, A. and O. Reiner, *Linking cytoplasmic dynein and transport of Rab8 vesicles to the midbody during cytokinesis by the doublecortin domain-containing 5 protein.* J Cell Sci, 2011. **124**(Pt 23): p. 3989-4000.

249. Xiong, Y., V.L. Dawson, and T.M. Dawson, *LRRK2 GTPase dysfunction in the pathogenesis of Parkinson's disease.* Biochem Soc Trans, 2012. **40**(5): p. 1074-9.

250. West, A.B., et al., *Parkinson's disease-associated mutations in leucine-rich repeat kinase 2 augment kinase activity.* Proc Natl Acad Sci U S A, 2005. **102**(46): p. 16842-7.

251. Ito, G., et al., *Lack of correlation between the kinase activity of LRRK2 harboring kinase-modifying mutations and its phosphorylation at Ser910, 935, and Ser955.* PLoS One, 2014. **9**(5): p. e97988.

252. Reynolds, A., et al., *LRRK2 kinase activity and biology are not uniformly predicted by its autophosphorylation and cellular phosphorylation site status.* Front Mol Neurosci, 2014. **7**: p. 54.

253. Nixon-Abell, J., et al., *Protective LRRK2 R1398H Variant Enhances GTPase and Wnt Signaling Activity.* Front Mol Neurosci, 2016. **9**: p. 18.

XI. List of papers

I. Blanca Ramirez, M., et al., LRRK2 and Parkinson s disease: from lack of structure to gain of function. Curr Protein Pept Sci, 2016.

Factor de impacto: 2.441 Quartil: Q2

II. Blanca Ramirez, M., et al., LRRK2: from kinase to GTPase to microtubules and back. Biochem Soc Trans, 2017. 45(1): p. 141-146.

Factor de impacto: 2.26 Quartil: Q1

III. Blanca Ramirez, M., et al., GTP binding regulates cellular localization of Parkinsons disease-associated LRRK2. Hum Mol Genet, 2017.

Factor de impacto: 5.985 Quartil: Q1

Additional publications

IV. Madero-Perez, J., et al., Cellular effects mediated by pathogenic LRRK2: homing in on Rab-mediated processes. Biochem Soc Trans, 2017. 45(1): p. 147-154.

Factor de impacto: 2.26 Quartil: Q1

V. Law, B.M., et al., A direct interaction between leucine-rich repeat kinase 2 and specific beta-tubulin isoforms regulates tubulin acetylation. J Biol Chem, 2014. 289(2): p. 895-908.

Factor de impacto: 4.573 Quartil: Q1

VI. Gomez-Suaga, P., et al., LRRK2 delays degradative receptor trafficking by impeding late endosomal budding through decreasing Rab7 activity. Hum Mol Genet, 2014. 23(25): p. 6779-96

Factor de impacto: 6.393 Quartil: Q1

VII. Gomez-Suaga, P., et al., Novel insights into the neurobiology underlying LRRK2-linked Parkinson's disease. Neuropharmacology, 2014. 85: p. 45-56.

Factor de impacto: 5.106 Quartil: Q1

VIII. Gomez-Suaga, P., et al., A Link between Autophagy and the Pathophysiology of LRRK2 in Parkinson's Disease. Parkinsons Dis, 2012. 2012: p. 324521.

Factor de impacto: 1.27 Quartil: Q2